AN ABSTRACT OF THE THESIS OF

Yongsheng Feng for the degree of Doctor of Philosophy

in Soil Science presented on August 22, 1990

Title: A Continuum Model of Plant Root Growth

Redacted for Privacy

Abstract approved: _____
Larry Boersma

The continuum theory provides a framework in which the growth of a plant root as a dynamic process involving interactions among transport of water and solute, cell division, and the subsequent cell elongation can be described. A plant root is modeled as a one–dimensional, multi–phase, mathematical continuum. The network of cell walls constitute the solid phase of the system. The symplast and the apoplast pathways reside in this network of cell walls. Water and carbohydrates move in opposite directions through the apoplast and symplast pathways within the deforming network of cell walls. The division and elongation of cells depends on the mechanical stress imposed on the cell walls, the rate of metabolic stress relaxation process, and the physical properties of the cell walls.

The model consists of five systems of differential equations. The kinematic equations are derived which allow, specifically, the different roles of cell division and elongation in root growth to be considered. These provide the reference system of the model. Equations of water transport in the coupled system of apoplast and symplast pathways are

derived from considerations of theories of transport in the porous media and the cellular and membrane properties of the plant root. Equations of solute transport are derived by considering, specifically, the mechanisms involved in solute transport both at the membranes separating individual cells and within the cytoplasm. The rate of cell elongation is described as a function of the mechanical stress in the cell walls, the viscoelastic properties of the cell walls, and a metabolically controlled strain energy relaxation process. Growth in the meristem is modeled as the result of continuous cell elongation and division.

The equations of water and solute transport, cell elongation, and meristem growth are solved simultaneously under the reference system provided by the kinematic theory. The model is used to examine the effects of soil water stress, soil resistance to root penetration, and temperature, as well as the carbohydrate supply from the upper part of the plant on the dynamic process of root elongation. The close correspondence between the material coordinate system and the underlying cellular structure of the root allows the comparison between the continuum theory and the results of cell growth studies. Agreement of the model predictions of the pattern of growth along the root axis, as well as the effects of temperature and soil water stress on root growth, with the experimental measurements reported in the literature provides the justification for the theories.

A Continuum Model of Plant Root Growth

by

Yongsheng Feng

A THESIS

submitted to

Oregon State University

in partial fulfillment of

the requirements for the

degree of

Doctor of Philosophy

Completed August 22, 1990

Commencement June 1991

APPROVED:

Redacted for Privacy

Professor of Soil Science in charge of major

Redacted for Privacy

Head of department of Crop and Soil Science

Redacted for Privacy

Dean of Graduate School

Date thesis is presented August 22, 1990

Typed by Yongsheng Feng for Yongsheng Feng

ACKNOWLEDGEMENTS

I would like to express my deep appreciation to Dr. Larry Boersma for his support, encouragement and understanding during my graduate program. His guidance has made my stay in Oregon State University a truly a learning experience.

Special appreciation is extended to the members of my graduate committee for their careful review of this thesis and many helpful suggestions.

I would also like to express my gratitude to members of the Department of Soil Science and my fellow graduate students who has made my stay truly enjoyable.

Special thanks are due to my wife, Xiaomei Li. for her love, support, and confidence, she deserves all my love and gratitude.

TABLE OF CONTENTS

LIST OF FIGURES

LIST OF TABLES

A CONTINUUM MODEL OF PLANT ROOT GROWTH

INTRODUCTION

It is through the root system that a plant comes into intimate contact with the soil environment. Continuous growth of roots enables a plant to explore the soil environment for water and essential mineral nutrients to meet the increasing demand during growth.

The axial growth of plant roots consists of cell multiplication in the meristematic region at the root apex and cell extension in the elongation region following the meristem (Green, 1976). The meristematic growth of a plant root is characterized by maximum production of cytoplasm and cell wall materials, such as DNA, RNA, protein, pectins, and cellulose (Burstrom, 1974). The cell elongation in the elongation region is characterized by extension and biosynthesis of cell walls and by water uptake. Despite the controversy regarding the distinction between cell multiplication and cell elongation regions, and the overlap of the two processes, the above general description provides a realistic picture of root axial growth. The description is also simple enough to serve as the basis for a mathematical description of plant root growth.

A large body of literature exists with respect to plant growth. Detailed reviews were written by Cleland (1971), Taiz (1984), Cosgrove (1986) and Dale (1988). The main component of the elongation rate of a plant root or shoot is contributed by elongating cells. Consequently, the literature on plant growth has concentrated on mechanisms of cell elongation. Cell division and its contribution to plant growth has, to a

large extent, been ignored. Meristematic cell division may contribute little to the instant rate of axial elongation of a root, but its long term effect on the total length of the root is expected to be much more significant than its contribution to the instant rate of growth. Stopping cell division may have little effect on the root growth rate at the instant, but root elongation will stop at a later time because there would be no more cell that could elongate. Little has been written in the literature concerning this aspect of axial growth.

It is concluded from the extensive research on growth that: (a) the driving force for cell extension is turgor pressure; (b) cell enlargement involves both mechanical stretching and biosynthesis of cell walls; (c) growth is an active process that requires energy from respiration; (d) continuous synthesis of cell contents such as DNA and protein is necessary; (e) a continuous supply of nutrients is necessary for any significant growth; (f) growth is affected by environmental conditions such as temperature, water stress, and soil resistance; and (g) the rate of growth in many higher plants is regulated by auxin. The problem is to organize this information into a coherent picture of growth so that a comprehensive understanding of plant growth is possible. Few researches have been attempted in this area (McCoy and Boersma, 1984).

Particular difficulty is imposed on plant root growth researches by their minute size and also by the inaccessibility of the soil environment in which the roots reside. The observation of growth rate and the time course of root length development has many difficulties, while a similar observation in the aerial part of the plant is readily performed. The streak photography technique initiated by Erickson and Sax (1956a) makes

the continuous observation of the growth of a plant root possible. There is the question, however, whether the observations correspond to the real situation in the soil, since in these experiments the roots are exposed to conditions drastically different from that in the soil in terms of water uptake and the mechanical resistance of the soil to root elongation. It is, at least, partly due to these difficulties that much of the research on root growth has been concerned with cell extension.

A second difficulty with root growth research is the large number of factors involved. These include the carbohydrate supply from the shoot, soil water stress, soil compaction, temperature, the mechanical properties of the cell walls, and the biochemical process of cell wall loosening and synthesis. Each of these factors works in close interaction with all the others to affect root growth. Much of the literature on root growth has been concerned with either one or two of these factors. The multi–factor nature of root growth and the close interactions between these factors has received less attention.

The difficult and complex nature of plant root growth research makes a mathematical model an ideal research tool. A mathematical model can be formulated to incorporate the main features of the growth activity based on current research findings. A model thus developed can then be used to theoretically examine various aspects of growth activity and to quantitatively predict the effects and interactions of factors affecting plant growth.

The growth activity of a plant can be described as a totality of multiplication and expansion of individual cells. Alternatively, it can be described as the continuous deformation and biosynthesis of a multicellular

plant tissue as a mathematical continuum (Silk and Erickson, 1979). The merit of the first approach lies in its ability to provide the detailed information of the behavior of individual cells and to relate the information to the biochemical processes that take place within these cells. This approach faces the difficulty of extrapolating the results and the observations to predict the behavior of the whole plant or a plant part. The deductions regarding the growth of a plant or a plant tissue obtained from these models, at its best, can only be qualitative. This is because that the processes involving interactions among plant cells, such as the transport of water and solute, cannot be adequately described by observing individual cells.

The second approach is to study the growth of a multicellular plant tissue as a whole. This approach is best represented by the continuum theory pioneered by Silk and Erickson (1979). This approach does not provide definite correlation with the specific biochemical processes taking place in individual cells, nor is it likely that the detailed biochemical process information will be explicitly incorporated in the continuum models. The continuum models work in the area where the "cellular" approach falls short, i.e., in studying the growth of a plant tissue, such as a root, and its interaction with processes that involve more than one cell, such as the transport of water and available carbohydrate. It provides mechanistic and quantitative information concerning how, and to some extent, why factors such as soil water stress, soil resistance, and soil temperature affect root growth, as well as information about the interaction among these factors. Although the continuum theory is not concerned with the detailed cellular structure of

the plant tissue. its development relies on the information regarding behavior and the inter–relations of individual cells. The basic starting point of the theory, which is the stress–strain properties of the tissue and the role of biosynthesis on cell extension relies on detailed studies of individual plant cells.

The two approaches, the cellular and the continuum, complement each other to provide a more comprehensive understanding of plant growth activity, rather than compete with each other. Their relations resemble that of the molecular theory and the continuum theory of fluid flow.

The one–dimensional nature of axial root growth makes it an ideal candidate for the application of the continuum theory because of the relative simplicity of mathematical treatments involved. Research in this area has, in the past, concentrated on the kinematics of the root growth (Silk and Erickson, 1979: Gandar, 1983a,b), its application in describing the measured growth and cell division patterns (Bertaud and Gandar, 1985; Carmona and Cardrado, 1986; Sharp et al., 1988; Pahlavanian and Silk, 1988), and the application of the law of mass balance to produce the local rate of biosynthesis of structural materials (Silk and Erickson, 1980; Silk et al., 1984; Silk et al., 1986). McCoy and Boersma (1984) treated the rate of root elongation from the perspective of conservation of thermodynamic free energy during tissue deformation. They presented equations that describe the steady state elongation of the plant root. The steady state model they derived applies only under constant soil environment conditions, which is rarely seen in practical situations.

No attempts have been made to model the growth response of

plant roots in a dynamic environment nor has it been attempted to incorporate into the models the viscoelastic properties of the cell walls, the different roles of cell division and elongation in root growth, the dynamic interactions between growth and the transport of water and solute, and the metabolically controlled cell wall loosening processes.

The need for a comprehensive approach to the study of plant root growth is evident. It will enable one to examine the roles of water and solute transport, the available carbohydrate supply from shoots, the physical properties of the cell wall, the cell division in the meristem region, and the cell elongation in the elongation region during the dynamic process of root growth. It will also enable one to evaluate how plant root development is affected by environmental factors, such as soil water potential, soil resistance, and soil temperature, in a dynamically changing soil environment.

Continuum theory is ideally suited for the development of such a comprehensive description of root growth. A number of problems are involved with an integrated approach. Firstly, the different roles played by cell division in the meristem and the cell elongation in the elongation region need to be incorporated into the kinematic theory of root growth. The traditional continuum theory, because of its basic assumption of one–to–one correspondence between material points and space points at all times, is inadequate for this task. Modifications must be made to accommodate the cell production in the meristem. Secondly, a stress–strain relation, or constitutive equation, must be developed for the cell walls which describes the elongation of cells as controlled by the metabolic processes of the cells, other than simple yielding of cell walls

under mechanical stress. Thirdly, water uptake from the soil, and transport of water and solute in the root must be adequately included in such a model. Finally, the mechanical resistance of soil to root elongation must also be included in such a model.

The objective of this thesis is the development of an integrated model of plant root elongation. The model will be used to theoretically examine various aspects of plant root growth and their relation to the physical and physiological properties of the root and to examine the response of the plant root growth in a dynamic soil environment.

This thesis consists of six parts. In the first chapter, the kinematic theory of axial root elongation is developed which describes root growth as a result of cell division in the meristem and subsequent elongation in the elongation region from a continuum perspective. This provides the framework in which the transport of water and solute, as well as division and elongation of cells, are represented. Chapter two describes the theory of cell elongation as a metabolically controlled process. Equations describing cell growth as a function of viscoelastic properties of cell walls and the metabolically controlled cell wall loosening processes are derived. Theory of water transport in a growing plant root, consisting of dynamic interactions between the apoplast and the symplast pathways is developed in Chapter 3. Equations describing the transport of solute in a growing root by facilitated diffusion both at the membranes and in the cytoplasm, mass flow, and active transport at the membranes are derived in Chapter 4. Chapter 5 integrates the theories of growth and transport developed in the previous chapters into a coherent, integrated model of plant root elongation. The model described in chapter 5 is solved in chapter 6.

Results of model simulations are discussed in chapter 6.

1. KINEMATICS OF AXIAL PLANT ROOT GROWTH

Yongsheng Feng and Larry Boersma
Department of Soil Science, Oregon State University
Corvallis, OR 97331

ABSTRACT

Axial growth of plant roots is a continuous process in both time and space. The growth consists of cell multiplication in the meristem and cell extension in the elongation region. The conventional continuum theory is inadequate for describing this process. When applied to the growth of a plant root as a function of time, it produces infinite extension at the apex. The theory lacks the desired correspondence between material points and the cellular structures of the root, i.e. a material point may not necessarily correspond to the same group of cells at different times. A new approach is proposed which adequately describes both the cell multiplication and the cell elongation aspects of root growth and has the desired feature of material point and cellular structure correspondence.

The meristem of a plant root where cells are continuously produced by cell division is idealized as being located at the root apex. Every elementary segment of the root is associated with a unique instant of time at which it was produced by the meristem. Elongation takes place after the root element leaves the meristem. Under steady state conditions, the rate of elongation of a particular segment of the root is a function of its age only. The total rate of root elongation at any instant is equal to

the sum of the rate of elongation of all root elements present at the moment plus the contribution of cell division at the meristem. The total length of the root at any instant is determined by integrating over the lengths of all the root segments present.

The theory developed in this study is used to describe the effects of water stress and temperature on root growth. The effect of water stress is characterized by a reduction in both the rate of cell division in the meristem and subsequent cell elongation. The combined effect of a lower rate of cell growth and a shorter elongation region results in greater reduction in the rate of root elongation. A 10 per cent reduction in the rate of cell growth results in a 30% reduction in the rate of steady state root elongation. The effect of temperature is characterized by a temperature–time equivalence effect. This concept allowed the calculation of an apparent activation energy for axial root elongation. An activation energy value of 50 kJ mol^{-1} was calculated for corn root growth, which is within the accepted range for biochemical reactions, suggesting that root growth is controlled by cell metabolic processes.

INTRODUCTION

The growth of a plant tissue is the result of division and extension of individual cells. In plant roots, cell production occurs primarily in a meristem region near the root apex; cell elongation occurs in a elongation region following the meristem (Green, 1976). The meristem of the primary root of corn (*Zea mays*) occupies a region of 1–2 mm at the root apex. The elongation region extends over the length of about 10 mm from the root meristem (Erickson and Sax, 1956a,b; Sharp et al., 1988; Pahlavanian and Silk, 1988). Despite controversies about the division and overlap of meristem and elongation regions (Green, 1976), the simple description of axial plant root growth as outlined above is useful in formulating mathematical models because of its simplicity and close approximation to the physical reality.

An alternative and equally fruitful approach in growth studies is to regard the plant root as a one–dimensional mathematical continuum consisting of material points distributed continuously over space (Erickson, 1976; Silk and Erickson, 1978; Gandar 1983a,b; McCoy and Boersma, 1984). The growth of the root is expressed as the motion of these material points through space. This approach focuses on the growth of a plant root as a whole, on the macroscopic scale, rather than on individual cells.

The concept of plant growth as a continuous process was applied in the early experimental studies of Goodwin and Stepka (1945) and Erickson and Sax (1956a,b). They defined such quantities as the cell density distribution in a plant root, the distance of an identifiable point

on the root surface from the root apex, and the velocity at which such a point is displaced away from the root apex during growth, as continuous functions both in space and time. Differentiation of those quantities yielded information that included elemental rate of root elongation and elemental rate of cell production which applied to infinitesimal portions of the root. Silk and Erickson (1978) applied the concept of considering a plant tissue as a mathematical continuum in analyzing the growth pattern of hypocotyl curvature of lettuce seedlings (*Lactuca sativa*) and proposed a mathematical model for describing the development of hypocotyl curvature as a continuous function. Silk and Erickson (1980) applied the law of mass conservation to root growth studies and derived the local rate of biosynthesis of cytoplasmic constituents in a growing root. These studies demonstrate that the continuum assumption can be used as a tool in plant growth studies, despite the fact that a plant root is composed of discrete cell entities.

The validity of the continuum assumption in plant growth studies is analogous to the assumption regarding fluids and elastic solids as mathematical continuums despite the discrete molecular nature of these materials in conventional continuum mechanics. Silk and Erickson (1979) examined the concept of plant tissue as a continuum and the analogy between plant growth and fluid flow. These authors concluded that for those processes involving individual cell differentiation, the continuum assumption may not apply, but for processes involving gross morphological changes in a plant tissue, such as cell expansion and division, the continuum assumption is appropriate.

The kinematic theory in continuum mechanics describes the

deformation of a material body or the motion of material points through space without consideration of the underlying mechanisms. The deformation of a continuum is described from two equivalent perspectives. In the first, attention is focused on the fixed points in space and the deformation is described by studying the motion of the material at these spatial points. This is the spatial or Eulerian description of motion. The second perspective follows specific material points as they move through space. This is often referred to as the material or Lagrangian description of motion. The various branches of continuum mechanics, such as the theory of linear elasticity and the theory of fluid mechanics, are built upon the kinematic theory with specific physical laws governing the material behavior. The kinematic theory of plant growth is an integral part of the continuum theory of plant growth describing the physical motion of the material points in a plant tissue through space. Silk and Erickson (1979) adopted the kinematic theory of conventional continuum mechanics to describe the growth of a plant tissue. They introduced the strain tensor and the continuity equation as defined in continuum mechanics to plant growth studies. These authors discussed the importance of distinction between material and spatial description of growth and the choice of appropriate coordinate systems. Gandar (1983a) discussed plant growth as described by a displacement tensor, a strain tensor, and a rate of deformation. The theory was applied in the analysis of growth in the root apex (Gandar, 1983b). McCoy and Boersma (1984) proposed a model of plant root growth by combining the kinematic theory of plant growth with a Hookian–like constitutive relation governing the stress–strain relations of a plant root, along with equations of water and

solute transport. The model was later used in the study of penetration of soil by plant roots (McCoy and Boersma, 1984).

These researches established the foundation for a theory which provides a consistent framework for quantitative and precise description of growth of plant tissues. However, some fundamental aspects of plant growth were not adequately addressed in these studies. First, fundamental differences exist between the roles of cell division and cell expansion in plant growth (Green, 1976). Cell expansion starts after a cell is produced by cell division. Cell division and extension may respond differently to factors such as water potential and availability of carbohydrates due to the differences of the physiological processes involved. The cells in a plant tissue are at different ages. The size of a mature cell changes very little regardless of the water potential (Taiz, 1984). The kinematic theory of continuum mechanics, when introduced to plant growth studies "as is", is awkward, if not incapable, in dealing with these aspects which are specific to a plant tissue. Furthermore, the kinematic theory in conventional continuum mechanics applies to infinitesimal deformations. The growth of a plant tissue, on the contrary, is anything but "infinitesimal". In the primary root of *Zea mays*, the length of a cell expands over an order of magnitude during cell extension (Erickson and Sax, 1956a,b).

In this study, we develop a set of simple kinematic equations for plant root growth by modifying the kinematic theory of the conventional continuum mechanics. The axial growth of a plant root is described as the result of meristem cell production and subsequent cell extension. It also addresses the fact that the axial root growth represents a finite deformation of the plant root as a mathematical continuum. An attractive

feature of the theory which is not present in previous researches (Silk and Erickson, 1979; Gandar, 1983a,b) is the close correspondence between the material points and the underlying cellular structure of the plant root. This allows us to compare the results of the continuum theory to those of plant cell growth studies which are found in great quantity in the literature. The one–dimensional nature of root growth simplifies the mathematical operations which makes it more suitable for theoretical analysis. The extension of the theory to more complicated growth patterns of two or three dimensions would be straight–forward. The validity of the theory is illustrated with the experimental data of Erickson and Sax (1956a,b), Sharp et al. (1988), and Pahlavanian and Silk (1988).

THEORY

Kinematic theory of continuum mechanics

A brief discussion of the principles of the kinematic theory of conventional continuum mechanics is presented in the following discussion. More detailed discussions were presented by Silk and Erickson (1979) and Gandar (1983a).

The motion of a typical material point, denoted by **X**, is expressed as

$$\mathbf{x} = \mathbf{x}(\mathbf{X}, t) \ , \qquad [1]$$

where the **x** on the left hand side is the spatial position of the material point **X** at time t; and the **x** on the right hand side refers to a function with independent variables **X** and t. The bold face letters represent vector quantities. The corresponding scalar quantities are denoted by normal face letters. The capital letters will be used to denote the quantities in material coordinates and the corresponding quantities in spatial coordinates will be denoted by lower case letters. This method of notation is employed throughout this thesis.

It is assumed that a unique inverse of [1] exists, which is expressed as

$$\mathbf{X} = \mathbf{X}(\mathbf{x}, t) \ . \qquad [2]$$

Equation [1] describes the spatial position of a typical material point as a function of time, and equation [2] describes material points occupying a specific spatial location at different instances in time.

Central to the kinematic theory of continuums are the concepts of initial undeformed state and the deformed state, the assumption of

non–penetrability of matter, and the continuity assumption. The material points in a continuum are identified by their spatial position in the initial undeformed state

$$\mathbf{X} = \mathbf{x}(\mathbf{x}, 0) \ . \qquad [3]$$

Equation [3] is the mathematical statement that material point **X** is the part of the continuum occupying spatial position **x** in the initial undeformed state. Equations [1] and [2] describe the motion of those material points through space during deformation. The assumption of non–penetrability of matter states that at any given moment each material point occupies a unique point in space and no two material points may occupy the same spatial position at the same time. An alternative statement of this assumption is the equivalence of material and spatial points (Gandar, 1983a). This assumption is satisfied by the unique inverse relation between equations [1] and [2]. The continuity assumption requires that the neighboring material particles remain being neighbors during deformation. The equivalent mathematical statements of this assumption are:

$$\lim_{\delta \mathbf{X} \to 0} \left[\mathbf{x}(\mathbf{X}+\delta\mathbf{X}, \ t) \ - \ \mathbf{x}(\mathbf{X}, \ t) \right] \ = \ 0 \qquad [4]$$

and

$$\lim_{\delta \mathbf{x} \to 0} \left[\mathbf{X}(\mathbf{x}+\delta\mathbf{x}, \ t) \ - \ \mathbf{X}(\mathbf{x}, \ t) \right] \ = \ 0 \ . \qquad [5]$$

The displacement of material particles away from their position in the initial undeformed state is expressed as a displacement vector, $\mathbf{U}(\mathbf{X},t)$ and $\mathbf{u}(\mathbf{x},t)$, in the material and spatial coordinate systems respectively,

$$\mathbf{u}(\mathbf{X},t) \ = \ \mathbf{x}(\mathbf{X},t) \ - \ \mathbf{x}(\mathbf{X},0) \qquad [6]$$

and

$$U(\mathbf{x},t) = X(\mathbf{x},t) - X(\mathbf{x},0) \quad . \qquad [7]$$

Silk and Erickson (1979) and Gandar (1983a,b) presented detailed discussions of these aspects of the continuum mechanics theory and their applications in plant growth studies.

Plant growth as deformation of a continuum

According to the continuum assumption, a plant tissue is regarded as a mathematical continuum which is composed of material points distributed continuously in space. The growth of the plant tissue or the deformation of a continuum is described as the physical motion of these material points through space (Silk and Erickson, 1979; Gandar, 1983a).

The continuum theory, when applied to plant growth, is concerned essentially with the macroscopic properties of the plant tissue. In describing these properties, we may disregard the fact that a plant tissue must be regarded as discrete on the cellular scale. In attempting to explain these properties, however, it may be necessary to take into account the cellular structure of the plant tissue. In light of these arguments, it is desirable that the material points of any continuum theory of plant growth correspond to the underlying cellular structure of the plant tissue. For simplicity, our discussions will focus on plant roots.

The concept of an "infinitesimal material point" is central to the continuum theory and some clarification is needed before further discussion. First, continuum theory is a macroscopic theory. It deals with the macroscopic behavior of a plant tissue which is the manifestation of the average behavior of the individual cells. A material point in the continuum theory is defined as an identifiable elementary volume of the

plant tissue consisting of large quantities of cells so that its properties represent the mean of these cells. Yet, it must be small enough on an macroscopic scale to be considered "infinitesimal", and to have uniform material properties. The correspondence between material points and the cellular structure of the plant tissue requires an identifiable material point to represent the same group of cells throughout the process of growth. Because of this close correspondence, the terms "material point" and "cells" are interchangeable in the discussions that follow.

A conceptual growth process of a plant root is illustrated in figure 1.1. It is assumed that the cells, or material points, are produced in a meristem located at the tip of the root. Cell extension occurs after a cell is produced by the meristem and continues until it reaches maturity. Axial growth of the root is characterized by the cell production at the meristem and the subsequent cell elongation.

In Figure 1.1, at time t=0, cell 1 is produced at the root tip. As time progresses, $t=t_1$, cell 2 is produced at the tip and, at the same time, cell 1 has elongated. Thus, the root growth is initiated. Growth is maintained by continuous production of new cells at the meristem and the extension of the existing cells. In continuum mechanics terms, as $\delta t=t_2-t_1=t_3-t_2\cdots$ approaches zero, each of the "cells" in figure 1.1 will represent an infinitesimal material point which corresponds to a specific group of cells. It is worth noticing that both the spatial position and the relative distance between any two cells varies as growth progresses. To identify material points by their spatial position or their position relative to other material points, such as the root tip (Gandar, 1983a), it is necessary to completely describe the growth pattern of the root.

Applicability of the conventional continuum concept to plant roots

A number of questions are raised about the applicability of the continuum theory outlined in the previous section to the process of root growth because of the inability of the theory to account for the difference between cell division and elongation in plant roots. In the following discussion we examine the applicability of the concept of initial undeformed state, the assumption of material and spatial point equivalence and the assumption of continuity as defined in the previous section.

Each of the cells in a growing plant root may be at a different stage of development and deformation. At any given moment, there are cells at the whole spectrum of states ranging from newly–produced to maturity. There are cells that have just begun elongation, cells that are undergoing rapid elongation, and cells that have reached maturity. A specific time may be defined appropriately as the initial state for one group of cells but not for others. The concept of initial undeformed state must be applied to individual cells or material points. The concept of the initial undeformed state thus is not applicable to the plant root as a whole.

A basic assumption of the continuum theory is the one–to–one correspondence between material and spatial points, or the assumption of material and spatial point equivalence (Gandar, 1983a). In terms of plant root growth, the applicability of this assumption is subject to debate. The spatial position of a particular material point could only be defined unambiguously after it is produced by the meristem. In light of the root growth process illustrated in Figure 1.1, there is no easy way of defining the spatial positions of cells 2 and 3 at time 0. If we regard the

material points corresponding to specific cells in the root as having the same spatial position as the meristem, i.e., the root apex, before they are produced, the assumption of material and spatial point equivalence fails since cells 2 and 3 would have occupied the same spatial position at time 0. One may argue that the material points in the continuum theory may not correspond to the cellular structure of the plant root (McCoy and Boersma, 1984). They could be represented by the identifiable points on the surface of the root, such as those points identified in streak photography (Erickson and Sax, 1956a; Sharp et al., 1988). However, this would make it difficult to examine the continuum theory against the results of cellular growth studies because the material points of the continuum theory would not correspond to the underlying cellular structure of the root. Another consequence of this lack of correspondence between the material points and the cellular structure is the possibility of infinite elongation of a given root segment. To illustrate this point, examine the root segment between a mark on the tip of the root and a mark at a finite distance from the root apex, such as the base of the root. The elongation of this segment is regarded as a continuous deformation process. Since a root is capable of continuous growth, a material segment so defined must be capable of infinite deformation. But it is known that plant cells only grow to a finite size. It is concluded from these arguments that the material and spatial points equivalence assumption must be modified for the plant root in order to account for the effects of cell division in the meristem and the fact that cells grow to finite sizes.

The continuity assumption of the conventional continuum theory

also needs examination in terms of its applicability to plant growth. As discussed in the previous section, this assumption requires that neighboring material points remain being neighbors during deformation. If we require that the material points in a plant tissue correspond to the underlying cellular structure, then the neighboring materials may be separated during growth as a result of cell division. Fortunately, this situation is avoided in the case of plant root growth, since cell division occurs in the meristem located at the tip of the root.

Kinematic theory of plant root elongation

The previous discussions indicate that the kinematic theory of continuum mechanics is not appropriate for describing the axial growth of plant roots. Modifications of the theory are required in order to take into account both the effects of cell division and cell elongation.

The time at which a material point is produced by the meristem in a plant root increases monotonically from t_0, when the root growth starts, at the base of the root to the present time, t, at the meristem. Thus each material point along the root axis is related to a unique time, t', at which it was produced by cell division in the meristem. Instead of its spatial position in an undefinable initial undeformed state of the root, a material point can be identified by its unique time of production, t'. The initial undeformed state can then be defined for each material point individually as the state it was in when it was first produced by the meristem. The spatial position of a material point is defined only after its production.

Under these conditions, equation [1] is modified for a plant root as:

$$x = x[X(t'),\ t]\ ,\qquad t'\leq t\ . \tag{8}$$

The condition of non–penetrability of matter is stated for a plant root as: any moment, $t\geq t'$, an arbitrary material point $X(t')$ occupies a unique spatial position, and no two material points $X(t'_1)$ and $X(t'_2)$, $t'_1\neq t'_2$, may occupy the same spatial position at times $t\geq\max(t'_1,t'_2)$. These statements are equivalent to stating that a unique inverse of [10] exists so that

$$X(t') = X(x,\ t)\ ,\qquad t'\leq t, \tag{9}$$

The continuity condition, as stated in equations [4] and [5] for a general continuum, are similarly modified. For axial plant root growth, the continuity condition requires that

$$\lim_{\delta t'\to 0}\Big[x[X(t'),t] - x[X(t'-\delta t'),\ t]\Big] = 0,\ t'\leq t \tag{10}$$

and

$$\lim_{\delta t'\to 0}\Big[X(x,t) - X(x-\delta x,t)\Big] = 0,\ t'\leq t\ . \tag{11}$$

Equations [10] and [11] are the mathematical statements of the fact that neighboring material points which were produced next to one another must occupy neighboring spatial locations throughout the growth process.

Under these conditions, the initial undeformed state is defined for each individual material point as the state it was in at the moment when it was produced by the meristem instead of defining an arbitrary initial state for the whole root. This method of identifying the material points also enables us to consider the growth of each individual cell along the root axis as a function of its own experience in terms of water stress and carbohydrate availability, as well as age. This will allow the axial

growth process of plant roots to be modeled more realistically than would be possible using the conventional continuum mechanics theory.

We further assume that the relations defined by equations [8] and [9] are smooth and differentiable over their range of definition. The following quantities are defined under this assumption

$$\Lambda'(t',t) = \lim_{\delta t' \to 0} \left[\frac{x[X(t'),t] - x[X(t'-\delta t'),t]}{\delta t'} \right], \quad t' \leq t, \ \delta t > 0 \qquad [12]$$

and

$$\aleph(t') = \Lambda'(t',t') \ . \qquad [13]$$

Since a material point, $X(t')$, is at the initial undeformed state at $t=t'$,

$$x[X(t'),t'] - x[X(t'-\delta t'),t'] = X(t') - X(t'-\delta t') \qquad [14]$$

at the limit as $\delta t'$ approaches zero. Combining equations [12] and [14] we define

$$\frac{dX(t')}{dt'} = \aleph(t') \ . \qquad [15]$$

Elongation of the elementary root element produced at time t' is defined as the ratio between its length at time t and its initial length

$$\Lambda(t',t) = \frac{dx[X(t'),t]}{dX(t')} = \frac{\Lambda'(t',t)}{\aleph(t')} \ , \ t' \leq t \ . \qquad [16]$$

The quantity $\aleph(t')$ is viewed as the rate of root production (mm/hr) at the meristem at time t', and $\Lambda'(t',t)$ is the current length of the material segment produced between t' and t'+dt'. After a group of cells are produced at time t', they begin elongation. because the material points correspond closely to the cellular structure of the root, $\Lambda(t',t)$ is equal to the ratio between the current length of the cells and their

initial length.

$\aleph(t')$, the rate of root production at the meristem, depends on the biological activity of the meristem cells, the carbohydrate availability in the meristem, and the environmental conditions such as temperature and water stress. The elongation of the cells is described by the function $\Lambda(t-t')$. In general terms, $\Lambda(t-t')$ is a function of temperature, carbohydrate availability, physical properties of the cell walls, soil water potential, and soil resistance to root penetration.

The general requirements for the function $\Lambda(t',t)$ are

$$\Lambda(t',t') = 1 \qquad [17]$$

and

$$\Lambda_{inf} = \lim_{t'\to\infty} \Lambda(t',t) < \infty \ . \qquad [18]$$

Equation [17] is the mathematical statement of the fact that the elongation of cells in a plant root starts at their initial lengths. Equation [18] states the fact that plant cells only grow to finite sizes.

The Henky strain measure used in describing deformation of plastic materials can be used to describe the finite deformation of a plant tissue. The local strain, or local deformation, is written for one–dimensional plant root elongation as:

$$\exists(t',t) = \ln[\Lambda(t',t)] \ , \qquad [19]$$

where $\exists$ is the local longitudinal strain in the material coordinate system. The rate of deformation, expressed as the time rate of strain, is given by

$$\dot{\exists}(t',t) = \frac{\partial \exists(t',t)}{\partial t} = \frac{1}{\Lambda(t',t)} \frac{\partial \Lambda(t',t)}{\partial t} \ . \qquad [20]$$

Alternative terms for the strain rate defined in equation [20] are the local elementary rate of elongation (Erickson and Sax, 1956b; Gandar, 1983a),

or local relative rate of elongation (Sharp et al., 1988).

The growth pattern of a root is specified by the meristematic production function, $\aleph(t')$, and the cell elongation function, $\Lambda(t',t)$. Both material and spatial coordinate systems are be defined so that the origin is located at the base of the root and the positive direction is toward the tip of the root. Under these definitions, the spatial position of any material point is calculated as

$$x[X(t'),t] = \int_0^{t'} \aleph(g)\Lambda(g,t)dg \ . \qquad [21]$$

Equation [21] is the mathematical statement that the distance of a material point from the origin at any time equals the total length of all the material preceding it. The velocity at which a material point travels is the time derivitive of its spacial position

$$v[X(t'),t] = \frac{dx[X(t'),t)]}{dt} = \int_0^{t'} \aleph(g)\frac{\partial\Lambda(g,t)}{\partial t}\, dg \ . \qquad [22]$$

The total length and the total rate of root elongation at any moment are described by the spatial position and the velocity of the root tip, respectively, as:

$$L(t) = \int_0^{t} \aleph(g)\Lambda(g,t)dg \qquad [23]$$

and

$$v(t) = \int_0^{t} \aleph(g)\frac{\partial\Lambda(g,t)}{\partial t}\, dg + \aleph(t) \ . \qquad [24]$$

Equations [21]–[24] describe the growth of a plant root as a function of time. From these equations, quantities including the local rate of elongation, the age of root elements at various positions along the root axis, and the process of cell extension as a function of time can all be

calculated. One particular application of these equations results from the fact that the material points so defined closely correspond to the cellular structure of the root. Therefore, it is possible to calculate the growth pattern of a root as a continuum by examining the cellular structure of the root. This aspect of the theory is discussed in detail. A second application of these equations is to examine the effect of altered rate of cell division which are represented by changes in the rate of root element production at the meristem on the root tip as a result of changing environmental conditions.

Steady state root growth

It is reasonable to assume that the rate of root production in the meristem remains constant under steady state conditions, i.e., $\aleph(t)=\aleph$. Equation [24] can then be written as:

$$\mathbf{v}(t) = \aleph\int_0^t \frac{\partial\Lambda(g,t)}{\partial t}\, dg + \aleph \ . \qquad [25]$$

Under steady state conditions, there is no reason to believe that the elongation process of the cells produced at different times would be different since all cells would be under the same constant environmental conditions. It may therefore be assumed that $\Lambda(t',t)$ of an arbitrary material point is a function of its age only, so that

$$\Lambda(t',t) = \Lambda(t-t'), \quad t\geq t' \ . \qquad [26]$$

Substituting equations [26] and [17] into equation [25] yields

$$\mathbf{v}(t) = \aleph\cdot\Lambda(t), \ t\geq 0 \ . \qquad [27]$$

As time progresses, $\Lambda(t)$ approaches Λ_{inf} so that

$$\mathbf{v} = \aleph\cdot\Lambda_{inf} \quad \text{for large } t, \qquad [28]$$

where v is the constant, steady state root elongation rate. These arguments show that under constant environmental conditions, constant, steady state root elongation is achieved only at sufficiently large t when the elongation of the cells produced at the beginning of the root growth has stopped. The rate of root elongation before this time is transient, even under constant environmental conditions, starting at $v=\aleph$ at t=0 and approaches $v=\aleph\Lambda_{inf}$ at large t.

Steady state root growth is characterized by constant cellular structure as a function of distance from the root tip (Erickson and Sax, 1956a,b). Cell size and local rate of elongation depend only on the distance from root apex. Consider an arbitrary point along the root axis which is at a fixed distance from the root tip. As the root grows, older cells at that point are continuously displaced away from the root tip and replaced by arriving younger cells. However, the cell size, age, and rate of elongation will remain the same at that point during steady state root growth. The root growth described by equations [25]–[28] satisfies these requirements. To illustrate this, consider the distance between cells with age a=t–t' and the root tip. Under steady state conditions, this is given by

$$d(a) = \int_{t-a}^{t} \aleph \cdot \Lambda(t-t')dt' \quad . \qquad [29]$$

where d is distance from root tip. Equation [29] can be written in terms of cell age as:

$$d(a) = \int_{0}^{a} \aleph \cdot \Lambda(a')da' \quad , \qquad [30]$$

which is independent of time and hence satisfies steady state conditions.

APPLICATIONS

The theory outlined in the previous section provides a mathematical framework with which the longitudinal growth of a plant root can be described. Erickson and Sax (1956a,b) reported measurements of the rate of root elongation, average cell length and local rate of extension along the root axis of a corn root during steady state growth. Sharp et al. (1988) measured the steady state elongation process of the primary root of maize growing in vermiculite at various water potentials. Pahlavanian and Silk (1988) reported measurements of temperature effects on the elongation of maize primary root. In the following discussion, the theory outlined in the previous section is applied to these experimental observations and the validity of the theory is examined.

Steady state root elongation

The relative cell length as a function of distance from the root tip for a corn root during steady state growth is plotted in figure 1.2 using data reported by Erickson and Sax (1956a). The Y–axis is the relative cell length calculated as the average cell length along the root axis divided by the average cell length in the meristem. This quantity corresponds to the local material elongation, Λ defined in equation [16]. In calculating Λ, it is assumed that because this is steady state growth, the initial length of all cells is the same and equals the cell length in the meristem. The meristem is assumed to be located at 1 mm from the tip of the root because it corresponds to the point of minimum cell length and maximum rate of cell division (Erickson and Sax, 1956a,b).

The top 1 mm of the root was regarded as the root cap and was not included in the following calculations. Cells are at their initial length at the meristem, so that Λ is equal to 1 at 1 mm from the root tip where the meristem is assumed to be located. The length of the cells increases with increasing distance from the meristem as a result of cell elongation. At a distance of about 8 mm from the root tip, the cell length reaches a constant value as the cell reach matures.

Λ_{inf} is the ratio between the length of mature cells and their initial length. Figure 2 suggests that 13.0 is a reasonable estimate of Λ_{inf}. The total rate of root elongation under steady state conditions reported by Erickson and Sax (1956a) was 1.75 mm/hr. Substituting these two values into equation [28] results in the steady state root production rate by the meristem as $\aleph$=0.135 mm/hr. According to the theory outlined in the previous section, the process of axial root growth is characterized by $\aleph$ and Λ. With Λ as a function of distance from root tip given in figure 1.2 and the $\aleph$ calculated above, the steady state growth process of the root is specified. Other quantities related to root growth, such as age of the cells and the rate of displacement along the root axis are calculated from $\aleph$ and Λ. The agreement between the quantities calculated and direct experimental measurements illustrates the applicability of the kinematic theory of longitudinal root growth developed in the previous section.

Figure 1.2 shows the function $\Lambda(d)$ where d is the distance from root root tip. The discussions of theories in the previous section defined Λ under steady state conditions as a function of cell age (equation [26]). Therefore Λ is calculated as a function of the age of cells. To do this,

we express Λ as a function of cell age as:

$$\Lambda(a) = \Lambda[d(a)] \ , \qquad [31]$$

where d is distance from meristem. The function $d(a)$ for steady state root growth is given by equation [30]. Substituting equation [31] into equation [30] and differentiating with respect to a produces

$$\frac{\mathrm{d}}{\mathrm{d}a} \ d = \aleph\Lambda(d) \ . \qquad [32]$$

Equation [32] is integrated subject to the boundary condition

$$d(0) = 0 \ . \qquad [33]$$

The d, distance from the meristem, as a function of a, the age of cells, calculated from equations [32] and [33] using the $\Lambda(d)$ function shown in figure 1.2 is plotted in figure 1.3. In addition figure 1.3 illustrates the results calculated from streak photography measurements by Erickson and Sax (1956b). Figure 1.3 shows that there is good agreement between the predicted and the measured values. The discrepancy near the root tip is a result of the fact that active cell division occurs over the range from 1 to 2 mm from the root tip, not at a single point as was assumed in the theoretical analysis. However, the validity of the calculation of cell age from measurements such as streak photography is also questionable because of the distributed nature of cell division. Despite the small discrepancy, we conclude that the calculations based on our theoretical analysis agree with the streak photography measurements.

The total local material extension, Λ, as a function of cell age is calculated by combining the functions shown in figures 1.2 and 1.3 using equation [31]. The results are illustrated in figure 1.4. These curves reveal that the rate of extension of a cell accelerates with time over a period of approximately 11 hours. As the cell approaches the maximum size, the

rate of extension quickly decreases to zero.

The axial growth of a plant root is usually expressed as the rate of displacement of a material point away from the root tip as a function of distance from the root apex (Erickson and Sax, 1956a,b; List, 1969; Sharp et al. 1988). This is the rate at which the distance between the root apex and a material point located at d from the root tip increases with time. As d increases, this rate of displacement approaches the rate of total axial root elongation. The rate of displacement between a material point and the root tip under steady state conditions is expressed as:

$$\frac{d}{dt}d[X(t'),t] = \int_{t'}^{t} \aleph \frac{d\Lambda(t-t')}{dt}dt' = \aleph\Lambda(t-t') \quad . \qquad [34]$$

The results of equation [34] are plotted in figure 1.5 along with the results obtained from steak photography measurements (Erickson and Sax, 1956a). The calculation agrees well with the results of the measurements except for a small discrepancy near the root tip.

Effect of water stress on steady state root elongation

Root production in the meristem, $\aleph$, and the strain rate, $\dot{\exists}$, defined by equations [13] and [20] correspond to the local growth rates in the meristem and in the elongation region. It is reasonable to assume that under steady state conditions, a constant water stress reduces $\aleph$ and $\dot{\exists}$ by

$$\aleph_{\Psi} = \beta(\Psi)\cdot\aleph_0 \qquad [35]$$

and

$$\dot{\exists}_{\Psi}(t-t') = \alpha(\Psi)\cdot\dot{\exists}_0(t-t') \quad , \qquad [36]$$

where $\beta(\Psi)\leq 1$ and $\alpha(\Psi)\leq 1$ are functions of soil water potential, $\aleph_0$ and $\dot{\exists}_0$ represent the rate of meristem production and the rate of strain at the reference level of soil water potential. Substituting equation [36] into equation [19] results in

$$\Lambda_\Psi(t',t) = [\Lambda_0(t-t')]^\alpha \ . \qquad [37]$$

Sharp et al. (1988) observed that cessation of longitudinal growth occurred in tissue of approximately the same age regardless of spatial location or water status which is reflected in equation [36]. The strain rate, $\dot{\exists}$, of a material point, under steady state conditions, is a function of its age. When the longitudinal growth of a group of cells stops at a certain age, represented by $\dot{\exists}=0$, equation [36] indicates that it would stop at the same age for all soil water potentials. The rate of displacement away from the root tip as a function of distance from the root apex is calculated by substituting equations [35] and [36] into equation [34]. Results of that calculation are shown in figure 1.6. The curve marked "unstressed" is the same as the curve shown in figure 1.5. It is plotted here as a basis of comparison. The low stress curve in figure 1.6 was calculated assuming that water stress results in a 10% reduction in both the meristem production and cell strain rate, whereby $\alpha=\beta=0.9$. The high stress curve was calculated assuming $\alpha=\beta=0.8$. These values were chosen so that the reductions in total root elongation rates approximately correspond to those reported by Sharp et al. (1988) (figure 1.7). A mild 10% reduction in $\aleph$ and $\dot{\exists}$ results in a 30% reduction in the rate of steady state root elongation, and a 20% reduction in $\aleph$ and $\dot{\exists}$ may result in a 52% reduction in root elongation rate. This results from the

combined effects of lower cell elongation rate and a shorter elongation region, as is shown in figure 1.6. The relationship between reduction of cell production–elongation and the reduction in total root elongation rate is plotted in figure 1.8.

Sharp et al. (1988) measured the response of longitudinal growth of maize primary roots to water stress. The response curves reported by these authors are reproduced in figure 1.8, showing exactly the same trend as illustrated in figure 1.6. The analysis of response of longitudinal root growth to water stress based on direct observation of the longitudinal displacement rate curves, such as those shown in figure 1.6, can be misleading. By observing the response of the rate of longitudinal displacement along the root axis to water stress (similar to the curves shown in figure 1.6), Sharp et al. (1988) concluded that the inhibition of root elongation at low water potentials was not explained by a constant decrease in growth along the length of the elongation zone. The longitudinal expansion was insensitive to water stress in the early ontogenetic phase of growth but was increasingly inhibited as cells were displaced away from the root apex. However, our analysis reveals that cell division and expansion are similarly inhibited throughout the elongation region of the root axis, as suggested by constant α and β values used in generating the curves in figure 1.6. The fact that the rates of longitudinal displacement under different water stress conditions are non–distinguishable near the root apex is the combined result of the manner in which root elongation and cell expansion is related and the way the data were presented, rather than the evidence that the cells along the root axis are affected differently by water stress.

Effect of temperature on steady state root elongation

Pahlavanian and Silk (1988) observed that for the primary root of maize, the length of the elongation region was independent of temperature. In the following discussions, we will demonstrate that this is equivalent to stating that an increase in temperature increases the rate of biological processes in the root so that a shorter time is required to produce the same amount of growth, provided other conditions remain the same. In other words, this is stated as the temperature–time equivalence.

Assuming that cells in a plant root reach their final length after a_f hours, a_f being a function of temperature, the total length of the elongation region under steady state conditions is calculated by applying equation [30] as:

$$L_e = \aleph(T)\int_0^{a_f} \Lambda(a',T)da' \quad , \qquad [38]$$

where L_e is the length of the elongation region, a' is the age of the cells, and T is the temperature. In equation [38], $\aleph$ and Λ are explicitly expressed as functions of temperature. We are interested in finding out the manner in which $\aleph$, Λ, and a_f vary with temperature so that the total length of the elongation zone would be independent of temperature as was observed by Pahlavanian and Silk (1988).

First, we define an arbitrary reference temperature T_o. The ratio between the length of the elongation region at temperature T and T_o is

$$\frac{L_e(T)}{L_e(T_o)} = \frac{\aleph(T)}{\aleph(T_o)} \frac{\int_0^{a_f(T)} \Lambda(a',T)da'}{\int_0^{a_f(T_o)} \Lambda(a',T_o)da'} \quad . \qquad [39]$$

Letting

$$\frac{\aleph(T)}{\aleph(T_o)} = \alpha(T) \ , \qquad [40]$$

the requirement that the length of the elongation region be independent of temperature dictates that

$$\frac{\int_0^{a_f(T)} \Lambda(a',T)\,da'}{\int_0^{a_f(T_o)} \Lambda(a',T_o)\,da'} = \frac{1}{\alpha(T)} \ . \qquad [41]$$

It can be shown that for an arbitrary function, $\Lambda(a, T)$, equation [41] is true under the conditions

$$\Lambda(a,T) = \Lambda[\alpha(T)a \ ,T_o] \qquad [42]$$

and

$$a_f(T) = \frac{a_f(T_o)}{\alpha(T)} \ . \qquad [43]$$

Equations [42] and [43] are the mathematical statement of the temperature–time equivalence concept with respect to plant root elongation. Figure 1.9 illustrates the rate of displacement of a material point away from the root apex as a function of distance from the root tip at three arbitrary temperatures. The curve marked T_o, which is used as a reference, and is the same as the "unstressed" curve in figure 1.6, was calculated from the data reported by Erickson and Sax (1956a,b). The curves marked T_1 and T_2 were calculated using arbitrary values of $\alpha(T_1) = 0.8$ and $\alpha(T_2) = 0.6$, respectively.

The rate of total longitudinal root elongation, shown as the rate of displacement of the mature region away from the root apex in figure 1.9, is reduced by exactly the same proportion as $\alpha(T_1)$ and $\alpha(T_2)$, thus differing from the effect of water stress where the reduction in the rate of total longitudinal root elongation was significantly higher than the

reduction in the rate of cell extension.

Pahlavanian and Silk (1988) measured the response of longitudinal growth of maize primary root to temperature over the range from 16 to 29°C. Their results are reproduced in figure 1.10. The agreement between figures 1.9 and 1.10 suggests that the theoretical analysis outlined in this work is valid. To further illustrate this, the distance of a material point from the root apex as a function of time was calculated using equation [30], with the same $\alpha(T)$ values that were used in producing figure 1.9. Theresults are plotted in figure 1.11. During root elongation, a material point initially located at the meristem was displaced away from the root tip as new cells were produced and then elongated. This rate of displacement evetually reaches a constant value which is equal to the rate of root elongation as it reaches the mature region of the root. A longer time is required at lower temperature (T2) for a cell to reach a given distance from the meristem. figure 1.12 shows the $\Lambda(a,T)$ function for the three arbitrary temperatures. It illustrates that lower temperature (T2) slowed cell elongation. However, elongation of the cells would only stop after reaching a certain length regardless of the temperature. figures 1.13 and 1.14 are experimentally measured curves corresponding to figures 1.11 and 1.12, respectively (reproduced from Pahlavanian and Silk, 1988).

The principle of temperature–time equivalence has been widely applied in the studies of viscoelastic materials (Haughton and Sellen, 1969; Sellen, 1980) where temperature was used to control the rate of the physical stress relaxation process. Measurements at different temperatures are combined applying the principle of temperature–time equivalence to obtain the kinetic behavior of the process over a wide span of time. The

principle of temperature–time equivalence is imbedded implicitly in such concepts as "degree–days" and Q_{10} in plant growth and development studies. Because plant cell expansion is biologically controlled viscoelastic expansion of the cell walls, it is not suprising to find that the principle applies to the longitudinal root expansion as well.

The temperature–time equivalence coefficient, $\alpha(T)$, represents the response of the rate of plant root elongation to temperature. Because plant root elongation is the result of a combination of complex physical and biological processes, $\alpha(T)$ as a function of temperature reflects the response of the slowest, or the control process. Assuming that the rate of this control process as a function of temperature is described by the Arrhenius equation, at least over the temperature range below the optimum temperature, we can write

$$\alpha(T) = \alpha_0 e^{-\frac{E_a}{RT}}, \qquad [44]$$

where α_0 is a constant, E_a is the activation energy, R is the universal gas constant, and t is temperature. The $\alpha(T)$ values for the primary root of maize, calculated from the data presented in figure 1.13 are listed in table 1. Twenty nine degree was used as the reference temperature in these calculations since it represents the highest elongation rate in the measurements by Pahlavanian and Silk (1988). A least square fitting of the $\alpha(T)$ values in table 1 to equation [46] results in an activation energy E_a = 50±3 kJ/mol. This value is well within the range for the activation energy of most biochemical reactions (Dixon, 1964). The activation energy for the physical extension of plant cell walls is 100–200 kJ/mol (Sellen, 1980). This result suggests that cell elongation during root

growth is controlled by biochemical processes (Cleland, 1987). In other words, extension of cell walls during cell expansion is controlled by biochemical reactions, not by the physical properties of the cell walls.

CONCLUSION

The kinematic theory of conventional continuum mechanics is inappropriate in describing the axial growth of plant roots as a one–dimensional continuous process due to its inability to account for differences between cell division and cell extension. A kinematic theory for plant root growth that accounts for both cell division in the meristem and the subsequent cell extension is proposed. Two functions were introduced: $\aleph(t')$ which describes cell division in the meristem and $\Lambda(t',t)$ which describes cell extension. There is good agreement between the theoretical calculations and the experimental measurements of corn root growth.

The kinematic theory developed in this study could serve as the basis of continuum theory of plant root growth, similar to the role of conventional kinematic theory in continuum mechanics. Root growth models could be developed by combining the kinematic theory of root growth developed in this study and the models of meristem activity, $\aleph$, and cell extension, Λ. The close correspondence between the material coordinate system and the cellular structure of the plant roots makes it possible to combine the information derived from cell growth studies and the continuum theory for a better understanding of the process of plant root elongation and its response to environmental conditions.

Table 1. The temperature–time equivalence coefficient, $\alpha(T)$, calculated from data by Pahlavanian and Silk (1988). The reference temperature was chosen as 29 C.

Temp. ($^{\circ}$C)	16	19	24	29
$\alpha(T)$	0.389	0.558	0.677	1.000

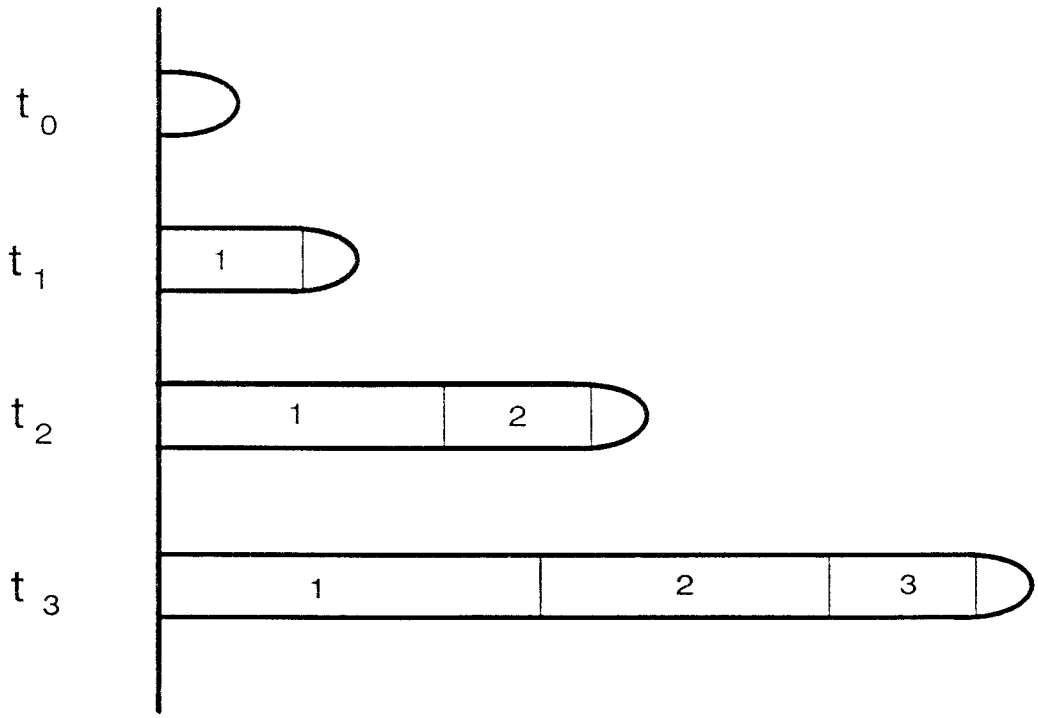

Figure 1.1. Conceptual process of plant root elongation. Cells are produced by the meristem located at the root tip. Cell extension follows cell production. Root elongation is the result of cell production and subsequent cell extension.

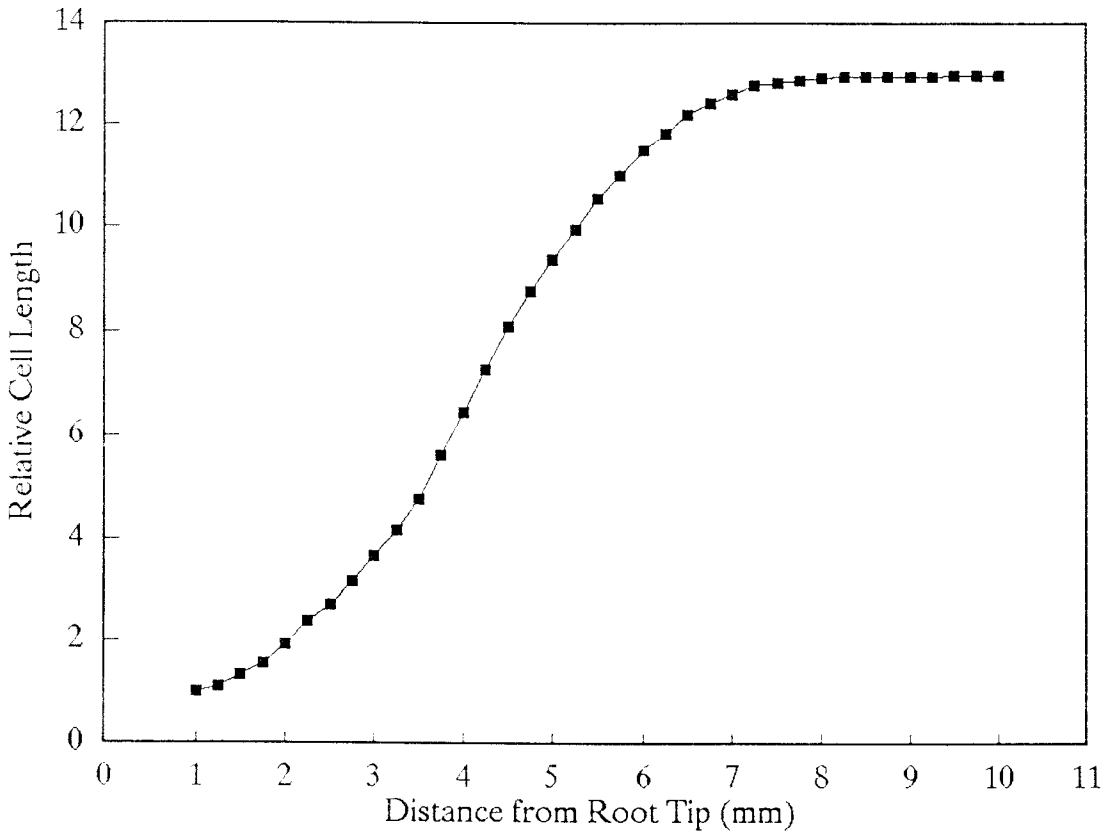

Figure 1.2. Relative cell length of a primary maize root calculated as the cell length along the root axis divided by cell length in the meristem, as a function of distance from root tip. This equals the total cell elongation from their initial length when the cells were produced by the meristem. (Calculated from data of Erickson and Sax, 1956b).

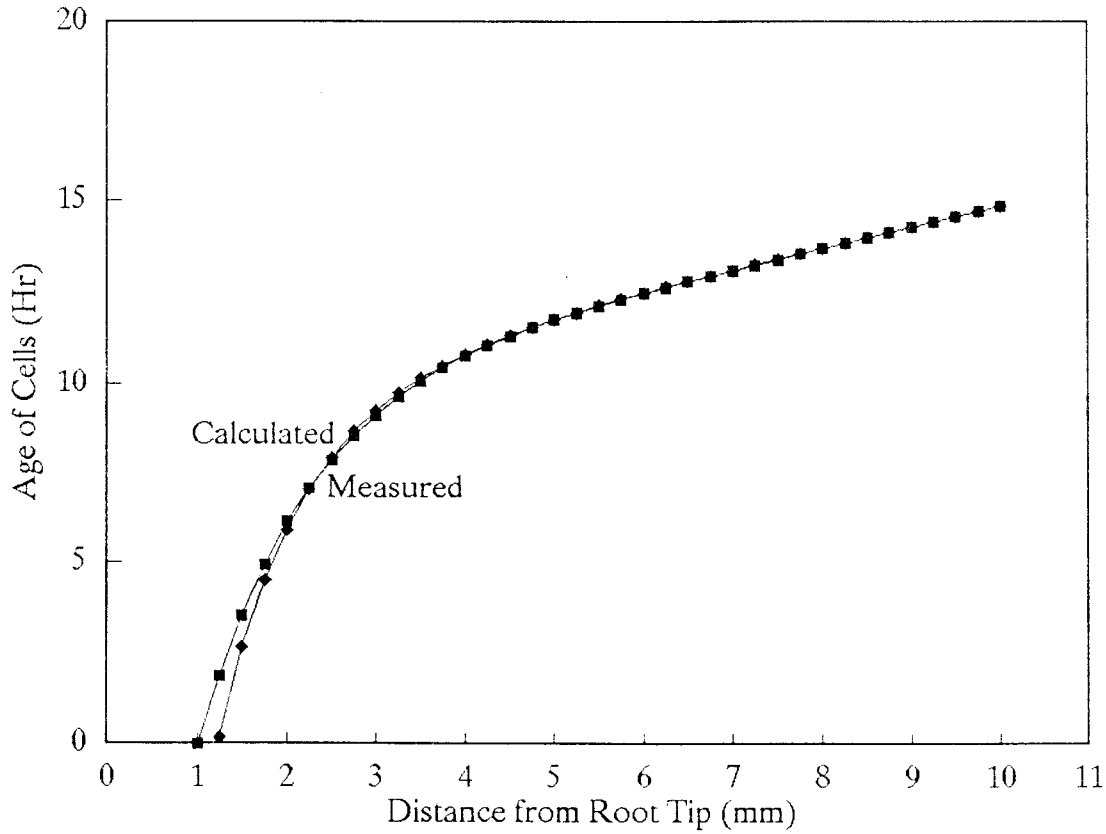

Figure 1.3. Age of the cells of a primary maize root as a function of distance from root tip. The "Calculated" curve was obtained from the kinematic theory and the "Measured" curve was obtained from streak photography measurements by Erickson and Sax (1956b).

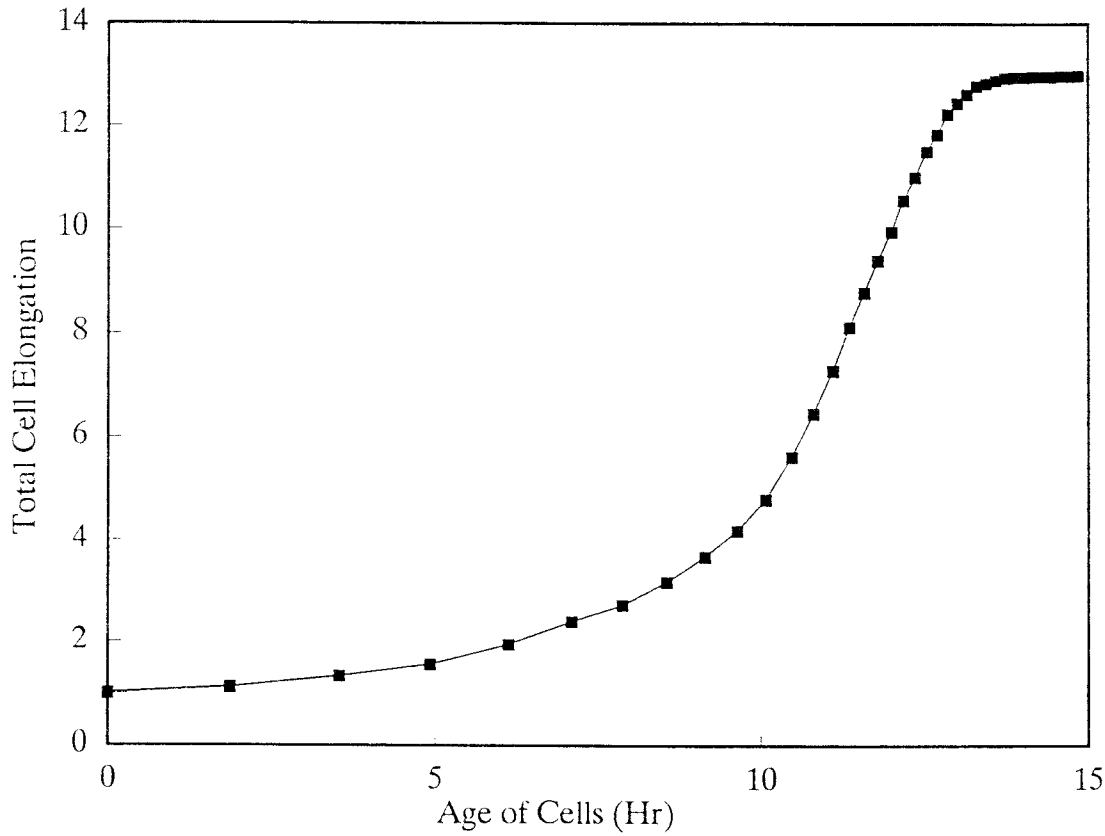

Figure 1.4. Relative cell length as a function of cell age. The relative cell length was calculated as current cell length divided by initial cell length. This quantity indicates the total amount that the cells have elongated after being produced by the meristem.

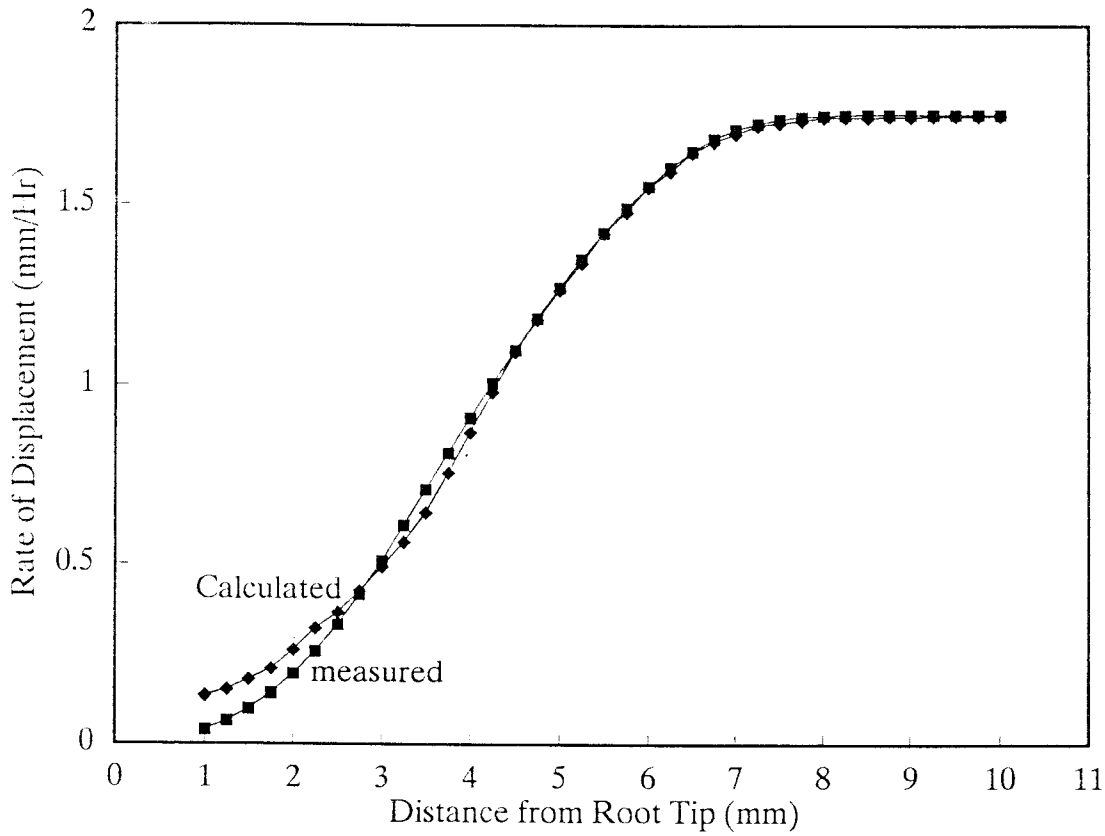

Figure 1.5. Rate of displacement away from the root tip of a material point along the root axis as a function of distance from the root apex. The "Calculated" curve was derived from the kinematic theory and the "Measured" curve was obtained from streak photography measurements by Erickson and Sax (1956b).

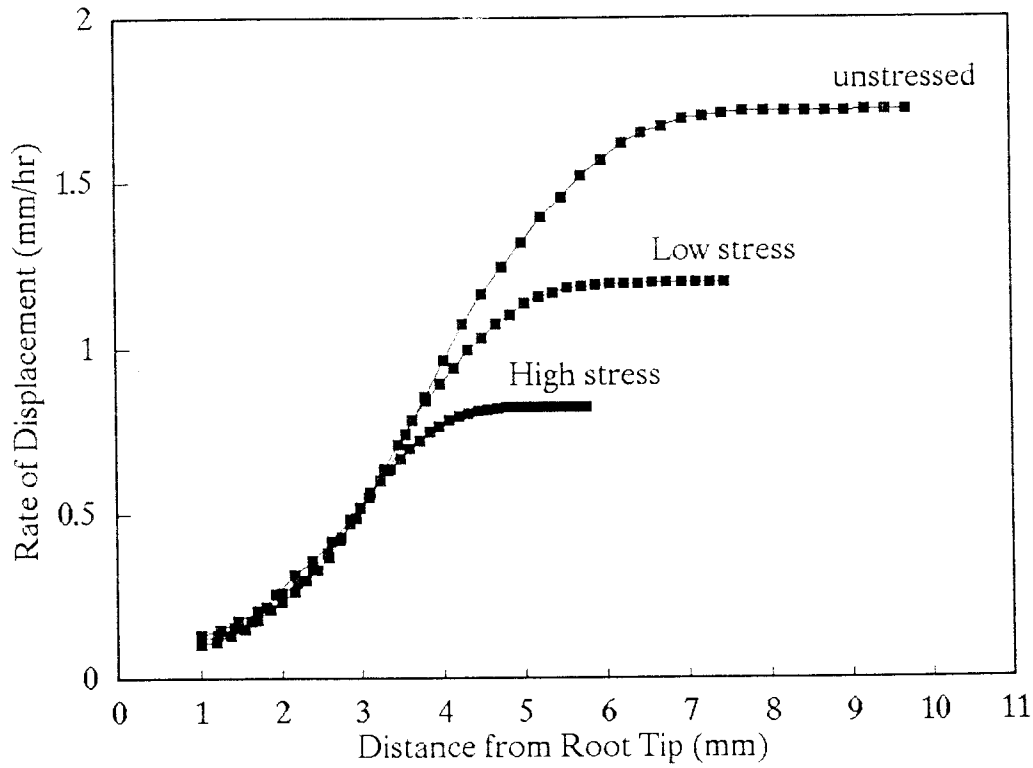

Figure 1.6. Calculated rate of displacement away from root tip of material points along the root axis under different water stress conditions. The assumption for the calculations was that under steady state conditions water stress reduces the rate of cell extension and production by a constant proportion.

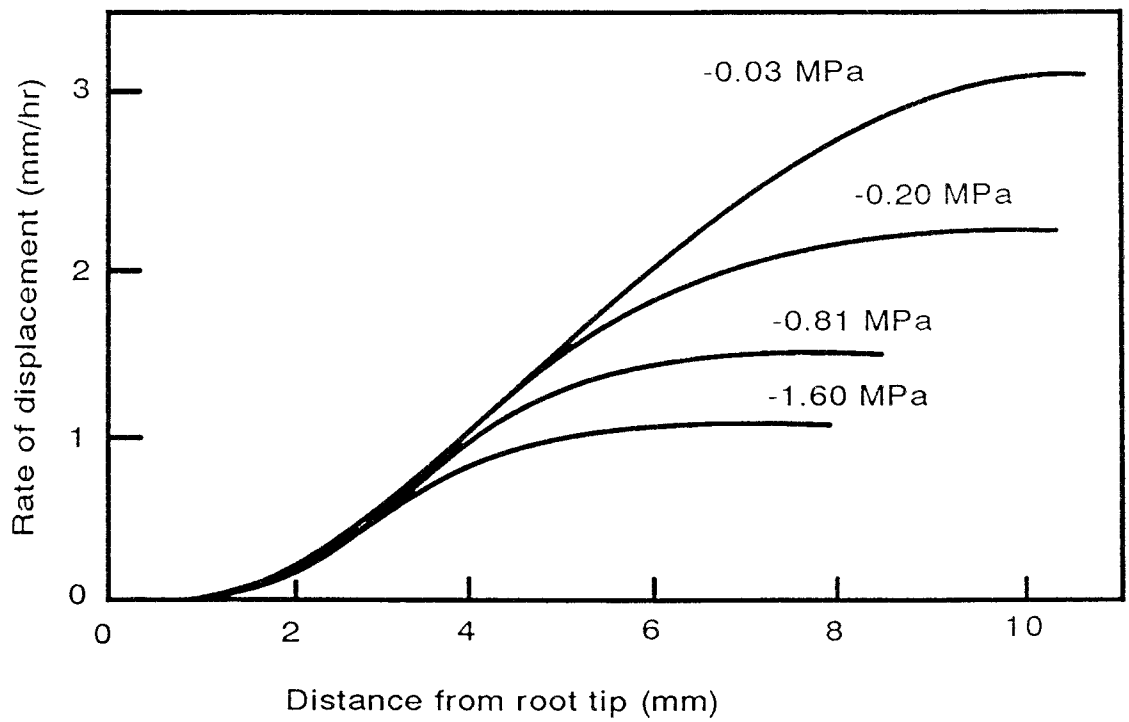

Figure 1.7. Measured rate of displacement away from the root tip of material points along the root axis under different soil water potentials (redrawn after Sharp et. al., 1988).

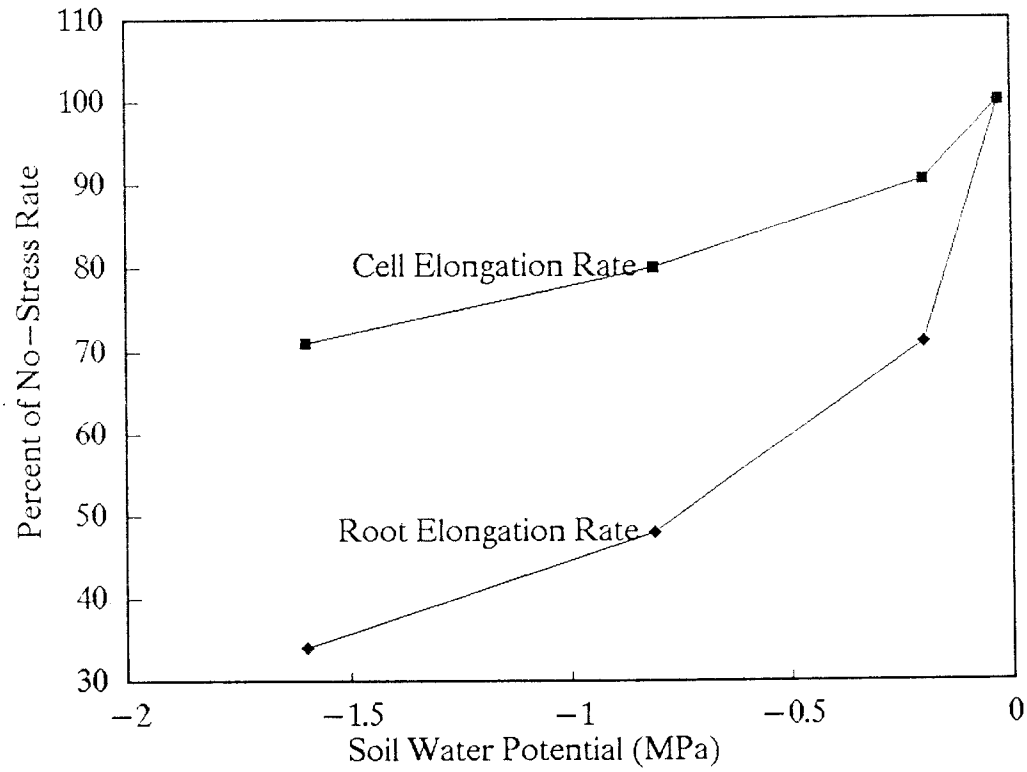

Figure 1.8. Cell extension rate and root elongation rate as functions of soil water potential. The root elongation rates were adopted from data by Sharp et al. (1988). Cell elongation rates at different soil water potentials were calculated using the kinematic theory so that the same reductions in total root elongation relative to the no–stress condition as those measured by Sharp et al. (1988) were obtained.

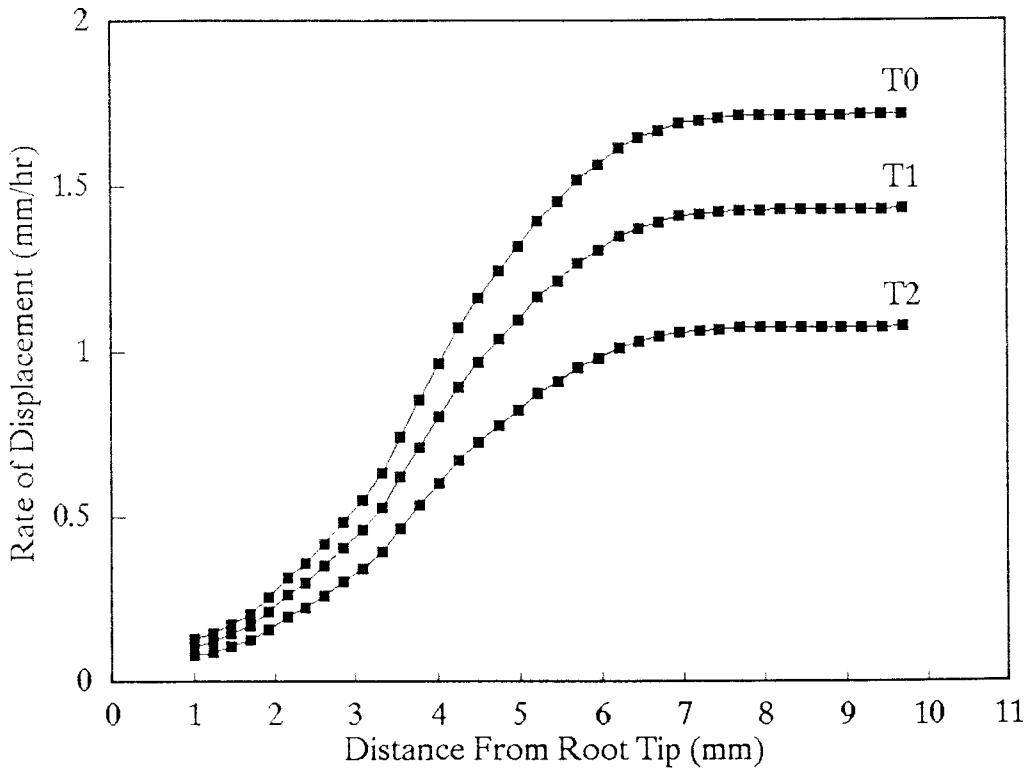

Figure 1.9. Predicted effect of temperature on the rate of displacement away from the root tip of material points along the root axis. Curves at different temperatures were calculated using the principle of temperature–time equivalence.

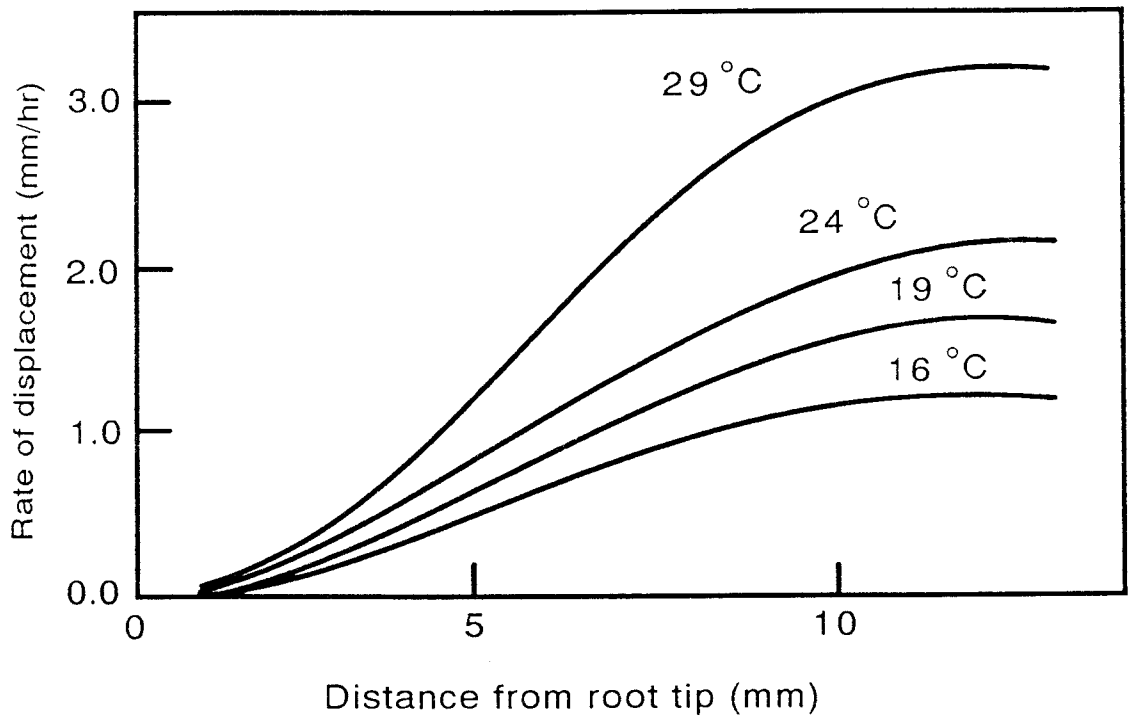

Figure 1.10. Measured rate of displacement away from the root tip of material points along the root axis under different temperatures (redrawn after Pahlavanian and Silk, 1988).

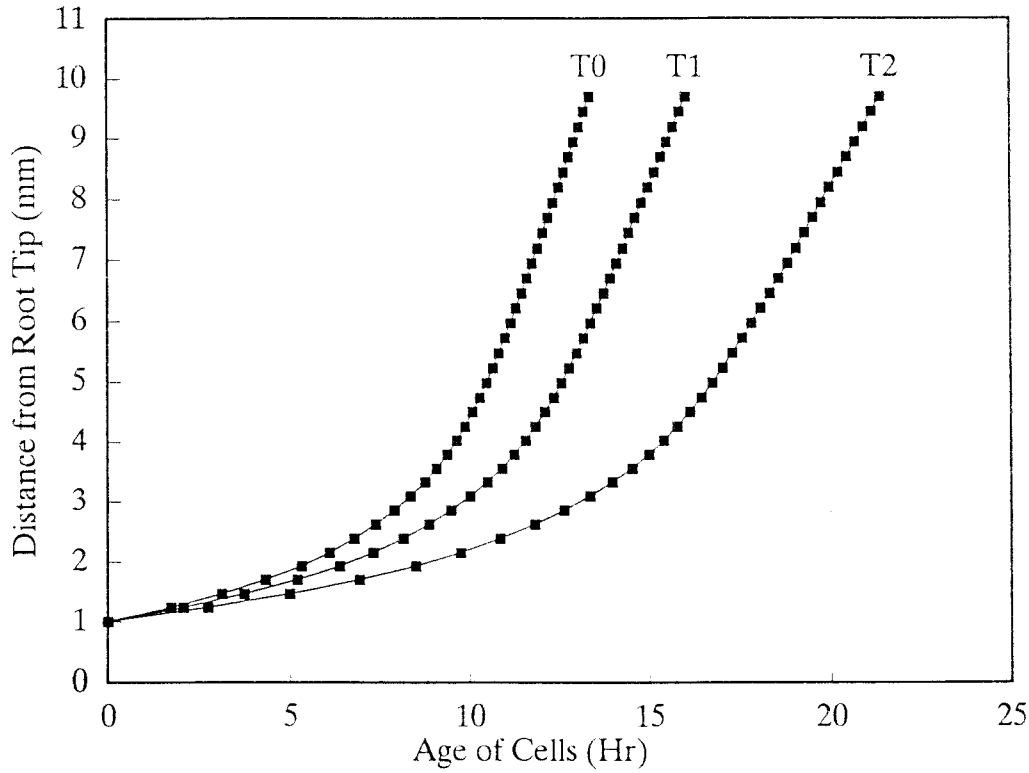

Figure 1.11. Predicted distance of material points from the root apex as a function of age at different temperatures.

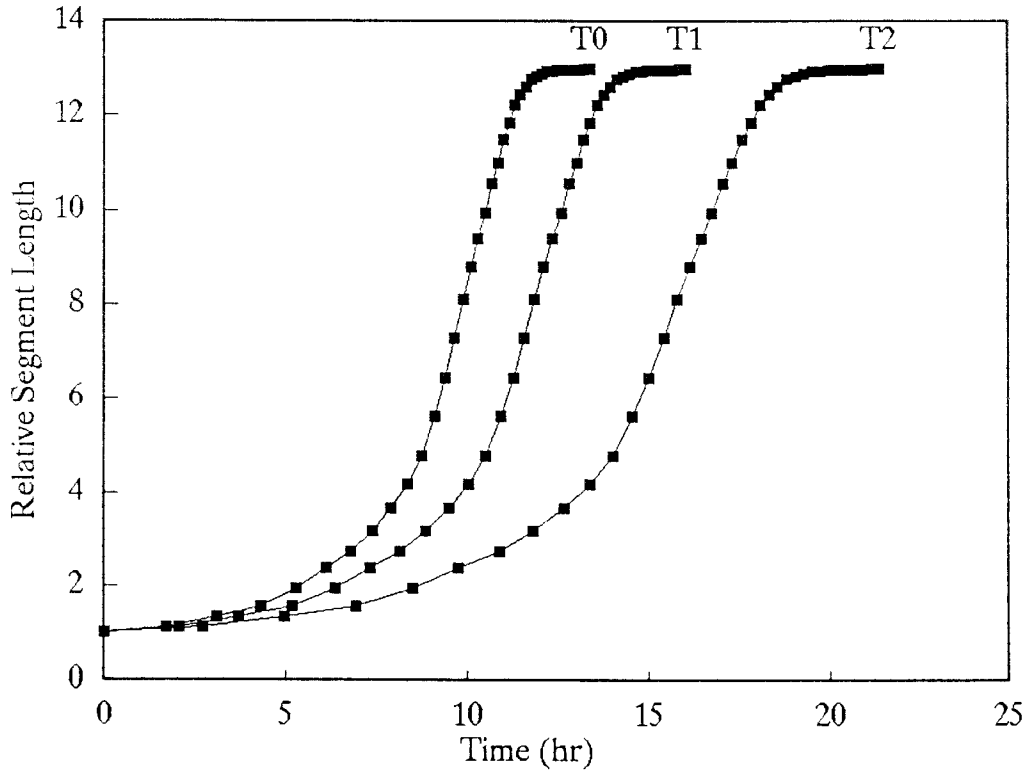

Figure 1.12. Predicted relative cell length as a function of cell age at different temperatures.

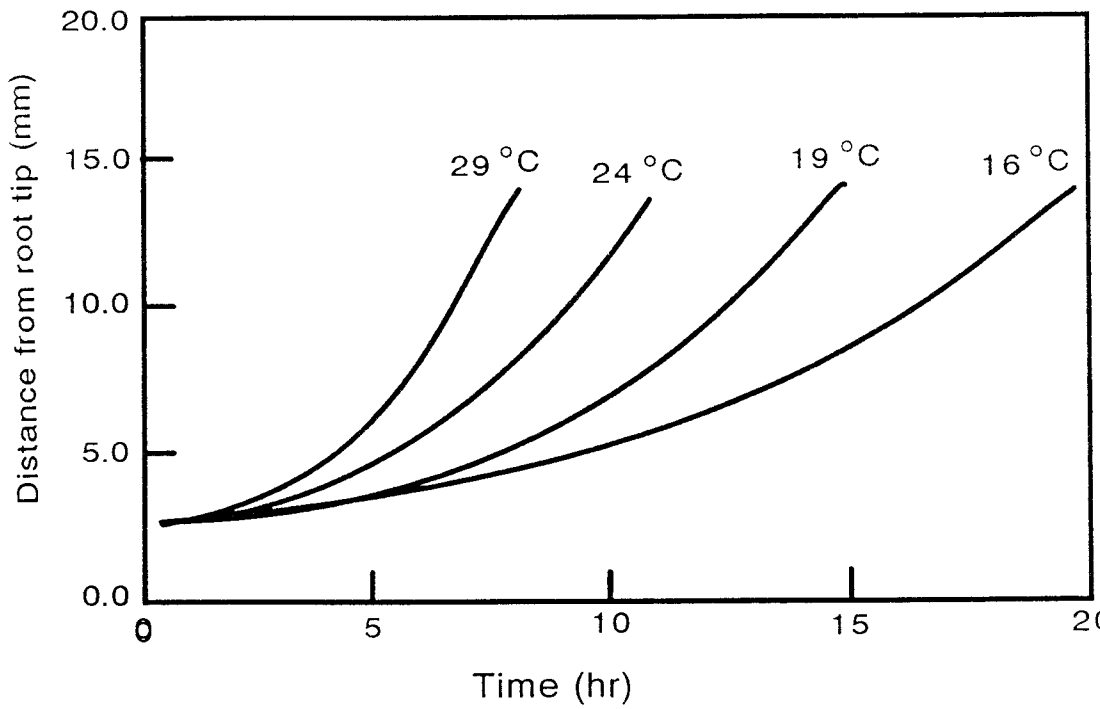

Figure 1.13. Measured distance of a material point from the root tip as a function of age at different temperatures (redrawn after Pahlavanian and Silk, 1988).

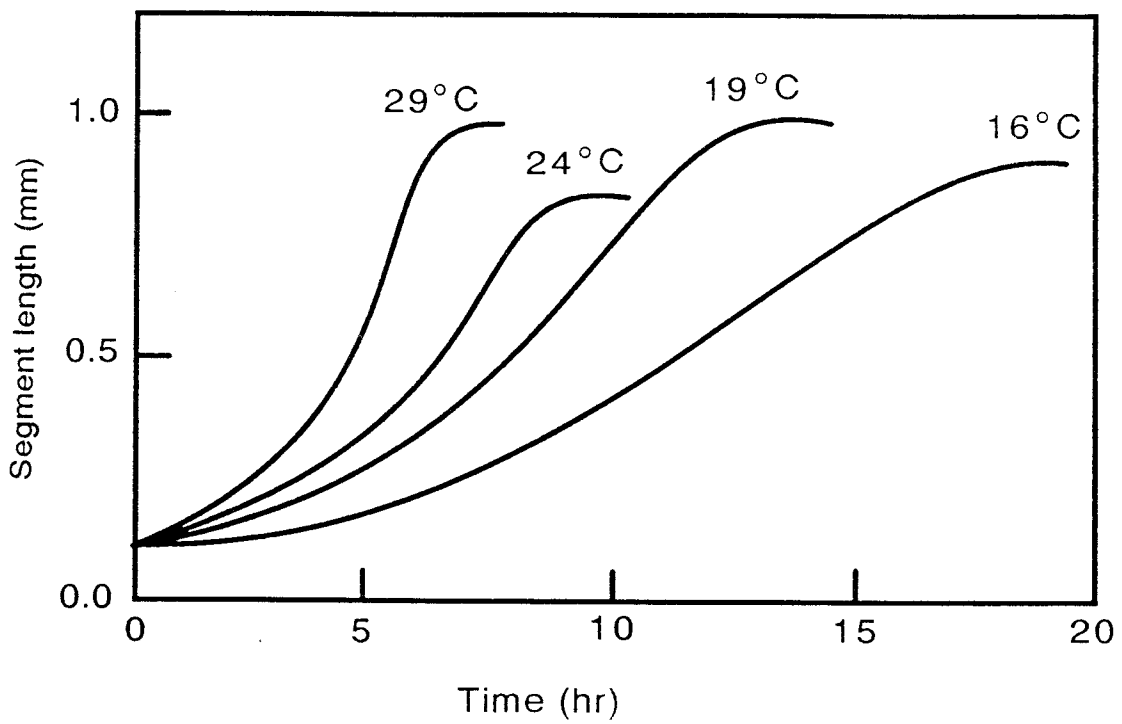

Figure 1.14. Measured length of a segment between two marks on the root surface as a function of time. The increase in the length of the segment results from cell elongation. The segment was initially located between 2.5 and 2.6 mm from the root tip (redrawn after Pahlavanian and Silk, 1988).

LIST OF SYMBOLS AND UNITS

t	current time	s
t'	past time	s
t_o	starting time	s
v	rate of displacement	m s^{-1}
x	spatial coordinate	m
E_a	activation energy	J mol^{-1}
L	total root length	m
L_e	length of elongation region	m
R	universal gas constant	J mol^{-1} K^{-1}
T	temperature	^oK
T_o	reference temperature	^oK
X	material coordinate	m
a	age of cells	s
a_f	age of cells when reaching maturity	s
d	distance from root tip	m
$\alpha(\Psi)$	reduction of $\dot{\epsilon}$ by water stress	dimensionless
$\alpha(T)$	temperature–time equivalence factor	dimensionless
α_o	value of $\alpha(T)$ under zero activation energy	dimensionless
ϵ	elemental strain or deformation	dimensionless
$\dot{\epsilon}$	rate of strain or deformation	s^{-1}
$\dot{\epsilon}_\Psi$	$\dot{\epsilon}$ under water stress	s^{-1}
$\dot{\epsilon}_o$	$\dot{\epsilon}$ under reference conditions	s^{-1}
$\aleph(t')$	rate of meristem production at t'	m s^{-1}

$\aleph_\Psi$	$\aleph$ under water stress	m s^{-1}
$\aleph_o$	$\aleph$ under reference conditions	m s^{-1}
$\Lambda(t',t)$	current length divided by initial length of cells produced at t'	dimensionless
Λ_Ψ	Λ under water stress	dimensionless
Λ_o	Λ under reference conditions	dimensionless
Λ_{inf}	maximum value of Λ at maturity	dimensionless

LITERATURE CITED

Cleland, R. E., 1987. The mechanisms of wall loosening and wall extension. *In* D. J. Cosgrove and D. P. Knievel (ed.) Physiology of cell expansion during plant growth. Am. Soc. Plant Physiol., Penn. State Univ., pp18–27.

Dixon, M., and E. L. Webb, 1964. Enzyme. Longmans, London. 1116pp.

Erickson, R. O., 1976. Modeling of plant growth. Ann. Rev. Plant Physiol., 27:407–434.

Erickson, R. O., and K. B. Sax. 1956a. Elemental growth rates of the primary root of *Zea mays*. Proc. Am. phil. Soc., 100:487–497.

Erickson, R. O., and K. B. Sax. 1956b. Elemental growth rates of the primary root of *Zea mays*. Proc. Am. Phil. Soc., 100:499–513.

Gandar, P. W., 1980. The analysis of growth and cell production in root apices. Bot. Gaz., 141:131–138.

Gandar, P. W., 1983a. Growth in root apices. I. Kinematic description of growth. Bot. Gaz., 144:1–10.

Gandar, P. W., 1983b. Growth in root apices. II. Deformation and rate of deformation. Bot. Gaz., 144:11–19.

Goodwin, R. H., and W. Stepka, 1945. Growth and differentiation in the root tip of *Phleum pralense*. Am. J. Bot., 32:36–46..

Greecen, E. L., and J. S. Oh, 1972. Physics of root growth. Nature, New Biol., 235:24–25.

Green, P. B., 1976. Growth and cell pattern formation on an axis. Critique of concepts, terminology, and modes of study. Bot. Gaz., 137:187–202.

Haughton, P. M., and D. B. Sellen, 1969. Dynamic mechanical properties of the cell walls of some green algae. J. Exp. Bot., 20:516–535.

Hejnowicz, Z., 1982. Vector and scalar fields in modeling of growth response in plants to changes in external water potential: *Zea mays* primary root. J. Theor. Biol., 96:161–173.

Kirkham, M. B., W. R. Gardner, and G. C. Gerloff, 1972. Regulation of cell division and cell enlargement by turgor pressure. Plant Physiol., 49:961–962.

List, A. Jr., 1969. Transient growth responses of the primary roots of *Zea mays*. Planta, 87:1–19.

McCoy, E. L., and L. Boersma, 1984. The principles of continuum mechanics applied to transport processes and deformation in plant tissue. J. Theor. Biol., 111:687–705.

Meyer, R. F., and J. S. Boyer, 1972. Sensitivity of cell division and cell elongation to low water potentials in soybean hypocotyls. Planta, 108:77–87.

Pahlavanian, A. M., and W. K. Silk, 1988. Effect of temperature on spatial and temporal aspects of growth in the primary Maize root. Plant Physiol., 87:529–532.

Plant, R. E., 1982. A continuum model for root growth. J. Theor. Biol., 98:45–59.

Salamon, P. A., A. List and P. S. Grenetz, 1973. Mathematical analysis of plant growth. *Zea mays* primary roots. Plant Physiol., 51:653–640.

Sellen, D. B., 1980. The mechanical properties of plant cell walls. *In* The mechanical properties of biological materials. Symp. Soc. Exp.

Biol. 34:315–329. Cambridge univ. Press, Cambridge.

Sharp, R. E., W. K. Silk, and T. C. Hsiao, 1988. Growth of the Maize primary root at low water potentials. I. Spatial distribution of expansive growth. Plant Physiol., 87:50–57.

Silk, W. K., and R. O. Erickson. 1978a. Kinematics of hypocotyl curvature. Am. J. Bot., 65:310–319.

Silk, W. K., and R. O. Erickson. 1978b. Kinematics of plant growth. J. Theor. Biol., 76:481–501.

Silk, W. K., and R. O. Erickson, 1980. Local biosynthesis rates of cytoplasmic constituents in growing tissue. J. Theor. Biol., 83:701–703.

Taiz, L., 1984. Plant cell expansion: Regulation of cell wall mechanical properties. Ann. Rev. Plant Physiol., 35:585–657.

2. THE CONSTITUTIVE RELATIONS OF PLANT ROOT ELONGATION

Yongsheng Feng and Larry Boersma
Department of Soil Science, Oregon State University,
Corvallis, OR 97331

ABSTRACT

Growth of plant cells, defined as increase in volume, is the result of expansion of cell walls. It is well–established that the growth of plant cells depends on the physical stress in cell walls. The rate of growth at a given cell wall stress is a function of the physical properties of cell walls. It has been suggested that cell growth is controlled by the metabolic process of the cell. The growth of plant cells is perceived as biologically controlled creeping. The mechanism of this biological control, and the interactions between the physical properties of the cell walls and the biological processes, however, is not clear.

The goal of this study is to develop a mathematical theory of plant cell growth that includes mathematical representations of the control by the metabolic control of cell growth as part of the theory. The plant cell walls were modeled as simple viscoelastic materials. The stress relaxation process of plant cell walls was studied from the perspective of work–energy relations. When plant cell walls are under stress, chemical bonds in the cell wall polymers are strained. Two general classes of the chemical bonds are recognized: the weak cross–link bonds, mainly

hydrogen bonds, that undergo spontaneous break and reform processes to release strain energy, and the strong bonds, mainly covalent bonds, that do not undergo these processes. The physical stress relaxation process was characterized by a first order relaxation process of the strain energy stored in the weak cross–link bonds (the viscoelastic strain energy). It is postulated that the metabolic processes of the cell control growth by controlling the strain energy relaxation process. Unlike the physical stress relaxation process, the biological process of cell wall loosening releases strain energy in both classes of chemical bonds in the cell wall polymers. The biological process of wall loosening works only when the cell walls are under mechanical stress. When cell walls are not stressed, the chemical bonds in the cell walls are not strained. As a result, there is no strain energy to be released. Permanent growth cannot occur in the absence of biological wall loosening process, therefore, both physical stress in the cell wall and the biological wall loosening process are necessary for cell growth.

An equation was developed for describing the rate of cell growth as a function of physical properties of the cell wall and the biological cell wall loosening process. The rate of cell growth depends not only on the current value of the mechanical stress in the cell wall, but also on its recent stress history. In other words, the cell growth depends in part on conditions that existed in the near past in addition to current conditions. The duration of this memory depends on both the physical properties of the cell walls and the rate of physiological wall loosening. The equation reduces to Lockhart's equation under steady state conditions. However, there is one important difference. The cell wall extensibility, previously

defined as the physical property of the cell wall in the Lockhart equation, is expressed in the proposed equation as a function of both the physical properties of the cell wall and the metabolic activity of the cell.

The equation derived in this study describes the dynamic processes of cell growth. It provides a specific definition of the previously poorly–defined term "cell wall extensibility". The derivations in this work assume that the rate of the physiological cell wall loosening process is constant. The more general case where the metabolic rate of the cell varies with time due to changing environmental conditions can be derived following the same principles, as is demonstrated in Chapter 5 of this thesis.

INTRODUCTION

All materials deform under applied force. The constitutive relation describes the relationship between the force (stress) and the deformation (strain). For example, Hook's law states that for an elastic solid, the deformation (strain) is directly proportional to the applied force (stress),

$$\epsilon = K \cdot \sigma \ . \qquad [1]$$

where σ is the stress (N m^{-2}), ϵ is the strain (dimensionless), and K is a proportionality constant (m^2 N^{-1}). The deformation is elastic if the material recovers to its original state upon removal of the imposed stress, and plastic if there is no recovery. Materials can be classified according to the type and time dependence of the deformation they undergo under imposed stress. For an elastic material, the deformation is instantaneous and proportional to the stress. For a viscous material, the deformation is not instantaneous but proceeds with time. The rate of deformation is proportional to the applied shear stress. Given sufficient time, any arbitrarily small shear stress applied to a viscous material can produce an infinitely large deformation. Most materials containing polymers of the length commonly found in plant cell walls behave neither as elastic nor as viscous materials. When a constant stress is applied to such a material, there is a small instantaneous deformation. The deformation continues as a function of time. In many cases, the deformation continues at a rate approximately proportional to the logarithm of time (Haughton and Sellen, 1969; Sellen, 1980). Materials with this behavior are referred to as viscoelastic materials (Ferry, 1970). The behavior of these three types of materials exposed to a constant external stress which was applied

at time t=0 is illustrated in figure 2.1.

Plant tissues consist of continuous networks of cell walls. The apoplast and symplast systems reside in these networks. Elongational growth is the process by which cell walls undergo continuous deformation. This deformation is the result of the combined action of physical stress and physiological wall loosening and wall synthesis (Cleland, 1971; Brummel and Hall, 1985; Cleland, 1987; Ray, 1987).

Lockhart (1965) proposed a mathematical model which describes the growth of plant cells as resulting from the viscoelastic deformation of plant cell walls under mechanical stress,

$$\dot{\epsilon} = m(\sigma - Y) \ , \qquad [2]$$

where $\dot{\epsilon}$ is strain rate, or the relative rate of deformation, σ is the physical stress in the cell wall often equated with turgor pressure, m is referred to as the extensibility of the cell wall, and Y is the minimum threshold that σ must exceed before deformation occurs. The extensibility and the yield stress were considered to be the physical properties of the cell walls (Lockhart, 1967). Other models based on the assumed analogy between plant cell and some simple mechanical systems have also been proposed (Green et al., 1971; Hettiaratchi and O'Callaghan, 1974; Ortega, 1985). However, the Lockhart equation continues to be the most popular model for describing the biophysical aspects of plant growth (Cleland, 1971; Taiz, 1984; Cosgrove, 1986; Cleland, 1987; Ray, 1987).

Extensive researches have been conducted to further the understanding about the biophysical natures of m and Y. Research has revealed important differences between the mechanical behavior of *in vivo* and *in vitro* cell walls (Haughton and Sellen, 1969; Green et al., 1971;

Sellen, 1980; Cosgrove, 1985). Under constant mechanical stress, the growth, or deformation of *in vivo* plant cells was found to be a linear function of time (Green et al., 1971) while the deformation of *in vitro* plant cell walls was often found to be a linear function of the logarithm of time (Haughton and Sellen, 1969; Sellen, 1980). The total amount of deformation, or strain, obtainable under a given mechanical stress is often small in *in vitro* plant cell walls while a living plant cell could grow to ten times or more of its initial size, far beyond what could be obtained in *in vitro* cell walls. Another important difference between the behavior of *in vitro* and *in vivo* cell walls is the temperature response. The physical deformation of *in vitro* plant cell walls has Q_{10} values of approximately 1.1 while the growth of living cells often have Q_{10} values of 2 or greater (Cleland, 1987). Cleland (1971), Taiz (1984) and Cosgrove (1986) offer more detailed discussions.

Green et al. (1971) studied the response of growth of *Nitella* cells to the dynamic changes of turgor pressure. They suggested that both m and Y may be under metabolic control of the cell. Abdul–Baki and Ray (1971) reported that the onset of rapid cell elongation in pea stem tissues coincided with the increased rate of incorporation of exogenous sugars into the cell wall hemicellulose. Pritchard et al. (1988) reported that excision of the root apex decreased cell extensibility. Van Volkenburgh and Cleland (1981) demonstrated that the onset of light increased the rate of leaf expansion by increasing cell wall extensibility. It has also been found that sustained growth depends on the incorporation of new matrix cell wall components into the cell wall (Brummel and Hall, 1985; Morris and Arthur, 1985). These evidences strongly argue that the growth of plant

cells is under metabolic control of the cell. However, the mechanism of this control is not clear.

It has been hypothesized that the deformation of the cell walls during growth is controlled by a process of cell wall loosening or cell wall softening (Taiz, 1984; Cleland, 1987; Ray, 1987). One theory proposes that cell growth consists of a series of events (Taiz, 1984; Ray, 1987). Initially the cell wall was hypothesized to be rigid. Then the wall softening, or wall loosening, process of the cell softens the cell wall through some unknown mechanism, resulting in a extensible cell wall. The softened cell wall extends in response to the physical stress. A wall hardening process fixes the deformation resulting in a rigid, irreversibly deformed cell wall. Erickson (1976) discussed the mathematical formalism of such a model.

Despite these advances, the mechanism of plant cell wall loosening is still uncertain (Ray, 1987). The matrix of plant cell walls consists of a network of cross–linked polymers (Lockhart, 1967; Fry, 1986). During irreversible viscoelastic deformation, the cross–linking bonds undergo a process of breakage and reformation (Ferry, 1970; Dorrington, 1980; Sellen, 1980). It is possible that the wall loosening process during cell growth is related to the breakage of the load bearing bonds in the cell wall (Ray, 1987).

A constitutive relation of plant cell elongation describes the growth or deformation of a plant tissue as a function of cell wall stress and the biological activities of the cells. Such a relation is essential in a dynamic, mechanistic model of plant growth. Our objective is to develop a mathematical description of the growth process of a plant tissue based on

the physical and chemical properties of the cell walls as well as the physiological processes of cell wall loosening. Based on the evidences presented in the research literature, there are three fundamental requirements which should be satisfied by such a relation:

1) the total strain obtainable under a finite stress in the absence of the biological wall loosening processes should be finite;

2) the stress–strain relation should exhibit viscoelastic behavior in the absence of biological wall loosening processes, i.e. for a constant force, there should be an instantaneous elastic deformation followed by a slow but continuous deformation approximately proportional to the logarithm of time for small t, and approaching an asymptotic value as t continues to increase; and

3) the total strain should be approximately proportional to time instead of to the logarithm of time in the presence of constant biological wall loosening processes.

THEORY

The behavior of a material under applied stress can be discussed from two perspectives. One is to start with the force–deformation relation of the material. This starting point is used in most of the discussions of the mechanical properties of cell walls (Lockhart, 1965; Lockhart, 1967; Green et al., 1971; Hettiaratchi and O'Callaghan, 1974; Dorrington, 1980; Cosgrove, 1985). The alternative approach is to discuss the material behavior from the perspective of work–energy relations. The latter approach is followed in this manuscript.

We will first derive a simple stress–strain relation for cell walls during physical deformation. A discussion of the energy relation of the deforming cell wall follows. The biological wall loosening event will be modeled as the process by which the strain energy in the wall is released through the biological activity of the cells.

Work is done to a material when it is deformed under applied stress. For an elastic material, all of the work done to the material during deformation is stored as elastic strain energy. This energy is recovered upon release of stress. During a viscous deformation, all the work done to the material is dissipated as heat during the deformation process, assuming kinetic energy to be negligible. For a viscoelastic material, part of the work is stored in the form of strain energy and part of the work is dissipated as heat. The ratio of amount stored to amount dissipated depends on the physical properties of the material as well as on the deformation process.

The behavior of viscoelastic materials is often illustrated by creep

tests and stress relaxation tests (Ferry, 1970; Sellen, 1980; Dorrington, 1980). In a creep test, a constant stress is applied to the material at the beginning; the resulting deformation, or strain, is monitored over time. The strain, as a function of time for a creep test, is illustrated in figure 2.2. For both viscoelastic liquids and viscoelastic solids, there is generally a small instantaneous elastic deformation in response to the applied stress. If the applied stress is constant, the deformation (strain) in the viscoelastic materials continuously increases with time. There is an important difference between viscoelastic solids and viscoelastic liquids: the strain in a viscoelastic solid approaches a maximum value, which is proportional to the constant applied stress, during a creep test. For a viscoelastic liquid, there is no maximum value for the strain. The strain increases continuously with time while the rate of strain approaches a constant value which is proportional to the applied stress. Thus, at large t, the behavior of viscoelastic solids approaches that of solids and the behavior of viscoelastic liquids approaches that of liquids, as suggested by their names (Ferry, 1970).

In a stress relaxation test, a constant strain is applied to a material at the beginning and the resulting stress is monitored over time. The stresses as functions of time for the two types of viscoelastic materials during a stress relaxation test are illustrated in figure 2.3. For a viscoelastic liquid, the stress gradually relaxes to zero as time progresses. For a viscoelastic solid, the stress relaxes only to a finite value.

From the energetic perspective, we can discuss the behavior of the two types of viscoelastic materials by analyzing the work performed on

the material in relation to the energy stored and dissipated. For a viscoelastic solid, the initial work at t=0 is the amount that is required to impose the initial instantaneous elastic strain. Under a constant stress, the work that is done on such a material approaches a maximum value when the strain approaches its maximum. In other words, when the rate of strain approaches zero. The energy dissipated through viscous friction and the energy stored in elastic strain all approach their asymptotic values. For a viscoelastic liquid, the work done and the energy dissipated continue to increase and the stored elastic strain energy remains finite.

In the molecular sense, the viscoelastic solid consists of polymers with extensive cross–links, while the viscoelastic liquid consists of polymers without such extensive cross–links (Ferry, 1970; Haughton and Sellen, 1980). Plant cell walls are made up of cross–linked polymers and are expected to behave as viscoelastic solids (Haughton and Sellen, 1980; Dorrington, 1980; Biggs and Fry, 1987; Fry, 1986). In terms of plant cell growth, it is argued that this is the only acceptable condition for which a finite cell size is maintained under positive turgor pressure. If the cell walls were to behave as viscoelastic liquids, as was implied in the growth equations of Lockhart (1965, 1967), plant cells would keep elongating as long as the physical stress in the walls exceeded their yielding value. In absence of cell wall synthesis, this could eventually lead to bursting of the cells. As a consequence of cell walls being cross–linked polymers, biological activities, such as wall loosening and synthesis, must be present in order for any significant cell elongation to take place.

The behavior of viscoelastic materials is often illustrated with spring–dashpot models (Ferry, 1970; Green et al., 1971; Dorrington, 1980).

A spring and a dashpot connected in series is usually referred to as a Maxwell element. A Voigot element consists of a spring and a dashpot in parallel. In these elements, the spring represents the elastic behavior and the dashpot represents the dissipative or viscous behavior of the material (figure 2.4). A real viscoelastic material can be modeled by a number of Maxwell elements connected in parallel or by several Voigot elements connected in series. The two representations are equivalent. In fact, it has been stated that (Ferry, 1970) "If a system can be represented by a mechanical model, then it can be represented by an infinite number of mechanical models." Any real material behavior can be produced by an increasing the number of elements.

Physical cell wall deformation

The following discussion of material behavior of cell walls is limited to the one–dimensional aspect where the deformation, or strain, is equal to the axial extension and the stress is equal to the axial force per unit cross–sectional area. In terms of plant root growth, the one–dimensional strain corresponds to the local axial elongation of the root.

Hook's law describes the relation between stress and strain of an elastic material as:

$$\epsilon = K\sigma \ , \qquad [1]$$

where ϵ is the axial strain (dimensionless), σ is the stress (N m^{-2}), and K is a proportionality constant (m^2 N^{-1}). The strain at any moment depends only on the value of stress at that particular instant and on the proportionality constant. The response of strain or deformation to stress is instantaneous.

It is appropriate at this point to discuss the physical meanings of "instantaneous" and "time dependent" strain–stress relations. In an absolute sense, all deformations are time–dependent since deformation involves motion of material elements relative to one another and all motions are time–dependent. However, often in elastic behavior the time required to produce the deformation is so small that it can be regarded as "instantaneous" without introducing any significant error. Conversly, the response of many viscoelastic materials to a given stress is so slow that significant error will be introduced by an "instantaneous" response approximation. In general, whether a material response to a given stress can be regarded as "instantaneous" depends on the process being considered as well as the material involved.

For a viscoelastic material, the strain at any moment depends not only on the current value of the stress but also on the past history of the stress, and *vice versa.* For a linear viscoelastic material, stress and strain are related as follows:

$$\sigma = \int_0^t G(t-t')\dot{\epsilon}(t')dt' \qquad [3a]$$

and

$$\epsilon = \int_0^t J(t-t')\dot{\sigma}(t')dt' \ , \qquad [3b]$$

where $\dot{\epsilon}$ and $\dot{\sigma}$ are the time derivatives of ϵ and σ respectively; G is called the stress relaxation modulus (N m^{-2}), J is called the creep compliance modulus (m^2 N^{-1}), t is the current time, and $t' \leq t$ is the past time. In a stress relaxation experiment where a constant strain ϵ_0 is applied at t=0, equation [2a] yields

$$\sigma = G(t)\epsilon_0 \ . \qquad [4]$$

For a creep experiment where an constant stress σ_0 is applied at t=0, equation [2b] becomes

$$\epsilon = J(t)\sigma_0 \ . \qquad [5]$$

The stress relaxation modulus and the creep compliance modulus are related through the equations

$$\int_0^t G(t-t')J(t') = t \qquad [6a]$$

and

$$\int_0^t G(t')J(t-t') = t \ . \qquad [6b]$$

The nature of the functions G and J depends on the characteristics of the material. The functions are often measured with stress relaxation and/or creep experiments using equations [4] and [5]. For a single Maxwell element, we see that

$$G = G_0 e^{-t/\tau} \qquad [7a]$$

and

$$J = J_0 + \frac{t}{\eta} \ , \qquad [7b]$$

where t is time, τ is the relaxation time coefficient, η (kg m^{-1} s^{-1}) is a viscosity term , and G_0 (N m^{-2}) and J_0 (m^2 N^{-1}) are constants. Equations [7a] and [7b] are related through equation [6]. For a Maxwell model consisting of n Maxwell elements in parallel, equation [7a] becomes

$$G = \sum_{i=1}^{n} G_i e^{-t/\tau_i} \ , \qquad [8]$$

where τ_i and G_i' are the parameters of the i–th element. The parameters τ_i and G_i's are referred to as the discrete relaxation spectra of the material. In theory, a real stress relaxation curve can be approximated to any degree of accuracy by adding more terms in equation [8]. In actual

practice, it is nearly impossible to resolve more than a few terms when analyzing experimental data. Furthermore, this approach is rarely used because of its limited theoretical value.

As the number of elements in a Maxwell model increases, the discrete relaxation spectra approach a continuous spectrum. The stress relaxation modulus becomes

$$G = G_e + \int_0^\infty H(\tau)e^{-t/\tau}d\tau \ . \qquad [9]$$

Equation [9] is the mathematical definition of the stress relaxation modulus.

In this study of plant cell elongation, the behavior of the cell wall matrix under physical stress is approximated with a single relaxation time. The stress relaxation function in equation [9] reduces to

$$G = G_e + G_v e^{-t/\tau} \ , \qquad [10]$$

and the corresponding creep compliance modulus is

$$J = J_e + J_v(1 - e^{-t/\gamma}) \ , \qquad [11]$$

where G_e (N m^{-2}) is Young's modulus at equilibrium, J_e (m^2 N^{-1}) is related to the instantaneous elastic response, G_v (N m^{-2}) and J_v (m^2 N^{-1}) are constants related to the viscous behavior of the material, and τ (s) and γ (s) are time constants for stress relaxation and creep respectively. These equations are the mathematical expressions of the simple spring and dashpot model illustrated in Figure 5. This model is used partly because it provides a solvable system when the constitutive relation derived from such a model is used in a comprehensive model of plant root growth. This simple model satisfies the first two general requirements stated in the introduction for a constitutive relation of cell

enlargement.

The stress relaxation modulus expressed in equation [10] and the creep compliance modulus expressed in equation [11] are related through equation [6]. Given any one of the two functions, the second can be completely determined. The constants in the two equations are related by

$$J_e = \frac{1}{G_e + G_o} , \qquad [12a]$$

$$J_v = J_e \frac{G_o}{G_e} , \qquad [12b]$$

and

$$\gamma = (1 + \frac{G_o}{G_e})\tau . \qquad [12c]$$

Substituting equation [10] into equation [3a] yields the stress–strain relation for the physical extension of cell walls which is written as

$$\sigma = G_e\epsilon + G_o \int_0^t e^{-(t-t')/\tau} \dot{\epsilon}(t')dt'. \qquad [13]$$

The term $G_e\epsilon$ represents the contribution of the elastic component of the cell walls to total stress. This is the non–decaying component of the stress. The second term on the right hand side of equation [13] is the contribution of the viscoelastic component of the cell walls to the total stress. This term decays with time. With these observations in mind, equation [13] is written as

$$\sigma = \sigma_e + \sigma_v . \qquad [14]$$

where σ is the total stress (N m^{-2}), and σ_e (N m^{-2}) and σ_v (N m^{-2}) are the elastic and viscoelastic stress components, respectively.

Energy relations of cell wall deformation

Deformation implies the absorption of energy by the deforming

material. A perfectly elastic material stores all the energy in the form of elastic strain energy,

$$E_e = \frac{1}{2}K\epsilon^2 \quad , \qquad [15]$$

where E_e is the elastic strain energy, K is the Hook's law constant (equation [1]) and ϵ is strain. The strain energy remains preserved as long as the strain exists. Elastic strain energy is not dissipated. The energy is recovered at any time in the form of work. When stress is applied to a viscous material, all the work done is dissipated as physical or chemical energy. A viscous material cannot store energy for later release. A viscoelastic material, such as the plant cell wall, stores part of the work as strain energy and dissipates the remaining part as heat or chemical energy.

The rate of work that is performed on the material during deformation is the product of stress, σ, and strain rate, $\dot{\epsilon}$,

$$\frac{dW}{dt} = \sigma\dot{\epsilon} = \dot{\epsilon}\int_0^t G(t-t')\dot{\epsilon}(t')dt \quad , \qquad [16]$$

where W is work (J). Where $\dot{\epsilon}$ = constant, substituting equation [10] into [16] produces

$$\frac{dW}{dt} = G_e\dot{\epsilon}^2t + G_v\dot{\epsilon}^2\tau(1-e^{-t/\tau}) \quad . \qquad [17]$$

The strain energy stored during this process is given by (Ferry, 1970)

$$E_{st} = \frac{1}{2}G_e\dot{\epsilon}^2t^2 + \frac{1}{2}G_v\dot{\epsilon}^2\tau^2(1-e^{-t/\tau})^2 \quad , \qquad [18]$$

where E_{st} is stored strain energy (J m^{-3}). The first term on the right hand side of equation [18] is the strain energy stored by the elastic component which is nondissipating and therefore can be recovered. The second term is the energy stored by the viscoelastic component which is being dissipated, thus only partially recoverable. The first term of the

stored energy is called elastic strain energy, E_e, and the second term is called viscoelastic strain energy, E_v. Equation [17] can be written as:

$$E_{st} = E_e + E_v \ . \qquad [19]$$

The rate at which the stored energy increases is the time derivative of equation [18],

$$\frac{dE_{st}}{dt} = G_e\dot{\epsilon}^2 t + G_v\dot{\epsilon}^2\tau(1-e^{-t/\tau})e^{-t/\tau} \ . \qquad [20]$$

Two processes affect the rate at which the stored strain energy changes with time. The stored strain energy increases as a result of the work being done to the material. At the same time, the stored strain energy is dissipated through the strain energy dissipation, or stress relaxation process. The net rate of energy storage is the sum of the rate of work and the rate of energy dissipation, which is written mathematically as:

$$\frac{dE_{st}}{dt} = \frac{dW}{dt} + \left.\frac{dE_{st}}{dt}\right|_{disp} \ , \qquad [21]$$

where the second term on the right hand side of equation [21] is the change in stored strain energy due to dissipation. Combining equations [17], [20], and [21] yields

$$\left.\frac{dE_{st}}{dt}\right|_{disp} = \dot{\epsilon}^2 G_v\tau(1-e^{-t/\tau})^2 = -\frac{2}{\tau}E_v \ . \qquad [22]$$

Physically, the process of strain energy dissipation is considered as the rearrangement of the cross–links between polymers. The "soft" cross–link bonds between the polymers which have been strained, or put into higher energy states by physical straining of the cell walls, spontaneously rearrange into lower energy states thereby releasing the stored strain energy. The stress in the cell walls is released as a result of this rearrangement. Equation [22] states that the rate of strain energy

dissipation is proportional to the viscoelastic strain energy. In other words, the rate of the cross–link bond rearrangement is proportional to the degree of straining of these bonds expressed as the strain energy stored in these bonds.

Wall loosening as a strain energy releasing process

We postulate that the processes of cell wall loosening and the fixation of elastic strain into the permanent strain (Lockhart, 1967; Taiz, 1984; Fry, 1986) is a unified process in which the strain energy in the cell walls is relaxed as a result of the physiological processes in the cells. The mathematical description of the process of cell enlargement follows from this hypothesis.

The cell walls are first strained by the physical stresses resulting from turgor potential. Work is done during this process to deform the cell walls. Some of the energy is stored as strain energy in the cross–link bonds of the cell wall polymers. Two processes work simultaneously to release this strain energy in the cell walls; the physical stress relaxation described in the previous section and the physiological stress relaxation resulting from biochemical processes in the cell. Physical stress relaxation is the result of spontaneous rearrangement of the cross–links between polymer molecules under stress (Tobolsky and Eyring, 1943; Haughton and Sellen, 1973; Dorrington, 1980). The physiological processes release stress in a similar way. As new cell wall materials are synthesized, cross–links between existing polymers are broken and the newly synthesized material is inserted. As a result, the bonds in the polymers return to lower energy states and the strain energy is released. In order for this process to

proceed, the cell walls must be under stress so that the bonds are in energized states. Continued cell expansion requires that the stress in the cell wall exceeds a minimum value, which suggests that a minimum strain energy value is required for the physiological stress relaxation process to be initiated.

The discussion in the previous section demonstrated how the physical stress relaxation process releases the viscoelastic strain energy in the cell walls, and that the rate of energy relaxation is proportional to the stored viscoelastic strain energy (equation [22]). The division of strain energy into elastic and viscoelastic portions is for the convenience of discussion. There is no evidence suggesting that differentiation between elastic and viscoelastic strain energy exists in terms of biological cell wall loosening processes. However, neither is there solid reason to conclude that such a differentiation is not valid. We assume, for simplicity, that a linear relationship similar to equation [22] holds for the physiological energy relaxation process

$$\left.\frac{dE_{st}}{dt}\right|_{physiol.} = -\frac{2}{\kappa} E_{st} \quad . \qquad [23]$$

This equation is analogous to equation [22]. It was obtained by writing "physiol." for "disp." in the subscript on the left hand side and replacing "E_v" with "E_{st}" on the right hand side. The justification was discussed in the previous paragraph. Equation [23] states that the physiological processes do not differentiate between elastic and viscoelastic strain energy. The rate of physiological strain energy relaxation is represented by κ, which is a function of carbohydrate concentration (C), temperature (T), water stress (Ψ), and critical strain energy (E_c),

$$\kappa = f(C, T, \Psi, E_c) \quad . \qquad [24]$$

This quantity is considered the time coefficient of physiological strain energy relaxation. A large value of κ means a slow physiological cell wall loosening process and *vice versa*. The value of κ approaches infinity in the absence of physiological wall loosening as is expected in a mature cell or in *in vitro* cell walls. The total rate of strain energy relaxation is the sum of physical (equation [22]) and physiological processes (Equation [23]). Adding equations [22] and [23], and substituting equation [19] for E_{st} yields

$$\left.\frac{dE_{st}}{dt}\right|_{\text{tot disp.}} = \frac{2}{\kappa} E_e + \left(\frac{2}{\kappa} + \frac{2}{\tau} \right) E_v \ . \qquad [25]$$

With the physiological strain energy relaxation process incorporated into the definition of the problem, the stress relaxation modulus in equation [10] becomes

$$G = G_e e^{-t/\kappa} + G_v e^{-t(1/\kappa + 1/\tau)} \ . \qquad [26]$$

When the physiological wall loosening process stops, $1/\kappa=0$, equation [26] reduces to equation [10], as expected. The creep compliance modulus is obtained by applying relation [6] to equation [26] as follows:

$$J = J_e + J_v(1 - e^{-t/\gamma}) + \frac{t}{\eta} \ , \qquad [27]$$

where J_e ($m^2\ N^{-1}$) is the initial instantaneous elastic deformation, J_v ($m^2\ N^{-1}$) is the maximum viscoelastic creeping. The parameter η (kg $m^{-1}\ s^{-1}$) has the unit of viscosity and is a function of both the physical properties of the wall and the physiological wall loosening process of the cell. Defining

$$r_\tau = \frac{\kappa}{\tau} \ , \qquad [28a]$$

and

$$\bar{\tau} = \frac{\kappa \tau}{\kappa + \tau} \ , \qquad [28b]$$

it can be shown that the coefficients in equation [27] are given by

$$J_e = \frac{1}{G_e + G_o} , \qquad [29a]$$

$$\gamma = \frac{\kappa}{1 + J_e G_e r_\tau} , \qquad [29b]$$

$$\eta = \left[\frac{G_o}{1 + r_\tau} + G_e\right]\kappa , \qquad [29c]$$

and

$$J_v = \frac{\kappa + \bar{\tau} - \gamma}{\eta} - J_e . \qquad [29d]$$

In the absence of physiological cell wall loosening, $1/\eta$ becomes zero and equations [26], [27], and [29] reduce to equations [10], [11], and [12] respectively.

DISCUSSION

The above relations were derived for one–dimensional elongation of plant roots. They can, however, be applied to cell expansion studies when the strain is defined as the volumetric expansion and stress is defined as the pressure imposed on the cell contents by the cell wall. The stress equals the turgor pressure when there is no water exchange between cytoplasm and the environment outside the cell wall, or as the membrane and cell wall resistance to water transport is negligible.

Lockhart (1965) assumed that the strain rate of the cell wall is directly proportional to the stress in the wall above some critical yielding value (equation [2]). Despite a large number of investigations concerning this relationship (Green, 1968; Green et al., 1971; Cosgrove, 1985; Cleland, 1987; Taiz, 1984), several questions remain unanswered. One component that is missing from the theory originated by Lockhart (1965) is the biological activity of the cells. Although it has been shown that cell wall synthesis and cell wall loosening are essential for continued cell expansion (Cleland, 1987; Ray, 1987), these processes either have been ignored or avoided in most of the investigations of biophysics of plant cell expansion (Green et al, 1971; Cosgrove, 1985). When the biological cell wall loosening and synthesis events are treated, the biological and physical processes are usually treated separately (Green et al., 1971; Fry, 1986; Biggs and Fry, 1987) and the interactions between the two processes are not adequately described.

One model suggests that the cell growth consists of a series of discrete events (Taiz, 1984; Cleland, 1987). First, the cell wall loosening

event occurs in which the rigid cell wall is modified biochemically; then, elastic expansion by physical stress occurs; and finally, the elastic strain is fixed into permanent strain by biochemical processes. The net result of these steps is the expanded rigid cell wall. Continued cell growth is achieved by repetition of these steps. However, it seems more logical that the physical wall straining and biological wall loosening processes operate continuously and in cooperation with one another during cell expansion, as described in this work, rather than as discrete events.

Under conditions of constant stress and constant physiological activity in the cell, equation [27] approaches the Lockhart equation as time progresses, resulting in a constant rate of cell expansion. The extensibility in Lockhart's equation corresponds to $1/\eta$ in equation [27]. Despite its widespread use (Green et al., 1971; Cosgrove, 1985; Cosgrove, 1986), the extensibility remains a poorly defined concept. Effects of temperature, water stress, pH, and auxin on cell expansion has often been attributed to changes in cell wall extensibility (Cleland and Haughton, 1971; Ray, 1987; Taiz, 1984). If, as it was assumed, the wall extensibility is indeed a physical parameter of the walls, it would be logical to expect the same effects on *in vitro* experiments on cell walls. The evidence in the literature does not support this assertion (Green et al., 1971; Sellen, 1980). Other theories, such as the "shifting yielding stress" theory (Green, 1968; Green et al., 1971; Cleland, 1987) have also been proposed. Despite elaborate arguments, these theories are no more convincing than the "shifting wall extensibility" hypothesis and they provide little insight into the mechanisms of the processes involved. Equation [28] indicates that the cell wall extensibility depends on the physical properties of the cell wall

as well as on the biological processes taking place in the cell. It would be more logical to expect that temperature, water stress and auxin affect the biological activity of the cells as much as, or more than, they affect the physical properties of the cell walls. Further analysis of results of experiments in the literature along this dimension is needed.

Another phenomenon that has been troubling the "wall extensibility" theory of cell growth is the apparent discrepancy between the observations that stress relaxation of *in vitro* cell walls is proportional to the logarithm of time while cell expansion is proportional to time (Green et al., 1971; Haughton et al., 1968). As is described in this study, the difference between the two processes is the biological activity of the cell. With the physiological wall loosening, equation [27] describes a cell expansion process that is linear with time when the steady state is reached. As the biological activity of the cell is stopped during the preparation of the cell wall materials for *in vitro* studies, the governing equation reduces to equation [11] which predicts exponential behavior.

It is apparent from the above discussions that Lockhart's equation, as a special case of equation [27] at steady state, only can describe the steady state cell expansion. Thus, it is not surprising that satisfactory explanations for the difference between transient responses of *Avena* coleoptile (Cleland and Haughton, 1971) and *Nitella* (Green et al., 1971) cell expansion to a sudden drop in turgor pressure have not been presented (Taiz, 1984). In the case of *Avena*, there is at first a rapid elastic shrinkage, after which there is an intermediate period when the growth rate continues to readjust. Finally, a new steady state growth rate is reached. With *Nitella*, on the other hand, there is little elastic

shrinkage. First, there is an immediate cessation of growth. After a period of time, growth resumes at the original rate. It can be shown that the difference may be attributed to the differences between the physical properties (G_e, G_v, and τ) of the cell walls and the physiological cell wall loosening processes (κ) of the two species. Cell walls with higher values of G_e and G_v (stiffer cell walls) will shrink little upon a sudden drop in turgor, while cell walls with lower values of G_e and G_v will shrink more. Thus, it seems that *Nitella* cell walls have higher values of G_e and G_v values than the cell walls of *Avena* coleoptiles. The values of τ and κ control the dynamic response of the rate of growth to change in turgor pressure. Larger values of κ and τ result in slower response while smaller values of these variables result in an immediate response.

CONCLUSION

A mathematical model is presented which describes the process of plant cell growth as the result of processes of physical and metabolically controlled strain energy relaxation. The relaxation of strain energy in the cross–linking bonds of the cell wall polymers results from physical and metabolically controlled breakage and reformation processes of these bonds. The physical strain energy relaxation process occurs in the weak bonds, primarily hydrogen bonds, while the metabolic strain energy relaxation process is assumed to occur in both weak hydrogen bonds and the strong covalent bonds. The model presented in this study reduces to the Lockhart (1965) equation under steady state conditions. However, the parameter corresponding to the cell wall extensibility in the Lockhart (1965) equation is defined as a function of both the physical properties of the cell wall and the metabolic strain energy relaxation process. The model was derived under the condition of constant metabolic strain energy process. The dynamic situation where this process is a function of time can be treated following the similar approach. The model is used as the basic constitutive relation in a dynamic, mechanistic model of plant root elongation in following chapters.

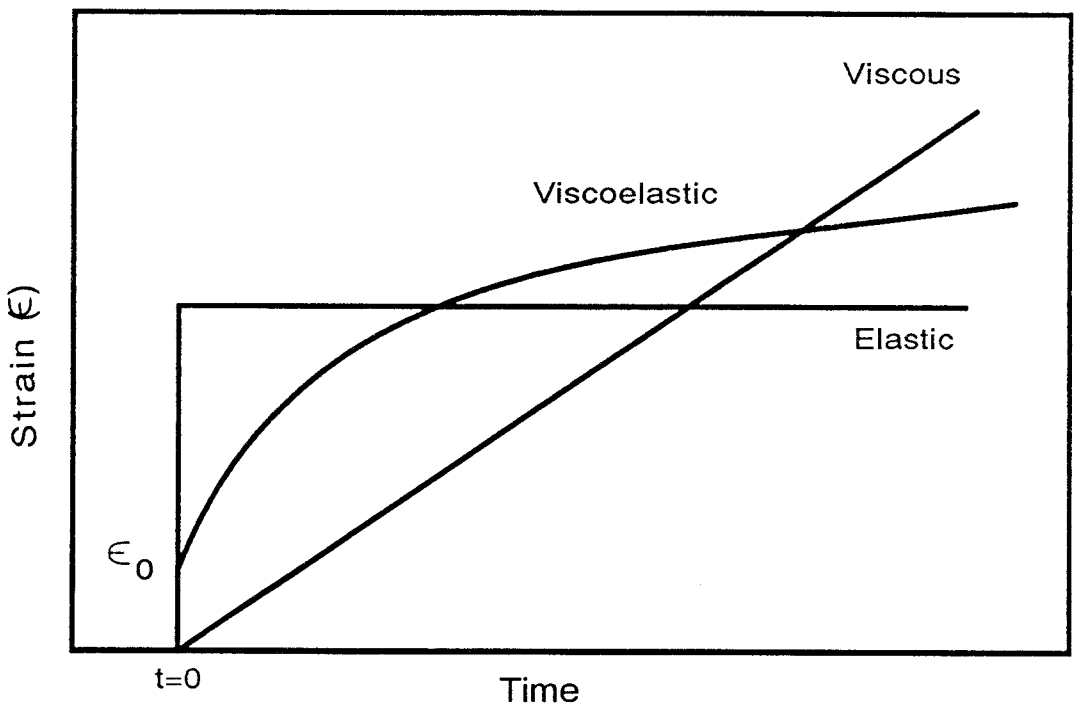

Figure 2.1. Response of three types of material to an instantaneous stress. A stress, σ_0, is imposed at t=0. Elastic material is characterized by an instantaneous strain proportional to the imposed stress. Viscous material is characterized by constant strain rate. Viscoelastic material exhibits an instantaneous elastic strain, ϵ_0, followed by a continuously increasing strain with a decreasing rate.

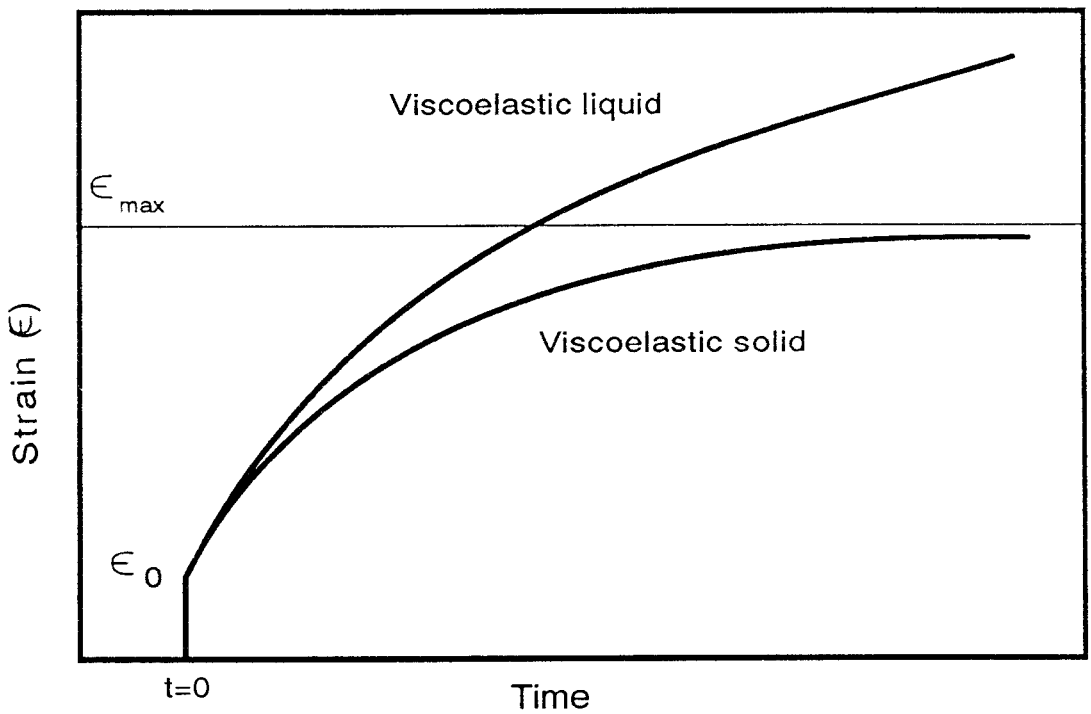

Figure 2.2. Response of two types of viscoelastic materials during a creep test. An finite stress is imposed instantaneously at t=0. Both types of material have a finite instantaneous elastic deformation, ϵ_0. As time progresses, the total strain of the viscoelastic solid approaches a finite asymptotic value, ϵ_{max} , which is a function of the imposed stress. The strain of the viscoelastic liquid does not exhibit an asymptotic value and increases continuously.

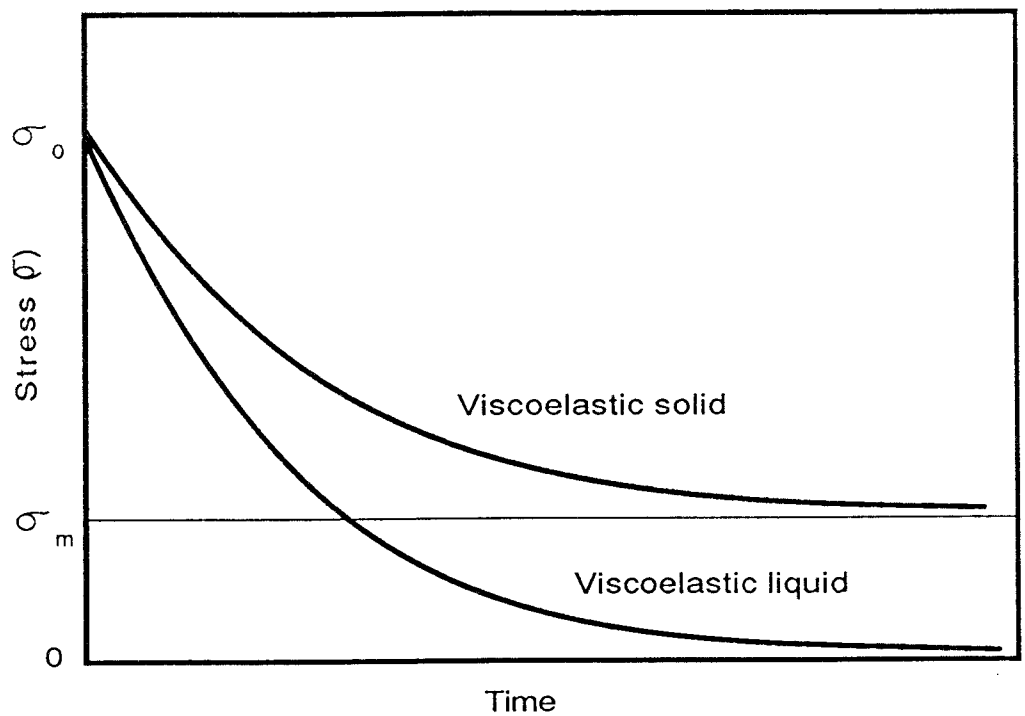

Figure 2.3. Response of two types of viscoelastic material during a stress relaxation test. A finite strain is imposed on the materials instantaneously at t=0. The σ_0 is the initial instantaneous stress. The stress of both types of materials decreases with time. Stress in the viscoelastic solid relaxes to a finite equilibrium value, σ_{min} . A equilibrium stress does not exist in the viscoelastic liquid, where the stress approaches zero as time progresses.

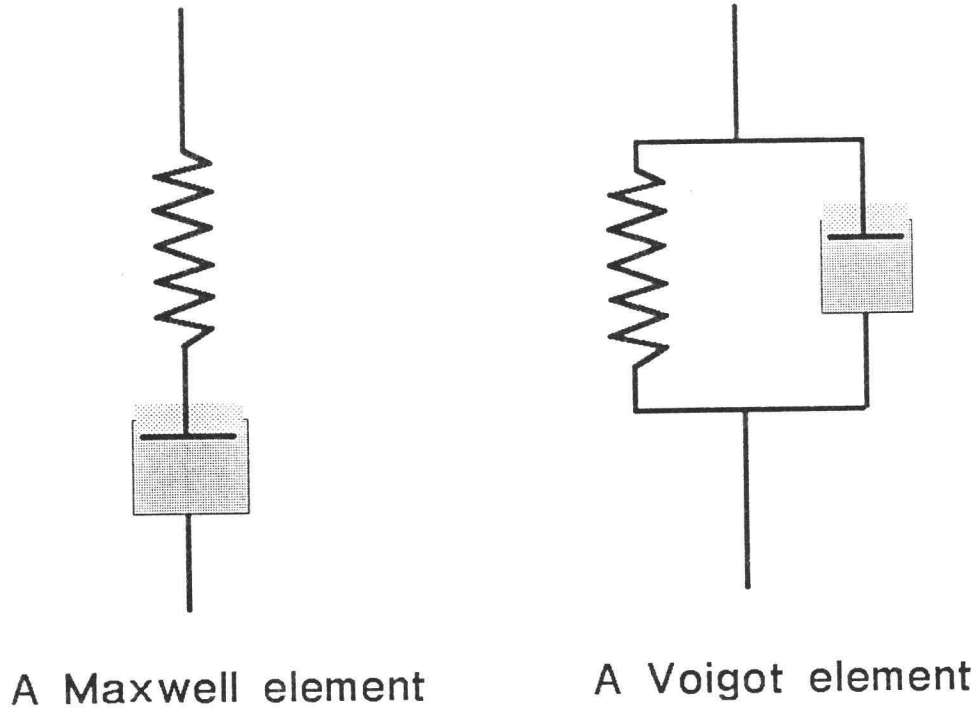

Figure 2.4. Schematic representation of two mechanical models of viscoelastic materials. A Maxwell element consists of a viscous (dashpot) and an elastic (spring) component connected in series. A Voigot element consists of a viscous and an elastic component connected in parallel. Behavior of any real viscoelastic material can be approximated by a number of these elements connected in different ways.

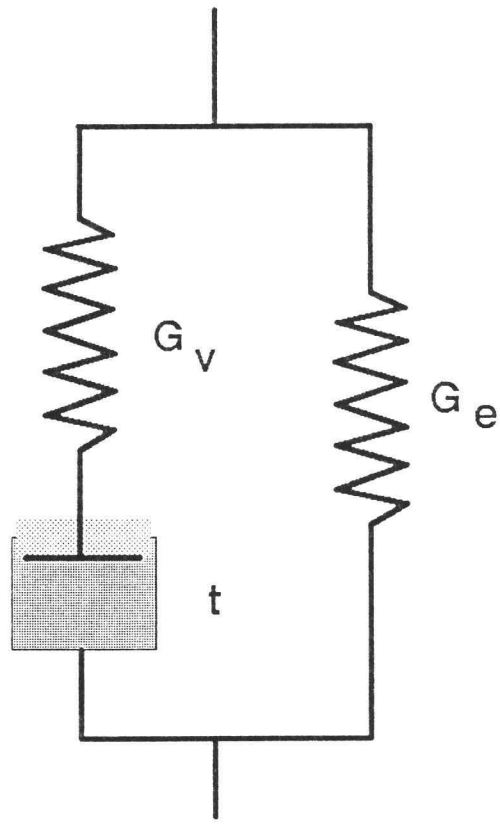

Figure 2.5. A schematic representation of a simple viscoelastic model of the mechanical properties of plant cell walls. G_v represents the strength of the hydrogen bond cross–links between polymers which undergo breaking and rearranging under physical stress, resulting in physical stress relaxation. The time coefficient, τ, of the dashpot represents the first order kinetics of this stress relaxation process. G_e represents the strength of the covalent cross–link bonds between polymers which normally do not break under imposed physical stresses.

LIST OF SYMBOLS AND UNITS

m	extensibility of the cell wall	$m\ s\ kg^{-1}$
t	current time	s
t'	past time ($t' \leq t$)	s
E_e	density of elastic strain energy	$J\ m^{-3}$
E_v	density of viscoelastic strain energy	$J\ m^{-3}$
E_{st}	density of stored strain energy	$J\ m^{-3}$
G	stress relaxation modulus	$N\ m^{-2}$
G_e	elastic strength of the cell wall	$N\ m^{-2}$
G_i	elastic strength of the i–th element in a Maxwell type model	$N\ m^{-2}$
G_o	elastic strength of a single Maxwell element	$N\ m^{-2}$
G_v	viscoelastic strength of the cell wall	$N\ m^{-2}$
H	continuous stress relaxation spectrum	$N\ m^{-2}$
J	creep compliance modulus	$m^2\ N^{-1}$
J_e	Young's modulus at equilibrium	$m^2\ N^{-1}$
J_o	Young's modulus at equilibrium for a single Maxwell element	$m^2\ N^{-1}$
J_v	viscoelastic creeping coefficient	$m^2\ N^{-1}$
K	Hook's law coefficient	$N\ m^{-2}$
W	work done on the cell wall during deformation	$J\ m^{-3}$
Y	yielding stress of the cell wall	$N\ m^{-2}$
ϵ	strain	no unit

$\dot{\epsilon}$	time rate of strain	s^{-1}
ϵ_o	initial instant strain in a stress relaxation test	no unit
γ	time constant of creep compliance	s
κ	time constant of biological strain energy relaxation	s
η	viscous coefficient of the cell wall	kg $m^{-1}s^{-1}$
σ	stress	N m^{-2}
$\dot{\sigma}$	time rate of stress	N m^{-2} s^{-1}
σ_e	elastic stress component	N m^{-2}
σ_v	viscoelastic stress component	N m^{-2}
σ_o	initial instant stress in a creep test	N m^{-2}
τ	time constant of physical stress relaxation	s
τ_i	time constant of stress relaxation for the i–th element in a Maxwell type model	s

LITERATURE CITED

Abdu–Baki, A. A., and P. M. Ray, 1971. Regulation by auxin of carbohydrate metabolism involved in cell wall synthesis by pea stem tissue. Plant Physiol., 47:537–544.

Biggs, K. J., and S. C. Fry, 1987. Phenolic cross linking in the cell wall. *In* D. J. Cosgrove and D. P. Knievel (Ed.) Physiology of cell expansion during plant growth. Am. Soc. Plant Physiol., Penn. State Univ..

Brummel, D. A., and J. L. Hall, 1985. The role of cell wall synthesis in sustained auxin–sensitive hypocotyl tissue. Planta, 139:227–237.

Carmona, M. J., and A. Cuadrado, 1986. Analysis of growth components in Allium roots. Planta, 168:183–189.

Cleland, R., 1971. Cell wall extension. Ann. Rev. Plant Physiol., 22:197–221.

Cleland, R., and P. M. Haughton, 1971. The effect of Auxin on stress relaxation in isolated *Avena* coleoptiles. Plant Physiol., 47:812–815.

Cleland, R., 1987. Mechanisms of wall loosening and wall extension. *In* D. J. Cosgrove and D. P. Knievel (Ed.) Physiology of cell expansion during plant growth. Am. Soc. Plant Physiol.. Penn. State Univ..

Cosgrove, D. J., 1985. Cell wall yield properties of growing tissue: Evaluation by *in vivo* stress relaxation. Plant Physiol., 78:347–356.

Cosgrove, D. J., 1986. Biophysical control of plant cell growth. Ann. Rev.

Plant Physiol., 37:377–405.

Dorrington, K. L., 1980. The theory of viscoelasticity in biomaterials. *In* The mechanical properties of biological materials. Symp. Soc. Exp. Biol., 34:315–329. Cambridge Univ. Press, Cambridge.

Erickson, R. O., 1976. Modeling of plant growth. Ann. Rev. Plant Physiol., 27:407–434.

Ferry, J. D., 1970. Viscoelastic properties of polymers. Second Edition. John Wiley and Sons, New York. 671pp.

Fry, S. C., 1986. Cross–linking of matrix polymers in the growing cell walls of angiosperms. Ann. Rev. Plant Physiol., 37:165–186.

Green P. B., 1968. Growth physics in *Nitella*: A method for continuous *in vivo* analysis of extensibility based on a micro–manometer technique for turgor pressure. Plant Physiol., 43:1169–1184.

Green, P. B., R. O. Erickson, and J. Buggy, 1971. Metabolic and physical control of cell elongation rate. *In vivo* studies in *Nitella*. Plant Physiol., 47:423–430.

Haughton, P. M., and D. B. Sellen, 1969. Dynamic mechanical properties of the cell walls of some Green algae. J. Exp. Bot., 20:516–535.

Haughton, P. M., and D. B. Sellen, 1973. Stress relaxation in regenerated cellulose. J. Physics, D: Applied Physics, 6:1998–2011.

Haughton, P. M., D. B. Sellen, and R. D. Preston, F. R. S., 1968. Dynamic mechanical properties of the cell wall of *Nitella opaca*. J. Exp. Bot., 19:1–12.

Hettiaratchi, D. R. P., and J. R. O'Callaghan, 1974. A membrane model of plant cell extension. J. Theor. Biol., 45:459–465.

Lockhart, J. A., 1967. Physical nature of irreversible deformation of plant

cells. Plant Physiol., 42:1545–1552.

Lockhart, J. A., 1965. An analysis of irreversible plant cell elongation. J. Theor. Biol., 8:264–275.

Morris, D. A., and E. D. Arthur, 1985. Invertase activity, carbohydrate metabolism and cell expansion in the stem of *Phaseolus vulgaris L.* J. Exp. Bot., 36:623–633.

Pritchard, J., R. G. Wyn Jones and A. D. Tomos, 1988. Control of wheat root growth. The effects of excision on growth, wall rheology and root anatomy. Planta, 176:399–405.

Ortega, J. K. E., 1985. Augmented growth equation for cell wall expansion. Plant Physiol., 79:318–320.

Ray, P. M., 1987. Principles of plant cell growth. *In* D. J. Cosgrove and D. P. Knievel (ed.) Physiology of cell expansion during plant growth. Am. Soc. Plant Physiol., Penn. State Univ..

Sellen, D. B., 1980. The mechanical properties of plant cell walls. *In* The mechanical properties of biological materials. Symp. Soc. Exp. Biol., 34:315–329. Cambridge Univ. Press, Cambridge.

Taiz, L., 1984. Plant cell expansion: Regulation of cell wall mechanical properties. Ann. Rev. Plant Physiol., 35:585–657.

Tobolsky, A., and H. Eyring, 1943. Mechanical properties of polymeric materials. J. Chem. Physics, 11:125–134.

Van Volkenburgh, E., and R. E. Cleland, 1981. Control of light–induced bean leaf expansion: Role of osmotic potential, wall yield stress, and hydraulic conductivity. Planta, 153:527–577.

3. TRANSPORT OF WATER IN A GROWING ROOT

Yongsheng Feng and Larry Boersma
Department of Soil Science, Oregon State University
Corvallis, OR 97331

ABSTRACT

Growth of plant roots is intimately related to the uptake and transport of water. Water transport in plant tissues occurs via two distinct pathways: the apoplast and the symplast. Rigorous treatment of the water transport process in plant roots from the standpoint of the continuum theory has been lacking in the past.

In this study, a system of mathematical equations that describes the dynamic interactions between water transport in the two pathways in plant roots and axial root elongation was derived from fundamental considerations of the physics of water transport in porous media as well as the considerations of the basic morphological properties of plant roots. Axial flux of water in both pathways is described by equations which formally resemble Darcy's law. The axial permeability in the apoplast pathway was derived as being constant in the spatial coordinate system while the axial permeability in the symplast pathway was shown to be essentially constant in the material coordinate system. The Munch pressure flow hypothesis results naturally from the equation of axial water transport in the symplast pathway as the conducting vessels develop, which is represented by a decrease in the solute reflection coefficient in the axial direction. The permeability between the two pathways was

derived as a function of cell size, membrane permeability, and the volume fractions of the apoplast and symplast pathways.

Continuity equations for water transport in both pathways were derived which describe the dynamic interactions between water transport in the two pathways and axial root elongation. The processes of water transport in the two pathways was coupled by continued exchange of water along the entire length of the root axis.

The mathematical descriptions of the dynamic processes of water transport in a growing plant root derived in this work can serve as the theoretical basis for evaluating the effects of soil water stress and root elongation rates on the water status of plant roots and ultimately, the whole plant. The equations can be integrated into a dynamic model of plant root growth so that interactions between water, solute transport, and growth can be simulated.

INTRODUCTION

Growth of plants is intimately associated with uptake and transport of water (Molz and Boyer, 1978; Kramer, 1983; Boyer, 1985, 1988). The root system provides the contact between plants and their soil environment. Water and mineral nutrients are taken up from the soil by the roots and transported to the upper parts of the plant to meet the demands as plants grow (Gardner, 1960; Dalton, 1975; Passioura, 1980). Availability, uptake and transport of water during plant growth has been a major area of concern in the past (Turner, 1986, 1987).

Water moves in plant tissue via two distinct pathways: the apoplasmic and symplasmic pathways (Molz, 1976; Kramer, 1983; Moon et al., 1986). Cell walls in plant tissue form a continuous, water conducting network referred to as the apoplast. The symplast is the system consisting of the parts of plant tissue bounded by plasmalemma membranes and interconnected by plasmodesmata (Kramer, 1983; Nobel, 1983; Hanson et al., 1985). In a plant root, water moves both axially through each pathway and laterally between the two pathways. During root elongation, the volume of the cytoplasm increases as a result of cell enlargement. Water moves laterally from the apoplast to the symplast to fill the space created by the expanding cell.

Mathematical analysis of water movement in plant tissues has traditionally been developed by considering behavior of individual cells (Molz, 1976). Mathematical description of the macroscopic behavior of plant tissue in terms of water transport were developed by considering a flow domain with dimensions much larger than those of an individual

cell. Mathematical expressions of water transport over such a domain were derived by averaging the behavior of the individual cells comprising the domain. This approach provides the connection between the behavior of individual cells at the microscopic scale and that of a plant tissue at the macroscopic scale. This approach, however, does not allow for consideration of interactions of water flow and local rate of growth (McCoy and Boersma, 1984).

An alternative approach is to consider a plant tissue as a mathematical continuum and derive the mathematical expressions for water transport from a continuum mechanics point of view (Silk and Wagner, 1980; McCoy and Boersma, 1984). Although a plant tissue consists of an assemblage of individual cells, the tissue, as a whole, can be viewed as a mathematical continuum (Silk and Erickson, 1979; McCoy and Boersma, 1984). Quantities such as density and velocity can then be assigned to material and spatial points of such a continuum. Continuum theory in the past has been used to describe the growth of plant roots (Silk and Erickson, 1979; Bertaud and Gandar, 1985; Carmona and Cuadrado, 1986), as well as transport of water and solute in plant tissues (Silk and Wagner, 1980; McCoy and Boersma, 1984)

Studies of water movement in plant roots have mostly been concerned with the lateral movement of water from the soil to the root surface and then to the xylem vessels (Lang and Gardner, 1970; Reicosky and Ritchie, 1976; McCully and Canny, 1988; Passioura, 1988). Few studies of axial water movement in the growth region of plant roots have been reported (Silk and Wagner, 1980; St. Aubin et al., 1986). McCoy and Boersma (1984) derived equations of axial water and solute transport

in plant roots from a continuum perspective. However, the difference between apoplasmic and symplasmic pathways were not addressed. The effect of soil water potential and the different roles played by the meristem and the elongation region did not receive appropriate treatment.

This study develops a complete mathematical description of axial water movement in the growth region of a plant root from a continuum perspective. The plant root is treated as a one–dimensional mathematical continuum consisting of two distinct water pathways: the apoplast and the symplast. The uptake of water from soil and the moving meristem at the tip of the root will be explicitly considered. Mathematical expressions of axial water permeability in both pathways, as well as the water permeability between the two pathways, are derived from fundamental considerations of physics of water movement in a growing plant tissue.

THEORY

Water transport in both the symplast and apoplast pathways is usually described by Darcy's law (Phillip. 1957; Kramer, 1983). This relation can be derived from considerations of basic physical principles governing viscous flow of water and the law of mass balance. Raats and Klute (1968a,b) derived water transport equations for porous media from considerations of basic principles of continuum theory. Sposito (1978a,b) arrived at the same results using an approach based on statistical mechanics. Similar work for the transport of water in plant tissues has not been reported. In this study, the mathematical description of water transport in a plant tissue is derived following a less rigorous but more intuitive approach.

Throughout the discussions in this chapter, vector quantities are denoted by symbols with a **bold** face and scalar quantities are denoted by symbols with a normal face. *Italic* symbols are used to denote quantities at microscopic scales, such as in a pore for a porous medium and in a cell for a plant tissue. The quantities at the macroscopic scale, a scale at which variations between individual pores or cells can be ignored, are denoted by the corresponding symbols of normal type. When a particular symbol is not available in italics, a bar on top of the symbol, e.g., $\bar{\rho}$, is used to denote the quantity at the microscopic scale.

Balance of linear momentum–Darcy's law

Equations for the axial transport of water in a plant root can be derived by considering the balance of linear momentum. Newton's law of

conservation of linear momentum states that the rate at which the linear momentum of a system changes is equal to the total force acting on the system. In the case of fluid flow, we start by considering an arbitrary volume $\mathcal{V}$ with a boundary $\mathcal{S}$ in a spatial coordinate system. The mathematical statement of the law of conservation of linear momentum is written as

$$\frac{d}{dt}\int_{\mathcal{V}}(\rho_\ell \mathbf{v})d\mathcal{u} + \int_{\mathcal{S}}(\rho_\ell \mathbf{v})(\mathbf{n}\cdot\mathbf{v})d\mathcal{a} = \int_{\mathcal{V}}\rho_\ell \mathbf{f} d\mathcal{u} + \int_{\mathcal{S}}\mathbf{t}\cdot\mathbf{n}\ d\mathcal{a}\,, \qquad [1]$$

where ρ_ℓ is fluid density (kg m^{-3}), $\mathbf{v}$ is the velocity vector (m s^{-1}), $\mathbf{n}$ is a unit vector normal to the surface, $\mathbf{f}$ is the body force (N kg^{-1}), $\mathbf{t}$ is the surface traction tensor (N m^{-2}), $\mathbf{n}$ is a unit vector normal to the surface bounding $\mathcal{V}$, and $\mathcal{u}$ and $\mathcal{a}$ are volume and area elements, respectively.

Equation [1] is the mathematical statement of Newton's law of conservation of linear momentum. The first term on the left hand side of equation [1] is the rate of linear momentum change in volume $\mathcal{V}$ due to change in fluid velocity. The second term on the left hand side of equation [1] is the change of linear momentum in volume $\mathcal{V}$ due to the flow of fluid across the boundary. The right hand side of equation [1] represents the sum of all forces acting on volume $\mathcal{V}$. The first term is the body force, including the gravitational force. The second term is the surface traction including all forces acting on the surface of volume $\mathcal{V}$, such as external pressure.

Next we consider fluid flow in a porous medium. For simplicity, we consider a system which consists of a solid phase and a fluid phase, i.e., the case of saturated flow, since this is the case in a plant root.

Differentiation between microscopic and corresponding macroscopic quantities must be made when considering point functions that are defined on spatial or material points, such as flow velocity, in a porous medium. For example, we can consider either a microscopic fluid flow velocity or a macroscopic fluid flow velocity. At the microscopic scale, fluid velocity may vary from one pore space to another or even from one point to another within a single pore. It is not practical, nor necessary, to describe fluid velocity in such detail when only the macroscopic behavior of the system is of interest. In this case, only the average value of the fluid velocity over a sufficiently large volume is needed to adequately describe the motion of the fluid. The macroscopic value of an arbitrary quantity at a point x is defined as its volume average,

$$\mathrm{m} = \frac{1}{\mathrm{V}} \int_{\mathrm{V_f}} m \, \mathrm{d}\boldsymbol{u} \,, \qquad [2]$$

where m is an arbitrary quantity and m is its volume average, i.e., the macroscopic counterpart of of m, V is an elemental volume centered at x, and $\mathrm{V_f}$ is the volume of fluid contained in V. The size of V over which this average must be carried out depends on the geometric structure of the porous medium as well as the quantity concerned. V is the minimum volume in which the definition of m in a macroscopic sense is meaningful.

For the fluid in an arbitrary volume, $\mathscr{V}$, of a porous medium which is bounded by a surface $\mathscr{S}$, equation [1] is written as

$$\frac{\mathrm{d}}{\mathrm{dt}} \int_{\mathscr{V}_\mathrm{f}} (\bar{\rho}\boldsymbol{v}) \mathrm{d}\boldsymbol{u} + \int_{\mathscr{S}_\mathrm{f}} (\bar{\rho}\boldsymbol{v})(\boldsymbol{n}\cdot\boldsymbol{v}) \mathrm{d}\boldsymbol{a} = \int_{\mathscr{V}_\mathrm{f}} \bar{\rho}\boldsymbol{f} \, \mathrm{d}\boldsymbol{u} + \int_{\mathscr{S}_\mathrm{f}} \boldsymbol{t}\cdot\boldsymbol{n} \, \mathrm{d}\boldsymbol{a} \,, \qquad [3]$$

where $\mathscr{V}_\mathrm{f}$ is the portion of $\mathscr{V}$ occupied by the fluid, $\mathscr{S}_\mathrm{f}$ is the boundary

of the fluid phase, and $\boldsymbol{n}$ is a unit vector on $\mathscr{S}_f$ pointing away from the liquid phase. The boundary of the fluid phase, $\mathscr{S}_f$, consists of two parts: the area of the surface bounding $\mathscr{V}$ that is occupied by the liquid phase, $\mathscr{S}_e$, and the solid–liquid interface within the volume $\mathscr{V}$, $\mathscr{S}_i$. Mathematically, this can be stated as

$$\mathscr{S}_f = \mathscr{S}_e + \mathscr{S}_i \ . \qquad [4]$$

The terms on the left hand side of equation [3] represent the inertial forces. For fluid flow in porous media, the effects of inertial forces are small and under many circumstances these terms can be safely neglected (Raats et al., 1968; Sposito, 1978). After neglecting the inertial forces, equation [3] is written as

$$\int_{\mathscr{V}_f} \bar{\rho} \boldsymbol{f} \, \mathrm{d}\mathscr{u} + \int_{\mathscr{S}_f} \boldsymbol{t}\cdot\boldsymbol{n} \, \mathrm{d}\mathscr{a} = 0 \ . \qquad [5]$$

In our study of water movement in the plant root, water is considered incompressible, thus, $\bar{\rho}$ is a constant. The gravitational force, g, is the only contributor to the body force, $\boldsymbol{f}$. Under these conditions,

$$\int_{\mathscr{V}_f} \bar{\rho} \boldsymbol{f} \, \mathrm{d}\mathscr{u} = \int_{\mathscr{V}} \theta \rho_\ell \mathbf{g} \mathrm{d}\mathscr{u} \ , \qquad [6]$$

where θ is porosity. Water transport in a plant root is considered as saturated flow, therefore θ equals to the volume fraction of water.

The second term in equation [5] can be written as

$$\int_{\mathscr{S}_f} \boldsymbol{t}\cdot\boldsymbol{n} \, \mathrm{d}\mathscr{a} = \int_{\mathscr{S}_e} \boldsymbol{t}\cdot\boldsymbol{n} \, \mathrm{d}\mathscr{a} + \int_{\mathscr{S}_i} \boldsymbol{t}\cdot\boldsymbol{n} \, \mathrm{d}\mathscr{a} \qquad [7]$$

by applying equation [4]. The first term on the right hand side of equation [7] is the force between the liquid phase in volume $\mathscr{V}$ and the surrounding liquid phase. It is equal to the hydrostatic pressure,

$$\boldsymbol{t}\Big|_{\mathscr{S}_e} = p\mathbf{I} \ , \qquad [8]$$

where p is the hydrostatic pressure, and $\mathbf{I}$ is a second rank unit tensor. The second term on the left hand side of equation [7] is the force exerted on the liquid phase by the solid phase at the liquid–solid interface. The force between the liquid and the solid phase can be divided into two components: the component normal to the interface that is due to the hydrostatic pressure, and the component tangential to the interface, i.e., the sheer stress, that is due to the viscous friction. Mathematically, this is expressed as

$$\boldsymbol{t}\Big|_{\mathscr{S}_e} = -\,p\mathbf{I}\Big|_{\mathscr{S}_e} + -\,\mu\boldsymbol{d}\Big|_{\mathscr{S}_e} \quad , \qquad [9]$$

where μ is the viscosity coefficient. The minus signs on the right hand side of equation [9] indicate that the force being considered is imposed on the liquid phase by the solid phase. The rate–of–deformation tensor, $\boldsymbol{d}$, is related to the velocity gradient by

$$\boldsymbol{d} = \tfrac{1}{2}(\nabla\boldsymbol{v}+\nabla\boldsymbol{v}') \quad . \qquad [10]$$

Combining equations [7]–[9] and [4] results in

$$\int_{\mathscr{S}_f} \boldsymbol{t}\cdot\boldsymbol{n}\ \mathrm{d}\mathscr{a} = \int_{\mathscr{S}_f} p\mathbf{I}\cdot\boldsymbol{n}\ \mathrm{d}\mathscr{a} + \int_{\mathscr{S}_i} \mu\boldsymbol{d}\cdot\boldsymbol{n}\ \mathrm{d}\mathscr{a} \quad . \qquad [11]$$

We assume that the tangential stress at the liquid–liquid boundary, $\mathscr{S}_e$, is small compared to the contribution from the liquid–solid interface, thus,

$$\int_{\mathscr{S}_i} \mu\boldsymbol{d}\cdot\boldsymbol{n}\ \mathrm{d}\mathscr{a} = \int_{\mathscr{S}_f} \mu\boldsymbol{d}\cdot\boldsymbol{n}\ \mathrm{d}\mathscr{a} \quad . \qquad [12]$$

Combining equations [5], [6], [11], and [12] results in

$$\int_{\mathscr{V}} \theta\rho_w\mathbf{g}\ \mathrm{d}\mathscr{u} - \int_{\mathscr{S}_f} p\mathbf{I}\cdot\boldsymbol{n}\ \mathrm{d}\mathscr{a} - \int_{\mathscr{S}_f} \mu\boldsymbol{d}\cdot\boldsymbol{n}\ \mathrm{d}\mathscr{a} = 0 \quad . \qquad [13]$$

Applying the divergence theorem to convert the surface integrals to the volume integrals, equation [13] becomes

$$\int_{\mathscr{V}} \theta\rho_w \mathbf{g}\, d\mathscr{u} + \int_{\mathscr{V}_f} \nabla p\, d\mathscr{u} + \int_{\mathscr{V}_f} \mu\nabla\cdot\boldsymbol{d}\, d\mathscr{u} = 0 \ . \qquad [14]$$

According to equation [2], the macroscopic quantities p and **d** may be defined by

$$\nabla p = \frac{1}{\nabla} \int_{V_f} \nabla p\, d\mathscr{u} \qquad [15]$$

and

$$\nabla\cdot\mathbf{d} = \frac{1}{\nabla} \int_{V_f} \nabla\cdot\boldsymbol{d}\, d\mathscr{u} = \frac{1}{\nabla} \int_{S_i} \boldsymbol{d}\cdot\boldsymbol{n}\, d\mathscr{a} \ , \qquad [16]$$

where S_i is the liquid–solid interface in V. It can be shown that the relation corresponding to equation [14] for these macroscopic quantities written as

$$\int_{\mathscr{V}} \theta\rho_\ell \mathbf{g}\, d\mathscr{u} + \int_{\mathscr{V}} \theta\nabla p\, d\mathscr{u} + \int_{\mathscr{V}} \theta\mu\nabla\cdot\mathbf{d}\, d\mathscr{u} = 0 \ , \qquad [17]$$

so that

$$\rho_\ell \mathbf{g} - \nabla p - \mu\nabla\cdot\mathbf{d} = 0 \ . \qquad [18]$$

Equation [18] is the momentum balance equation for the liquid phase in a porous medium. The first term represents gravity, the second term is the gradient of hydrostatic pressure. These two terms together are the driving force for water movement. The third term in equation [18] is the friction between the moving liquid and the solid phase. This term reduces to zero when there is no water movement as suggested by equation [10]. To derive the constitutive relation of water transport in a porous medium, it is necessary to further examine this term.

We start by considering the motion of water in a hypothetical pore as shown in figure 3.1. A plant root consists of the assembly of many such pores extending throughout the solid phase. The water transport property of the plant root is the macroscopic average of the

behavior of the individual pores. The pore considered here is a hypothetical pore used to illustrate the basic physical principles involved. This pore may be considered as part of a continuous path that a water molecule follows as it moves through the pore space in a plant root. The magnitude of the total viscous frictional force between the moving fluid and the side wall of the pore, t_f , is expressed as

$$t_f = \mu \int_v |\nabla \cdot \boldsymbol{d}| \, d\boldsymbol{\alpha} \, , \qquad [19]$$

where v is the volume of the pore. For a cylindrical pore, the integration of equation [19] results in

$$t_f = \frac{8\mu l}{\bar{\rho} r^2} \, q \, , \qquad [20]$$

where r is the radius of the pore, l is the length of the pore, and q is the rate of discharge of water through the pore. This is the Poiseuille equation (Hillel, 1982). The proportionality between t_f and q can readily be shown for a number of other types of pores, such as rectangular, elliptic, etc.

Assuming that the linear relation between t_f and q can be extended to arbitrary pores in a porous medium results in

$$t_{f,j} = \mu k_j q_j, \; j = 1, 2, 3, \cdots, \qquad [21]$$

where the subscript j denotes the j–th pore, and k_j is a proportionality constant, given by equation [20] for a cylindrical pore. Let e_j be a unit vector located at the center of the j–th pore along the direction defined by the line connecting its two end points, such as indicated in figure 3.1, v_j be the volume of the j–th pore, and a_j be the cross sectional area of the j–th pore. The following local vector quantities can then be defined

$$t_{f,j} = - \frac{t_{f,j}}{v_j} \, e_j \, , \qquad [22]$$

and

$$\boldsymbol{q}_j = \frac{q_j}{a_j}\, \boldsymbol{e}_j \ . \qquad [23]$$

Equations [21]–[23] suggest

$$\boldsymbol{t}_{f,j} = -\frac{\mu k_j a_j}{v_j}\, \boldsymbol{q}_j \ . \qquad [24]$$

The macroscopic water flux, $\mathbf{q}$ can be calculated by combining equations [2] and [23] as follows:

$$\mathbf{q} = \frac{1}{\nabla} \int_{V_f} \boldsymbol{q}\ \mathrm{d}\boldsymbol{\omega} = \sum_{j=1}^{N} \boldsymbol{q}_j v_j = \sum_{j=1}^{N} q_j \frac{v_j}{a_j}\, \boldsymbol{e}_j \ , \qquad [25]$$

where N is the total number of pores in volume V. The macroscopic quantity for the viscous friction between the liquid and the solid phases is calculated by combining equations [16], [19], and [24], resulting in

$$\nabla\cdot\mathbf{d} = \frac{1}{\nabla} \int_{V_f} \nabla\cdot\boldsymbol{d}\ \mathrm{d}\boldsymbol{\omega} = \frac{1}{\mu} \sum_{j=1}^{N} \boldsymbol{t}_{f,j} v_j = -\sum_{j=1}^{N} k_j q_j \boldsymbol{e}_j \ . \qquad [26]$$

Assuming that a linear relation analogous to equation [24] also exists on the macroscopic scale produces

$$\nabla\cdot\mathbf{d} = -\, R\cdot\mathbf{q} \ , \qquad [27]$$

where $\mathbf{R}$ is a constant, second–rank tensor. This is so only if

$$\sum_{j=1}^{N} k_j q_j \boldsymbol{e}_j = R \cdot \sum_{j=1}^{N} q_j \frac{v_j}{a_j}\, \boldsymbol{e}_j \qquad [28]$$

over an elementary volume of the porous medium. For an isotropic porous medium, equation [28] is independent of the spatial directions, leading to

$$R = R\mathbf{I} \ . \qquad [29]$$

where R is a constant, and $\mathbf{I}$ is a unit second–rank tensor. Equation [28] becomes, for an isotropic porous material,

$$R = \frac{\sum_{j=1}^{N} k_j q_j e_j}{\sum_{j=1}^{N} q_j \frac{v_j}{a_j} e_j} = \text{constant} \ . \qquad [30]$$

$\boldsymbol{R}$ and R are called the resistivity tensor and the resistivity coefficient, respectively. For the simplest case of cylindrical pore geometry, equation [30] becomes

$$R = \frac{\sum_{j=1}^{N} (r_j^2 l_j \nabla p \cdot e_j) e_j}{\sum_{j=1}^{N} (r_j^4 l_j \nabla p \cdot e_j) e_j} \ . \qquad [31]$$

Letting

$$\mathbf{k} = R^{-1} \qquad [32]$$

and

$$k = R^{-1} \ , \qquad [33]$$

and substitution of equations [27] and [32] into equation [18] results in

$$\mathbf{q} = - \frac{\mathbf{k}}{\mu} \cdot (\nabla p - \rho_\ell \mathbf{g}) \ , \qquad [34]$$

which is Darcy's law. The $\mathbf{k}$ in equation [34] is the permeability tensor. For an isotropic material, equation [34] becomes

$$\mathbf{q} = - \frac{k}{\mu} (\nabla p - \rho_\ell \mathbf{g}) \ , \qquad [35]$$

where k is the permeability coefficient. Since axial water transport in a plant root is approximated as a one–dimensional flow, equation [35] can be used to describe axial water transport in plant roots.

Axial water transport in the apoplast pathway

Water moves in a plant root via the apoplast and symplast pathways. Assuming that Darcy's law is applicable and that the effect of gravitational force is negligible compared to that of the water potential

gradient, the equation of axial water transport for the apoplast pathway is written as

$$q_a = -\frac{k_a}{\mu}\frac{\partial \Psi_a}{\partial x} , \qquad [36]$$

where q_a is the axial water flux in the apoplast, k_a is axial water permeability of the apoplast, μ is the viscosity coefficient of water, Ψ_a is the apoplast water potential, and x is the spatial distance along the root axis.

The apoplast of the root deforms during root elongation. We assume that the deformation during root elongation results only in macroscopic volume changes in the apoplast but the microscopic pore structure remains constant on a statistical basis so that the apoplast water permeability, k_a, in equation [36] remains constant during growth. This requires that the statistical relation between the microscopic pore structure and macroscopic water permeability described by equation [30] does not change during root elongation.

For our study, it is desirable to write equation [36] in the material coordinate system which deforms along with the growing root. Equation [36] in the material coordinate system becomes

$$Q_a = -\frac{k_a}{\mu}\frac{1}{J}\frac{\partial \Psi_a}{\partial X} , \qquad [37]$$

where Q_a is flux in the material coordinate system, X is the material coordinate, and J is the Jacobian defined by

$$J(X,t) = \frac{\partial x}{\partial X} . \qquad [38]$$

Letting

$$K_a = \frac{k_a}{J(X,t)} , \qquad [39]$$

where K_a is the axial apoplast water permeability in the material

coordinate, equation [37] is written as

$$Q_a = - \frac{K_a}{\mu} \frac{\partial \Psi_a}{\partial X} \quad . \qquad [40]$$

The material coordinate, X, is related to the spatial distance along the root axis, x, by

$$x = x(X(\tau), t), \text{ for } \tau \leq t \quad , \qquad [41]$$

where t is present time and τ is past time. The relation described by equation [41] depends, not only on the current conditions of the root at time t, but also on its past history of growth.

Axial water transport in the symplast pathway

Analogous to equations [36] and [4], the equations of axial water transport for the symplast pathway are written as

$$q_s = - \frac{k_s}{\mu} \frac{\partial}{\partial x} (P + s_x \Pi) \qquad [42]$$

for the spatial coordinate system and

$$Q_s = - \frac{K_s}{\mu} \frac{\partial}{\partial X} (P + s_x \Pi) \qquad [43]$$

for the material coordinate system, where q_s and Q_s are the axial water flux in the symplast for the spatial and material coordinate systems, respectively, k_s and K_s are the axial water permeability of the symplast for the spatial and material coordinate systems, respectively, P is turgor potential, Π is osmotic potential, and s_x is the plant cell membrane reflection coefficient in the axial direction. When $s_x \longrightarrow 0$, presumably in the well developed phloem elements, equation [42] describes the axial water transport in the symplast pathway as driven by turgor potential gradient (Fiscus, 1975; Newman, 1976). By defining

$$\Psi_{sx} = P + s_x \Pi = P - s_x CRT \quad , \qquad [44]$$

where C is solute concentration, R is the universal gas constant, and T is absolute temperature, equations [42] and [43] formally resemble equations [36] and [37].

The assumption of constant axial water permeability in the spatial coordinate system, however, cannot be made for the symplast. The symplast pathway consists of cytoplasms of individual cells bounded by the cytoplasm membranes and interconnected by plasmodesmata. Equation [31] suggests that the contribution of individual pores to the resistivity coefficient is proportional to r^{-2}. The radius of cytoplasm in a plant tissue is typically in the order of micrometers while the radii of plasmodesmata are in the order of nanometers. Thus, the ratio between the contribution of cytoplasm and the contribution of plasmodesmata to the resistivity coefficient of the symplast pathway is in the order of 10^{-6}. Although these are only crude estimates, they clearly indicate that the contribution by cytoplasm to the symplast resistance to water flow is negligible. The total resistance in the symplast pathway between any two points depends only on the number of cytoplasm membranes encountered and the size and number of plasmodesmata on the cytoplasm membranes as water flows from cell to cell.

Consider two material points X_a and X_b along the root axis. Since these material points are fixed on the root, the root segment between X_a and X_b corresponds to the same group of cells during elongational growth. The sum in equation [28] remains unchanged during root elongation, assuming that the size and number of plasmodesmata on the membranes of these cells does not change. Letting $\Psi_{sx,a}$ and $\Psi_{sx,b}$ denote the symplast water potential at X_a and X_b, respectively, the axial

water flux in the symplast pathway is

$$Q_a = - \frac{1}{\mu R'_s(X_b,X_a)} \frac{\Psi_{sx,b} - \Psi_{sx,a}}{X_b - X_a} , \qquad [45]$$

where $R'_s(X_a,X_b)$ is the total symplast resistance to axial water transport over the distance between X_a and X_b . According to the argument in the previous paragraph, R'_s will remain constant during elongational growth. Considering the limit of $(X_b - X_a) \rightarrow 0$ in the macroscopic sense, equation [45] becomes equation [43] where the symplast water permeability at an arbitrary material point X is defined as

$$K_s(X) = \lim_{\delta X \rightarrow 0} \frac{1}{R'_s(X-\delta,X+\delta)} . \qquad [46]$$

The permeability of the symplast pathway in the material coordinate system, as defined in equation [46], is constant during elongational growth. Similar to equation [39], the permeability to axial water transport in the symplast pathway in the material and the spatial coordinate systems are related by

$$K_s(X) = \frac{k_s}{J(X,t)} . \qquad [47]$$

There is an important difference between the two pathways. For the symplast pathway, K remains constant during elongational growth while for the apoplast pathway, k remains constant during elongational growth (Passioura, 1984a,b).

Water transport between the two pathways

In addition to axial flow in both pathways, water moves laterally between the two pathways. The apoplast and symplast pathways in a plant tissue are separated by cytoplasm membranes. A plant tissue

consists of an assemblage of discrete cells. The mathematical description of water transport between the two pathways on the macroscopic scale is obtained by considering the water transport across the cytoplasm membranes of individual cells.

The rate at which water flows across the cytoplasm membrane of a cell is proportional to the total water potential difference between the cytoplasm and the cell wall,

$$q'_{as,j} = L_{m,j} a_{m,j} (\psi_{a,j} - \psi_{s\ell,j}) \ , \qquad [48]$$

where q'_{as} is the rate of flow, L_m is the membrane conductance, a_m is the area of the cytoplasm membrane, and ψ_a is the total water potential of the apoplast. The quantity $\psi_{s\ell}$ is defined by

$$\psi_{s\ell} = P + s_\ell \Pi \ , \qquad [48a]$$

where s_ℓ is the reflection coefficient of the cell membrane separating the symplast and the apoplast pathway. The membrane reflection coefficient s_ℓ is assumed to be different from s_x because of the existence of plasmodesmata for cell–to–cell transport of water in the symplast pathway. The subscript j in equation [48] refers to the j–th cell in a volume V.

We define a microscopic flow density over the volume of the j–th cell, $v_{c,j}$, as

$$q_{as,j} = \frac{L_{m,j} \frac{a_{m,j}}{\mu} (\psi_{a,j} - \psi_{s\ell,j})}{v_{c,j}} \ . \qquad [49]$$

The macroscopic flow density function, q_{as} , is calculated as

$$q_{as} = \frac{1}{V} \int_V q_{as} d\mathcal{V} = \frac{\sum_{j=1}^{N} q_{as,j} v_{c,j}}{\sum_{j=1}^{N} v_{c,j}} \ , \qquad [50]$$

where N is the total number of cells in volume V. Substituting equation [49] into equation [50] yields, after rearranging,

$$q_{as} = \frac{\frac{1}{N}\sum_{j=1}^{N}\left[(L_{m,j}\ \frac{a_{m,j}}{\mu v_{c,j}})(\psi_{a,j} - \psi_{s\ell,j})v_{c,j}\right]}{\frac{1}{N}\sum_{j=1}^{N} v_{c,j}} . \qquad [51]$$

When a macroscopic quantity is calculated, it is assumed that N is large. Thus, the averages calculated in the numerator and in the denominator of equation [51] are equal to their respective statistical expectations, so that

$$q_{as} = \frac{E\left[(L_m\ \frac{a_m}{\mu v_c})(\psi_a - \psi_{s\ell})v_c\right]}{E(v_c)} , \qquad [52]$$

where E( ) refers to statistical expectation. Assuming that ψ_a, $\psi_{s\ell}$, and L of individual cells in an elementary macroscopic volume of a plant tissue are statistically independent of the sizes of individual cells, equation [51] becomes

$$q_{as} = \frac{E(L_m\ \frac{a_m}{\mu v_c})E\left[(\psi_a - \psi_{s\ell})v_c\right]}{E(v_c)} . \qquad [53]$$

The macroscopic symplast and apoplast water potential are defined similar to equation [50], as

$$\Psi_a = \frac{1}{V}\int_V \psi_a\ d\mathcal{V} = \frac{\sum_{j=1}^{N} \psi_{a,j} v_{c,j}}{\sum_{j=1}^{N} v_{,j}} \qquad [54]$$

and

$$\Psi_{s\ell} = \frac{1}{V}\int_V \overline{\Psi}_{s\ell}\, d\mathcal{V} = \frac{\sum_{j=1}^{N} \psi_{s\ell,j} v_{c,j}}{\sum_{j=1}^{N} v_{c,j}} \quad . \qquad [55]$$

It can easily be shown by combining equations [53]—[55] that

$$q_{as} = \frac{1}{\mu}\left[E(L_m \frac{a_m}{v_c})\right](\Psi_a - \Psi_{s\ell}) \quad . \qquad [56]$$

Setting

$$k_{as} = E(L_m \frac{a_m}{v_c}) \quad , \qquad [57]$$

the equation for water transport between the two pathways is

$$q_{as} = \frac{k_{as}}{\mu}(\Psi_a - \Psi_{s\ell}) \quad , \qquad [58]$$

where k_{as} is the permeability between the two pathways. This is the equation governing water transport between the apoplast and the symplast pathways.

The macroscopic water permeability between the two pathways, k_{as}, is a function of the size and shape distribution of individual cells in a plant tissue. The cells in a plant root elongate primarily in the axial direction during root elongation, changing both the size and the shape of the cells. As a result, the water permeability between the two pathways is constant along the root axis.

To derive an expression of k_{as} as a function of growth along a root axis, we consider the ideal case where cells are cylindrical with their axies lined up with the root axis. We Assume that the axial lengths of the cells initially are the same as their diameters and that the volume fraction of the symplast remains constant during cell elongation. Under these assumptions, it can be shown that

$$\frac{a_{m,j}}{v_{c,j}} = \frac{\bar{\omega}_{s,j}}{r_{c,j}} \left[2 + \frac{2r_{c,j}}{l_{c,j}} \right] , \qquad [59]$$

where the subscript j refers to the j-th cell, $\bar{\omega}_s$ is the volume fraction of the symplast for the cell, r_c is the cell radius, and l_c is the length of the cell after elongation.

The quantities involved in equations [57] and [59] may vary from cell–to–cell on the microscopic scale. In calculating the macroscopic water permeability between the two pathways as given by equation [57], the statistical expectations were taken over the cells in a local region of the plant tissue. The cells in such a local region would have the same origin. It is reasonable to assume that any variation of the parameters are random. Defining

$$L_{ma} = E(L_m) , \qquad [60a]$$

$$r_{ca} = E(r_c) , \qquad [60b]$$

and

$$\omega_s = E(\bar{\omega}_s) , \qquad [60c]$$

and substituting equations [60] and [59] into [57] yields

$$k_{as} = \frac{L_{ma}\,\omega_s}{r_{ca}} \left[2 + E\left(\frac{2r_c}{l_c}\right) \right] . \qquad [61]$$

In equation [61], $2r_c$ is the initial axial length of a cell in the root, and l_c is the length after growth. The ratio between the two is the inverse of the axial elongation of the cell. The statistical average of the axial deformation of individual cells is the macroscopic elongation of the root in the axial direction,

$$E\left(\frac{2r_c}{l_c}\right) = \frac{dX}{dx} = \frac{1}{J} . \qquad [62]$$

Substitution of equation [62] into equation [61] yields the final expression

for the macroscopic water permeability between the two pathways in a growing plant root,

$$k_{as} = \frac{L_{ma}\omega_s}{r_{ca}} \left[2 + \frac{1}{J} \right] . \qquad [63]$$

The water flux between the two pathways in the spatial coordinate system, q_{as} in equation [58], has the dimension of density. If we let Q_{as} denotes the corresponding quantity in the material coordinate system, the two are related by

$$Q_{as} = J\ q_{as} . \qquad [64]$$

Combining equations [58], [63] and [64] results in

$$Q_{as} = \frac{K_{as}}{\mu} (\Psi_a - \Psi_{s\ell}) , \qquad [65]$$

where

$$K_{as} = J\ k_{as} = \frac{L_{ma}\omega_s}{r_{ca}}(2J + 1) \qquad [66]$$

is the water permeability between the apoplast and symplast pathways in the material coordinate system. Unlike the axial water permeability coefficients for the apoplast and symplast, the permeability for water transport between the two pathways varies during growth in both the spatial and material coordinate systems.

Water uptake from the soil

Water moves from soil to the surface of the plant root according to water potential gradient. Assuming cylindrical geometry, the water flux toward root surface is given by

$$q'_{sr} = \frac{2\pi r}{\mu} k_{sl}(\Psi) \frac{\partial \Psi}{\partial r} , \qquad [67]$$

where r is the radial distance from the center of the root, k_{sl} is the soil permeability to water which is a function of soil water potential, Ψ is

soil water potential, and q'_{sr} is the rate of water uptake by the plant root in units of mass per unit root length per unit time. Under steady state conditions, q'_{sr} is a constant. Assuming the following boundary conditions,

$$\Psi\Big|_{r=r_r} = \Psi_a \qquad [68a]$$

and

$$\Psi\Big|_{r=r_d} = \Psi_{sl} \ , \qquad [68b]$$

where r_r is the radius of the root, r_d is some distance from the root surface where soil water potential is a constant, Ψ_a is the apoplast water potential of the root, and Ψ_{sl} is the water potential of the bulk soil. Equation [67] is integrated, resulting in

$$q'_{sr} = -\frac{k'_{sr}}{\mu}(\Psi_a - \Psi_{sl}) \ , \qquad [69]$$

where k'_{sr} is a function of both Ψ_a and Ψ_{sl},

$$k'_{sr} = \frac{2\pi}{\ell n\left[\frac{r_d}{r_r}\right](\Psi_a - \Psi_{sl})} \int_{\Psi_a}^{\Psi_{sl}} k_{sl}(\Psi)d\Psi \ . \qquad [70]$$

The rate of water uptake, q'_{sr}, in equation [69] has the units of mass per unit root length per unit time. To convert this into the units of mass per unit volume per unit time, we divide q'_{sr} by the cross sectional area of the root,

$$q_{sr} = \frac{q'_{sr}}{\pi r_r^2} = -\frac{k_{sr}}{\mu}(\Psi_a - \Psi_{sl}) \ , \qquad [71]$$

where

$$k_{sr} = \frac{k'_{sr}}{\pi r_r^2} \qquad [72]$$

is the water permeability at the root–soil boundary. The rate of water

uptake in a material coordinate system is expressed as

$$Q_{sr} = -\frac{K_{sr}}{\mu}(\Psi_a - \Psi_{si}) \ , \qquad [73]$$

where K_{sr}, the water conductance at the root–soil interface in the material coordinate system, is related to k_{sr} by

$$K_{sr} = k_{sr} \ J \ . \qquad [74]$$

Equations [71] and [72] are the governing equations for plant root water uptake from soil. The conductance at the root–soil interface depends on both the properties of the root and the properties of the soil. The properties of the root involved in the conductance are the radius of the root and the root apoplast water potential. The properties of the soil involved are the bulk soil water potential and the soil water permeability function.

The continuity equations

The transport equations derived in the previous section describes the instantaneous rates of water transport. Continuity equations are needed to describe the dynamic processes of water transport during root growth as functions of time.

We start our discussion with the mass balance of water in the apoplast. Similar arguments apply to water in the symplast.

Consider the section of a plant root between two material points, X_a and X_b. The principle of mass balance states that the change in the total mass of water in the apoplast of the root segment between X_a and X_b is equal to the total amount of water flowing in minus the total amount of water flowing out of the system. Mathematically, this is expressed by

$$\frac{d}{dt}\int_{X_a}^{X_b} (\rho_\ell \omega_a \theta_a) dx = q_a\Big|_{X_a} - q_a\Big|_{X_b} - \int_{X_a}^{X_b} q_{as} dx + \int_{X_a}^{X_b} q_{sr} dx \ , \qquad [75]$$

where ω_a is the volume fraction of the apoplast, and θ_a is the porosity of the apoplast. The left hand side of equation [75] is the rate of change of the total mass of water in the apoplast between X_a and X_b. On the right hand side of equation [75], the first and the second terms are the axial water flow at X_a and X_b, respectively, the third term is water flow from the apoplast to the symplast, and the fourth term is water uptake from the soil. In equation [75], X_a and X_b are material points fixed to the root which move along with the plant root as a root elongates. In a spatial coordinate system, these end points are functions of time.

To avoid differentiating the limits of integration, we convert equation [75] into a material coordinate system in which X_a and X_b become constant. In a material coordinate system, equation [75] becomes

$$\frac{d}{dt}\int_{X_a}^{X_b} (\rho_w \omega_a \theta_a) J dX = Q_a\Big|_{X_a} - Q_a\Big|_{X_b} - \int_{X_a}^{X_b} Q_{as} dX + \int_{X_a}^{X_b} Q_{sr} dX \ . \qquad [76]$$

For our purpose, ρ_ℓ, ω_a, and θ_a are assumed to be constant. Since the limits of integration are constants in equation [76], we can switch the order of differentiation and integration on the left hand side of equation [76]. After dividing both sides of equation [76] by $X_b - X_a$ and then taking the limit as $X_b \longrightarrow X_a$, equation [76] becomes

$$(\rho_\ell \omega_a \theta_a)\frac{dJ}{dt} = -\frac{\partial Q_a}{\partial X} - Q_{as} + Q_{sr} \ . \qquad [77]$$

The Jacobian, J, for plant root elongation as a one–dimensional process equals the ratio between initial length of an infinitesimal root

segment and its length after growth. If we define the axial deformation of a root segment with a length ℓ by

$$\dot{\epsilon} = \frac{1}{\ell}\frac{d\ell}{dt} , \qquad [78]$$

then it can be shown that the local rate of deformation at a material point X along the root axis is expressed as

$$\dot{\epsilon} = \frac{1}{J}\frac{dJ}{dt} . \qquad [79]$$

Substituting equations [40], [65], [73], and [79] into equation [77] results in, after rearranging,

$$\frac{\partial}{\partial X}(K_a \frac{\partial \Psi_a}{\partial X}) - K_{as}(\Psi_a - \Psi_{s\ell}) - K_{sr}(\Psi_a - \Psi_{sl}) - (\mu\rho_\ell\omega_a\theta_a)J\dot{\epsilon} = 0 , \qquad [80]$$

where K_a, K_{as}, and K_{sr} are given by equations [39], [66], and [74], respectively. It can be shown that the equation of mass balance in the spatial coordinate system for the apoplast pathway is

$$\frac{\partial}{\partial x}(k_a \frac{\partial \Psi_a}{\partial x}) - k_{as}(\Psi_a - \Psi_{s\ell}) - k_{sr}(\Psi_a - \Psi_{sl}) - (\mu\rho_\ell\omega_a\theta_a)\dot{\epsilon} = 0 , \qquad [81]$$

where k_a, k_{as}, and k_{sr} are defined by equations [36], [63], and [72], respectively.

The continuity equations for water transport in the symplast are derived following similar arguments. The resulting equations are

$$\frac{\partial}{\partial X}(K_s \frac{\partial \Psi_{sx}}{\partial X}) + K_{as}(\Psi_a - \Psi_{s\ell}) - (\mu\rho_\ell\omega_s)J\dot{\epsilon} = 0 \qquad [82]$$

for the material coordinate system and

$$\frac{\partial}{\partial x}(k_s \frac{\partial \Psi_{sx}}{\partial x}) + k_{as}(\Psi_a - \Psi_{s\ell}) - (\mu\rho_\ell\omega_s)\dot{\epsilon} = 0 \qquad [83]$$

for the spatial coordinate system. The axial permeability of the root symplast to water, K_s, in the spatial coordinate system and k_s in the material coordinate system, are given by equations [47] and [42],

respectively.

Equations [80]–[83] are the governing equations for axial water transport in the plant root. The equations for the apoplast and symplast pathways are coupled and must be solved simultaneously. These equations can be solved either in the spatial or material coordinate system along with appropriate boundary conditions. The solutions in the two coordinate systems are equivalent.

Boundary conditions

The boundary conditions for the systems of equations for water transport are given at the tip of the root and at the base of the root. The origin of the material coordinate system is defined at the base of the root. It is assumed that the apoplast and symplast water potentials at the base of the root are the same and are equal to the xylem water potential,

$$\Psi_a = \Psi_x \quad \text{for } X = 0 \qquad [84a]$$

and

$$\Psi_{s\ell} = \Psi_x \quad \text{for } X = 0 \ , \qquad [84b]$$

where Ψ_x is the xylem water potential which must be specified. In the most general case, Ψ_x may be specified as a function of time to reflect plant water potential change in response to the changing transpiration demands.

The boundary conditions must also be specified at the tip of the root. The root meristem is located at the tip of the root. At this point water must flow through the apoplast and symplast pathways to the meristem to meet the requirement of cellular division in the meristem.

Thus,

$$(\omega_a K_a \frac{\partial \Psi_a}{\partial X} + \omega_s K_s \frac{\partial \Psi_{sx}}{\partial X})\Big|_{X(t)} = -\mu\rho_\ell(\omega_{sm} + \omega_{am}\theta_a)\aleph(t) \ , \qquad [85a]$$

where X(t) denotes the position of the root tip in the material coordinate system which is a function of time, and $\aleph(t)$ is the rate at which new root elements are produced by the meristem. An additional boundary condition at the root tip is obtained by considering the mass balance of the symplast pathway. The requirement for water by the growing symplast in the meristem is satisfied by axial water transport through the symplast pathway and water uptake from the apoplast. Therefore

$$(L_{mstm}K_{as}(\Psi_{s\ell} - \Psi_a) + \omega_s K_s \frac{\partial \Psi_{sx}}{\partial X})\Big|_{X(t)} = -\mu\rho_\ell\omega_{sm}\aleph(t) \ . \qquad [85b]$$

Similar relations can be written for the spatial coordinate system. It should be noted that J=1 at the tip of the root because elongation of cells in a plant root starts at the root tip, hence the deformation at the root tip is zero.

The continuity equations and the corresponding boundary conditions define the system of differential equations that describe axial water transport in the plant root. The system can be solved to produce water potential distribution in each of the two pathways of the plant root along the axis of a growing plant root. Soil water potential affects water status of a plant root by directly affecting the water potential gradient across the soil–plant interface and the permeability through the interface. The model presented above can be used to examine effects of soil water

potential, the morphological properties of plant roots, as well as the rate of root elongation on the water potential distributions along the root axis.

CONCLUSION

A mathematical model was presented that describes the coupled transport of water in the apoplast and symplast pathways of a plant root. Transport of water in both pathways was described by Darcy's law. Mathematical descriptions of the permeabilities in both pathways were derived from considerations of the fundamental morphological properties of the root. The systems of the water transport equations can be solved under prescribed growth and soil water potential conditions to evaluate the effects of soil water stress, membrane permeability, cell size, and the rate of root elongation on the water status of the root. The mathematical model developed in this study can also serve as part of a dynamic plant root growth model, along with models of solute transport and cell growth, to simulate the dynamic interactions between water transport, solute transport, and root growth. Such a model is presented in the latter part of this thesis.

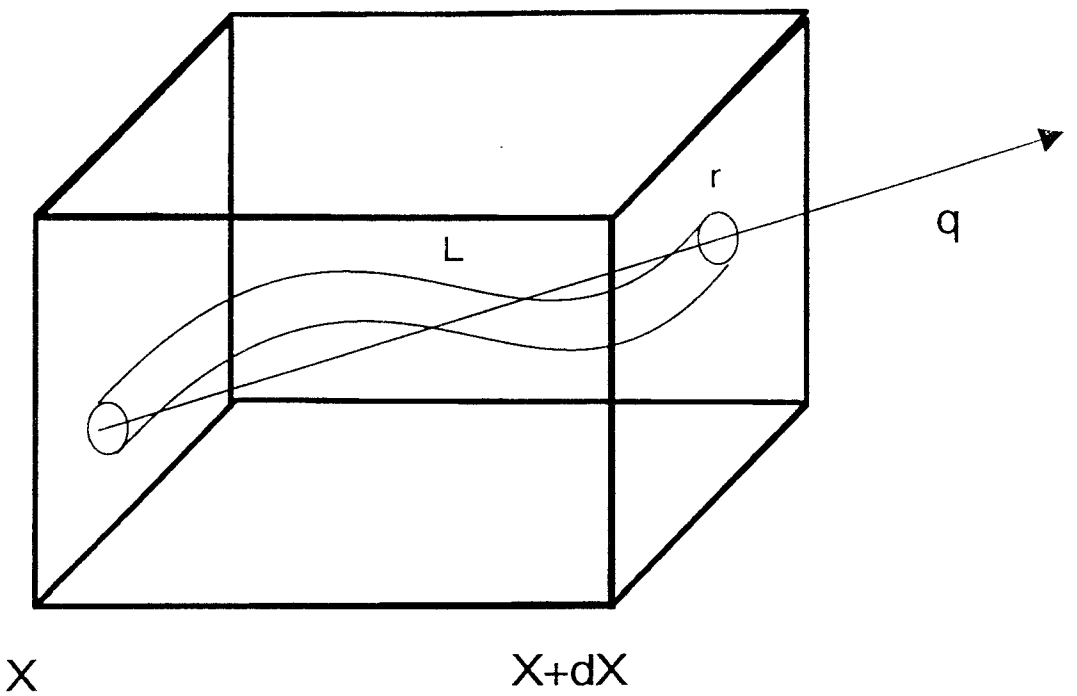

Figure 3.1. Diagram illustrating the water transport through a single hypothetical pore in a porous medium.

LIST OF SYMBOLS AND UNITS

$\mathbf{d}$	rate of deformation tensor	s^{-1}
$\mathbf{f}$	body force	N kg^{-1}
$\mathbf{g}$	gravitational force	N kg^{-1}
k	permeability coefficient	kg m^{-1}
$\mathbf{k}$	permeability tensor	kg m^{-1}
k_a	apoplast permeability in spatial coordinate system	kg m^{-1}
k_s	symplast permeability in spatial coordinate system	kg m^{-1}
k_{as}	permeability between the two pathways in spatial coordinate system	kg m^{-1}
k'_{sr}	soil to root boundary permeability	kg m^{-1}
k_{sr}	volume averaged soil–root boundary permeability	kg m^{-3}
m	an arbitrary quantity	
$\mathbf{n}$	a unit vector	dimensionless
p	hydroscopic pressure	N m^{-2}
$\mathbf{q}$	macroscopic water flux	m s^{-1}
q_a	apoplast water flux in spatial coordinate system	kg m^{-2} s^{-1}
q_{sr}	volume averaged soil–root water flux	kg m^{-3} s^{-1}
s_x	axial membrane reflection coefficient	dimensionless
s_ℓ	membrane reflection coefficient between apoplast and symplast pathways	dimensionless

$\mathbf{t}$	surface traction tensor	$N\ m^{-2}$
$\mathbf{v}$	velocity	$m\ s^{-1}$
C	solute concentration	$mol\ m^{-3}$
$\mathbf{I}$	identity tensor	dimensionless
J	Jacobian	dimensionless
K_a	apoplast permeability in material coordinate system	$kg\ m^{-1}$
K_{as}	permeability between the two pathways in material coordinate system	$kg\ m^{-3}$
K_s	symplast permeability in material coordinate system	$kg\ m^{-1}$
K_{sr}	soil–root permeability in material coordinate system	$kg\ m^{-1}$
L_{mstm}	length of the meristem	m
P	turgor potential	$N\ m^{-2}$
$\mathbf{Q}_a$	apoplast water flux in material coordinate system	$kg\ m^{-2}\ s^{-1}$
$\mathbf{Q}_{as}$	water flux between the two pathways in material coordinate system	$kg\ m^{-3}\ s^{-1}$
$\mathbf{Q}_s$	symplast water flux in material coordinate system	$kg\ m^{-2}\ s^{-1}$
Q_{sr}	volume averaged soil–root water flux in material coordinate system	$kg\ m^{-3}\ s^{-1}$
R	universal gas constant	$J\ mol^{-1}K^{-1}$
T	temperature	$^{\circ}K$
V	an elementary volume	m^3

V_f	volume in V occupied by fluid	m^3
a	cross sectional area of a pore	m^2
a_m	area of membrane of a cell	m^2
$\boldsymbol{d}$	microscopic rate of deformation tensor	s^{-1}
$\boldsymbol{e}$	microscopic unit vector	dimensionless
$\boldsymbol{f}$	microscopic body force	N kg^{-1}
k	proportionality constant between rate of discharge and viscous friction in a pore	m^2 kg^{-1}
l	pore length	m
l_c	length of a cell	m
$\boldsymbol{n}$	microscopic unit vector	dimensionless
p	microscopic hydrostatic pressure	N m^{-2}
q	rate of water discharge though a pore	kg s^{-1}
$\boldsymbol{q}$	rate of water discharge vector in a pore	kg s^{-1}
q_{as}	membrane flux averaged over cell volume	kg m^{-3} s^{-1}
q'_{as}	water flux across a cell membrane	kg s^{-1}
q'_{sr}	water flux from soil to root	kg m^{-2} s
r	pore radius	m
r_c	radius of a cell	m
r_{ca}	averaged cell radius	m
$\boldsymbol{t}$	microscopic surface traction tensor	N m^{-2}
t_f	magnitude of viscous friction at fluid–solid boundary of a pore	N
t_f	viscous frictional force in a pore	N
v	volume of a pore	m^3
$\boldsymbol{v}$	microscopic velocity vector	m s^{-1}

v_c	cell volume	m^3
L_m	cell membrane permeability	kg m^{-1}
L_{ma}	averaged membrane permeability	kg m^{-1}
$\boldsymbol{R}$	macroscopic resistivity tensor	m kg^{-1}
R	macroscopic resistivity coefficient	m kg^{-1}
R_s	symplast resistivity	m kg^{-1}
μ	viscosity coefficient	kg m^{-1} s^{-1}
ω_s	volume fraction of symplast	dimensionless
$\overline{\omega}_s$	volume fraction of symplast of a cell	dimensionless
ω_{sm}	volume fraction of symplast in meristem	dimensionless
ω_{am}	volume fraction of apoplast in meristem	dimensionless
θ	porosity	dimensionless
ρ_ℓ	density of water	kg m^{-3}
$\overline{\rho}$	microscopic water density	kg m^{-3}
$\psi_{s\ell}$	symplast flow potential between the two two pathways in a cell	N m^{-2}
Π	osmotic potential	N m^{-2}
Ψ_a	apoplast water potential	N m^{-2}
Ψ_{sx}	axial symplast flow potential	N m^{-2}
$\aleph$	rate of material production in meristem	m s^{-1}

LITERATURE CITED

Bertaud, D. S., and P. W. Gandar, 1985. Referential descriptions of cell proliferation in roots illustrated using *Phleum pratense L.* Bot. Gaz., 146:275–287.

Boyer, J. S., 1985. Water transport. Ann. Rev. Plant Physiol., 36:473–516.

Boyer, J. S., 1988. Cell enlargement and growth–induced water potentials. Physiol. Plant., 73:311–316.

Carmona, M. J., and A. Cuadrado, 1986. Analysis of growth components in Allium roots. Planta, 168:183–189.

Dalton, F. N., P. A. C. Raats, and W. R. Gardner, 1975. Simultaneous uptake of water and solutes by plant roots. Agron. J., 67:334–339.

Fiscus, E. L., 1975. The interaction between osmotic– and pressure–induced water flow in plant roots. Plant Physiol., 55:917–922.

Gardner, W. R., 1960. Dynamic aspects of water availability to plants. Soil Sci., 89:63–73.

Hanson, P. J., Sucoff E. I., and Markhart A. H., 1985. Quantifying apoplast flux through red pine root systems using tri–sodium, 3–hydroxy–5, 8, 10–pyrenetri–sulfonate. Plant Physiol., 77:21–24.

Hillel, D., 1982. Introduction to soil physics. Academic press, New York. 364pp.

Kramer, P. J., 1983. Water relations of plants. Academic Press, Orlando. 189pp.

Lang A. R. G., and W. R. Gardner, 1970. Limitation to water flux from soil to plants. Agron. J., 62:693–695.

McCoy, E. L., and L. Boersma, 1984. The principles of continuum mechanics applied to transport processes and deformation in plant tissue. J. Tehor. Biol., 111:687–705.

McCully, M. E.. and M. J. Canny, 1988. Pathways and processes of water and nutrient movement in roots. Plant and Soil, 159–170.

Molz, F. J., 1976. Water transport through plant tissue: the apoplasm and symplasm pathways. J. Theor. Biol., 59:277–292.

Molz, F. J., and J. S. Boyer, 1978. Growth induced water potentials in plant cells and tissues. Plant Physiol., 62:423–429.

Moon, G. J., B. F. Clough, C. A. Peterson, and W. G. Allaway, 1986. Apoplastic and symplastic pathways in *Avicenia merina (Forsk) Vierh.* roots reveled by fluorescent tracer dyes. Aust. J. Plant Physiol., 13:637–648.

Newman, E. I., 1976. Interaction between osmoti– and pressure– induced water flow in plant roots. Plant Physiol., 57:738–739.

Passioura, J. B.. 1980. The transport of water from soil to shoot in wheat seedlings. J. Exp. Bot., 31:333–345.

Passioura, J. B.. 1984a. Hydraulic resistance of plants. I. Constant or variable? Aust. J. Plant. Physiol., 11:333–339.

Passioura, J. B.. 1984b. Hydraulic resistance of plants. II. Effects of rooting medium, and time of day, in barley and lupin. Aust. J. Plant Physiol., 11:341–350.

Passioura, J. B.. 1988. Water transport in and to roots. Ann. Rev. Plant Physiol., 39:245–265.

Phillip, J. R., 1957. The physical principles of soil water movement during the irrigation cycle. Proc. Int. Congr. Irrig. Drain..

8:125–154.

Raats, P. A. C., and A. Klute, 1968a. Transport in soils: the balance of mass. Soil Sci. Soc. Am. Proc., 32:161–166

Raats, P. A. C., and A. Klute, 1968b. Transport in soils: the balance of momentum. Soil Sci. Soc. Am. Proc., 32:452–456.

Reicosky, D. C., Ritchie J. T., 1976. Relative importance of soil resistance and plant resistance in root water absorption. Soil Sci. Soc. Am. Proc., 40:293–297.

Silk, W. K., and R. O. Erickson, 1979. Kinematics of plant growth. J. Theor. Biol., 76:481–501.

Silk, W. K., and K. K. Wagner, 1980. Growth sustaining water potential distributions in the primary corn root. A noncompartmental continuum model. Plant physiol., 66:859–863.

Sposito, G., 1978a. The statistical mechanical theory of water transport through unsaturated soil. 1. The conservation laws. Water Res. Res., 14:474–478.

Sposito, G., 1978b. The statistical mechanical theory of water transport through unsaturated soil. 2. Derivation of the Buckingham–Darcy flux law. Water Res. Res., 14:479–484.

St. Aubin, G., Canny M. J., and McCully M. E., 1986. Living vessel elements in the late metaxylem of sheathed maize roots. Ann. Bot., 58:577–588.

Turner, N. C., 1986. Adaptation to water deficits: a changing perspective. Aust. J. Plant Physiol., 13:175–190.

Turner, N. C., 1987. Crop water deficits: a decade of progress. Adv. Agron., 39:1–51.

4. TRANSPORT OF SOLUTE IN A GROWING ROOT

Yongsheng Feng and Larry Boersma
Department of Soil Science, Oregon State University
Corvallis, OR 97331

ABSTRACT

Solute transport is necessary for maintaining plant growth. Transport of carbohydrates in a multicellular plant tissue, such as a root, occurs in the symplast pathway. The convection–dispersion equation which is generally used for describing solute transport processes in porous media has been used in the past to describe solute transport process in plant tissues. However, such application has not been fully justified.

A plant tissue differs from an ordinary porous medium, such as soil, because of the existence of the semipermeable cell membranes and the active solute transport processes that occur across these membranes. In this manuscript, mathematical descriptions of solute transport processes in a multicellular plant tissue at the macroscopic scale were developed from considerations of mechanisms of solute transport that occur across the cell membranes and in the cytoplasm of individual cells. The mechanisms of solute transport in the cytoplasm include facilitated diffusion, dispersion, and convection. The mechanisms of solute transport across the membranes separating the individual cells include, in addition, enzyme mediated active transport. Also, the process of convective transport depends on the reflection coefficient of the membranes.

The mathematical equation derived in this manuscript which

describes the solute transport process in a multi–cellular plant tissue at the macroscopic scale formally resemble the traditional convection–dispersion equation, with an additional active transport term. The apparent coefficient of dispersion (D_d) and the coefficient of active transport (D_a) are expressed explicitly ad functions of solute permeability of the membranes (D_m), solute dispersion coefficient in the cytoplasm (D_o), and the average size of the cells (d_{ci}). The coefficient of convection (D_q) depends, in addition, on the reflection coefficient of the membranes (s_x).

When the dispersion coefficient in the cytoplasm dominates ($D_o >> D_m$), the apparent coefficient of dispersion in the material coordinate system remains constant during growth, the coefficient of convection reaches its minimum value of $1–s_x$, and the active transport process reaches maximum efficiency with $D_a=1$. At the other extreme, when the permeability of the membranes dominates ($D_m >> D_o$), the behavior of a plant tissue in terms of solute transport would approach that of an ordinary porous medium. The apparent dispersion coefficient in the spatial coordinate system approaches constant ($d_d=D_o$), the coefficient of dispersion reaches its maximum value ($D_q=1$), and the coefficient of active transport becomes zero. A plant tissue generally lies between these two extremes. Calculations assuming identity between $1–D_d$ and s_x leads to under–estimate of the the membrane reflection coefficient. The magnitude of the error depends on the relative magnitude of D_m and D_o. These analysis provide at least partial explanations for the low values of membrane reflection coefficient often reported in the literature.

INTRODUCTION

Plant growth depends on the adequate transport and distribution of nutrients and carbohydrates. Inorganic nutrients absorbed from soil by the root systems are transported to the upper parts of the plant. At the same time, products of photosynthesis, i.e. carbohydrates must be transported from the upper part of the plant to the roots. The long distance transport of carbohydrates from the upper part of the plant to the root occurs by mass flow in the phloem, driven by the turgor potential gradient. The short distance transport of the carbohydrate in regions where the phloem system has not been developed, such as near the apex of a root, must rely on cell to cell transport across the membranes (Canny, 1971; Tyree and Dainty, 1975; Nobel, 1983; Reinhold and Kaplan, 1984).

Mechanisms of solute transport in a multi–cellular tissue generally include carrier mediated diffusion (Nobel, 1983), mass flow (Canny, 1971; Christy and Ferrier, 1973; Tyree and Dainty, 1975; Reinhold and Kaplan, 1984), and energy requiring active transport (Luttge and Pitman, 1976; Stein, 1977; Reinhold and Kaplan, 1984). Movement of solutes by molecular diffusion alone is often inadequate to satisfy the requirements for solute transport in a plant tissue, even for a short distance (Tyree and Dainty, 1975; Nobel, 1983).

Diffusion of solutes across the cell–to–cell membrane barrier is believed to be assisted by carriers (Stein, 1977; Feher, 1983; Nobel, 1983). Inside the plasmalemma membrane, solute diffusion is assisted by the streaming motion of the cytoplasm. These processes are referred to as

facilitated diffusion (Nobel, 1983). Chen and Russel (1989) reported that facilitated diffusion increased the rate of transport of glutamine in bacterial cells at least 1000 fold. Mass flow is the process in which solutes are transported by the moving fluid. This is by far the most important mechanism of long distance solute transport. Tyree and Dainty (1975) calculated that a mere 10^{-6} m s^{-1} flow rate in the phloem produces a solute flux 100 times greater than that due to diffusion. For cell–to–cell transport of solute in a multi–cellular tissue, mass transport may also be an important factor. However, the amount of the solute that is carried by water flux in the symplast pathway may be limited by the reflection coefficients of the membranes. Evidences of active transport include sensitivity to metabolic inhibitors (Gayler and Glasziou, 1972; De Mechelis et al., 1978) and temperature dependence, with Q_{10} values in the range commonly found for metabolic processes (Wyse, 1979; Thorne, 1982). For both facilitated diffusion and active transport, the relationship between the rate of transport and the substrate concentration often resembles the Michaelis–Menten equation (Cleland, 1970; Stein, 1977; Komor et al., 1981; Nobel, 1983) although the exact meaning of the parameters may be quite complicated, depending on the assumptions used in deriving the models (Reinhold and Kaplan, 1984).

It has been shown in the past that a plant tissue may be regarded as a mathematical continuum despite the fact that it is composed of discrete cellular entities (Silk and Erickson, 1979; Silk, 1984). The continuum concept has been applied to the mathematical description of the patterns of growth (McCoy and Boersma, 1984), patterns of cell proliferation (Bertaud and Gandar, 1985) and the patterns of synthesis of

cytoplasm and cell wall components (Silk and Erickson, 1980; Silk et al., 1984; Silk et al., 1986), as well as transport of water (Silk and Wagner, 1980). However, its use in describing the transport of solutes in a multi–cellular plant tissue has not been attempted.

Past researches regarding transport of solutes in plants have focused on the phloem transport (Canny, 1971; Tyree and Dainty, 1975; Milburn and Kallarackal, 1989) and mechanisms and kinetics at the cellular level (Reinhold and Kaplan, 1984; Madore and Lucas, 1989). Continuum theory is a macroscopic theory. When used to describe the transport of solute in a plant tissue, it describes solute movement on a scale many times larger than that of the individual cells without being concerned about the cell–to–cell variations. However, detailed derivation and interpretation of such a continuum model of solute transport must be based on consideration of the cellular structures of plant tissues.

Transport of solutes in a porous medium, in a continuum sense, is often described by the well–established convection–dispersion equation (Nielsen, 1986). The convection term describes the motion of solute as a result of bulk flow of the fluid phase. The dispersion term describes the motion of solute resulting from molecular diffusion and hydrodynamic dispersion. McCoy and Boersma (1984) assumed plant tissue to be a porous medium and applied the convection–dispersion equation to describe the solute motion in the plant tissue. Justifications of such assumptions were not discussed.

In this work, we derive mathematical descriptions of solute transport in a plant root as a one–dimensional continuum. Specific considerations are given to the relationships between the macroscopic

description of solute transport and the fundamental processes at the cellular level.

THEORY

Discussions of solute transport processes in a growing multi–cellular plant tissue can be performed from two equivalent perspectives: the material and spatial coordinate systems (Silk and Erickson, 1979; Chapter 1). The material coordinate system corresponds to the cellular structure of the root and moves along with the growing tissue. Thus, in a material coordinate system, one focuses on the behavior of specific material points. A spatial coordinate system is fixed in space. A specific point in such an spatial coordinate system may correspond to different material points as the plant tissue grows. Thus, in a spatial coordinate system, one focuses on the events at specific points in the space. Equivalence between the descriptions in the two systems is assured by the space and material equivalence and continuity requirements in defining such coordinate systems (Chapter 1). Discussions in this work focus on the description of solute transport near the apex of a growing plant root in a material coordinate system. Corresponding relations in a spatial coordinate system are presented.

The following convention of notations are used. Capital letters are used to denote quantities in the material coordinate system. Corresponding quantities in the spatial coordinate system are denoted by lower case letters. Vector and tensor quantities, such as velocity and flux, are denoted by **bold** face symbols. Scalar quantities, such as density, are denoted by symbols of normal face. Quantities at the cellular level are denoted by *italic* letters. When an italic letter corresponding to a specific symbol is not available, a bar over the symbol, e.g., $\bar{\rho}$, will be used to

denote the microscopic quantity.

Equations of transport

Different processes occur at the barrier separating the cells and in the cytoplasm in terms of solute transport. In the following discussions, the barrier for solute transport between individual cells, consisting of plasmalemma membranes and connecting plasmodesmata, will be referred to as plasmodesmata membrane (Molz, 1976), or simply membrane. Processes that occur at the plasmodesmata membrane include facilitated diffusion through the plasmodesmata, active transport, and mass flow. Processes that occur in the cytoplasm include facilitated diffusion, hydrodynamic dispersion, and mass flow. The solute transport by mass flow at the plasmodesmata membrane is limited by the reflection coefficient of the membrane, while inside the cytoplasm there is no such limitation. These processes are illustrated in figure 4.1, where a plant root is simplified as consisting of a single file of cells.

Let x_{-i} and x_{+i} denote the material coordinate at the two sides of the i–th membrane and c_{-i} and c_{+i} denote the corresponding solute concentration. The solute flux through the membrane due to facilitated diffusion is assumed to be proportional to the concentration difference across the membrane. Mathematically, this is expressed by

$$\mathbf{q}^{d}_{c,i} = - D_m(c_{+i} - c_{-i})\mathbf{i} \ , \qquad [1]$$

where $\mathbf{q}^{d}_{c,i}$ is the solute flux through the i–th membrane by facilitated diffusion, D_m is the coefficient of facilitated diffusion through the membrane, and $\mathbf{i}$ is a unit vector along the root axis pointing toward the positive direction of the material coordinate system. In addition to

facilitated diffusion, solutes may also move across the membrane carried by the bulk flow of water in the symplast pathway. The flux of solute across the membrane by this mechanism is expressed by

$$q^{m}_{c,i} = (1-s_x) q_{s,i} c_{-i} \quad , \qquad [2]$$

where $q^{m}_{c,i}$ denotes the solute flux across the i–th membrane due to mass flow, s_x is the membrane reflection coefficient in the axial direction of the root, and $q_{s,i}$ is the symplast water flux across the i–th membrane. The s_x is specifically referred to as the reflection in the axial direction because the reflection coefficient for axial, cell–to–cell, solute transport may differ from that for the lateral transport between symplast and apoplast pathways as a result of the existence of plasmodesmata for the cell–to–cell solute transport. The third mechanism by which solutes may travel across the membrane is active transport. It is assumed that the rate of active transport at the membrane is a function of solute concentration next to it, whereby

$$q^{a}_{c,i} = A(c_{-i})\mathbf{i} \quad . \qquad [3]$$

Studies have demonstrated that the function $A(c)$ generally resembles the Michaelis–Menten equation (Reinhold and Kaplan, 1984). For simplicity, the exact functional form of $A(c)$ will not be expressed explicitly in the following discussions.

The total solute flux across the i–th membrane is the sum of the contributions from facilitated diffusion, mass flow, and active transport,

$$q_{c,i} = -D_m(c_{+i} - c_{-i})\mathbf{i} + (1-s_x) q_{s,i} c_{-i} + A(c_{-i})\mathbf{i} \quad . \qquad [4]$$

The solute concentration difference across the membrane is obtained by rearranging equation [4],

$$\Delta c_i = \frac{-q_{c,i} + (1-s_x)\, q_{s,i} c_{-i} + A(c_{-i})}{D_m} , \qquad [5]$$

where $\Delta c_i=(c_{+i}-c_{-i})$, $q_{c,i}$ is the magnitude of $\boldsymbol{q}_{c,i}$, and $q_{s,i}$ is the magnitude of $\boldsymbol{q}_{s,i}$.

The total solute flux through the cytoplasm space bounded by membranes stated in the material coordinate system is

$$\boldsymbol{q}_c = - D_o \frac{\partial c}{\partial x} \mathbf{i} + \boldsymbol{q}_{s,i} c , \qquad [6]$$

where x represents spaces between two membranes separating individual cells, and D_o is the coefficient of facilitated diffusion within the cytoplasm. The total concentration difference across the cytoplasm space bounded by the i and the i+1 −th membranes is calculated as

$$\Delta c_{i,i+1} = \int_{x_{+i}}^{x_{-i+1}} \frac{-q_c + q_{s,i} c}{D_o} \, dx . \qquad [7]$$

Our goal is to derive a relationship between the concentration gradient and the solute flux along the root axis at the macroscopic scale. To do this, consider the ideal plant root consisting of a single file of cells as illustrated in figure 4.1. Let Δc denote the macroscopic concentration difference between x and x+Δx along the root axis. Then Δc is the sum of the concentration differences across all the cell membranes between x and x+Δx plus the sum of the concentration differences in the cytoplasm of all cells located between x and x+Δx. Mathematically, this is expressed as

$$\Delta c = \sum_i \Delta c_i + \sum_i \Delta c_{i,i+1} . \qquad [8]$$

Substituting equations [5] and [7] into [8] yields:

$$\Delta c = \sum_i \left[\frac{-q_{c,i} + (1-s_x)\, q_{s,i} c_{-i} + A(c_{-i})}{D_m} \right] + \int_{\Delta x_s} \frac{-q_c + q_{s,i} c}{D_o} \, dx ,$$

[9]

where Δx_s represents all the spaces between x and x+Δx occupied by cytoplasm. Under steady state conditions, all solutes that enter a cell from one end will exit from the other, as does water. Thus, solute and water fluxes throughout the distance from x to x+Δx are uniform. This condition is expressed as

$$\begin{cases} q_c = q_{c,i} = q_c \\ q_s = q_{s,i} \end{cases} \quad 0<i<n \ , \qquad [10]$$

where n is the total number of cells between x and x+Δx. Under these conditions, equation [9] is rewritten

$$\Delta c = \sum_i \left[\frac{-q_c + (1-s_x) q_s c_{-i} + A(c_{-i})}{D_m} \right] + \int_{\Delta x_s} \frac{-q_c + q_s c}{D_o} dx \ . \qquad [11]$$

Letting c be the macroscopic quantity representing the average solute concentration between X and X+ΔX, the integration in equation [11] can be approximated by

$$\int_{\Delta x_s} \frac{-q_c + q_s c}{D_o} dx = \frac{-q_c + q_s c}{D_o} \Delta x_s \ . \qquad [12]$$

During the axial growth of a plant root, the distance between any two spatial points may represent different groups of cells at different times when the root elongates since the cells move along the root axis during elongation. Thus, summation and the integration in equations [11] and [12] may depend on time. It is desirable to write equations [11] and [12] in the material coordinate system where the coordinate system moves along with the root during growth so that the root segment between any two points in such a coordinate system always represents the same group

of cells. The equivalents of equations [11] and [12] in the material coordinate system are

$$\Delta C = \sum_i \left[\frac{-Q_c + (1-s_x) Q_s C_{-i} + A(C_{-i})}{D_m} \right] + \int_{\Delta X_s} \frac{-Q_c + Q_s C}{D_o} J dX \qquad [13]$$

and

$$\int_{\Delta X_s} \frac{-Q_c + Q_s C}{D_o} J \, dX = \frac{-Q_c + Q_s C}{D_o} J \Delta X_s \, , \qquad [14]$$

where J is the Jacobian between the two coordinate systems defined by

$$J = \frac{dx}{dX} \, . \qquad [15]$$

Substituting equation [14] into equation [13] and then carrying out the summation yields, after rearranging,

$$\frac{\Delta C}{\Delta X} = -Q_c \left[\frac{1}{D_m} \frac{N}{\Delta X} + \frac{J}{D_o} \frac{\Delta X_s}{\Delta X} \right] + Q_s \left[\frac{(1-s_x)}{D_m} \frac{\Sigma C_{-i}}{\Delta X} + \frac{J}{D_o} \frac{\Delta X_s}{\Delta X} C \right] + \frac{\Sigma A(C_{-i})}{D_m \Delta X}, \qquad [16]$$

where N is the total number of cells between X and X+ΔX. It can be shown that at the macroscopic scale,

$$\frac{1}{N} \Sigma C_{-i} \simeq C \qquad [17]$$

and

$$\frac{1}{N} \Sigma A(C_{-i}) \simeq A(C) \, . \qquad [18]$$

Substituting equations [17] and [18] into equation [16] results in

$$\frac{\Delta C}{\Delta X} = -Q_c \left[\frac{1}{D_m} \frac{N}{\Delta X} + \frac{J}{D_o} \frac{\Delta X_s}{\Delta X} \right] + C Q_s \left[\frac{(1-s_x)}{D_m} \frac{N}{\Delta X} + \frac{J}{D_o} \frac{\Delta X_s}{\Delta X} \right] + \frac{A(C)}{D_m} \frac{N}{\Delta X} \, . \qquad [19]$$

In deriving equation [19], N is the total number of cells between X and X+ΔX. The average length of the cells is defined as

$$d_c = \frac{\Delta x}{n} = \frac{\Delta X}{N} J \ . \qquad [20]$$

At the initial undeformed state, i.e., at the moment before cell elongation starts, J=1, thus,

$$\frac{N}{\Delta X} = \frac{1}{d_{ci}} \ . \qquad [21]$$

Another quantity in equation [16] that needs further explanation is $\Delta X_s/\Delta X$ which is the proportion of space occupied by the cytoplasm in the material coordinate system. Assuming that the cells are isotropic before elongation starts, this quantity is equal to the volume fraction of the cytoplasm in the initial undeformed state. As the cells elongate, the fraction of space in the axial direction that is occupied by the cytoplasm increases, since the change in the thickness of the lateral cell walls is negligible compared to the total increase in the axial dimension of the cells. It can be shown, assuming the lateral cell wall thickness remains constant during cell elongation, that

$$\frac{\Delta X_s}{\Delta X} = 1 - \frac{1}{J} \omega_{ai} \ , \qquad [22]$$

where $\omega_{ai} = 1 - \omega_{si}$ is the initial volume fraction of apoplast. Substituting equations [21] and [22] into equation [19] and then taking the limit as $\Delta X \longrightarrow 0$ at the macroscopic scale results in, after rearranging,

$$Q_c = -D_d \frac{\partial C}{\partial X} + D_q Q_s C + D_a A(C) \ , \qquad [23]$$

where

$$D_d = \frac{d_{ci} D_o D_m}{D_o + D_m d_{ci} (J - \omega_{ai})} \ , \qquad [24]$$

$$D_q = 1 - \frac{s_x D_o}{D_o + D_m d_{ci} (J - \omega_{ai})} \ , \qquad [25]$$

and

$$D_a = \frac{D_o}{D_o + D_m d_{ci}(J-\omega_{ai})} \quad . \qquad [26]$$

In the following discussions, D_d is referred to as the apparent dispersion coefficient, D_q as the convection coefficient, and D_a as the active transport coefficient. Since the actual rate of active transport in equation [23] is the product of D_a and the rate of active transport process at the membrane, A(C), D_a can be regarded as the coefficient of efficiency of the active solute transport process. These are the parameters that determine the solute transport process at the macroscopic scale. In vector notation, equation [23] is written as

$$\mathbf{Q}_c = -D_d \frac{\partial C}{\partial X} \mathbf{I} + D_q \mathbf{Q}_s C + D_a A(C) \mathbf{I} \quad . \qquad [27]$$

Equation [27] formally resembles the convection–dispersion equation used by McCoy and Boersma (1984), with an additional term describing the process of active transport at the cell membrane. However, instead of the direct application of the convection–dispersion theory of solute transport to the root as a porous medium as proposed by McCoy and Boersma (1984), equation [27] was derived from considerations of the fundamental solute transport processes at the cellular level. The macroscopic parameters that appear in the convection dispersion equation are now all expressed explicitly as functions of the fundamental properties of plant cells in the root, such as size of the cells, facilitated diffusion coefficients both across the cell membranes and within the cytoplasm, as well as an active transport process.

Equation [27] can also be written with respect to the spatial coordinate system, resulting in

$$\mathbf{q}_c = -D_d J \frac{\partial c}{\partial x} \mathbf{i} + D_q \mathbf{q}_s c + D_a A(c) \mathbf{i} \quad . \qquad [28]$$

Equations of mass balance

The transport equations describe the solute flux as a function of the local concentration gradient, the symplast water flux, and an active solute transport process. The mathematical description of the dynamic changes of solute concentration both with time and with the position along the axis of a plant root during root growth are derived from considerations of mass balances.

To start, consider the mass balance of the solute of a root segment bounded by two arbitrary points a and b. Assume that a and b represent material points that move along with the growing root. The total amount of solute within such a root segment is calculated by

$$\int_a^b \mathscr{A}\omega_S C J dX \ , \qquad [29]$$

where $\mathscr{A}$ is the cross–sectional area of the root, ω_S is the volume fraction of the symplast pathway, or the volume fraction of the cytoplasm, and J is the Jacobian. $\mathscr{A}\omega_S$ represents the cross–sectional area of the cytoplasm. Since only the axial transport of the solute is being considered, the net rate of solute transport into the root segment equals the rate at which solute enters this root segment at a minus the rate at which solute leaves the root segment at b. Mathematically, this is expressed as

$$\mathscr{A}\omega_S(Q_{c,a} - Q_{c,b}) = -\int_a^b \mathscr{A}\omega_S \frac{\partial Q_c}{\partial X}\, dX \ . \qquad [30]$$

The total rate of solute consumption within the root segment includes respiration, synthesis of cell walls, and synthesis of cytoplasm components. This is expressed as

$$\int_a^b \mathscr{A}\omega_S(R_r + S_w + S_s)JdX \ , \qquad [31]$$

where R_r is the rate of respiration, S_w is the rate of cell wall synthesis, S_s is the rate of cytoplasm component synthesis, all expressed as moles per unit time per unit volume of cytoplasm.

The law of mass balance dictates that the rate at which the total amount of solute in such a root segment changes with time equals the net rate at which solute enters the segment through its boundaries minus the rate of metabolic solute consumption within the segment. The mathematical statement of the law of mass balance with respect to such an arbitrary root segment is expressed as

$$\frac{\partial}{\partial t}\int_a^b \mathscr{A}\omega_S CJdX = \int_a^b \mathscr{A}\omega_S \frac{\partial Q_c}{\partial X}dX - \int_a^b \mathscr{A}\omega_S(R_r+S_w+S_s)JdX \ . \qquad [32]$$

Since a and b are constants in the material coordinate system, we can move the differentiation with respect to time at the left hand side of equation [32] under the integral sign obtaining, after rearranging,

$$\int_a^b \mathscr{A}\omega_S\left[\frac{\partial}{\partial t}(CJ) + \frac{\partial Q_c}{\partial X} + (R_r+S_w+S_s)J\right]dX = 0 \ , \qquad [33]$$

assuming that the rate at which $\mathscr{A}$ and ω_S change with time are negligible. Because a and b are arbitrary material points along the root axis, equation [33] is true only if

$$\frac{\partial}{\partial t}(CJ) + \frac{\partial Q_c}{\partial X} + (R_r+S_w+S_s)J = 0 \ . \qquad [34]$$

It can be shown that (Chapter 3)

$$\frac{\partial J}{\partial t} = J\dot{\epsilon} \ , \qquad [35]$$

where $\dot{\epsilon}$ is the local rate of axial extension, or local elemental growth rate. Substituting equation [35] into [33] yields

$$J\frac{\partial C}{\partial t} + \frac{\partial Q_c}{\partial X} + (\dot{\epsilon}C + R_r+S_w+S_s)J = 0 \ . \qquad [36]$$

Equation [36], with Q_c given by equations [23]–[26], is the governing equation of axial solute transport in a growing plant root. When the growth field $\dot{\epsilon}$ is specified, equation [36], along with appropriate boundary and initial conditions, can be solved for the axial profile of solute concentration as a function of the position along the root axis.

Under certain circumstances, the spatial description of solute transport may be preferable over the material description. The equation of mass balance in the spatial coordinate system corresponding to equation [36] is written as

$$\frac{\partial c}{\partial t} + \frac{\partial q_c}{\partial x} + (\dot{\epsilon} c + R_r + S_w + S_s) = 0 \ . \qquad [37]$$

Boundary condition at the root tip

Root elongation resulting from production of new cells in a meristem located at the tip of the root and the subsequent elongation of the cells was described mathematically in Chapter 1. The solute requirements of the meristem for growth and metabolism must be satisfied by axial solute transport. As a result of this conceptual description of root growth, the boundary condition for solute transport at the root tip is expressed as

$$Q_c\big|_{tip} = (S_{sm} + S_{wm} + R_{rm}) L_{mstm} \ , \qquad [38]$$

where L_{mstm} is the finite length of the meristem, S_{wm}, S_{sm}, and R_{rm} are the rates of cell wall synthesis, cytoplasm component synthesis, and respiration, in the meristem, respectively.

The boundary condition at the base of the root depends on the

supply of photo–assimilates from the upper part of the plant. In the most general form, this boundary condition may be written as

$$\beta_1 \frac{\partial C}{\partial X} + \beta_2 C + \beta_3 = 0, \quad X=0. \qquad [39]$$

where β_1, β_2, and β_3 may be constants or functions of time, depending on the photosynthesis and translocation processes. The exact form of the mathematical representation of these parameters is beyond the scope of this analysis.

DISCUSSION

This analysis demonstrates that the general form of the convection–dispersion equation which describes solute transport in porous materials may be applied to describe solute transport in a multi–cellular tissue, such as the axial transport of solutes in a plant root. Explicit mathematical expressions were derived which describe the macroscopic parameters that appear in convection–dispersion type equations as functions of properties of the cells. The apparent dispersion coefficient, coefficient of convection, and the coefficient of active transport are functions of coefficients of facilitated diffusion across the cell membranes and in the cytoplasm, as well as the average sizes of the cells.

The implications of the theory developed in this manuscript are illustrated by considering some extreme cases: the membrane limiting transport process characterized by $D_o >> D_m d_{ci}$, the cytoplasm limiting transport process characterized by $D_o << D_m d_{ci}$, and the extreme cases for the membrane reflection coefficient, $s_x=1.0$, and $s_x=0.0$.

Membrane limiting solute transport

The condition $D_o >> D_m d_{ci}$ is equivalent to the statement that the resistance for solute transport results mainly from the membranes separating individual cells. This is likely to be the case in a multicellular tissue where development of phloem systems for solute transport has not begun. In plant roots, the elongation region near the root apex is an example of such an un–differentiated plant tissue. Under these conditions, the apparent dispersion coefficient is approximated by

$$D_d \simeq D_m d_{ci} \quad , \qquad [40]$$

which is equivalent to the statement that the apparent dispersion coefficient in the material coordinate system remains constant during root elongation. For the spatial coordinate, the apparent dispersion coefficient is expressed as

$$d_d \simeq \frac{1}{J} D_m d_{ci} \quad , \qquad [41]$$

which varies during elongation. A similar condition exists for the axial permeability of water in the symplast pathway, which was shown to be approximately a constant in the material coordinate system, but a variable in the spatial coordinate system during root elongation (Chapter 3).

Under the condition of $D_o >> D_m d_{ci}$, the convection coefficient defined by equation [25] is approximated by

$$D_q = 1 - s_x \quad , \qquad [42]$$

which is exactly the same as the expression used by McCoy and Boersma (1984). The active transport coefficient defined by equation [26] becomes

$$D_a = 1 \quad , \qquad [43]$$

which implies that the rate of active solute transport at the macroscopic scale is the same as the active transport rate at the membranes. Since 1 is the maximum value possible for D_a, the condition $D_o >> D_m d_{ci}$ is also the condition for maximum efficiency of the active solute transport mechanism.

Cytoplasm limiting solute transport

This is the case where resistance to solute transport results mainly from the cytoplasm. This condition is equivalent to the hypothetical

condition where the cell–to–cell barrier for solute transport has disappeared. A plant tissue differs from a typical porous material, such as soil, in terms of solute transport because of the existence of membrane barriers. If these barriers did not exist, as implied by the condition $D_o << D_m d_{ci}$, the equation describing the solute transport in plant tissues would reduce to the convection–dispersion equation describing solute transport processes in normal porous materials.

Under the condition of $D_o << D_m d_{ci}$, equations [24]–[26] lead approximately to,

$$D_d = \frac{1}{J} D_o \ , \qquad [44]$$

$$D_q = 1 \ , \qquad [45]$$

$$D_a = 0 \ , \qquad [46]$$

assuming ω_{ai} to be small. Substituting equations [44]–[46] into equation [28] results in a form of the convection–dispersion that is generally used to describe solute transport processes in porous materials, as was expected from the arguments of the previous paragraph.

Convective solute transport and the reflection coefficient

Solute transport due to convection is a function of the membrane reflection coefficient, s_x, as stated by equation [25]. Existence of the membrane generally reduces the efficiency at which the solute is transported by the bulk water flux in the symplast pathway, as is implied by the fact that D_q defined by equation [25] may never be greater than 1.

Membranes completely permeable to the solutes are characterized by $s_x=0$. Under this condition, equation [25] reduces to $D_q = 1$. This may

represent the condition in the phloem elements where solutes are carried by the bulk water flux crossing the sieve plates. At the other extreme, perfectly semipermeable membranes are characterized by $s_x=1$. Under this condition, equation [25] states that as long as the facilitated diffusion across the membrane occurs, represented by $D_m>0$, one still has $D_q>0$. As a result, the convection term in the solute transport equation persists even when $s_x=1$.

If the convection coefficient, D_q, in equation [20] is identified with $1-s_x$ (McCoy and Boersma, 1984), an underestimate of s_x results since the factor multiplying s_x in equation [25] is generally less than 1. The magnitude of the error depends on the relative magnitudes of D_o and D_m. This may be for the values of reflection coefficient often reported in the literature which are apparently too low (Reinhold and Kaplan, 1984; Steudle, Oren and Schulze, 1987).

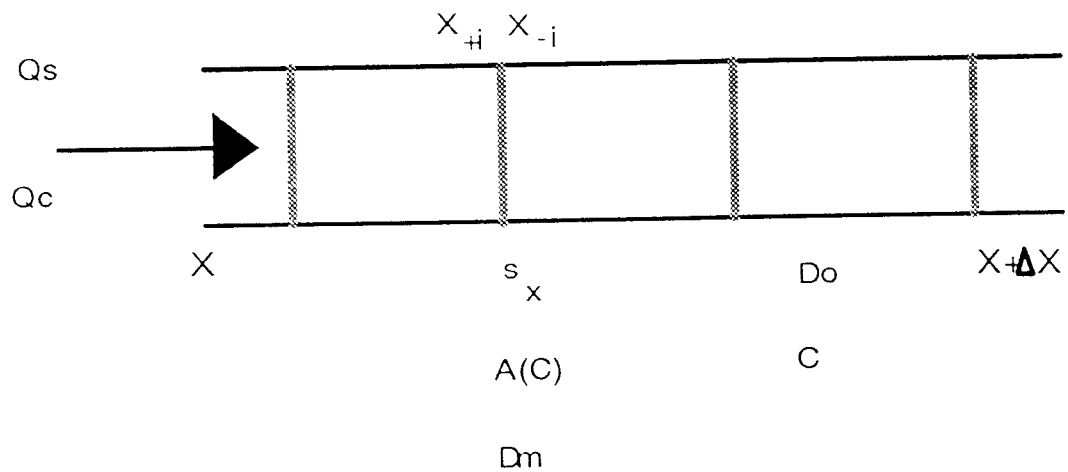

Figure 4.1. Schematic diagram of a plant root idealized as consisting of a single file of cells, illustrating the processes of axial solute transport.

LIST OF SYMBOLS AND UNITS

c	microscopic solute concentration	mol m^{-3}
d_c	average length of cells	m
q_c	solute flux	mol m^{-3}
q_c^a	solute flux by active transport	mol m^{-2} s^{-1}
q_c^d	solute flux by diffusion	mol m^{-2} s^{-1}
q_c^m	solute flux by mass flow	mol m^{-2} s^{-1}
q_s	symplast water flux	m s^{-1}
s_x	axial membrane reflextion coefficient	dimensionless
x	spatial distance	m
x_{+i}	positive side of i–th membrane	m
x_{-i}	negative side of i–th membrane	m
$A(c)$	active transport function	mol m^{-2} s^{-1}
C	solute concentration in material system	mol m^{-3}
D_a	active transport coefficient	dimensionless
D_d	apparent tissue dispersion coefficient	m^2 s_m^{-1}
D_m	membrane dispersion coefficient	m s^{-1}
D_o	cytoplasm dispersion coefficient	m^2 s^{-1}
D_q	convection coefficient	dimensionless
J	Jacobian	dimensionless
L_{mstm}	length of meristem	m
Q_c	solute flux in material system	mol m^{-2} s^{-1}
Q_s	symplast water flux in material system	m s^{-1}
R_r	rate of respiration	mol m^{-3} s^{-1}
S_s	rate of cytoplasm synthesis	mol m^{-3} s^{-1}

S_{sm}	rate of cytoplasm synthesis in meristem	mol m^{-3} s^{-1}
S_w	rate of cell wall synthesis	mol m^{-3} s^{-1}
S_{wm}	rate of cell wall synthesis in meristem	mol m^{-3} s^{-1}
β_1, β_2, β_3	boundary condition coefficients	
$\dot{\epsilon}$	rate of deformation	dimensionless
ω_{ai}	initial volume fraction of apoplast	dimensionless
ω_s	volume fraction of symplast	dimensionless
$\mathscr{A}$	cross sectional area of root	m^2

LITERATURE CITED

Bertaud, D. S., and P. W. Gandar, 1985. Referential descriptions of cell proliferation in roots illustrated using *Phleum pratense L.* Bot. Gaz., 146:275–287.

Canny, M. J., 1971. Translocation: Mechanisms and kinetics. Ann. Rev. Plant Physiol.. 22:237–260.

Chen, G., nd J. B. Russel, 1989. Transport of glutamine by *Streptococcus bovis* and conversion of glutamine to pyroglutamic acid and amonia. J. Bacteriol., 171:2981–2985.

Christy, A. L., and J. M. Ferrier, 1973. A mathematical treatment of Munch's pressure flow hypothesis of phloem translocation. Plant Physiol., 52:531–538.

Cleland, W. W., 1970. Steady state kinetics. In P. D. Boyer (ed.) The enzymes, kinetics and mehanism, II. Academic press, New York. 584pp.

De Mechelis, M. I., M. Radice, R. Columbo, and P. Lado, 1978. Evidences for an active transport of methyl–α–D–glucopyranoside in pea stem segments. Plant Sci. Lett., 12:93–99.

Feher, J. J.. 1983. Facilitated calcium diffusion by intestinal calcium–binding proterin. Am. J. Physiol., 244:303–307.

Gayler, K. R., and K. T. Glasziou, 1972. Carrier mediated active transport of glucose. Plant Physiol., 49:563–568.

Komor, E., M. Thom, and A. Maretzki, 1981. The mechanism of sugar uptake by sugarcane suspension cells. Planta, 153:181–192.

Luttge, U., and M. G. Pitman, 1976. Transport and energy. in Luttge,

U., and M. G. Pitman (ed.) Encycl. Plant Physiol., vol. 2: Transport in plants II, Part A: Cells. Spring–Verlag, Berlin. 400pp.

Madore, M. A., and W. J. Lucas, 1989. Transport of photoassimilates between leaf cells. In D. A. Baker and J. A. Milburn (ed.) Transport of photoassimilates. Longman Sci. Tech., 384pp.

McCoy, L. E., and L. Boersma, 1984. The principles of continuum mechanics applied to transport processes and deformation in plant tissue. J. Theol. Biol., 111:687–705.

McCully, M. E., and M. J. Canny, 1988. Pathways and processes of water and nutrient movement in roots. Plant and Soil, 111:159–170.

Milburn, J. A. and K. Kallarackal, 1989. Physiological aspects of phloem translocation. In D. A. Baker and J. A. Milburn (ed.) Transport of photoassimilates. Longman Sci. Tech., 384pp.

Molz, F. J., 1976. Water transport through plant tissue: the apoplasm and symplasm pathways. J. Theor. Biol., 59:277–292.

Nielsen, D. R., 1986. Water flow and solute transport processes in unsaturated zone. Water Res. Res., 22:89s–108s.

Nobel, P. S., 1983. Biophysical plant physiology and ecology. Freeman and Company, New York. 608pp.

Reinhold, L., and A. Kaplan, 1984. Membrane transport of sugars and amino acids. Ann. Rev. Plant Physiol., 35:45–83.

Silk, W. K., 1984. Quantitative descriptions of development. An. Rev. Plant Phyiol., 35:479–518.

Silk, W. K., and R. O. Erickson, 1979. Kinematics of plant growth. J. Theor. Biol., 76:481–501.

Silk, W. K., and R. O. Erickson, 1980. Local biosynthesis rates of

cytoplasmic constituents in growth tissue. J. Theor. Biol., 83:701–703.

Silk, W. K., R. C. Walker, and J. Labavitch, 1984. Uronide deposition rates in the primary root of *Zea mays*. Plant Physiol., 74:721–726.

Silk, W. K., T. C. Hsiao, U. Diedenhofen, and C. Matson, 1986. Spatial distributions of potassium, solutes, and their deposition rates in the growth zone of the primary corn root. Plant Physiol., 82:853–858.

Stein, W. D., 1977. Testing and characterizing a simple carrier model for co–transport. in M. Kramer and F. Lauterbach (ed.) Intestinal permeation. p. 262–274. Excerpta Medica, Amsterdam. 449pp.

Steudle, E., R. Oren, and E. D. Schulze, 1987. Water transport in maize roots: Measurement of hydrolic conductivity, solute permeability, and of reflection coefficients of excised roots using the root pressure probe. Plant Physiol., 84:1220–1232.

Thorne, J. H., 1982. Characterization of the active sucrose transport system of immature soybean embryos. Plant Physiol., 70:953–958.

Tyree, M. T., and J. Dainty, 1975. Theoretical considerations. in M. H. Zimmermann and J. A. Milnurn (ed.) Encycl. Plant Physiol., vol. 1. Transport in plants I: Phloem transport. Spring–Verlag, Berlin. 535pp.

Wyse, R., 1979. Sucrose uptake by sugar beet tap root tissue. Plant Physiol., 64:837–841.

5. A CONTINUUM MODEL OF PLANT ROOT GROWTH: Model Development

Yongsheng Feng and Larry Boersma
Department of Soil Science, Oregon State University
Corvallis, OR 97331, U.S.A.

ABSTRACT

A plant root may be modeled as a one–dimensional continuum with a meristem located at the root tip. Axial growth of the root is the result of production of new cells by the meristem and the subsequent elongation of these cells. Cell elongation is driven by the physical stress in the cell walls while the rate and the amount of elongation is controlled by the biological processes of cell wall loosening. The physical stress in the cell walls is a function of local water potential components, the axial water potential gradients, as well as the soil resistance to root growth. Under static conditions where there is no axial water potential gradient and the soil resistance is negligible, the physical stress in the cell walls equals the turgor pressure. Equations describing the local rate of elongation as a function of wall stress and the biological wall loosening process described in Chapter 2 of this thesis were modified to include the situation where the rate of biological wall loosening is not a constant. Equations relating cell wall stress to local water potential components, axial water potential gradient, and soil resistance to root growth were derived by considering the force balance of an arbitrary segment of the

root. These equations, along with equations for water and solute transport and the appropriate boundary and initial conditions, define the model for root growth. The implications of the model are discussed and the method of solution is outlined.

INTRODUCTION

Expansion of plant cells involves intimate interaction between biophysical water uptake and biochemical cell wall loosening and synthesis (Lockhart, 1965; Taiz, 1984; Brummell and Hall, 1985; Ray, 1987). In a multicellular tissue, transport of water and solute also plays an important role (Silk and Wagner, 1980; Ho and Baker, 1982; Boyer, 1988).

Much of the research on the biophysics of plant cell growth are based on a mathematical model presented by Lockhart (1965). In this theory, the growth rate of individual cells is controlled by turgor potential, cell wall extensibility and yielding stress. Cell growth ceases as the turgor potential becomes lower than a minimum stress, termed the yielding stress. Above the yielding stress, the rate of growth is proportional to the difference between the turgor potential and the yielding stress. The proportionality constant is termed the wall extensibility. The turgor is the driving force for the cell growth. The cell wall extensibility and the yielding stress are often regarded as properties of the cell wall (Lockhart, 1967; Green, Erickson and Buggy, 1971; Cosgrove, 1986, 1987). Growth of the cell is considered as viscous flow of the cell wall in response to pressure from the symplast. In his analysis, Lockhart (1965) also indicated that turgor potential depends on the rate of water uptake.

Extensive experimental research has been conducted to investigate the effects of environmental and metabolic factors on the parameters in the Lockhart (1965) equation. In *Nitella*, wall extensibility decreases with decreasing osmotic potential of the bathing medium (Green et al., 1971).

Changes of yield stress under water stress have been observed in sunflower leaves (Mathews et. al., 1984). Auxin stimulates growth by increasing the wall extensibility (Cleland, 1971; Green and Cummins, 1977; Boyer and Wu, 1978). The slowing of growth due to aging has also been attributed to decreased extensibility (Green et al., 1971). In addition, tissue extensibility has been observed to change with water stress (Mathews et al., 1984) and light (Van Volkenburgh and Cleland, 1981).

Growth is a process that occurs in living organisms. It is natural to expect that cell growth is under metabolic control. Ray and Ruesick (1962) and Brummell and Hall (1985) demonstrated that plant growth rate decreased immediately in the presence of metabolic inhibitors. In fact, respiration is required for continued growth (Taiz, 1984). Cell metabolic processes control growth, presumably through control of wall extensibility and yielding stress (Green et. al., 1971; Cleland, 1987; Theologis, 1987). The extensibility and yielding stress can not be simply the properties of the cell wall as it is implied by the Lockhart equation (1965). It is difficult to imagine growth in a lifeless cell no matter what the stress in the cell wall may be. Sellen (1982) describes cell growth as biologically controlled creep. However, the question of how this control is achieved remains to be answered .

Models based on the Lockhart (1965) concept fail to recognize the biological control of growth. Plant cells are treated as mechanical objects and growth is simply the response of this mechanical object to the external force. Even though it has been suggested that growth is under metabolic influence (Sellen, 1982; Cleland, 1987; Theologis, 1987), the metabolic mechanisms and their implications have not yet been

incorporated into plant growth models.

The growth of a multicellular tissue involves influences of intercellular transport of water and solutes in addition to tissue deformation. The continuum theory provides a powerful tool (Silk and Erickson, 1979; Plant, 1982; Gandar, 1983a,b; McCoy and Boersma, 1985) for modeling the growth of multicellular tissues. Silk and Erickson (1979) argued convincingly that the continuum theory can be applied to studies of expansive plant growth where cell differentiation is not involved. In an earlier study, Erickson and Sax (1956a,b) successfully applied the continuum assumption to corn root elongation and derived such quantities as local rate of elongation and cell division. To date, most applications of continuum theory to plant growth studies deal with kinematics of growth (Gandar, 1983a,b; Bertaud and Gandar, 1985) and the application of the law of mass conservation (Silk and Erickson, 1980; Silk et. al., 1986) to obtain local rates of synthesis of plant constituents from measurements of concentration distribution and growth pattern. McCoy and Boersma (1985) developed a mathematical model of plant root elongation based on the continuum theory. They considered the root as a conserving system and employed the change of thermodynamic potential energy as the process providing the energy that is driving the process of growth. The influence of water and solute potential was not specifically considered in this model, although it was implied indirectly.

Mathematical models based on the theory initiated by Lockhart (1965) have been developed to consider specifically the growth of multicellular tissues (Grenetz and List, 1973; Cosgrove, 1981; Plant, 1982; McCoy and Boersma, 1985). Most of these models fail to include the

dynamic interactions between water and solute transport and cell growth. In plant root growth, previous modeling efforts have failed to include the influence of soil resistance and to differentiate the different roles played by the meristem and the elongation region (Plant, 1982; McCoy and Boersma, 1985).

In this manuscript, we present a model of axial plant root growth based on the continuum assumption. The conceptual root consists of a meristem located at the root tip, an elongation zone and the mature region. Biological control of growth is achieved by the metabolic strain energy relaxation process (Chapter 2). The dynamic interactions between water uptake and transport, availability and transport of carbohydrates, as well as the effects of soil water stress and soil resistance are considered and simulated in this model. The solution of the model provides the dynamic response of rate of root elongation as well as the growth pattern along the root axis to the changing environmental conditions.

THEORY

The growth of a plant root can be expressed as the deformation of a one–dimensional continuum (Silk and Erickson, 1979; McCoy and Boersma, 1985). The processes involved include cell expansion and division in the meristem, cell elongation in the elongation region, transport of water in the apoplast and symplast pathways, and transport of solute (sugar). The metabolic processes that must be considered include respiration, synthesis and metabolic loosening of the cell wall, and synthesis of the cytoplasm constituents.

Kinematics of root elongation

A set of kinematic equations based on the principles of continuum mechanics were developed in Chapter 1 of this thesis. The equations describe the axial growth of a plant root as the result of cell production in the meristem and subsequent cell elongation in the elongation zone. Some of the important results are summarized below.

In continuum mechanics terms, a plant root is considered a one–dimensional continuum consisting of material points distributed continuously along the root axis. The growth of the plant root is described by the motion of these material points through space. The material points along a root axis are identified by the time at which they were produced by the meristem,

$$X = X(t') \ , \qquad [1]$$

where $t' \leq t$ is the past time. The spatial positions of these material points during root growth as a function of time are expressed by

$$\mathbf{x} = \mathbf{x}[\mathbf{X}(t'),\ t],\quad t' \leq t\ , \qquad [2]$$

where $\mathbf{x}$ denotes the spatial position along the root axis. The axial growth pattern of the root can be completely described once the functional relation in equation [2] is specified.

It was demonstrated in Chapter 1 that the axial growth of a plant root is characterized by two functions: the rate of cell production ($\aleph(t')$), and, at any moment t, the ratio between the length of cells produced at $t' \leq t$ and their initial length, $\Lambda(t',t)$. It follows from these definitions that the Jacobian between the spatial and material descriptions of root growth are defined as

$$J = \frac{dx}{dX} = \Lambda(t',t)\ , \qquad [3]$$

and the local rate of strain or the local rate of relative cell elongation is given as

$$\dot{\varepsilon}(t',t) = \frac{1}{\Lambda(t',t)} \frac{\partial \Lambda(t',t)}{\partial t} = \frac{1}{J} \frac{\partial J}{\partial t}\ . \qquad [4]$$

With these relations, the spatial position of any material point, as stated by equation [2], is expressed by

$$\mathbf{x}[(\mathbf{X}(t'),t] = \int_0^{t'} \aleph(g)\Lambda(g,t)dg\ . \qquad [5]$$

The total length of the root is calculated by

$$L(t) = \int_0^{t} \aleph(g)\Lambda(g,t)dg\ , \qquad [6]$$

and the rate of root elongation represented by

$$\mathbf{v}(t) = \int_0^{t} \aleph(g)\frac{\partial \Lambda(g,t)}{\partial t}dg + \aleph(t)\ . \qquad [7]$$

In a dynamic model of plant root growth, $\aleph(t')$ and $\Lambda(t',t)$ can be calculated using constitutive relations of meristem growth and cell elongation. The growth pattern along the root axis can then be calculated

using the above outlined kinematic equations.

Equations of cell elongation

Growth, or the deformation of a plant tissue occurs when cell walls are physically stressed and the biochemical wall loosening process is taking place. Neither of the two processes, physical stress or wall loosening can result in growth without the presence of the other. A cell wall cannot be loosened unless it is stressed, and permanent growth or deformation cannot take place without the cell wall loosening process.

Plant cell walls have the properties of viscoelastic materials (Sellen, 1980). As the cell walls are stressed, energy is stored in the cell walls in the form of strain energy. The total strain energy of the cell wall consists of two parts: elastic strain energy (E_e) and viscoelastic strain energy (E_v). The elastic strain energy (E_e) represents the energy stored in strong bonds of the cell wall polymers, mostly covalent bonds. The viscoelastic strain energy (E_v) represents the energy stored in weak bonds, mostly hydrogen bonds between polymers (Ferry, 1970; Chapter 2). When under stress, weak bonds rearrange spontaneously into lower energy states through a break and reform process. As a result, the viscoelastic strain energy is dissipated. For a simple viscoelastic material, the viscoelastic strain energy is dissipated by a first degree process (Chapter 2)

$$\left.\frac{dE_v}{dt}\right|_{disp} = -\frac{2}{\tau} E_v \ , \qquad [8]$$

where τ (sec) is the time constant of physical stress relaxation. The biochemical wall loosening is considered a process in which the rearrangement of both the weak hydrogen bonds and the strong covalent bonds in the cell walls are facilitated by biochemical reactions. Thus, in

the presence of biochemical wall loosening,

$$\left.\frac{dE_{st}}{dt}\right|_{disp} = \left.\frac{dE_v}{dt}\right|_{disp} + \left.\frac{dE_e}{dt}\right|_{disp} = -2(\frac{1}{\tau} + \frac{1}{\kappa})E_v - \frac{2}{\kappa}E_e \ , \qquad [9]$$

where κ (sec) is the time coefficient of biochemical strain energy relaxation, which is a function of temperature, availability of carbohydrates, and other factors that affect the metabolic activity of the cell. The biochemical wall loosening process may also require a minimum value for cell wall strain energy, corresponding to the yielding stress, in order to be activated. The strong bonds are relaxed only through the biochemical reactions and the weak bonds are relaxed by both the biochemical and physical energy relaxation processes.

It can be shown that the growth, or deformation, is then given by (Chapter 2)

$$\epsilon = \int_0^t J(t-t')\dot{\sigma}(t')dt' \ , \qquad [10]$$

where ϵ is strain, or growth, J is the creep compliance function, $\dot{\sigma}$ is the time derivative of stress, and $t' \leq t$ is the past time. The creep compliance function J is expressed by

$$J = J_e + J_v(1 - e^{-t/\gamma}) + \frac{t}{\eta} \ . \qquad [11]$$

Setting

$$r_\tau = \frac{\kappa}{\tau} \qquad [12a]$$

and

$$\bar{\tau} = \frac{\kappa\tau}{\kappa + \tau} \ , \qquad [12b]$$

it can be shown that the coefficients in equation [11] are

$$J_e = \frac{1}{G_e + G_v} \ , \qquad [13]$$

$$\gamma = \frac{\kappa}{1 + J_e G_e r_\tau} \ , \qquad [14]$$

$$\eta = \left[\frac{G_v}{1 + r_\tau} + G_e\right]\kappa \ ,$$

and [15]

$$J_v = \frac{\kappa + \bar{\tau} - \gamma}{\eta} - J_e \ , \qquad [16]$$

where G_e and G_v represent the strength of the strong and weak bonds in the cell walls, respectively, J_e corresponds to the initial instantaneous elastic deformation, and J_v is related to the maximum viscoelastic creeping in absence of biological wall loosening. The parameter η has the units of viscosity and is a function of both the physical properties of the wall and the biochemical wall loosening process of the cell.

Equation [10] describes the relationship between cell wall stress and growth. In the derivation of equation [10], κ was assumed to be constant (Chapter 2). However, during the growth of a plant root, each cell may experience a gradient of environmental conditions as it is displaced from the root tip to a more mature region of the root (Silk and Erickson, 1980; Silk, Walker, and Labavitch, 1984; Silk et al., 1986). The availability of carbohydrates may also vary during cell growth. Age is another factor that changes the metabolic activity of the cell. Therefore, the metabolic activity and hence κ, the metabolic wall loosening process, should not be a constant. An alternative equation is needed to account for the time dependence of κ.

In a simple viscoelastic material, the total strain energy is divided into the elastic and the viscoelastic strain energy (Chapter 2). Likewise, the total stress in the cell wall is divided into the elastic (σ_e) and the viscoelastic (σ_v) stress, supported by strong and weak bonds in the cell wall polymers, respectively. Mathematically, this is expressed as

$$\sigma = \sigma_e + \sigma_v \quad . \qquad [17]$$

During deformation, the rate of strain energy change equals the sum of the rate of work done by the external stress and the rate of strain energy dissipation. The rate of work is the product of stress and the rate of strain. Mathematically, this is

$$\frac{dE_e}{dt} = \sigma_e \dot{\epsilon} + \left.\frac{dE_e}{dt}\right|_{disp} \qquad [18]$$

and

$$\frac{dE_v}{dt} = \sigma_v \dot{\epsilon} + \left.\frac{dE_v}{dt}\right|_{disp} \quad . \qquad [19]$$

The strain energy–stress relation of each group of bonds is described by

$$E_{\cdot} = \frac{1}{2G_{\cdot}} \sigma^2 \quad , \qquad [20]$$

where the "$\cdot$" in the subscript may be replaced by "e" for elastic and by "v" for viscoelastic strain energy. Substituting equations [20] and [9] into equations [18] and [19] yields

$$\frac{d\sigma_e}{dt} = G_e \dot{\epsilon} - \frac{1}{\kappa} \sigma_e \qquad [21]$$

and

$$\frac{d\sigma_v}{dt} = G_v \dot{\epsilon} - (\frac{1}{\kappa} + \frac{1}{\tau})\sigma_v \quad . \qquad [22]$$

Combining equations [21], [22] and [17] yields

$$\frac{d\sigma}{dt} = (G_e + G_v)\dot{\epsilon} - \frac{1}{\kappa}\sigma - \frac{1}{\tau}\sigma_v \quad . \qquad [23]$$

In the general problem of plant root growth, the wall stress σ and the rate at which σ changes with time can be obtained by solving the water and solute transport equations. Once the stress function is obtained and the rate of wall loosening as a function of time (κ) is known, equations [21]–[23] can be solved to obtain the rate of growth ($\dot{\epsilon}$). Total growth is then obtained by integrating the growth rate function.

Rate of metabolic cell wall loosening, $1/\kappa$

For the derivation of equations [21]–[23], it was not necessary to define κ as a constant. Thus, κ may vary with the metabolic activity of the cell as it moves toward more mature regions. It can be shown that in the case of a constant κ, equations [21]–[23] produce the same solution as equation [11]. Therefore, equation [11] is the special case of equations [21]–[23] under the condition of constant κ.

Since $1/\kappa$ represents the rate of metabolic cell wall loosening, we may assume that it is proportional to the concentration of an enzyme system, [E]. This assumption is expressed mathematically as

$$\frac{1}{\kappa} = K_m[E] \ , \qquad [24]$$

where K_m is a proportionality constant. The rate constant K_m represents the activity of the enzyme system, [E], and may be affected by temperature, water stress, and other environmental stresses. Equation [24] implies that growth of cells occurs when [E] is synthesized in the cell and stops when the concentration of the enzyme system, [E], equals zero, or the activity of the enzyme system, K_m, equals zero.

We assume that the concentration of the enzyme system, [E], is controlled by a synthesis process and a first order decay process. Under this assumption, cell growth is initiated by the synthesis of the enzyme system. When the cell reaches maturity, the process of [E] synthesis is terminated and growth stops after the remaining [E] decomposes.

To derive a mathematical expression of $1/\kappa$ as a function of time during growth, consider a material segment bounded by a and b at two ends. The a and b move along with the root during growth, just like marks on the root surface, so that the segment between these two points

would always represent the same group of cells during growth. Under these conditions, the relation

$$\frac{\partial}{\partial t}\int_a^b [E]\ dx = \int_a^b S_e\ dx - \int_a^b K_d[E]\ dx \qquad [25]$$

exists, where S_e is the rate of synthesis of [E], and $K_d[E]$ is the rate of the first order decay process of [E] with K_d being the rate constant. Since the spatial positions of a and b are functions of time, we cannot simply move the differentiation operator at the left hand side of [25] to the inside of the the integral operator. We can write equation [25] in terms of material coordinate X as

$$\frac{\partial}{\partial t}\int_a^b [E]JdX = \int_a^b S_eJdX - \int_a^b K_d[E]JdX\ , \qquad [26]$$

where J is the Jacobian of the coordinate system. Since a and b are constants in the material coordinate system, equation [26] is rearranged to produce

$$\int_a^b \left\{\frac{\partial}{\partial t}\Big[[E]J\Big] - S_eJ + K_d[E]J\ dX\right\} = 0\ . \qquad [27]$$

Equation [27] is true for arbitrary a and b only if

$$\frac{\partial}{\partial t}\Big[[E]J\Big] - S_eJ + K_d[E]J\ dX = 0\ . \qquad [28]$$

By expanding equation [28] and noting that for a one–dimensional system,

$$\frac{\partial J}{\partial t} = J\dot{\epsilon}\ , \qquad [29]$$

we obtain

$$\frac{\partial[E]}{\partial t} = S_e - (K_d + \dot{\epsilon})[E]\ . \qquad [30]$$

Equations [23] and [17] are combined to produce

$$\frac{\partial}{\partial t}\frac{1}{\kappa} = K_\kappa - (K_d + \dot{\epsilon})\frac{1}{\kappa}\ , \qquad [31]$$

where $K_\kappa = K_mS_e$.

Equation [31] is our final expression for the rate of metabolic cell

wall loosening as a function of time. If the mechanical stress, σ, in the cell wall as a function of time is known, equation [31] can be solved along with equations [21]–[23] as a system to yield ϵ as a function of time. The ratio between cell length at an arbitrary moment and the initial cell length, or the Jacobian J, can be calculated from ϵ by

$$J = e^{\epsilon} \quad . \qquad [32]$$

The mechanical stress in the cell wall, σ

The rate of root growth depends on the physical stress in the cell walls. In the most general case, stress in the cell walls is a function of turgor potential (P), the gradient of apoplast water potential ($\nabla\Psi_a$), as well as the resistance of soil to root elongation (f), so that

$$\sigma = \sigma(P, \nabla\Psi_a, f_r) \quad . \qquad [33]$$

The wall stress of a plant tissue balances turgor pressure when there is no water potential gradient and the soil resistance is zero. This is equivalent to the case of a single cell in a liquid medium whereby equation [34] is expressed as

$$\sigma = \frac{\omega_s}{\omega_w} P + \sigma_f(\nabla\Psi_a, f_r) \qquad [34]$$

with the condition

$$\sigma_f = 0 \text{ as } \nabla\Psi_a = 0 \text{ and } f_r = 0 \quad , \qquad [34a]$$

where σ_f is the wall stress induced by soil resistance and water potential gradient in the root, ω_s is the volume fraction of the symplast and ω_w is the volume fraction of the cell wall. Assuming that the structure of the plant root is isotropic, ω_s and ω_w also represent the area fraction of the symplast and cell wall at any cross section of the root.

The exact form of the function σ_f can be derived by considering the balance of linear momentum of an arbitrary segment of a plant root. Newton's second law of motion states that the rate of momentum change of an object equals the sum of forces acting on it. Mathematically, this translates to

$$\frac{d}{dt}\int_{\mathcal{V}} \bar{\rho}\ \bar{\mathbf{v}}\ dv = \oint_{\mathcal{S}} \bar{\mathbf{t}}\cdot d\mathbf{a} + \int_{\mathcal{V}} \bar{\mathbf{f}} dv\ , \qquad [35]$$

where $\bar{\rho}$ is the density, $\bar{\mathbf{v}}$ is the velocity vector, $\bar{\mathbf{t}}$ is the surface traction tensor, and $\bar{\mathbf{f}}$ is the body force. Consider an arbitrary segment of a plant root with two end points identified as a and b. For an arbitrary quantity $\overline{Q}$, the volume integral is expressed as

$$\int_{\mathcal{V}} \overline{Q}\ dv = \int_a^b \left[\int_{\mathcal{A}} \overline{Q} da \right] dx = \int_a^b Q\ dx\ , \qquad [36]$$

where Q is the linear density of $\overline{Q}$, and $\mathcal{A}$ is the cross–sectional area of the root. The surface integral can be expressed as

$$\begin{aligned}\oint_{\mathcal{S}} \overline{Q}\ da &= \int_a^b \left[\int_{\mathcal{C}} \overline{Q} ds \right] dx + \int_{\mathcal{A}} \overline{Q} da\Big|_{x=a} + \int_{\mathcal{A}} \overline{Q} da\Big|_{x=b} \\ &= \int_a^b Q dx + Q_a + Q_b\ , \end{aligned} \qquad [37]$$

where Q_a and Q_b are, respectively, the integral of $\overline{Q}$ at the cross–sections of two ends. Substituting equations [36] and [37] into equation [35] results in

$$\frac{d}{dt}\int_a^b \rho_w \mathbf{v}\ dx = \int_a^b \mathbf{f} dx + \mathbf{f}_a + \mathbf{f}_b\ , \qquad [38]$$

where $\mathbf{f}$ is the lumped one–dimensional body force, and $\mathbf{f}_a$ and $\mathbf{f}_b$ are forces acting on the root segment at the two end points respectively,

$$\mathbf{f} = \frac{\int_{\mathcal{A}} \bar{\mathbf{f}} da + \oint_{\mathcal{C}} \mathbf{t}\cdot\mathbf{n}\ ds}{\mathcal{A}}\ , \qquad [39]$$

$$f_a = \frac{\int_{\mathcal{A}} \bar{f}\, da\Big|_{x=a}}{\mathcal{A}} , \qquad [40]$$

and

$$f_b = \frac{\int_{\mathcal{A}} \bar{f}\, da\Big|_{x=b}}{\mathcal{A}} . \qquad [41]$$

The body force f consists of the gravitation force and the frictional force between soil and root. If we neglect gravity, f represents the frictional resistance between root and soil,

$$f = f_r . \qquad [42]$$

Taking the differentiation in equation [38] under the integral sign yields

$$\int_a^b \frac{D}{Dt}(\rho_w v)dx = \int_a^b f dx + f_a + f_b . \qquad [43]$$

The above equation can be approximated by

$$\frac{D}{Dt}(\rho_w v)(b-a) = f_r(b-a) + f_a + f_b , \qquad [44]$$

where f_a and f_b consist of the internal stress of the cell wall matrix (f_σ), the force acting on the cell wall by the symplast water (f_s), and the force from apoplast water (f_p), respectively,

$$f_a,\ f_b = f_\sigma + f_s + f_p . \qquad [45]$$

At $x=a$,

$$f_\sigma(a) = -\sigma(a)\omega_w , \qquad [46]$$

where $\sigma(a)$ is the internal stress of the cell wall at $x=a$, and ω_w is the volume fraction of the cell wall. The force by apoplastic water is expressed as

$$f_p(a) = \Psi_a(a)\omega_a , \qquad [47]$$

where Ψ_a is the water potential of the apoplast, and ω_a is the volume

fraction of the apoplast. The force from the symplastic water is similarly given by

$$f_s(a) = P(a)\omega_s \ , \qquad [48]$$

where P is the turgor pressure. Similar relations are for x=b,

$$f_\sigma(b) = \sigma(b)\omega_w \ , \qquad [49]$$

$$f_p(b) = -\Psi_a(b)\omega_a \ , \qquad [50]$$

and

$$f_s(b) = -P(b)\omega_s \ . \qquad [51]$$

Substituting equations [45]–[51] into equation [44] results in

$$\frac{D}{Dt}(\rho_w v)(b-a) = (\sigma(b)-\sigma(a))\omega_w - (P(b)-P(a))\omega_s - (\Psi_a(b)-\Psi_a(a))\omega_a + f_r \ . \qquad [52]$$

Dividing both sides of equation [52] by (b–a) and then taking the limit as $(b-a)\rightarrow 0$ yields

$$\frac{D}{Dt}(\rho_w v) = \omega_w \frac{\partial \sigma}{\partial x} - \omega_s \frac{\partial P}{\partial x} - \omega_a \frac{\partial \Psi_a}{\partial x} + f_r \ . \qquad [53]$$

The left hand side of equation [53] represents the change in the kinetic energy of a plant root as its velocity changes. For a growing plant root, it can be shown that this is negligible in magnitude compared to the terms on the right hand side of the equation. This is equivalent to the assumption that the inertia force resulting from acceleration due to growth is negligible. Thus, equation [53] can be well approximated by

$$\omega_w \frac{\partial \sigma}{\partial x} - \omega_s \frac{\partial P}{\partial x} - \omega_a \frac{\partial \Psi_a}{\partial x} + f_r = 0 \ . \qquad [54]$$

Integrating equation [54] yields

$$\sigma = \frac{\omega_s}{\omega_w} P + \frac{\omega_a}{\omega_w} (\Psi_a - \Psi_{atip}) - \int_x^{tip} f_r dx \ , \qquad [55]$$

where Ψ_{atip} is the apoplast water potential at the root tip. Cell wall stress σ can be calculated from equation [55] when the apoplast water

potential and turgor distribution along the root axis are known. That information can be obtained by solving the water and solute transport equations along the root axis.

The meristem

Growth in the meristem consists mainly of two concurrent processes: cell division and expansion (Green, 1982). In addition, synthesis of cytoplast contents (proteins, nucleic acids, etc.), synthesis of cell wall material, and respiration all occur during growth. These quantities act as sinks for sugar transport and, along with the rate of elongation, determine the quantities such as volume fraction of apoplast (ω_a) and the density of cytoplasm contents.

Following procedures similar to those used for deriving equation [31], it can be shown that the following relations exist:

$$\frac{dr_m}{dt} = (\dot{\epsilon} - b)r_m \ , \qquad [56]$$

$$\frac{d\omega_a}{dt} = \frac{1-\omega_a}{\theta\rho_w} S_w - \omega_a\dot{\epsilon} \ , \qquad [57]$$

and

$$\frac{d\rho_s}{dt} = S_s + \frac{\rho_s}{\omega_s}\frac{\partial\omega_a}{\partial t} - \rho_s\dot{\epsilon} \ , \qquad [58]$$

where r_m is the average radius of cells in the meristem, b is the rate of cell division, θ is the porosity of the apoplast, ρ_w is the cell wall density, S_w is the rate of cell wall synthesis in the meristem, ρ_s is the density of the cytoplast contents, and S_s is the rate of synthesis of cytoplast contents in the meristm.

Limited information is available regarding the rate of cell division in the plant root. Collins and Richmond (1962) and Tyson (1986)

presented models that describe the cell cycle in a bacterial population as a function of the rate of cell expansion. Tyson (1986) showed that the cell cycle in a bacterial population can be approximated by

$$\begin{cases} b = \dfrac{A(x - a)^2}{1 - x}\,\dot{\epsilon}\,, & a < x < 1, \\ b = 0\,, & x \geq 1,\ 0 < x < a \end{cases} \qquad [59]$$

where $x = r_m/r_{max}$ is the ratio between average cell size and the maximum cell size, A is a constant, and a is the minimum value of x where cell division is possible.

Equations [56]–[59] describe the growth of the meristem. In this model, it is assumed that the meristem contributes to the total elongation of the root by producing new tissue to the elongation zone next to the meristem. The rate at which these new tissues are produced is calculated by

$$\aleph = \dot{\epsilon}\, L_{mstm}\,, \qquad [60]$$

where L_{mstm} is the length of the meristem. Cells start elongation after they are produced by the meristem. The initial values of ρ_s, ω_a, ω_s, and r_{ci} at the moment a cell leaves the meristen are assumed to be the same as the corresponding values in the meristem at the same momemt.

The elongation region

Equations similar to equations [57] and [58] can be derived for the elongation region. These equations, along with equations governing the rate of cell elongation describe the growth in the elongation region.

Respiration, synthesis of cell wall, cytoplasm, and Se

Although it is safe to state that these processes, and $\dot{\epsilon}$ could not

be independent of one another, little information is available about the interactions among these individual processes. Because of lack of better information and for simplicity, the rate of respiration is assumed to be proportional to the density of the cytoplasm, and is related to sugar concentration by a Michaelis–Menten type equation. This leads to

$$S_r = \frac{K_{mr}\rho_s C}{k_r + C}, \qquad [61]$$

where C is the sugar concentration. A similar relation is assumed for the synthesis of the proposed enzyme system for cell wall loosening,

$$S_e = \frac{K_{me}\rho_s C}{k_e + C}. \qquad [62]$$

It is reasonable to expect that the rate of synthesis of cell wall material and the cytoplasm constituents during cell growth to be related to the rate of growth. This can be illustrated by considering the consequences if they were not related or independent. If the rate of cell wall synthesis were relatively higher than the rate of growth and were not regulated by growth rate, the proportion of the cell walls in the plant tissue would increase until all of the spaces were occupied by cell walls. If the rate of cell wall synthesis were lower than the rate of growth and were not regulated, the thickness of the cell walls would decrease until cells burst under internal turgor pressure. The fact that the growth of a plant tissue is a extremely stable process so that the conditions mentioned above do not occur suggests there must be a mechanism regulating the rate of cell wall and cytoplasm synthesis in relation to the rate of growth, or *vice versa*. However, little is known about such a regulating mechanism. For these reasons, the rate of synthesis of cell wall and cytoplasm in this model are assumed to be

proportional to $\dot{\epsilon}$, whereby

$$S_W = K_W \dot{\epsilon}, \qquad [63]$$

and

$$S_S = K_S \dot{\epsilon} \ , \qquad [64]$$

where K_W and K_S are constants. Equations [63] and [64] are equivalent to the statement that under constant environmental conditions, cell wall thickness and cytoplasm density approaches some stable values during growth. These stable values are determined by K_W and K_S. As more information becomes available, equations [63] and [64] can be replaced with more realistic relations. The values of the parameters in equations [61]–[64] may all be functions of temperature as well as water stress.

DISCUSSION

A number of mathematical models have been reported to simulate plant growth in terms of the physical properties of the plant tissue and the basic postulated mechanisms (Grenetz and List, 1973; Cosgrove, 1981; Plant, 1982; McCoy and Boersma, 1985). Most of these models are formulated on the basis of formal analogies between plant tissues and some simple mechanical systems. McCoy and Boersma (1985) followed a different approach by considering the laws of energy conservation in a plant tissue from basic thermodynamic principles in the formulation of their model. However, the dynamic interaction between water and solute transport and plant growth, and the effects of soil water stress and soil resistance to root elongation has not been explicitly modeled, nor has the role of metabolic cell wall loosening been considered in these models.

The mathematical model proposed in this manuscript explicitly describes the dynamic interaction between water and solute transport and root growth. In this model the growth of the plant root consists of cell division and expansion in the meristem and cell elongation in the elongation region. Sets of differential equations were developed to describe growth in the meristem and the elongation zone. These equations describe growth as being controlled by the metabolic process of cell wall loosening and driven by the mechanical stresses in the cell walls.

The metabolic processes considered in this model include respiration, synthesis and decay of the hypothetical cell wall loosening system, and synthesis of cell wall and cytoplasm constituents. The rates of respiration and synthesis of the hypothetical cell wall loosening system were asumed to be proportional to the availability of solute (sugar) and the content of

the cytoplasm constituents in the cells. The rates of cell wall and cytoplasm constituent synthesis were asumed to be proportional to the rate of cell elongation to provide the desired stability for the model. It is imaginable that in the nature, these processes must be coordinated so that the root elongates in a controlled fashion. However, the exact mechanisms of the coordination of these metabolic processes are not known at this time. As new information appears regarding the mechanisms of coordination between these metabolic processes, they can be easily incorporated into the mdoel.

Solution of the dynamic transport equations of water and solute along a growing root provides information regarding distribution of water potential, turgor, and solute concentration along the root axis. This information is used to calculate the rates of metabolic processes along the root axis and the physical stress in the cell walls from which the growth pattern of the root can be calculated.

The model presented in this manuscript is a dynamic model which includes interactions between growth and transport of water and solutes. Since growth is not only affected by water and solute transport, but in turn also affects the transport of water and solute, the transport equations and the equations of growth must be solved simultaneously.

This model can simulate the effects of temperature, water stress, soil compaction, as well as the availability of carbohydrates on the dynamic processes of plant root growth. Temperature effects on root growth are modeled through its effects on the physical processes of water and solute transport and, more importantly, through its effects on the metabolic processes. Water stress affects growth directly through its effect

on turgor potential, and hence the physical stress in the cell wall that is the driving force for growth. Water stress also affects growth by its effect on solute transport, since transport of water and solutes are coupled processes. In addition, water stress may directly affect the rates of metabolic processes by affecting their activation energy (Feng et al., 1990). The combined effects of temperature and water stress on metabolic processes may be modeled using equations discussed by Feng et al. (1990). The effect of soil compaction is expressed by the coefficients of soil resistance in the model. The effect of the availability of carbohydrates is modeled through the solute transport equations.

Limited validation of the model is provided by the solution of the growth equations under steady state conditions. A plant tissue typically shrinks approximately 5% upon suddenly losing turgor. Assuming an initial turgor of 0.5MPa, a volume fraction of cell walls, ω_a, equal to 0.2, and a porosity of the cell wall equal to 0.5, the change in physical stress in the cell walls upon losing turgor results from equation [55]:

$$\Delta\sigma = \frac{\omega_s}{\omega_w}\Delta P = \frac{(1-0.2)}{0.2\times 0.5} \times 0.5 \text{ MPa} = 4 \text{ MPa} . \qquad [65]$$

assuming apoplast water potential gradient and the soil resistance terms are negligible. Assuming that turgor was lost over a short period of time so that the effect of wall loosening was minimal, equation [23] can be approximated by

$$\Delta\sigma = (G_e + G_v)\Delta\epsilon . \qquad [66]$$

Using the values $\Delta\sigma = 4$ MPa and $\Delta\epsilon = 0.05$, we have $(G_e + G_v) = 80$ MPa. For the purpose of illustration, we assume that $G_e = G_v = 40$ MPa. The time coefficient of physical stress relaxation in plant cell walls

typically averages one hour. For our calculations, we assume τ = 1 hr. When cells reach maturity, the rate of elongation reduces from a maximum rate to nearly zero in approximately one hour after elongating for 9 hrs (Erickson and Sax, 1956a). Therefore, K_d = 0.5 hr and a stopping time of 9 hrs, after which K_κ is equal to zero would be reasonable estimates.

With these parameters and an initial K_κ = 7.5, equations [21]–[23] and [31] were solved simultaneously with the following initial conditions:

$$\sigma_v = \sigma = 4 \text{ MPa}, \ \epsilon = 0, \ 1/\kappa = 0, \text{ at } t=0 \ , \qquad [67]$$

to yield relative cell length as a function of time (figure 5.1). The growth curve calculated using equations of cell elongation which were derived from considerations of metabolic cell wall loosening, predict the general trend of cell growth, with a slow initial growth rate, followed by a quick, exponential growth, which stops after reaching maturity.

This simple example illustrates the validity of the basic assumptions of the model presented in this manuscript. The full validation of the model, however, can only be carried out when the growth equations are solved simultaneously with dynamic equations of water and solute transport. The model can then be used to simulate and predict dynamic responses of plant root elongation to varying environmental conditions, including temperature, water stress, soil compaction, and supply of photosynthates.

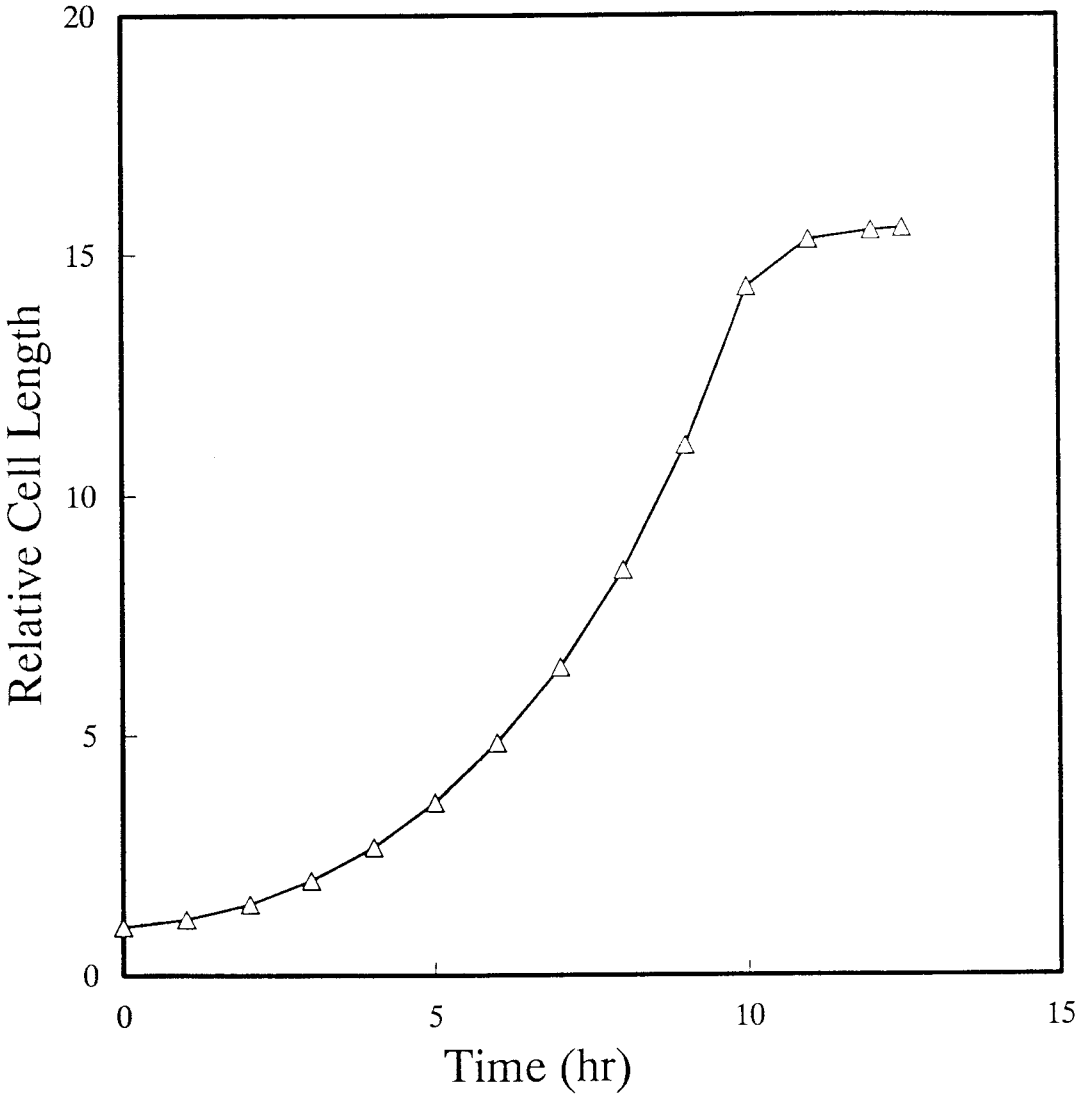

Figure 5.1. Relative cell length as a function of time calculated by solving the system of equations [21]–[23] and [31].

LIST OF SYMBOLS AND UNITS

a	minimum value of x for cell division	dimensionless
b	rate of cell division in meristem	s^{-1}
f	body force	$N\ m^{-3}$
$f_{a,b}$	axial force on cell wall matrix at a and b	$N\ m^{-2}$
f_r	frictional force between root and soil	$N\ m^{-3}$
f_σ	contribution of wall stress to axial force balance	$N\ m^{-2}$
f_s	contribution of symplast water potential to axial force balance	$N\ m^{-2}$
f_P	contribution of apoplast water potential to axial force balance	$N\ m^{-2}$
r_m	cell radius in meristem	m
r_{max}	maximum value of r_m	m
t	time	s
t'	past time ($t' \leq t$)	s
t	surface traction tensor	$N\ m^{-2}$
x	spatial coordinate	m
v(t)	rate of root elongation	$m\ s^{-1}$
v	displacement velocity	$m\ s^{-1}$
A	a coefficient of cell division	dimensionless
$E_.$	elastic or viscoelastic strain energy density	$J\ m^{-3}$
E_e	elastic strain energy density	$J\ m^{-3}$

E_v	viscoelastic strain energy density	J m^{-3}
E_{st}	total stored strain energy	J m^{-3}
[E]	concentration of biological cell wall loosening system	kg m^{-3}
$G_.$	elastic or viscoelastic strength of cell wall	N m^{-2}
G_e	elastic strength of cell wall	N m^{-2}
G_v	viscoelastic strength of cell wall	N m^{-2}
J	Jacobian	dimensionless
J_c	creep compliance modulus	m^2 N^{-1}
J_e	equilibrium Young's modulus	m^2 N^{-1}
J_v	viscoelastic creeping coefficient	m^2 N^{-1}
K_m	efficiency of metabolic wall loosening system	m^3 $kg^{-1}s^{-1}$
K_d	rate of first order degradation of metabolic cell wall loosening system	s^{-1}
K_κ	S_eK_m	s^{-2}
L	root length	m
L_{mstm}	length of meristem	m
P	turgor pressure	N m^{-2}
Q	an arbitrary quantity	
S_e	rate of synthesis of metabolic wall loosening system	mol $m^{-3}s^{-1}$
S_w	rate of cell wall synthesis	mol m^{-3} s^{-1}
S_s	rate of cytoplasm synthesis	mol m^{-3}

s^{-1}		
T	absolute temperature	^{o}K
X	material coordinate	m
$\cdot_{disp}$	in subscript refers to dissipation	
k_r	Michaelis–Menten coefficient of respiration	mol m^{-3}
k_e	Michaelis–Menten coefficient of cell wall loosening system synthesis	mol m^{-3}
K_{mr}	maximum rate respiration per unit mass of cytoplasm	mol $kg^{-1}s^{-1}$
K_{me}	maximum rate of wall loosening system synthesis per unit mass of cytoplast	mol $kg^{-1}s^{-1}$
K_s	coefficient of cytoplasm synthesis	mol $kg^{-1}m^{-3}$
K_w	coefficient of cell wall synthesis	kg m^{-3}
$\mathscr{A}$	cross sectional area of root	m^2
$\mathscr{C}$	circumference of the root	m
$\varkappa$	r_m/r_{max}	dimensionless
ϵ	strain	dimensionless
$\dot{\epsilon}$	time rate of strain	s^{-1}
γ	time constant of creep compliance	s
κ	time constant of biological strain energy relaxation	s^{-1}
η	viscous coefficient of cell walls	kg m^{-1} s^{-1}
ω_a	volume fraction of apoplast	dimensionless
ω_s	volume fraction of symplast	dimensionless

ω_w	volume fraction of cell wall	dimensionless
θ	porosity of cell wall	dimensionless
ρ_s	density of cytoplasm constituents	kg m^{-3}
ρ_w	density of cell wall	kg m^{-3}
σ	stress	N m^{-2}
σ_e	elastic stress	N m^{-2}
σ_v	viscoelastic stress	N m^{-2}
σ_f	stress induced by water potential gradients and soil resistance	N m^{-2}
τ	time coefficient of physical stress relaxation	s
$\aleph(t')$	rate of root production by meristem	m s^{-1}
$\Lambda(t',t)$	current length divided by initial length of cells produced at t'	dimensionless
Ψ_a	apoplast water potential	N m^{-2}

LITERATURE CITED

Bertaud, D. S. and P. W. Gandar, 1985. Referential descriptions of cell proliferation in roots illustrated using *Phleum pratense L.*, Bot. Gaz., 146:275–287.

Boyer, J. S., 1988. Cell enlargement and growth–induced water potentials. Physiol. Plant., 73:311–316.

Boyer, J. S., and G. Wu, 1978. Auxin increases the hydraulic conductivity of auxin–sensitive hypocotyl tissue. Planta, 139:227–237.

Brummell, D. A., and J. L. Hall, 1985. The role of cell wall synthesis in sustained auxin–induced growth. Physiol. Plant., 63:406–412.

Cleland, R. E., 1971. Cell wall extension. Ann. Rev. Plant Physiol., 22:197–222.

Cleland, R. E., 1987. The mechanisms of wall loosening and wall extension. in D. J. Cosgrove and D. P. Knievel (ed.) Physiology of cell expansion during plant growth. Am. Soc. Plant Physiol., Penn. State Univ..

Collins, J. F., and M. H. Richmond, 1962. Rate of growth of *Bacillus cereus* between divisions. J. Gen. Microbiol., 28:15–33.

Cosgrove, D. J., 1981. Analysis of the dynamic and steady–state responses of growth rate and turgor pressure to changes in cell parameters. Plant Physiol., 68:1439–1446.

Cosgrove, D. J., 1986. Biophysical control of plant cell growth. Ann. Rev. Plant Physiol., 37:377–405.

Cosgrove, D. J., 1987. Wall relaxation and the driving forces for cell expansive growth. Plant Physiol., 84:561–564.

Erickson, R. O., and K. B. Sax, 1956a. Elemental growth rates of the primary roots of *Zea mays*. Proc. Am. Phil. Soc., 100:487–497.

Erickson, R. O., and K. B. Sax, 1956b. Rates of cell division and cell elongation in the growth of the primary root of Zea mays. Proc. Am. Phil. Soc., 100:499–513.

Feng, Y., X. Li, and L. Boersma, 1990. The Arrhenius equation as a model for explaining plant responses to temperature and water stresses. Ann. Bot., 66:237–244.

Gandar, P. W., 1983a. Growth in root apices. I. Kinematic description of growth. Bot. Gaz., 144:1–10.

Gandar, P. W., 1983b. Growth in root apices. II. Deformation and rate of deformation. Bot. Gaz., 144:11–19.

Green, P. B., 1976. Growth and cell pattern formation on an axis. Critique of concepts, terminology, and modes of study. Bot. Gaz., 137:187–202.

Green, P. B., R. O. Erickson, and J. Buggy, 1971. Metabolic and physical control of cell elongation rate: in *vivo* studies in *Nitella*. Plant Physiol., 47:423–430.

Green, P. B., K. Bauer, and W. R. Cummins, 1977. Biophysical model for plant growth: auxin effect. in A. M. Jungreis et al. (ed.) Water relations in membrane transport in plants and animals. Academic press. New York.

Grenetz, P. S. and A. List, 1973. A model for predicting growth response in plants to changes in external water otential: *Zea mays* primary root. J. Theor. Biol., 39:29–45.

Ho, L. C. and D. A. Baker, 1982. Regulation of loading and unloading in

long distance transport systems. Physiol. Plant., 56:225–230.

Lockhart, J. A., 1965. An analysis of irriversible plant cell elongation. J. Theor. Biol., 8:264–275.

Lockhart, J. A., 1967. Physical nature of irriversible deformation of plant cells. Plant Physiol., 42:1545–1552.

Mathews, M. A., E. Van Volkenburgh, and J. S. Boyer, 1984. Acclimation of leaf growth to low water potentials in sunflower plant. Cell Environ., 7:199–206.

McCoy, E. L., and L. Boersma, 1984. The principles of continuum mechanics applied to transport processes and deformation in plant tissue. J. Theor. Biol., 111:687–705.

Plant, R. E., 1982. A continuum model for root growth. J. Theor. Biol., 98:45–59.

Ray, P. M., 1987. Principles of plant cell growth. in D. J. Cosgrove and D. P. Knievel (ed.) Physiology of cell expansion during plant growth. Am. Soc. Plant Physiol., Penn. State Univ..

Ray, P. M., and A. W. Reusink, 1962. Kinetic experiments on the nature of the growth mechanism in oat coleoptile cells. Dev. Biol., 4:377–397.

Sellen, D. B., 1982. The mechanical properties of plant cell walls. in The mechanical properties of biological materials. Symposia of Soc. Exp. Biol., 34:315–329. Cambridge Univ. Press, Cambridge.

Silk, W. K. and R. O. Erickson, 1979. Kinematics of plant growth. J. Theor. Biol., 76:481–501.

Silk, W. K. and R. O. Erickson, 1980. Local biosynthesis rates of cytoplasmic constituents in growing tissue. J. Theor. Biol.,

83:701–703.

Silk, W. K. and K. K. Wagner, 1980. Growth sustaining water potential distribution in the primary corn root. Plant Physiol., 66:859–863.

Silk, W. K., R. C. Walker, and J. Labavitch, 1984. Uronide deposition rates in the primary root of *Zea mays*. Plant Physiol., 74:721–726.

Silk, W. K., T. C. Hsiao, U. Diedenhofen, and C. Matson, 1986. Spatial distributions of ptasium, solutes, and their deposition rates in the growth zone of the primary corn root. Plant Physiol., 82:853–858.

Taiz, L., 1984. Plant cell expansion: Regulation of cell wall mechanical properties. Ann. Rev. Plant Physiol., 35:585–657.

Theologis, A., 1987. Possible link between auxin regulated gene expression, H^+ secretion, and cell elongation: a hypothesis. in D. J. Cosgrove and D. P. Knievel (ed.) Physiology of cell expansion during plant growth. Am. Soc. Plant Physiol., Rockville, Maryland.

Tyson, J. J., 1986. Sloppy size control of the cell division cycle. J. Theor. Biol., 118:405–426.

Van Volkenburgh, E., and R. Cleland, 1981. Control of light induced bean leaf expansion: role of osmotic potential, wall yield stress, and hydraulic conductivity. Planta, 153:572–577.

6. A CONTINUUM MODEL OF PLANT ROOT GROWTH: Model Solution and Application

Yongsheng Feng and Larry Boersma
Department of Soil Science, Oregon State University
Corvallis, OR 97331

ABSTRACT

The growth of a plant root involves interactions among division and elongation of cells, transport of water, and transport and availability of photoassimilates. Environmental factors such as soil water potential, soil temperature and the mechanical resistance of the soil to root penetration also play important roles in determining root growth. A more thorough understanding of the roles and interactions of the physical and biological processes involved in root growth, and mechanistic interpretation of the effects of environmental factors on root growth may be achieved by placing these processes under the context of a dynamically growing plant root.

In this manuscript, a plant root is modeled as a one dimensional continuum. The growth of the root is modeled with five systems of equations describing meristematic growth, cell elongation, transport of water in the apoplastic and the symplastic pathways, and the transport of solutes. Numerical simulations using the model yields information regarding elongation of the root as a whole, the spatial patterns of growth along the axis of the root, as well as information on the elongation process of

specific cells as functions of time.

The model were used to simulate effects of soil water potential, temperature, soil resistance, and carbohydrate supply on root growth. Lower soil water potential reduces the rate of root elongation mainly by reducing the length of the growth region near the root tip. It also reduces the rate of cell elongation nearly uniformly over the elongation region of the root. On the other hand, lower temperature affects root growth mainly be reducing the rate of cell elongation while the length of the growth region remains nearly constant. Effect of soil resistance on root growth is similar to that of lower soil water potential except that the elongation rate of younger cells are less affected than that of the more mature cells. Limiting carbohydrate supply reduces root growth by significantly reducing both the rate of cell elongation and the length of the growth region. Justification of the model was found in the agreement between model simulation and experimental measurements of effects of soil water stress and temperature on root growth reported in the literature.

The model presented in this manuscript provides the means to simulate mechanistically the response of the dynamic process of root growth to various environmental conditions. It also provides the theoretical framework under which the dynamic interactions between root growth and the transport of water and solutes in a growing root.

INTRODUCTION

Several models of plant growth have been reported (Lockhart, 1965, 1967; Green, Erickson, and Buggy, 1971; Grenetz and List, 1973; Plant, 1982; McCoy and Boersma, 1984). In a pioneering work, Lockhart (1965) developed equations describing elongation of plant cells as viscoelastic creeping of plant cell walls under turgor pressure. The rate of growth was assumed to occur when the turgor potential was greater than a minimum value, the cell wall yielding stress. The rate of growth was assumed to be proportional to the difference between turgor and the yielding stress. The proportionality coefficient was termed the cell wall extensibility. Green et al. (1971) measured the transient rates of cell elongation of *Nitella* cells under varying turgor potentials and postulated that the extensibility and the yielding stress of the cell, presumably the physical properties of cell walls, was under metabolic control. Plant (1982) attempted to model the axial growth at the root apex based on the Lockhart (1965) theory. However, he was forced to assume that the cell wall yielding stress first decreased and then increased with the distance from the root tip in order to reproduce the experimentally observed growth pattern along the root axis (Erickson and Sax, 1956a,b). Justification of the assumptions was not given.

It has been reported that total water potential and turgor potential distribution in a multi–cellular plant tissue are affected by growth (Molz and Boyer, 1978; Silk and Wagner, 1980; Boyer, 1988). Since it is generally recognized that turgor potential is directly involved in determining the rate of growth, it is reasonable to expect that water

potential and turgor distribution in a multicellular tissue may in turn affect the rate of growth. A model that involves mechanistic descriptions of growth as well as water and solute transport is needed to study the dynamic interactions between these processes. We are not aware of a such model, although the approach was implied by McCoy and Boersma (1984).

The continuum theory provides an ideal framework under which such a model can be developed. The hypothesis that the growth of a plant tissue can be considered as the deformation of a mathematical continuum, despite the fact that it consists of discrete cell entities, was formally introduced by Silk and Erickson (1979). Gandar (1983a,b) discussed the application of the kinematic theory of the continuum mechanics in describing the growth patterns at root apices. Continuum theory has been applied to modeling water transport in plant tissues (Molz, 1976; Silk and Wagner, 1982; McCoy and Boersma, 1984), cell proliferation along root axis (Bertaud and Gandar, 1985), synthesis and deposition of cell wall and cytoplasm constituents (Silk and Erickson, 1980; Silk, Walker and Labavitch, 1984), and longitudinal root growth (Plant, 1982; McCoy and Boersma, 1984).

These studies apply the continuum theory to pre–assumed steady state conditions. However, a dynamic model of plant root elongation must be able to describe the transient growth processes in a dynamically changing environment. As was shown in Chapter 1, the kinematic theory used in these studies is not adequate for this purpose since no distinction can be made regarding different roles played by cell division in the meristem and subsequent cell elongation in the elongation zone.

A dynamic model of one–dimensional plant root growth was

described in Chapter 5. The model describes the process of longitudinal growth of a plant root as the result of the continuous production of new cells by the meristem, which was assumed to be located at the tip of the root, and the subsequent elongation of these cells. Growth in both the meristem and the elongation region was modeled as driven by the mechanical stress in the cell walls and controlled by the process of metabolic cell wall loosening. The cell wall loosening process was modeled as the metabolically mediated strain energy relaxation process in the cell wall (Chapter 2).

In this study, these equations of growth are solved simultaneously with the dynamic equations of water and solute transport to simulate the dynamic process of longitudinal root elongation. The solutions of the model are given in the form of total root length and the rate of root elongation as functions of time, as well as the local rate of elongation along the root axis. The model is used to study the dynamic responses of plant root growth to temperature, water stress, soil compaction, and the supply of carbohydrates to the root.

MODEL DESCRIPTION

The model consists of five systems of inter–related equations that must be solved simultaneously:

1. equations for meristem growth,
2. equations for cell elongation in the elongation zone,
3. equations for water transport in the apoplast pathway,
4. equations for water transport in the symplast pathway, and
5. equations for solute (sugar) transport.

In addition, kinematic equations are needed to establish the framework under which these systems of equations can be solved. Equations that describe the metabolic processes in the root, i.e., respiration, cell wall and cytoplasm constituent synthesis, are also included. A complete list of all the mathematical equations included in the model can be found in the APPENDIX.

A system of seven first order differential equations define the growth in the meristem. Solution of these equations produces such quantities as average cell size, volume fraction of apoplast, density of cytoplasm constituents in the symplast, rate of metabolic cell wall loosening, and the rate of growth as functions of time. In addition, elastic and viscoelastic stresses in the cell walls are obtained. These quantities are needed in order to calculate the growth rate. The information needed for these calculations are solute concentration, turgor potential, and soil resistance to root penetration, along with initial values of the seven quantities that are being solved for. The initial values are needed to initiate the process. The solute concentration and turgor

potential of the meristem are obtained from solutions of water and solute transport equations.

A system of six first order differential equations defines the process of cell elongation along the root axis. These equations are similar to the growth equations for the meristem except that the equations for cell division are absent. Information needed for these calculations include apoplast water potential, turgor potential, and solute concentration distribution along the root axis. These quantities are obtained from solutions of water and solute transport equations. This system of equations must be solved for each material point along the root axis. Initial conditions for each of the material points are assumed to be the same as the conditions in the meristem at the moment when the particular material point is produced. Since the elongation of cells in the elongation zone depends on their individual history of water potential, turgor, and solute concentration, the model must be solved under the material coordinate system where the elongation of each material point as a function of time is calculated.

The mass balance of water in the apoplast consists of the terms describing axial Darcy flux in the apoplast, water uptake from the soil, water exchange between apoplast and symplast, and the effect of local elongation. The mass balance of water in the symplast pathway includes axial Darcy flux in the symplast, water uptake from the apoplast, and the effect induced by the local rate of elongation. Because of the existence of plasmodesmata in the membranes which separate cells, different values are assumed for the membrane reflection coefficients in the axial direction and the lateral direction between symplasm and

apoplasm.

Mass flux of solutes in the axial direction consists of three terms: dispersion, which is augmented by a facilitated diffusion factor, mass flux, and the energy requiring active transport. The sink term in the mass balance equation of solute includes contributions of cell wall synthesis, cytoplasm synthesis, respiration, and the local elongation rate. Respiration, facilitated dispersion, and active transport are assumed to be proportional to the local density of cytoplasm constituents in the symplast pathway. In addition, these quantities are assumed to be dependent upon the local solute concentration by Michaelis–Menten type relations.

The boundary conditions for the water and solute transport equations at the root tip were derived from mass balance considerations. The water requirement of the growing meristem is satisfied by axial water through the apoplast and symplast pathways to the meristem, plus water uptake by the meristem from the soil. The second boundary condition for water transport at the root tip is provided by the relation between water transport between the two pathways and the local rate of elongation. The boundary condition of solute transport at the root tip states that the solute requirement of the meristem is satisfied by the axial flux of solute at the root tip.

Since all five systems of equations are inter–related, they must be solved simultaneously. The growth equations describe the rate of growth as a function of local water status, solute concentration, and soil resistance. Once these quantities are known, the local rate of growth is calculated. Accumulated growth is calculated by integrating the rate of growth over time. The water transport equations, along with the solute

transport equations, provide the necessary information needed for the calculation of local rate of growth both along the root axis and in the meristem.

The equations of growth, water transport and solute transport, along with the appropriate boundary and initial conditions define the system. There are four unknown functions in the system: the rate of growth, apoplast water potential, turgor potential, and solute concentration. There are four systems of equations corresponding to these four unknown functions, with the equations of meristem growth defining the moving boundary at the root tip. Therefore, the number of equations matches with the number of unknowns and the system is properly defined.

The main steps during each time increment of the model simulation are summarized bellow:

1. the temperature at the next time interval is calculated;

2. soil water potential and soil water conductivity are calculated;

3. physical parameters, including viscosity, solute diffusivity, and membrane permeability are calculated;

4. the rates of metabolic processes, including respiration, cell wall and cytoplasm synthesis, and the synthesis of the cell wall loosening system, are calculated for the meristem;

5. the equations of meristem growth are solved;

6. the length of new root tissue produced by the meristem is calculated from the growth rate of the meristem as

$$dX = \frac{1}{2}(\dot{\epsilon}_{m,n-1} + \dot{\epsilon}_{m,n}) \times L_{mstm} \times dt \ ; \qquad [1]$$

7. the material coordinate of the new tip node, X_n, is calculated

as

$$X_{new\ tip} = X_{old\ tip} + dX \ , \qquad [2]$$

and the previous terminal node, $X_{old\ tip}$, becomes an internal node (figure 6.1).

8. the rates of metabolic processes along the root axis at the nodes X_1 to X_n are calculated;

9. growth equations are solved along the root axis for X_1 to X_n;

10. apoplast water transport equations are solved for values of apoplast water potential;

11. symplast water transport equations are solved for values of turgor potential;

12. solute transport equations are solved for the values of solute concentration and osmotic potential;

13. if the convergence criteria were not met, go back to step 4; and

14. project the values of all relevant variables for the next time increment.

During the calculations of steps 4–12, the updated values of all relevant variables are used whenever available. If updated values are not available, such as occurs during the first pass through the iteration routine, the values projected at the end of last time increment are used.

NUMERICAL PROCEDURES

Kinematic equations

The material coordinates of the system are defined by

$$X_{i+1} = X_i + \frac{1}{2}[\dot{\epsilon}_m(t_i) + \dot{\epsilon}_m(t_{i+1})] \times L_{mstm} \times (t_{i+1} - t_i) \ . \qquad [3]$$

The nodal point i+1 is not defined until after the i–th time step. The spatial position of the i–th material point X_i is calculated as

$$x_i = \sum_{2}^{i} \frac{1}{2}(J_i + J_{i+1})(X_i - X_{i-1}) \ . \qquad [4]$$

The total length of the root at the n–th step is calculated as

$$L(t_n) = x_n(t_n) \ . \qquad [5]$$

The rate of total root elongation is calculated as

$$v(t_n) = \frac{L(t_n) - L(t_{n-1})}{t_n - t_{n-1}} \ . \qquad [6]$$

High precision integration formulas are not necessary for the calculation of spatial quantities (equations [4]–[6]) since these quantities are not directly involved in the iteration scheme of the model. They are calculated only for the purpose of output.

Gradient and divergence operators

The interval between the nodal points of the system depends on step size in time and the rate of growth in the meristem. The system has unevenly spaced nodal points because the growth rate of meristem at any moment depends on the water status and solute concentration at the root tip, which are dynamic functions of time. The Lagrangian interpolation polynomial is used to calculate the differentials in the spatial

direction.

Given three nodal points X_1, X_2, and X_3, the Lagrangian interpolation polynomial for an arbitrary function F(X) is

$$F(X) = \frac{(X-X_2)(X-X_3)}{(X_1-X_2)(X_1-X_3)} f_1 + \frac{(X-X_1)(X-X_3)}{(X_2-X_1)(X_2-X_3)} f_2 +$$

$$\frac{(X-X_1)(X-X_2)}{(X_3-X_1)(X_3-X_2)} f_3 , \qquad [7]$$

where f_1, f_2, and f_3 are values of F(X) at X_1, X_2, and X_3 respectively. The first and the second order derivatives of equation [7] are

$$F'(x) = \frac{(X-X_2)+(X-X_3)}{(X_1-X_2)(X_1-X_3)} f_1 + \frac{(X-X_1)+(X-X_3)}{(X_2-X_1)(X_2-X_3)} f_2 +$$

$$\frac{(X-X_1)+(X-X_2)}{(X_3-X_1)(X_3-X_2)} f_3 , \qquad [8]$$

and

$$F''(X) = \frac{2}{(X_1-X_2)(X_1-X_3)} f_1 + \frac{2}{(X_2-X_1)(X_2-X_3)} f_2 +$$

$$\frac{2}{(X_3-X_1)(X_3-X_2)} f_3 . \qquad [9]$$

At $X=X_1$.

$$F'(X_1) = \frac{(X_1-X_2)+(X_1-X_3)}{(X_1-X_2)(X_1-X_3)} f_1 + \frac{X_1-X_3}{(X_2-X_1)(X_2-X_3)} f_2 +$$

$$\frac{X_1-X_2}{(X_3-X_1)(X_3-X_2)} f_3 \ . \qquad [10]$$

At $X=X_2$,

$$F'(X_2) = \frac{X_2-X_3}{(X_1-X_2)(X_1-X_3)} f_1 + \frac{(X_2-X_1)+(X_2-X_3)}{(X_2-X_1)(X_2-X_3)} f_2 +$$

$$\frac{X_2-X_1}{(X_3-X_1)(X_3-X_2)} f_3 \ . \qquad [11]$$

And at $X=X_3$

$$F'(X_3) = \frac{X_3-X_2}{(X_1-X_2)(X_1-X_3)} f_1 + \frac{X_3-X_1}{(X_2-X_1)(X_2-X_3)} f_2 +$$

$$\frac{(X_3-X_1)+(X_3-X_2)}{(X_3-X_1)(X_3-X_2)} f_3 \ . \qquad [12]$$

The discrete representation of an arbitrary continuous function defined along the root axis can be defined, in matrix notation, by

$$\mathbf{F} = \begin{bmatrix} f_1 \\ f_2 \\ \vdots \\ f_n \end{bmatrix} , \qquad [13]$$

$$\nabla\mathbf{F} = \begin{bmatrix} \nabla f_1 \\ \nabla f_2 \\ \vdots \\ \nabla f_n \end{bmatrix} . \qquad [14]$$

and

$$\nabla^2\mathbf{F} = \begin{bmatrix} \nabla^2 f_1 \\ \nabla^2 f_2 \\ \vdots \\ \nabla^2 f_n \end{bmatrix} , \qquad [15]$$

where $\nabla = \frac{\partial}{\partial X}$ is the gradient operator and $\nabla^2 = \frac{\partial^2}{\partial X^2}$ is the Laplace operator. By combining equations [10]–[12] and equation [14] we define the discrete form of the gradient operator as

$$\nabla = \mathbf{H} , \qquad [16]$$

where $\mathbf{H}$ is a matrix whose elements are given by

$$\begin{cases} H_{i,i-1} = \dfrac{X_i - X_{i+1}}{(X_{i-1}-X_i)(X_{i-1}-X_{i+1})} \\ H_{i,i} = \dfrac{2X_i - X_{i-1} - X_{i+1}}{(X_i - X_{i-1})(X_i - X_{i+1})} , \quad 1<i<n. \\ H_{i,i+1} = \dfrac{X_i - X_{i-1}}{(X_{i+1}-X_{i-1})(X_{i+1}-X_i)} \end{cases} \qquad [17]$$

The values of the elements at the two boundaries, X_1 and X_n, depend on the interpolation formula used. If the three–point interpolation formula is used at the boundaries, the values of the elements of $\mathbf{H}$ at the boundary are expressed by formulas corresponding to equations [10] and [12], respectively. If two–point interpolation formulas are used at the boundaries, simpler formulas can be obtained. For simplicity, these formulas will not be written explicitly.

Similar to equation [17], the discrete Laplace operator is defined as

$$\nabla^2 = \mathbf{B} . \qquad [18]$$

The elements of the matrix $\mathbf{B}$ are found by combining equations [9] and [15] as

$$\begin{cases} B_{i,i-1} = \dfrac{2}{(X_1-X_2)(X_1-X_3)} \\ B_{i,i} = \dfrac{2}{(X_2-X_1)(X_2-X_3)} \quad , \ 1<i<n \ . \\ B_{i,i+1} = \dfrac{2}{(X_3-X_1)(X_3-X_2)} \end{cases} \qquad [19]$$

The values of the elements of **B** at the two boundaries are defined by

$$B_{1,j} = B_{2,j} \ , \ j=1,2,3 \qquad [20]$$

and

$$B_{n,j} = B_{n-1,j}, \ j=n, \ n-1, \ n-2 \ . \qquad [21]$$

With these definitions, the gradient and divergence of a function **F**, whose values are designated at nodal points X_i, i=1,2,...n, are calculated as

$$\nabla \mathbf{F} = \mathbf{H}\cdot\mathbf{F} \ , \qquad [22]$$

and

$$\nabla^2 \mathbf{F} = \mathbf{B}\cdot\mathbf{F} \ . \qquad [23]$$

Assuming a second function K is also defined along the root axis, another operation often encountered is

$$\frac{\partial}{\partial X}\left(K\frac{\partial F}{\partial X}\right) = K\,\frac{\partial^2 F}{\partial X^2} + \frac{\partial K}{\partial X}\,\frac{\partial F}{\partial X} \ . \qquad [24]$$

With our notations, the discrete equivalent of equation [24] can be written as

$$\nabla(K\nabla F) = K(\mathbf{B}\cdot\mathbf{F}) + (\mathbf{H}\cdot K)(\mathbf{H}\cdot\mathbf{F}) \ . \qquad [25]$$

By defining

$$\mathbf{M} = K\mathbf{B} + (\mathbf{H}\cdot K)\mathbf{H} \ , \qquad [26]$$

equation [25] is simplified further as

$$\nabla(K\nabla F) = \mathbf{M}\cdot\mathbf{F} \ . \qquad [27]$$

For convenience, we have used the notation

$$(\mathbf{KB})_{ij}=K_i B_{ij}, \qquad [28]$$

where summation is not implied. This notation is used throughout this manuscript. These relations are used in formulating the discrete, finite difference equations of water and solute transports along the root axis.

Equations of apoplast water transport

Water transport in the apoplast pathway is described by (Chapter 3)

$$\frac{\partial}{\partial X}\left(K_a \frac{\partial \Psi_a}{\partial X}\right) - \frac{K_{sr}}{\omega_a}(\Psi_a - \Psi_{soil}) - \frac{K_{as}}{\omega_a}[\Psi_a - (P + s_\ell \Pi)] - \mu \rho_\ell \theta \dot{\epsilon} J = 0 \ . \qquad [29]$$

The terms in equation [29] are Darcy flux, water uptake from soil, water flow between apoplast and symplast pathways, and growth effect, respectively (chapter 3). All of the permeability parameters, the growth rate ($\dot{\epsilon}$), and Jacobian (J) may all vary with position as well as time. Using the discrete operators **II**, **B**, and **M** defined in the previous section, the finite difference form of equation [29] is written as

$$\left\{[\omega_a K_a \mathbf{B} + (\mathbf{II}\cdot K_a)\mathbf{II} - K_{sr}\mathbf{I} - K_{as}\mathbf{I}]\cdot \Psi_a\right\}^n = R_a \ , \qquad [30]$$

where

$$R_a = R_{a1}^n + R_{a2} \ . \qquad [31]$$

The terms in equation [31] are defined by

$$R_{a1}^n = \left\{-[K_{sr}\Psi_{soil} + K_{as}(P - s_\ell \Pi)]\right\}^n \qquad [32]$$

and

$$R_{a2} = \frac{1}{2}[(\mu\rho_\ell\omega_a\theta J)^n + (\mu\rho_\ell\omega_a\theta J)^{n-1}] \frac{\epsilon^n - \epsilon^{n-1}}{dt} . \quad [33]$$

Equations [30]–[33] define the implicit scheme for solving the apoplast water transport equation. This scheme is used in the initialization stage of the model. Once the model is initialized, the more stable Crank–Nickolson scheme should be used. This is achieved by redefining equation [31] as

$$R_a = R_{a1}^n + 2R_{a2} + R_{ac} , \quad [34]$$

where

$$R_{ac} = - \left\{[\omega_a K_a B + (H \cdot K_a)H - K_{sr}I - K_{as}I] \cdot \Psi_a\right\}^{n-1} + R_{a1}^{n-1} . \quad [35]$$

When the Crank–Nickolson scheme is invoked during a simulation, R_{ac} is calculated at the end of each time step and saved in a vector to be used for the next time step.

Equations of symplast water transport

Transport of water in the symplast pathway is described by (Chapter 3)

$$\frac{\partial}{\partial X}\left\{K_s \frac{\partial}{\partial X}(P + s_x\Pi)\right\} + \frac{K_{as}}{\omega_s}[\Psi_a - (P + s_\ell\Pi)] - \mu\rho_\ell\dot{\epsilon}J = 0 , \quad [36]$$

where the first term describes axial Darcy flux, the second term describes water uptake from the apoplast, and the third term describes the effect of growth (Chapter 3). The unknown quantity to be solved is turgor

potential. Procedures similar to those used in deriving the finite–difference equations for water transport in the apoplast pathway lead to

$$\left\{[\omega_s K_s B + (H\cdot K_s)H - K_{as} I]\cdot P\right\}^n = R_s \ , \qquad [37]$$

where

$$R_s = R_{s\pi}^n + R_{s1}^n + R_{s2} \ , \qquad [38]$$

with the terms defined by

$$R_{s\pi}^n = - \left\{[\omega_s K_s B + (H\cdot K_s)H]\cdot(s_x \Pi) - K_{as}(s_\ell \Pi)\right\}^n \ , \qquad [39]$$

$$R_{s1}^n = - \left\{K_{as}\Psi_a\right\}^n \qquad [40]$$

and

$$R_{s2} = \tfrac{1}{2}[(\mu\rho_\ell\omega_s J)^n + (\mu\rho_\ell\omega_s J)^{n-1}] \ \frac{\epsilon^n - \epsilon^{n-1}}{dt} \ . \qquad [41]$$

The finite difference scheme defined by equations [37]–[41] is called the implicit method. When the more stable Crank–Nickolson scheme is used,

$$R_s = R_{s\pi}^n + R_{s1}^n + 2R_{s2} + R_{sc} \ , \qquad [42]$$

where

$$R_{sc} = - \left\{[\omega_s K_s B + (H\cdot K_s)H - K_{as} I]\cdot P\right\}^{n-1} + R_{s\pi}^{n-1} + R_{s1}^{n-1} \ . \qquad [43]$$

During model simulation, the implicit scheme is used to initialize the system which is then converted to the Crank–Nickolson scheme. When the Crank–Nickolson scheme is used, the vector R_{sc} is calculated at the end of each time step and stored in the memory to be used for the next step.

Equations of solute transport

The mass balance of solute along the root axis is described by (Chapter 4),

$$J\frac{\partial C}{\partial t} = \frac{\partial}{\partial X}\left[\alpha_f D_d \frac{\partial C}{\partial X} - D_q C Q_{sx} - D_a A(C)\right] - J(\dot{\epsilon}C + S_w + S_s + R_r), \quad [44]$$

where

$$Q_{sx} = - K_s \frac{\partial}{\partial X}(P + s_x \Pi) \quad [45]$$

and

$$\Pi = - CRT \ . \quad [46]$$

The first term on the right hand side of equation [44] is the gradient of total axial solute flux. The second term includes the effects of growth, wall and cytoplasm synthesis, and respiration. Equation [44] states that the axial flux of solute has three components: facilitated dispersion, mass flow, and active transport (Chapter 4).

The finite difference equation of solute transport in the material coordinate system is

$$\left\{\{\alpha_f D_d B + [H\cdot(\alpha_f D_d)]H - D_q Q_{sx} I - A_g I\}\cdot C\right\}^n = R_c \ , \quad [47]$$

where

$$A_g = \frac{1}{2dt}(J^n + J^{n-1})[I + \frac{1}{2}(\epsilon^n - \epsilon^{n-1})] \ . \quad [48]$$

By defining

$$A_{-g} = \frac{1}{2dt}(J^n + J^{n-1})[-I + \frac{1}{2}(\epsilon^n - \epsilon^{n-1})] \quad [49]$$

and

$$A_s = \frac{1}{2}\left\{[J(S_w+S_s+R_r)]^n + [J(S_w+S_s+R_r)]^{n-1}\right\}, \quad [50]$$

the right hand side of equation [47] can be expressed by

$$\mathbf{R_c} = \mathbf{A_{-g}C^{n-1}} + \mathbf{A_s} + [\mathbf{H}\cdot(\mathbf{D_a A(C)})]^n \ . \qquad [51]$$

The scheme described by equations [47]–[51] is the implicit method that can be used to initialize the model. The equations for the more stable Crank–Nickolson scheme are

$$\left\{\{\alpha_f \mathbf{D_d B} + [\mathbf{H}\cdot(\alpha_f \mathbf{D_d})]\mathbf{H} - (\mathbf{I}-s_x)\mathbf{Q_{sx}I} - 2\mathbf{A_g I}\}\cdot\mathbf{C}\right\}^n = \mathbf{R_c} \ , \qquad [52]$$

and

$$\mathbf{R_c} = 2\mathbf{A_{-g}C^{n-1}} + 2\mathbf{A_s} + [\mathbf{H}\cdot(\mathbf{D_a A(C)})]^n + \mathbf{R_{cc}} \ , \qquad [53]$$

where

$$\mathbf{R_{cc}} = -\left\{\{\alpha_f \mathbf{D_d B} + [\mathbf{H}\cdot(\alpha_f \mathbf{D_d})]\mathbf{H} - (\mathbf{I}-s_x)\mathbf{Q_{sx}I}\}\cdot\mathbf{C}\right\}^{n-1} + [\mathbf{H}\cdot(\mathbf{D_a A(C)})]^{n-1} \ . \qquad [54]$$

When the Crank–Nickolson scheme is invoked, $\mathbf{R_{cc}}$ is calculated at the end of each time step and used in the subsequent step.

Boundary conditions

The boundary conditions for water and solute transport at the root tip are written as

$$\omega_a K_a \frac{\partial \Psi_a}{\partial X} + \omega_s K_s \frac{\partial}{\partial X}(P + s_x \Pi) + L_{mstm} K_{sr}(\Psi_a - \Psi_{soil}) = -\mu\rho_\ell(\omega_{sm} + \theta\omega_{am})\dot{\epsilon}_m L_{mstm} \ , \qquad [55]$$

$$L_{mstm} K_{as}[(P + s_\ell \Pi) - \Psi_a] + \omega_s K_s \frac{\partial}{\partial X}(P + s_x \Pi) = -\mu\rho_\ell \omega_{sm} \dot{\epsilon}_m L_{mstm} \ , \qquad [56]$$

and

$$\alpha_f D_d \frac{\partial C}{\partial X} - D_q Q_{sx} C - D_a A(C) = -(S_{sm} + S_{wm} + R_{rm}) L_{mstm} . \quad [57]$$

Equation [55] states that the water requirement of meristem growth is satisfied by axial water transport to the meristem via both apoplast and symplast pathways plus uptake of water by the meristem from soil. Equation [56] states that the water requirement of the growing symplast in the meristem is satisfied by axial transport via the symplast pathway and water flow from apoplast to symplast in the meristem. Equation [57] is equivalent to the statement that the solute requirement of the meristem for growth and metabolism must be supplied by axial solute transport.

Boundary conditions for water and solute transport at the base of the root are required in order to properly define the system. The boundary condition for apoplast water transport and solute transport at the root base are specified as input during model simulation. The boundary condition for water transport in the symplast pathway is calculated from

$$K_{as}[\Psi_a - (P + s_\ell \Pi)] = \mu \rho_\ell \omega_s J \frac{\epsilon^n - \epsilon^{n-1}}{dt} . \quad [58]$$

Equation [58] is the mathematical equivalent of the statement that cells must take up water in order to expand.

It can be shown that the boundary conditions of water and solute transport at both ends can be written in the general form

$$\beta_1 \frac{\partial F}{\partial X} + \beta_2 F = \beta_3 , \quad [59]$$

where F represents either Ψ_a, P, or C. The coefficients β_1, β_2, and β_3 may be constants or functions of time. Equation [59] may be written in the finite difference form as

$$\beta_1^n \, (\mathbf{H}\cdot\mathbf{F})_i^n + \beta_2^n \, f_i^n = \beta_3^n \ , \qquad [60]$$

for the n–th time step, if an implicit scheme is used. In equation [60], i could be either 1, for the boundary at the root base, or n for the boundary at the root tip. When the Crank–Nickolson scheme is used, equation [60] becomes

$$\beta_1^n \, (\mathbf{H}\cdot\mathbf{F})_i^n + \beta_2^n \, f_i^n = \beta_3^n + R_b \ , \qquad [61]$$

where

$$R_b = [\beta_3 - \beta_1 \, (\mathbf{H}\cdot\mathbf{F})_i + \beta_2 \, f_i]^{n-1} \ , \qquad [62]$$

which is calculated at the end of each time step, to be used in the subsequent step.

RESULTS AND DISCUSSION

Input data preparation

The parameters in the growth equations include the elastic strength (G_e) and viscoelastic strength (G_v) of the cell wall, time coefficient of physical cell wall stress relaxation (τ), coefficients of synthesis (K_κ) and degradation (K_d), and, for the elongation region, the age of the cells when elongation begins to stop (t_g). These parameters are estimated as $G_e=G_v=40$ MPa, $\tau=1$ hr, $t_g=9$ hr, $K_\kappa = 7.5$ hr^{-2}, and $K_d=0.5$ hr^{-1} for the elongation region (Chapter 5). For the meristem, a value of 3 hr^{-2} is assumed for K_κ. Other parameters are assumed to be the same for both the elongation region and the meristem. The length of the meristem is assumed to be 1×10^{-3} m. The constants A and a in equation [A16] that describe the rate of cell division are assumed to be 100 and 0.6, respectively (Tyson. 1986). The average cell radius in the meristem of the primary root of *Zea mays* is 1×10^{-5} m (Erickson and Sax, 1956). Assuming that the meristem was at the steady state, $dr_m/dt=0$, results in an estimate of the maximum cell radius $r_{m,max}=1.5\times10^{-5}$ m.

A value for the cell membrane reflection coefficient is needed in the equations of water and solute transport. The model allows different values for the reflection coefficient of the symplast–apoplast boundary (s_ℓ) and for cell–to–cell solute transport within the symplast pathway (s_x), because of the existence of plasmodesmata connecting neighboring cells in the symplast pathway. As the phloem elements mature, s_x decreases to zero. As a result, axial flow of water in the symplast pathway is

driven by a turgor potential gradient (equation 36), as described by the Munch pressure flow hypothesis. An initial value of 0.97 (Dainty, 1976) was assumed for both s_ℓ and s_x at the instant when the cells leave the meristem. It is assumed that s_x then decreases exponentially with a time constant of 15 hr as the cells mature.

The values of membrane permeability for water flow between the apoplast and the symplast pathways (L_c) and for cell–to–cell water flow within the symplast pathway (L_x) used in our simulations are $L_c=8\times10^{-12}$ kg m^{-2} and $L_x=3\times10^{-10}$ kg m^{-2} (Molz, 1976). Note that these are permeabilities. These values were calculated by multiplying the conductivities (m s^{-1} MPa^{-1}) with $\mu\rho_\ell$, where ρ_ℓ is the density and μ is the viscosity of water. The coefficients of diffusion for solute transport across the cell–to–cell membrane (D_m) and in the liquid phase within the cells (D_0) are 14×10^{-8} m s^{-1} and 0.7×10^{-9} m^2 s^{-1} respectively (Nobel, 1983). Molecular diffusion alone is inadequate to account for the transport processes of solute in plant tissues (Epstein, 1976; Nobel, 1983). Chen and Russell (1989) report that facilitated diffusion increased the glutamine transport rate in a bacterial culture by at least 1000 fold. Accordingly, a value of 10^4 was assumed for the coefficient of facilitated diffusion, α_f. Energy consuming active transport is another important mechanism of solute transport (Nobel, 1983; ref). Because of the lack of information, a value of 2×10^{-5} mol m^{-2} s^{-1} was assumed. This rate is sufficient to support the growth of a 10^{-3} m root segment growing at a typical rate of 4×10^{-5} s^{-1}. Since sucrose is the main transported carbohydrate, the molecular weight of the solute is 360×10^{-3} kg mol^{-1}.

Assuming that resistance to axial water transport in the symplast

pathway results mainly from membranes, the axial permeability of the symplast pathway is calculated from equation [A34] using the membrane permeability and cell size estimated above. This results in $K_s = 6\times10^{-15}$ kg m^{-1}. Since $K_{s,o}$ (equation [A34]) represents the permeability in the symplast pathway when there is no resistance from the cell membranes, or when the phloem elements are fully developed, it is assumed that $K_{s,o} = 6\times10^{-13}$ kg m^{-1}, which is 100 times higher than when there are membrane resistances. The permeability of cell walls may be 100 times higher than the permeability of cell membranes (Dainty, 1976; Lauchli, 1976). Therefore, $K_{a,o}$ is assumed to be 6×10^{-13} kg m^{-1}. A typical value of the permeability of a whole plant tissue is approximately 10^{-13} kg m^{-1} (Dainty, 1976; Lauchli, 1976; Silk and Wagner, 1980). These estimated values are within the acceptable range of the values reported in the literature.

Actively growing plant roots typically respire about 10% of the tissue dry weight per day. Assuming sucrose is the main substrate, it can be calculated that this is equivalent to a respiration rate of approximately 7.7×10^{-4} mol m^{-3} s^{-1} in the symplast. The rate of cell wall synthesis is chosen so that a constant apoplast fraction (ω_a) of 0.2 is maintained. The rate of cytoplasm synthesis in the meristem is chosen so that a constant cytoplasm constituent density of 120 kg m^{-3} is maintained. For the elongation region, it is assumed to be a fraction of the rate of cell wall synthesis. More realistic relations can be used when more information becomes available.

The rates of synthesis of the metabolic cell wall loosening system (K_κ), respiration (R_r), and active solute transport (α_a), as well as the

coefficient of facilitated diffusion (α_d), are all assumed to be proportional to the cytoplasm density and related to solute concentration by a Michaelis–Menten type relation. Because of lack of information, the values for the parameters in these Michaelis–Menten relations are all chosen so that the rates estimated in the previous paragraphs represent the conditions under a cytoplasm density (ρ_s) of 120 kg m^{-3} and a solute concentration of 0.4 M. The maximum rates are assumed to be twice the rates estimated in the previous paragraphs.

Finally, the density of the cell wall was assumed to be 800 kg m^{-3} with a porosity of 0.5. The radius of the root was 5×10^{-5} m and the average distance between neighboring roots was 10^{-2} m.

Root length as a function of time

The root length as a function of time, simulated using the parameters estimated in the previous section, is shown in figure 6.2. The soil water potential was assumed to be –0.25 MPa, and the soil water permeability was 10^{-10} kg m^{-2}. Soil resistance to root elongation was assumed to be zero. An apoplast water flux of -10^{-3} m s^{-1} was used as the boundary condition at the root base for water transport in the apoplast pathway. A constant solute concentration of 0.4 mol was used as the solute boundary condition at the root base.

The growth of a plant root starts with a meristem. At the beginning, root elongation consists of the contribution from the meristem only. Thus the total rate of root elongation is low. As the time progresses, the cells that are continuously produced by the meristem are displaced into the elongation zone. The number of cells that are

elongating increases, resulting in increased rate of root elongation. When the elongation zone is fully established, the rate of root elongation reaches its maximum. The time the root can continue elongating at this rate depends on the ability of the root to supply solutes to the growth zone. As the root grows, the distance that the solutes must be transported to reach the growing cells increases, and the concentration of solutes in these cells decrease. This results in reduction of turgor pressure as well as the rate of metabolic cell wall loosening process of these cells. As the driving force for growth—the cell wall stress and the biological wall loosening process decrease, the rate of root growth decreases. This is shown in figure 6.3.

Growth pattern along the root axis

The model yields information regrading to growth pattern along the axis of a plant root. Figure 6.4 is a plot of the rate at which a material point is displaced away from the root tip as function of spatial distance from the root tip. This plot is often measured and reported in studies of plant root growth (Erickson and Sax, 1956a; List, 1969; Carmona and Cuadrado, 1986; Pahlavanian and Silk, 1988; Sharp et al., 1988). Figure 6.4 is plotted by using the root tip as a convenient reference point, and viewing the material points along the root axis as being displaced away from the root tip. The rate at which a material point moves away from the root tip equals to the sum of the rate of elongation of all cells between such a material point and the root tip plus the rate of meristematic growth (Chapter 1). Thus, the rate at which a material point in the mature region of the root is displaced away from the root

tip equals to the rate of total root elongation. On the other hand, the material point next to
the meristem is displaced away from the root tip only by the growth of the meristem. It is worth notice that although root tip is a convenient reference point for describing root growth, it is the root tip that actually has the highest velocity of motion. The spatial positions of material points in the mature regions of the root remains constant during root growth. The rate at which a material point in the mature region is displaced away from the root tip is, actually, the velocity at which the root tip is moving in the space at the opposite direction.

Figure 6.4 shows that the rate of displacement is small near the root tip and increases with increasing distance from the root tip until reaching the mature region at about 10 mm from the root tip. At distances greater than 10 mm from the root tip, the rate of displacement remains constant.

Figure 6.5 is a plot of the rate of cell wall synthesis as a function of distance from the root tip. Since cell wall synthesis was assumed to be directly proportional to the local rate of growth, figure 6.5 also shows the pattern of local rate of growth, or strain rate, along the root axis. The rate of growth initially increases sharply to a maximum and then gradually decreases. The initial sharp increase is due to the production of cell wall loosening system in the cells. The gradual decrease after the maximum results mainly from decreasing turgor potential as well as lower cytoplasm density which was assumed to be directly proportional to the metabolic activity of the cells. As the mature region is reached, the rate of cell wall synthesis, and hence the rate of growth, quickly decreased.

Water potential distribution along the root axis

The equations of water and solute transport are solved along with the growth equations during model simulation, yielding information about distribution of water potential and its components along the root axis.

Figure 6.6 shows the distribution of apoplastic water potential along the root axis. In the actively growing region near the root tip, the root water potential is low since the growing cells must take up water from the soil environment. Apoplastic water potential increases towards the mature region of the root. The water potential decrease near the base of the root, between 15 to 18 mm from the root tip, is due to the specified boundary condition of a 1 mm hr^{-1} water flux at the base of the root. The water potential decrease from the mature region to the actively growing region of the root illustrates the concept of growth induced water potential (Boyer, 1988).

Osmotic potential at first increased slightly and then decreased continuously with increasing distance from the root tip (figure 6.7). The initial slight increase in osmotic potential is the result of active solute transport toward the root tip. On the one hand, the rate of growth near the root tip is relatively low. As a result, the rate of solute consumption is low. On the other hand, the size of the cells here is small, resulting in a higher rate of active solute transport. The net effect of these two processes is a slight accumulation of the solute near the root tip. As the distance from the root tip increases, the higher rate of growth results in higher rate of solute consumption along the root axis. At the same time, other mechanisms of solute transport such as convection and dispersion play increasingly more important roles. The net result is the steadily

decreasing osmotic potential with increasing distance from the root tip.

Turgor potential initially decreased with distance from the root tip as a result of the initial increase in osmotic potential (figure 6.8). It then increased gradually, as a result of the decrease in osmotic potential and the slight increase in apoplastic water potential with increasing distance from the root tip. When the mature region is reached, the turgor potential increased quickly as a result of the quick increase of apoplastic water potential. In the mature region, the turgor potential increased gradually towards the base of the root in response to the decrease in osmotic potential. It is interesting to notice that the turgor potential in the elongation region, where it is most needed, is the lowest. This is the consequence of the dynamic balance between water transport toward the elongation region and the rate of elongation.

Growth of a specific cell as functions of time

The model provides not only the information regarding the growth of a plant root as a whole, but also the information about the dynamic growth processes of material points, or cells, along the root axis as functions of time. Figure 6.9 shows the relative cell length, or the ratio between the current length and the initial length, of the cells produced at 2.5 hr after the growth starts as a function of time. Figure 6.10 is a plot of the rate of cell wall synthesis, which is proportional to the rate of cell elongation, of the same group of cells as a function of time. After a cell leaves the meristem, its rate of growth quickly increases to the maximum value as the cell wall loosening system is synthesized. Then the rate of growth decreases gradually with time. As the cell reaches

maturity, the rate of growth quickly decreases to zero. The curve in figure 6.9 resembles the general growth curve of plant cells with a slow, gradual initial growth followed by a quick, nearly exponential growth, and then a sudden stop as the cell reaches maturity (Erickson and Sax, 1986a; Sharp et al., 1988)

Effects of soil water potential

Lowering soil water potential results directly in lower root water potential. This causes decreased turgor potential and hence lower rate of root elongation. Figure 6.11 shows that be decreasing soil water potential from –2.5 to –3.5 MPa, the total length of the root after growing for 15 hr decreased from 18 to 13 mm, a 28% decrease. Figure 6.12 and 13 shows the effect of lowering soil water potential on the spatial pattern of growth along the root axis. Decrease in soil water potential has little effect on the rates of displacement of material points within the first 5 mm from the root tip, despite its large effect on the rate of total root elongation (figure 6.12). Same phenomenon was observed experimentally by Sharp et al. (1988). Figure 6.13 shows the effect of lowering soil water potential on the rate of cell wall synthesis, which is proportional to the local rate of elongation, along the root axis. Decreasing soil water potential from –2.5 to –3.5 MPa resulted only in less than 10% decrease in the rate of cell growth in the elongation region. However, the length of the elongation region decreased nearly 25%. The nearly 30% decrease in the rate of total root elongation is the consequence of the combined effects of shorter elongation region and lower rate of cell elongation. The decrease in the length of the elongation region plays a more important

role in determining the rate of root elongation under water stress.

The relatively small effect of lowering soil water potential on the rate of cell elongation can be explained by considering the interactions between growth and transport of water and solute. Lowering soil water potential causes the apoplastic water potential to decrease in order to maintain water uptake. At the same time, the slower rate of growth reduces the rate of solute consumption along the root axis. The shorter growth region also reduces the distance over which solute must be transported. As a result, the osmotic potential in the growth region near the root tip decreases. Figure 6.14 shows that osmotic potential near the root tip decreased nearly 0.05 MPa as soil water potential decreased from –0.25 to –0.35 MPa. This decrease in osmotic potential offsets partly the effect of lowering soil water potential on the turgor potential of the growth region. As a result, the effect of lowering soil water potential on the turgor potential is kept small, and thus its effects on the growth rate of the cells. This phenomenon is at least partly responsible for the often observed osmotic adjustment in water stressed plants.

Effects of temperature

Temperature affects both the physical and the biological processes involved in root growth, such as transport of water and solute, physical stress relaxation in cell walls, respiration, cytoplasm and cell wall synthesis, and the biological cell wall loosening. Complete quantitative information on the effects of temperature on these processes is lacking. However, it is possible to simulate the main features of temperature effects on root growth.

It is shown in Chapter 1 that effect of temperature on root growth may be characterized by the concept of temperature–time equivalence. This concept was used in obtaining parameter estimates to simulate the temperature effects on root growth. A temperature–time equivalence factor of 0.75 was used for the low temperature simulation. The rates of physical cell wall stress relaxation, biological cell wall loosening, and the degradation of the cell wall loosening system were all reduced by a factor of 0.75. In other words, the time required for these processes to proceed to the same degree at the low temperature is longer than that at the higher temperature by a factor of 0.75^{-1}. The maximum age of the cells when cell elongation stops was also increased by a factor of 0.75^{-1}. Since growth is controlled mainly by the processes of cell wall loosening, and the effects of temperature on the physical transport processes of water and solute are relatively small, the temperature effects on these physical processes may be ignored for a simulation aimed at illustrating the main features of temperature effects on root growth.

Figure 6.15 is a plot of the root length as functions of time at two different temperatures. The curve marked "High Temp." is the same as that in figure 6.2 and is plotted here as a basis of comparison. The curve marked "Low Temp." results from the low temperature simulation described in the previous paragraph. It shows that lowering temperature results in a horizontal shift of the curve in the time axis while the effect on the steady state root elongation rate, expressed as the slope of the linear section of the root length–time curve, is smaller. As a comparison, figure 6.11 shows that soil water potential affects mainly the steady state rate of root elongation while the position of the curve relative to the

time axis remains nearly unchanged.

Figure 6.16 compares the rate of displacement of a material point along the root axis as functions of distances from the root tip. It shows that the curves correspond to different temperatures separate near the tip of the root. The length of the growth region between the root tip and mature region remains approximately constant. Figure 6.17 clearly shows that temperature affects root growth mainly by affecting the rate of cell elongation.

Figure 6.18 illustrates the elongation processes of cells produced at 2.5 hr after root growth start at two different temperatures. Although the cells at the low temperature grow at lower rates, the final length of the cells at two different temperatures are approximately the same because the cells at the low temperature grow for longer time.

Pahlavanian and Silk (1988) showed, by measuring the growth pattern along the axis of primary roots of maize grown under different temperatures, that the length of the growth region and the final length of root cells were nearly independent of temperature. Excellent agreement is found between these results of our model simulation and the results of experimental measurements by these authors.

Similar to the effect of soil water potential, lower rate of growth at low temperature also results in an accumulation of solute near the root tip but to a less degree. Figure 6.18 shows that osmotic potential near the root tip at the lower temperature decreased about 0.03 MPa. However, this effect is expected to become even smaller if the temperature effect on solute transport processes are taken into account.

Effects of soil resistance

Soil resistance causes directly reduction in wall stress since part of the driving force for growth must be spend to push the root through the soil against soil resistance. However, as the growth rate decreases because of the soil resistance, the distance that solute must be transported in order to reach the growth zone decrease, leading to higher solute concentration in the growth zone. The increasing turgor pressure and biological activity due to higher solute concentration may then offset some of the effect caused by increased soil resistance.

Figures 6.20–6.23 illustrates the result of model simulation of the effects of soil resistance on root growth. The curves marked "Resist." resulted from model simulation where a friction coefficient of 1×10^{-4} MPa between soil and the root surface was assumed. The curves marked "No Resist." are the standard curves used as the basis of comparison where zero soil resistance was assumed. Comparison between figures 6.20–6.23 and figures 6.11–6.14 shows that the effects of soil resistance on the root growth is similar to the effect of soil water potential except a small difference between their effects on the rate of cell elongation along the root axis. Lowering soil water potential decreases the rate of cell elongation nearly uniformly throughout the growth region (figure 6.13). Soil resistance, on the other hand, has less effect on the rate of elongation of the cells near the tip of the root. Both soil resistance and soil water stress reduce the length of the growth region of the root.

Effects of carbohydrate supply

In our model simulations, availability of carbohydrates or solutes is

expressed as the solute concentration specified as the boundary at the base of the root. Lower solute concentration means lower turgor potential and lower rate of biological cell wall loosening, thus lower rate growth.

Simulations illustrating the effects of carbohydrate supply to root growth were run with two different solute concentrations at the base of the root, 0.4 mol as the standard and 0.3 mol as comparison. Figures 6.25–6.26 show that the effect of carbohydrate supply on the growth patterns of roots are somewhere between those of soil water potential and those of temperature. Both the length of the growth region and the rate of cell elongation are significantly reduced (figure 6.26). The rate of cell elongation reduced by about 15% as solute supply reduced from 0.4 mol to 0.3 mol, a 25% decrease. At the same time, the length of the growth region reduced by more than 50%. The combined effects of lower rate of cell elongation and shorter elongation region reduced the rate of total root elongation from 1.9 mm hr^{-1} to 0.6 mm hr^{-1}, by a factor of nearly 70% (figure 6.25).

CONCLUDING REMARKS

Growth of plant roots is the result of the interactions among production and elongation of individual cells in the meristem and elongation region, the processes of water and solute transport, and the mechanical interactions between root and soil. Understanding of actions and interactions of these processes in determining the process of root growth, as well as the effects of environmental factors such as soil water stress, temperature, and soil resistance, can not be achieved through studies of these individual factors and processes alone. Such an understanding can only be approached by placing these processes and factors in a comprehensive manner under the context of root growth. In addition, such an approach may provide means to examine the validity of the measurements of plant parameters, such as conductivities and diffusivities, as well as the theories upon which our current understanding of plant growth processes is based.

The complexity of such an task may seem overwhelming, since each of the processes involved in root growth alone may constitute a subject of study with formidable complexity of its own. However, our current under standing of these individual processes does permit such a comprehensive model to be built. The work reported in this study represents the first step toward this direction.

Many unknowns remain in our way toward understanding of plant growth. To name a few, little is known about the exact nature of the biological cell wall loosening process and the postulated enzymatic system which performs such task, about the coordination among the synthesis of cell walls, the synthesis of cytoplasm constituents and the rate of cell

elongation, and about the change in membrane properties such as solute and water permeability and reflection coefficient, as well as the changes in the mechanical properties of the cell walls, during cellular growth. Both experimental and theoretical works are needed for solving these unknowns.

However, despite our incomplete understanding of the processes involved in the growth of plant roots, the model developed in this study does allow us to describe, and to a certain extend, to predict the detailed growth patterns of a plant root under different temperature in a mechanistic manner. Future applications of the model may include simulations of root growth under dynamically changing conditions of soil water potential, soil temperature, as well as the rates of assimilation and translocation of photosynthates.

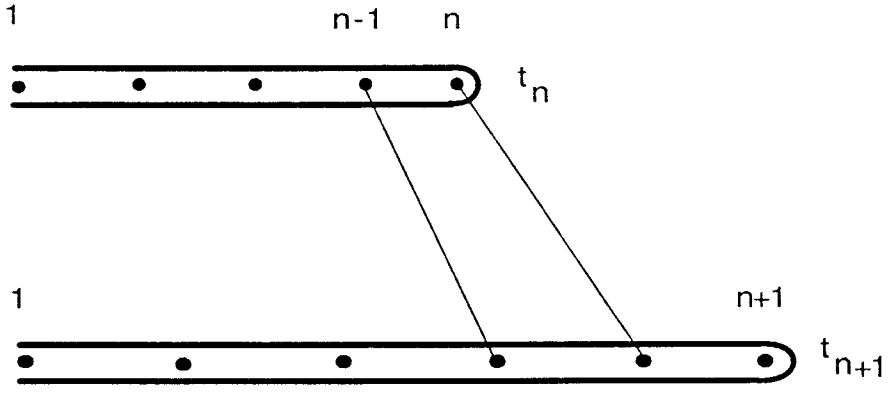

→ Figure 6.1. One dimensional growth process of a plant root. At the n–th time step, material nodal point n is produced by the meristem at the root tip and is the top boundary node for this time step. At the n+1–th time step, the new top boundary node, n+1, is produced and the n–th node becomes an internal node.

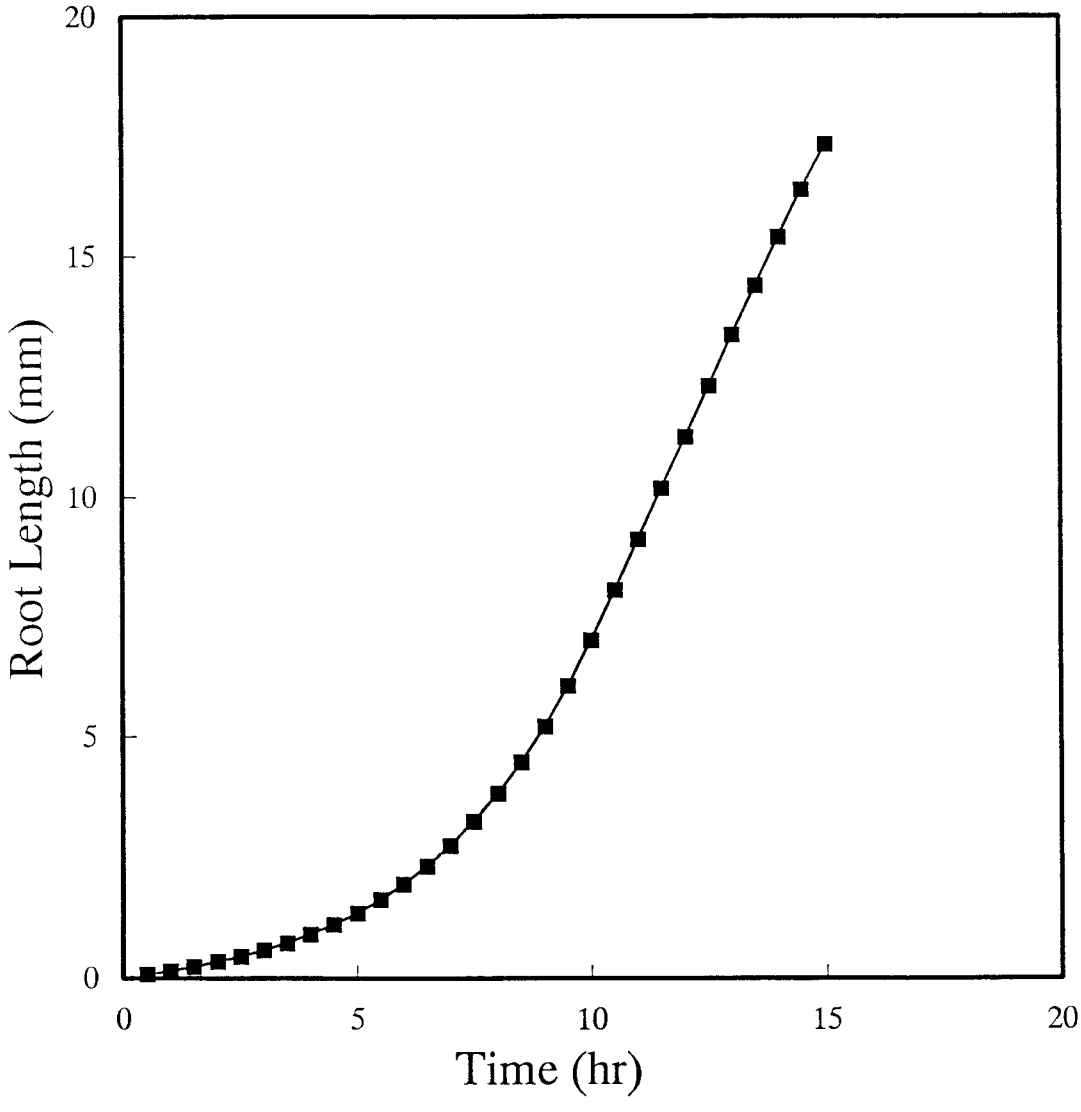

Figure 6.2. Root length as a function of time.

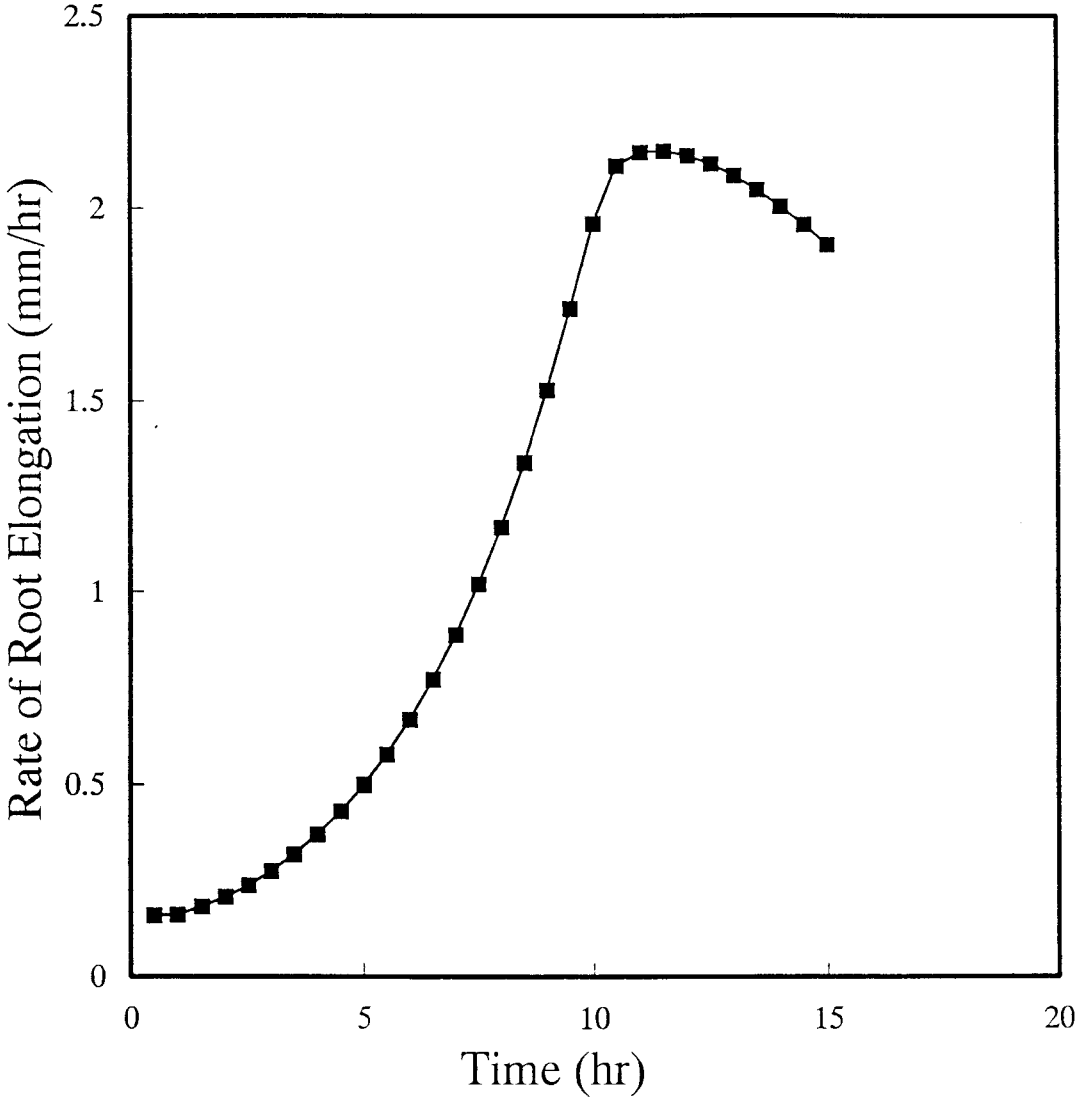

Figure 6.3. Rate of root elongation as a function of time.

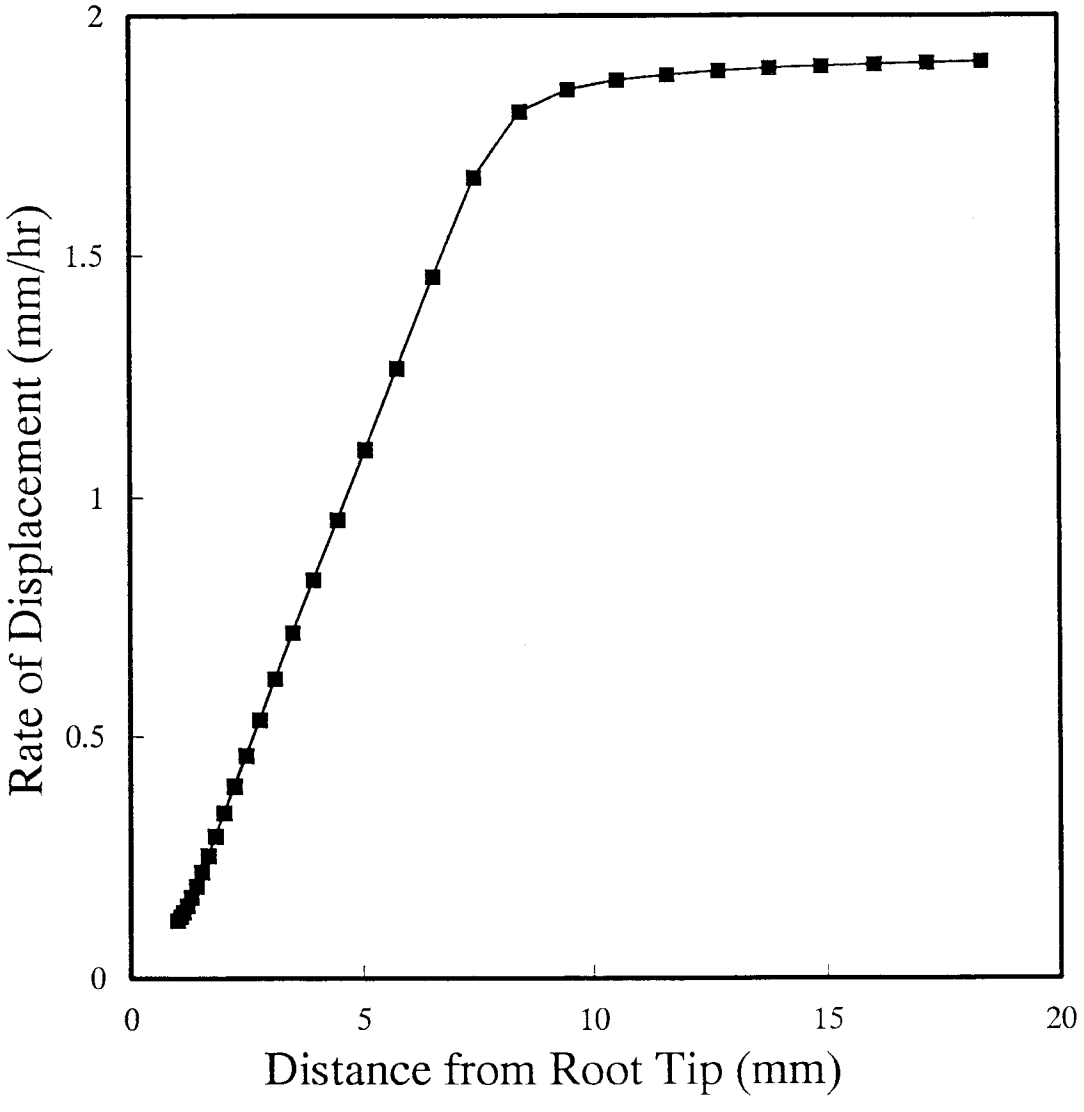

Figure 6.4. Rate of displacement from the root tip of a material point as a function of spatial distance along the root axis.

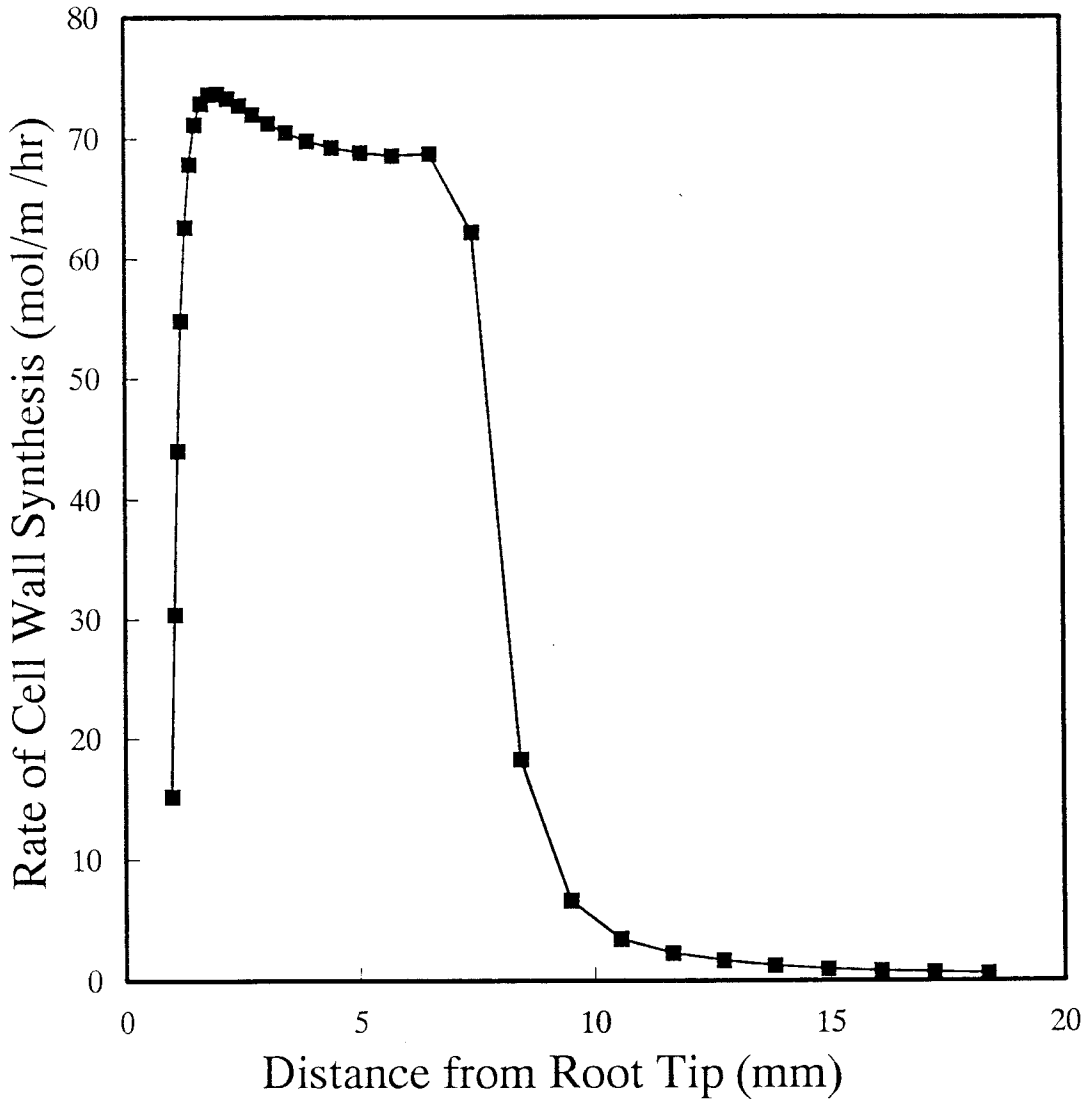

→ Figure 6.5. Rate of cell wall synthesis as a function of spatial distance along the root axis. In the model it is assumed to be proportional to the rate of cell elongation by a constant factor.

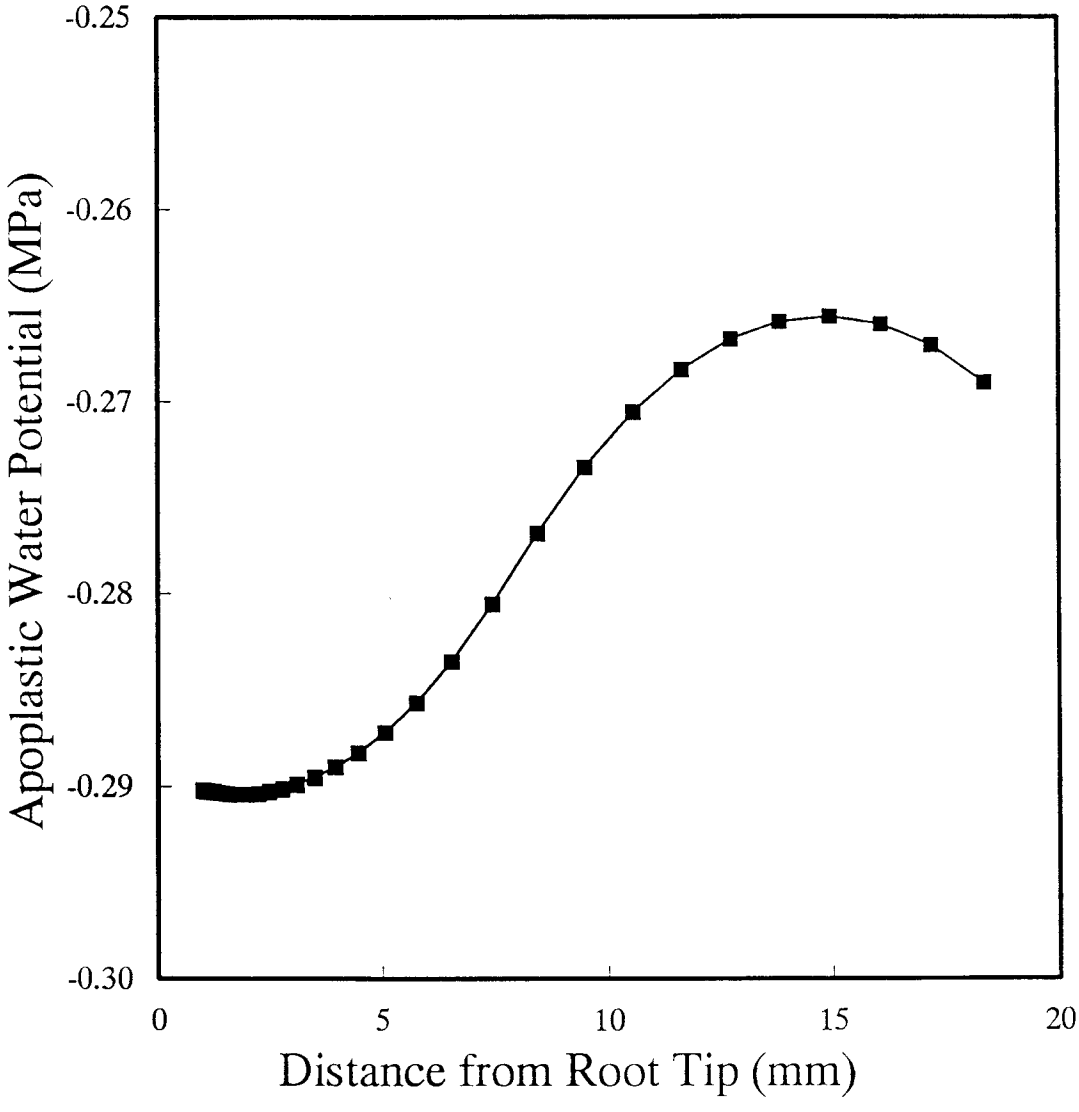

→ Figure 6.6. Apoplastic water potential distribution along the root axis after 15 hr of root growth.

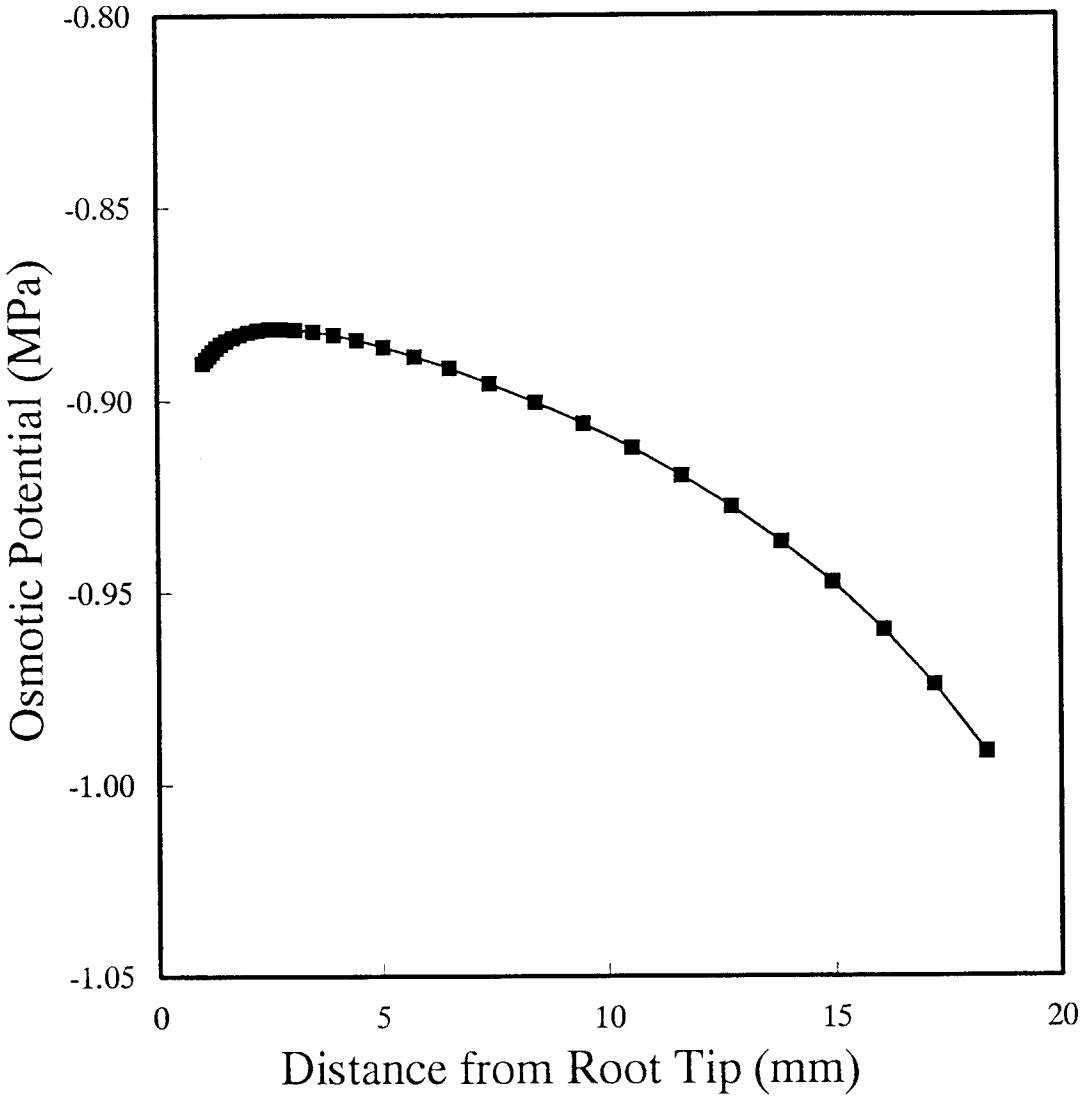

Figure 6.7. Osmotic potential distribution along the root axis after 15 hr of growth.

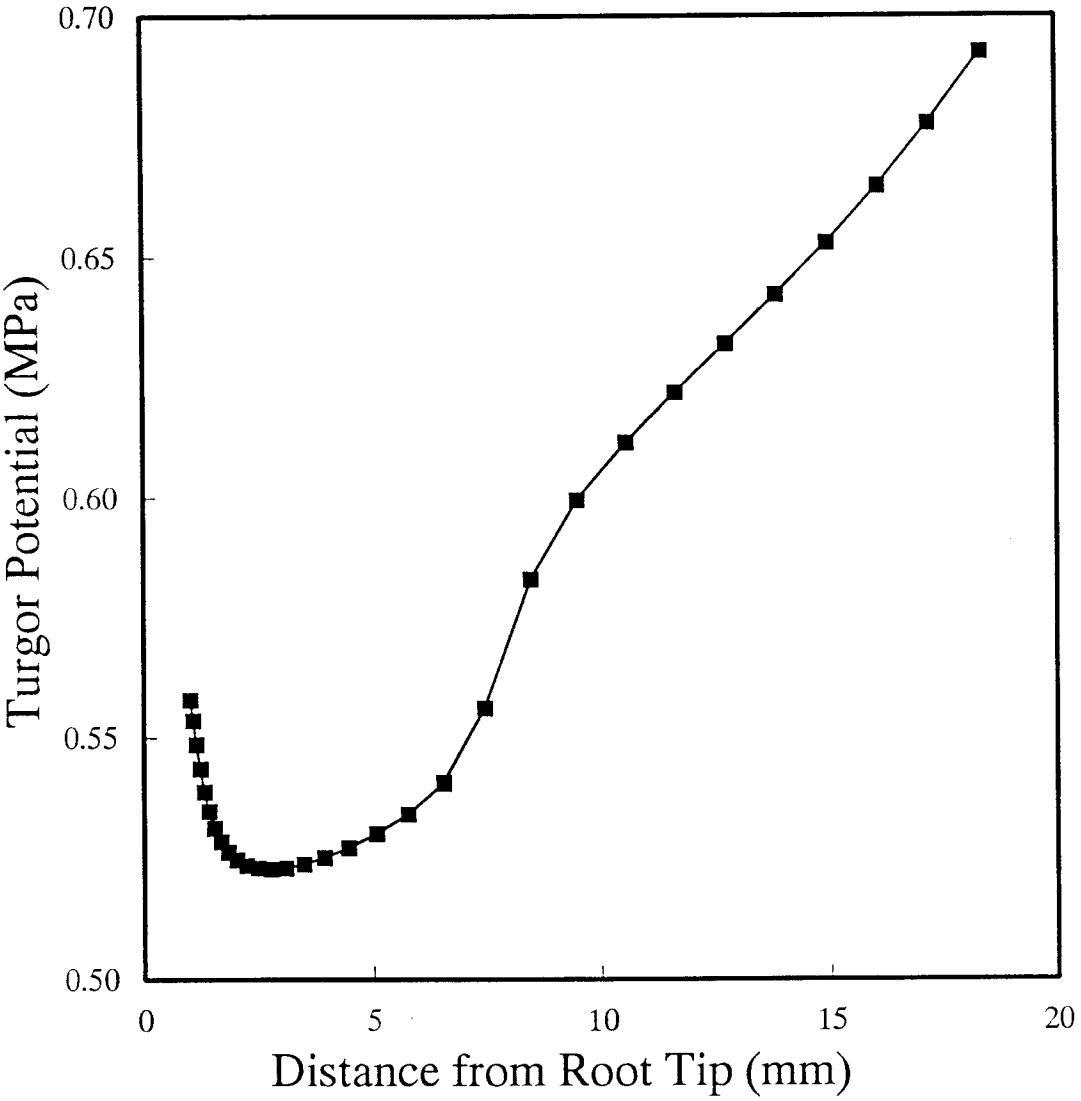

Figure 6.8. Turgor potential distribution along the root axis after 15 hr of growth.

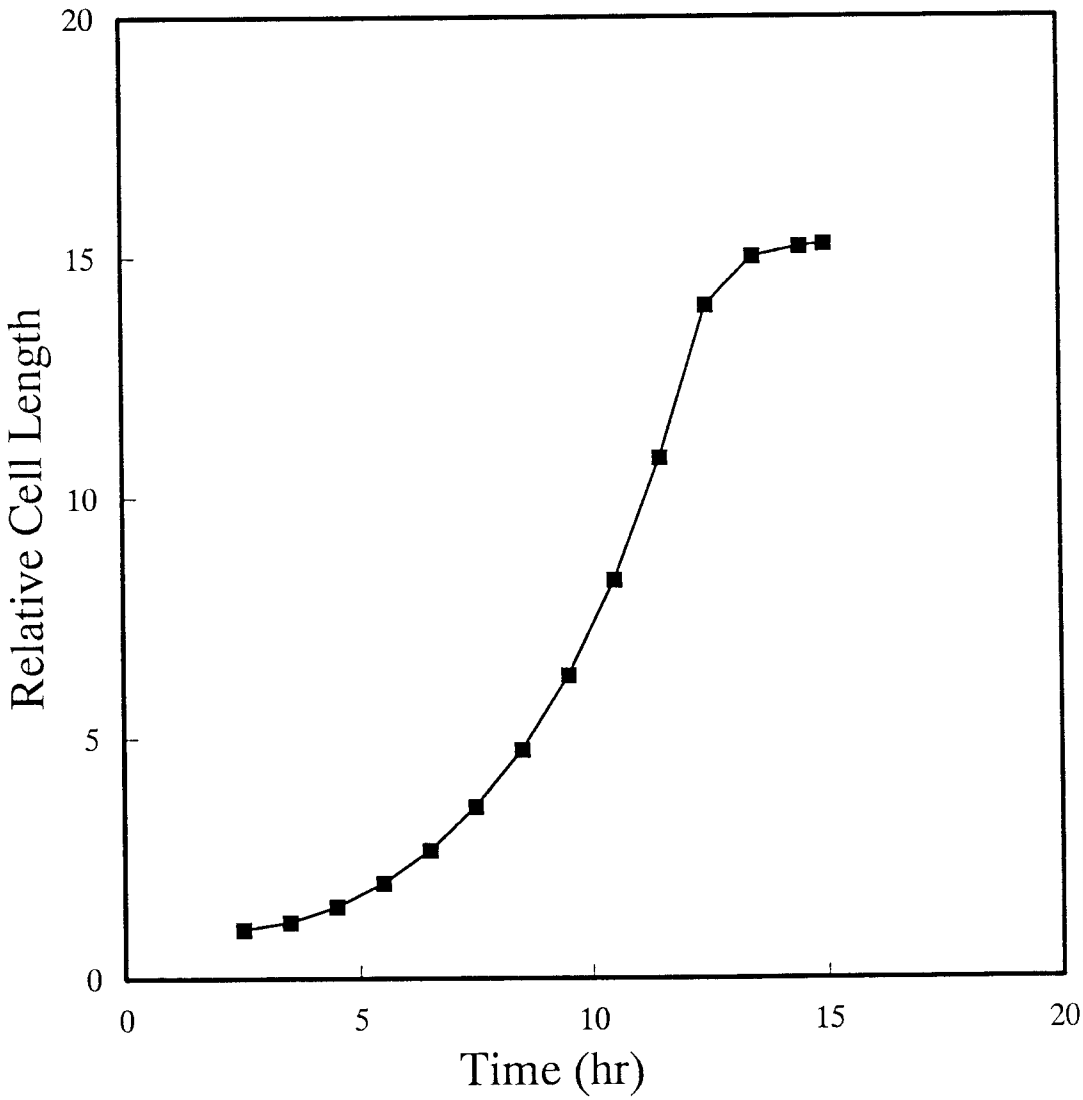

→ Figure 6.9. Elongation of a cells produced at t=2.5 hr as a function of time. Relative cell length is the current length divided by its initial length.

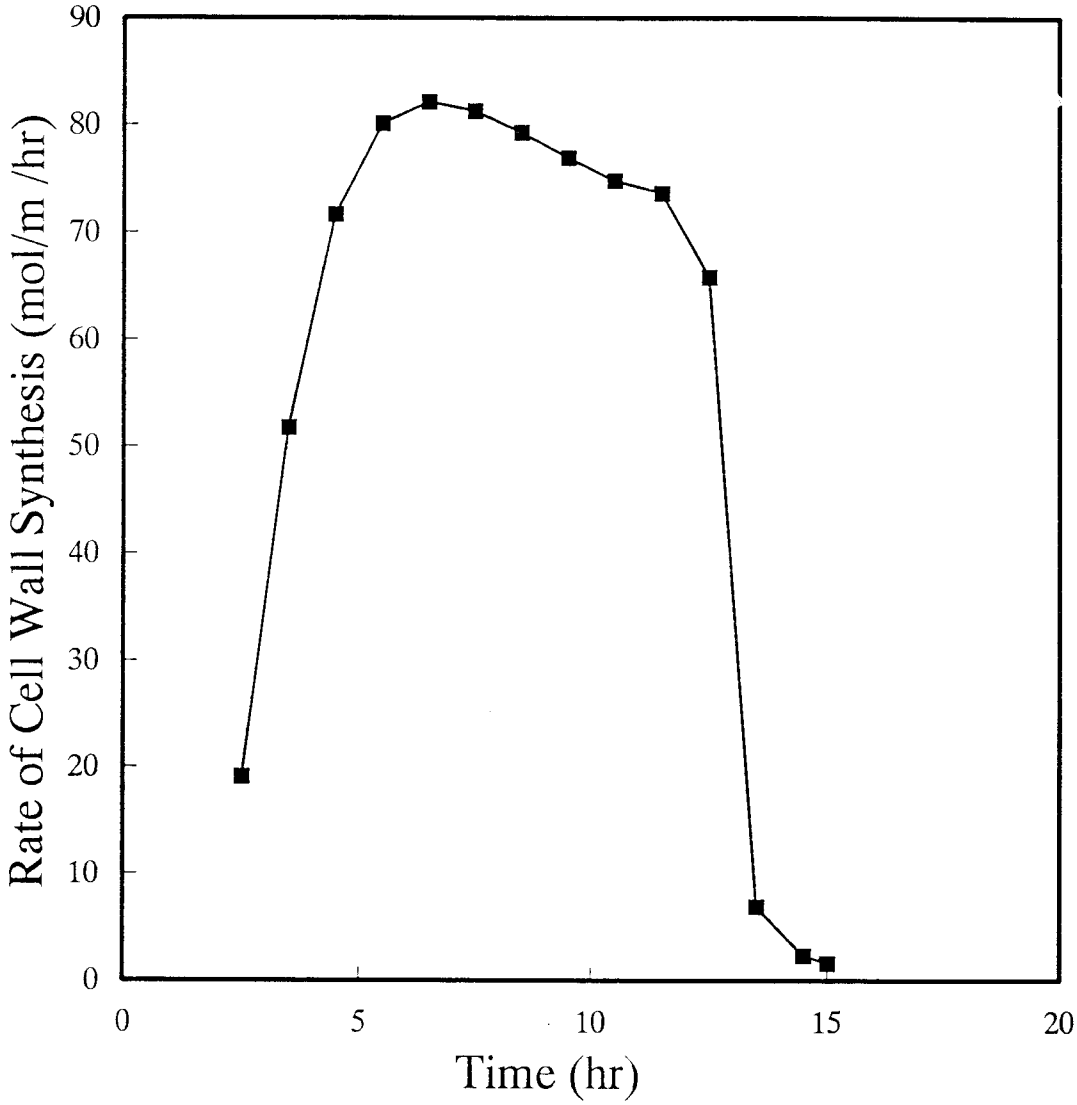

Figure 6.10. Rate of cell wall synthesis of the cells produced at t=2.5 hr as a function of time. It is assumed in the model to be proportional to the rate of cell elongation by a constant factor.

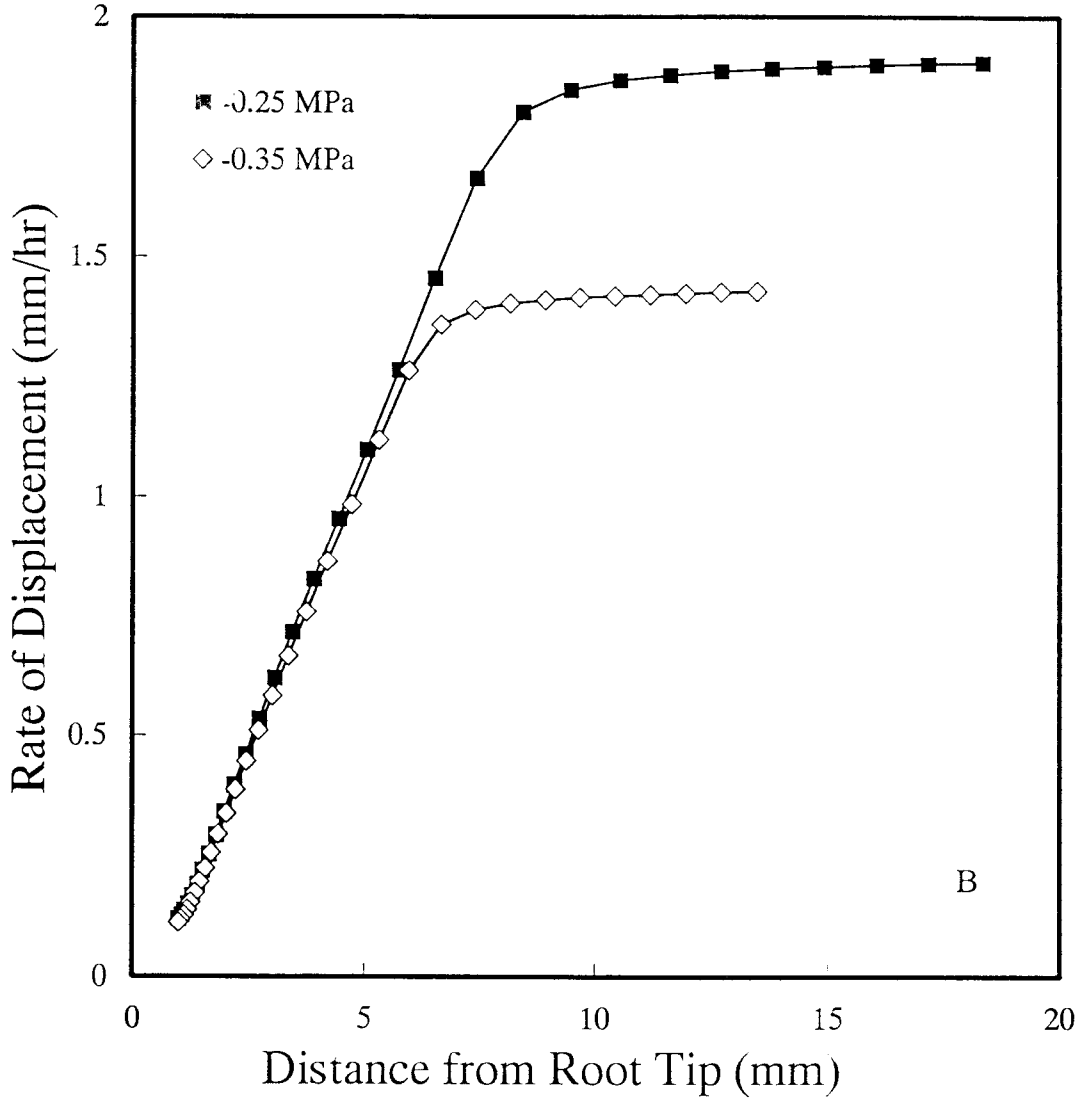

Figure 6.11. Effect of soil water stress on root length as functions of time.

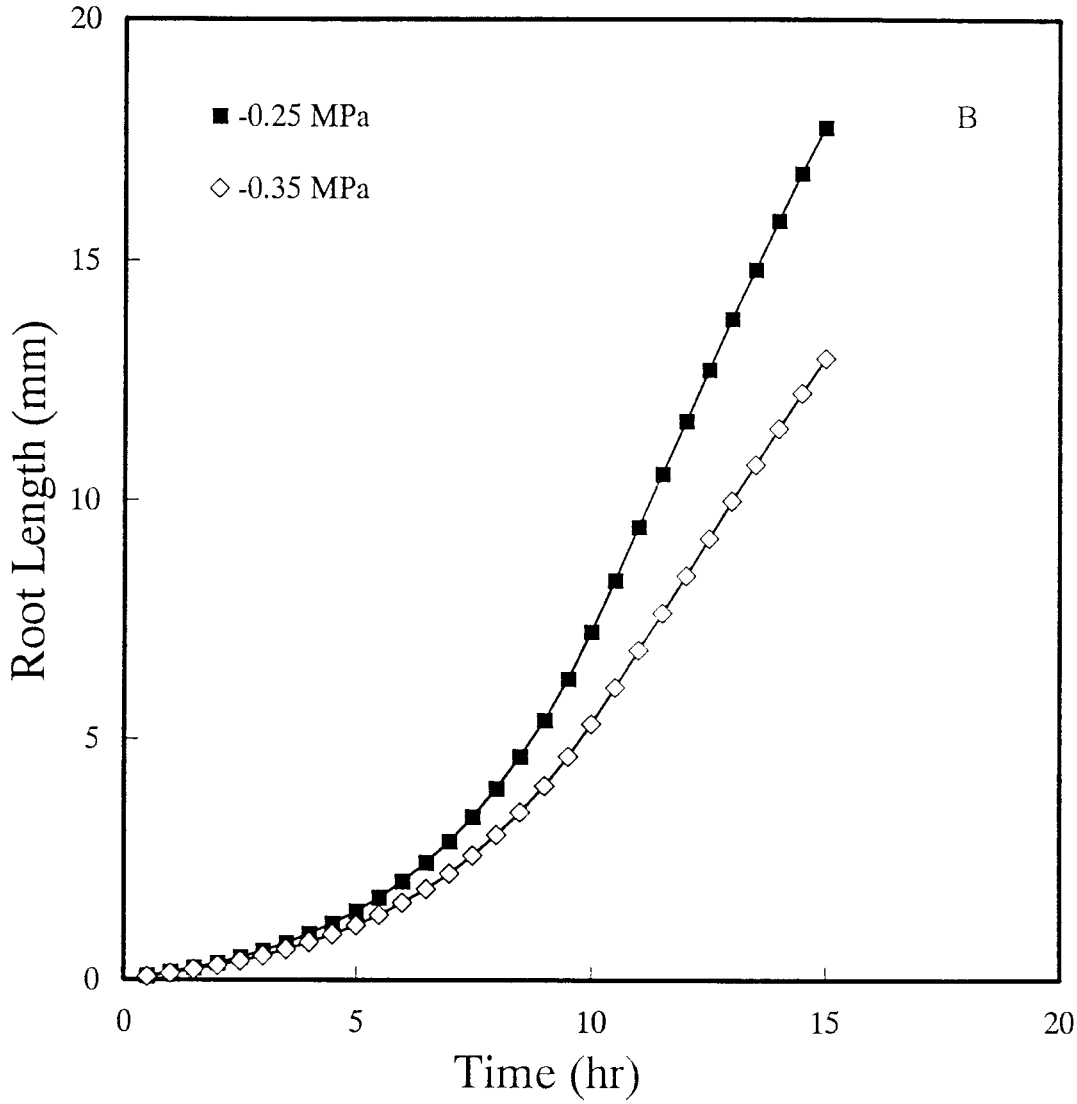

Figure 6.12. Effect of soil water stress on the rate of displacement from the root tip of a material point as functions of spatial distance along a root axis.

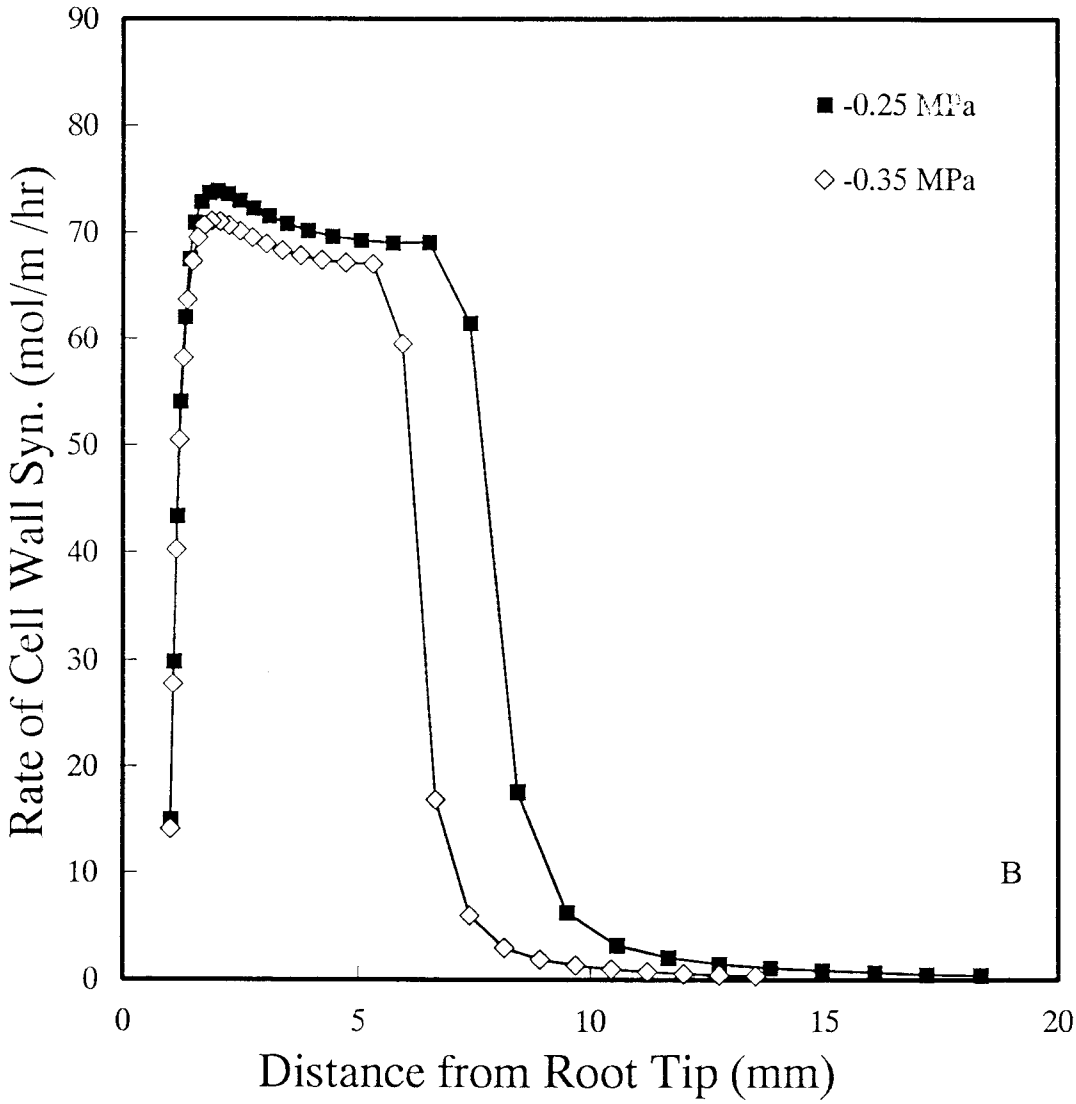

Figure 6.13. Effect of soil water stress on the rate of cell wall synthesis as a function of spatial distance along the root axis. It is assumed in the model to be proportional to the rate of cell elongation by a constant factor.

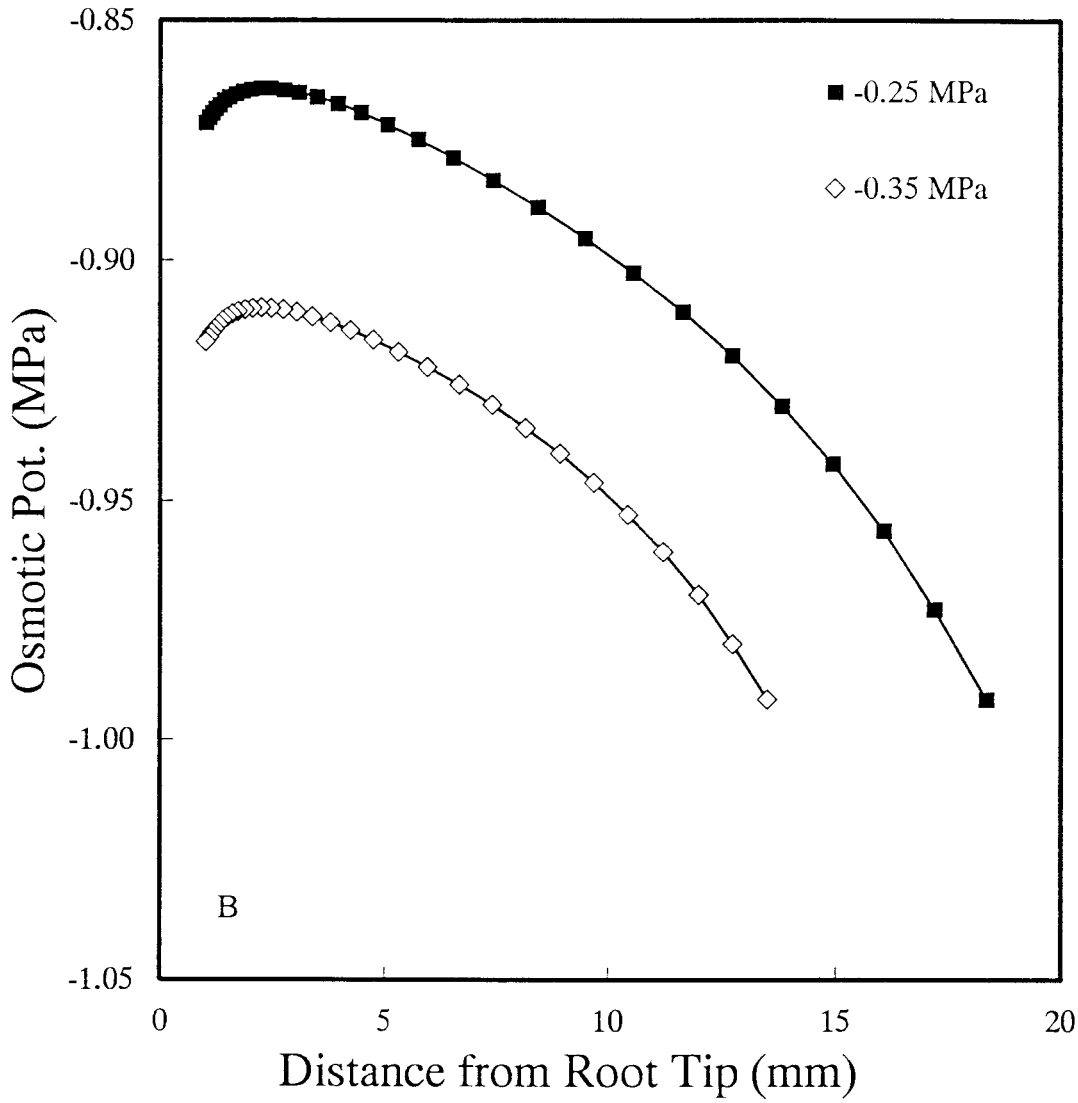

Figure 6.14. Effect of soil water potential on the distribution of osmotic potential along the root axis.

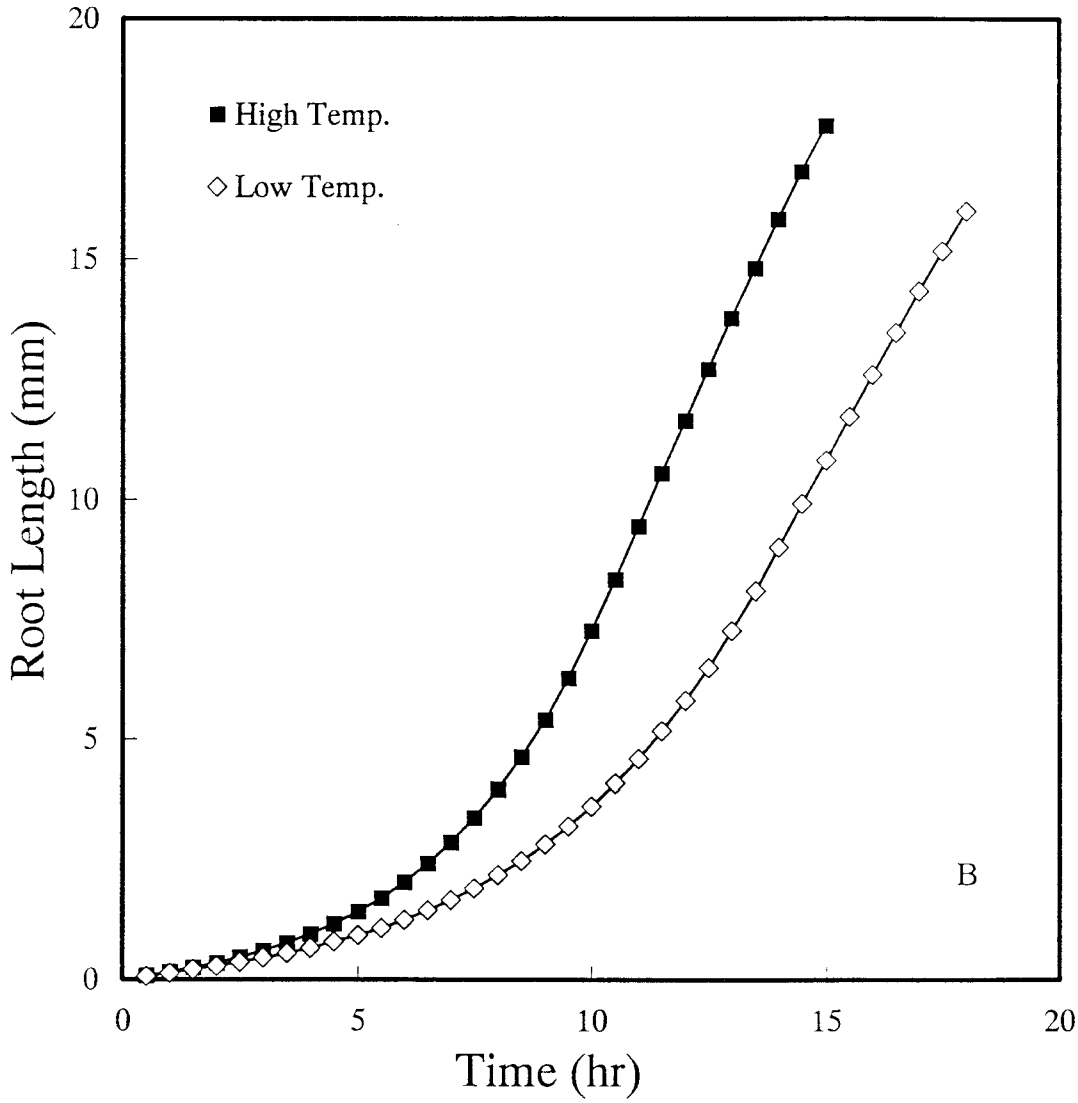

Figure 6.15. Effect of temperature on root length as functions of time.

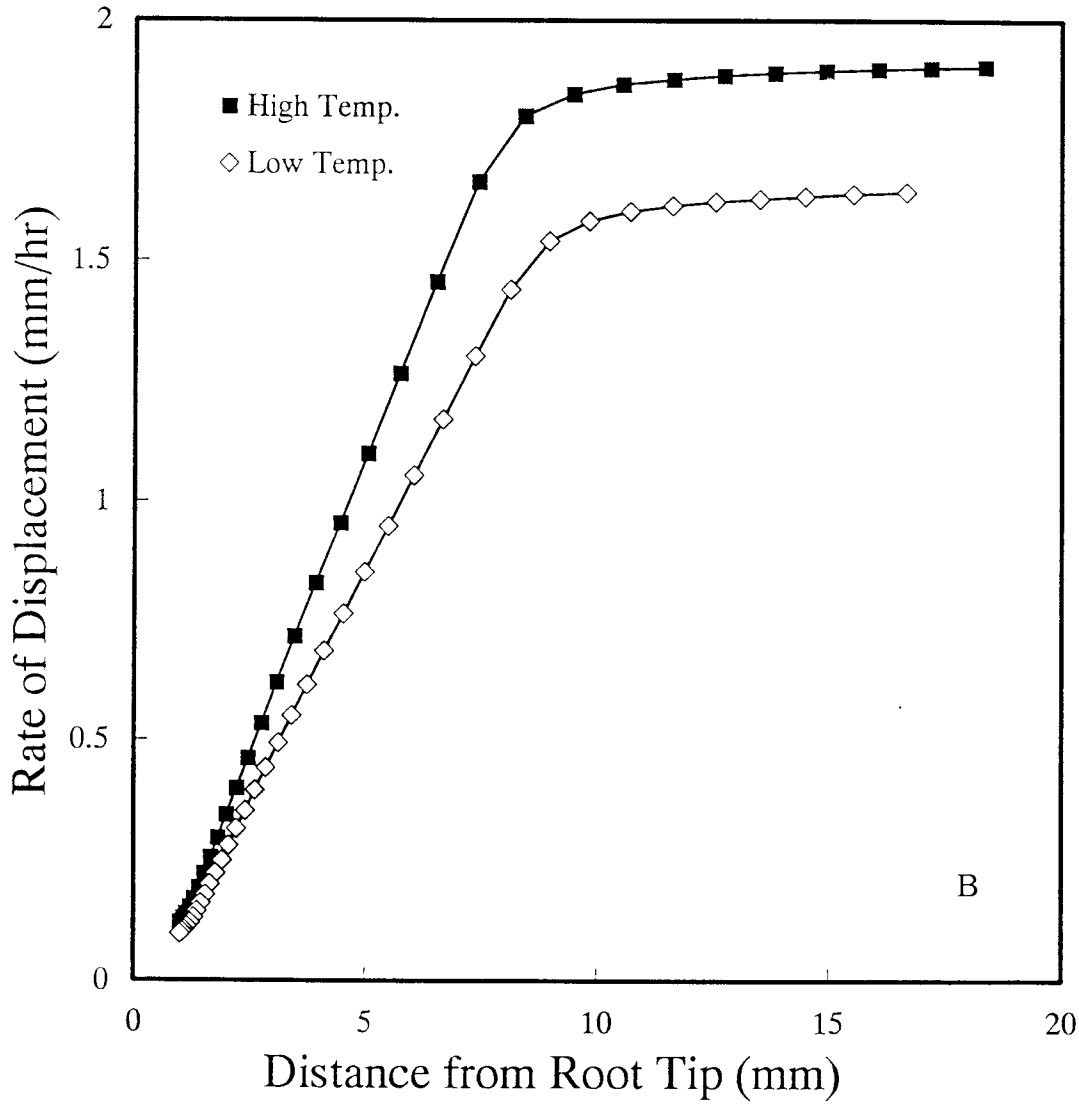

Figure 6.16. Effect of temperature on the rate of displacement of material points along the root axis from the root tip as functions of spatial distance along the root axis.

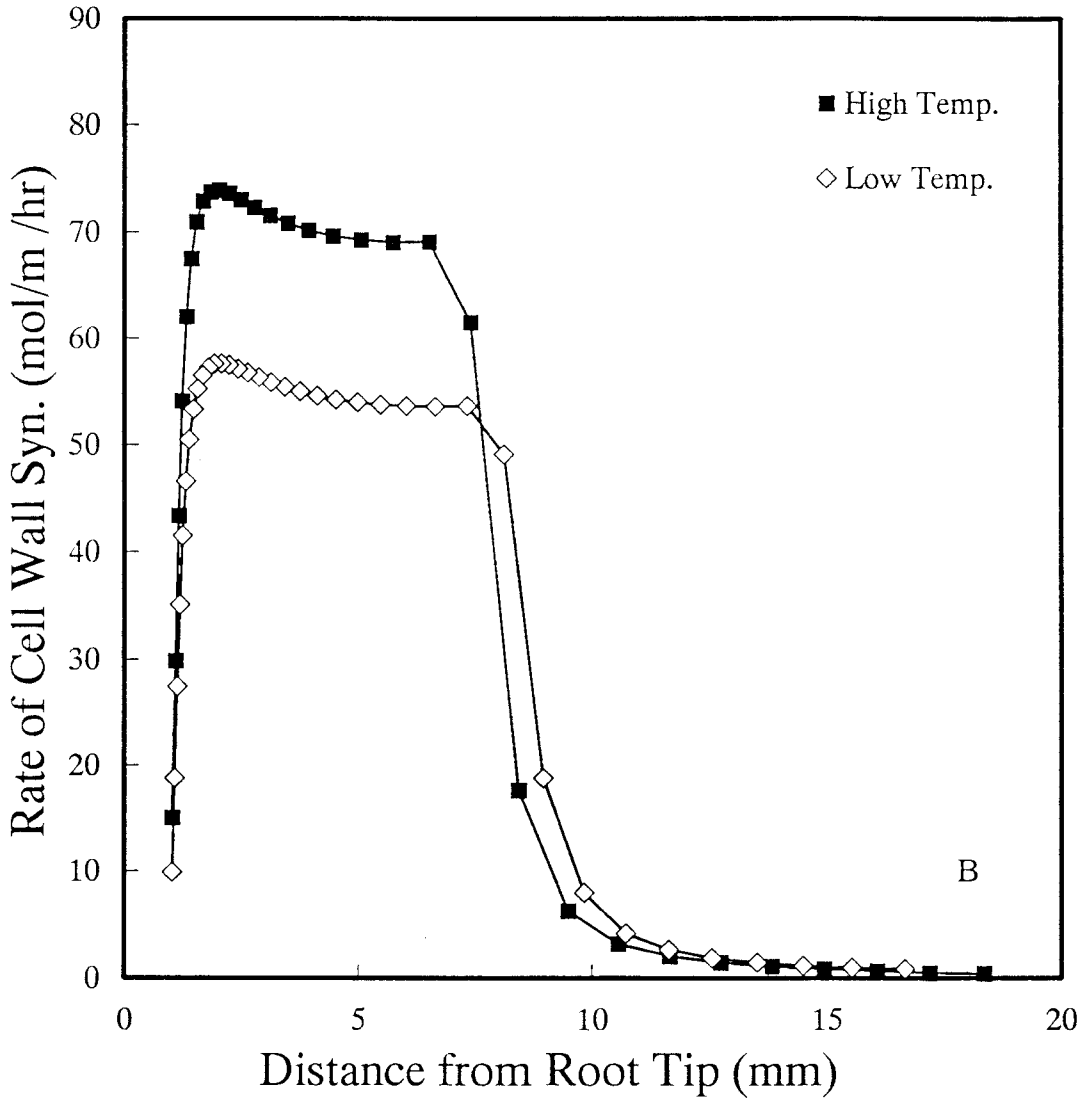

Figure 6.17. Effect of temperature the rate of cell wall synthesis as functions spatial distance along the root axis. It is assumed in the model to be proportional to the rate of cell elongation by a constant factor.

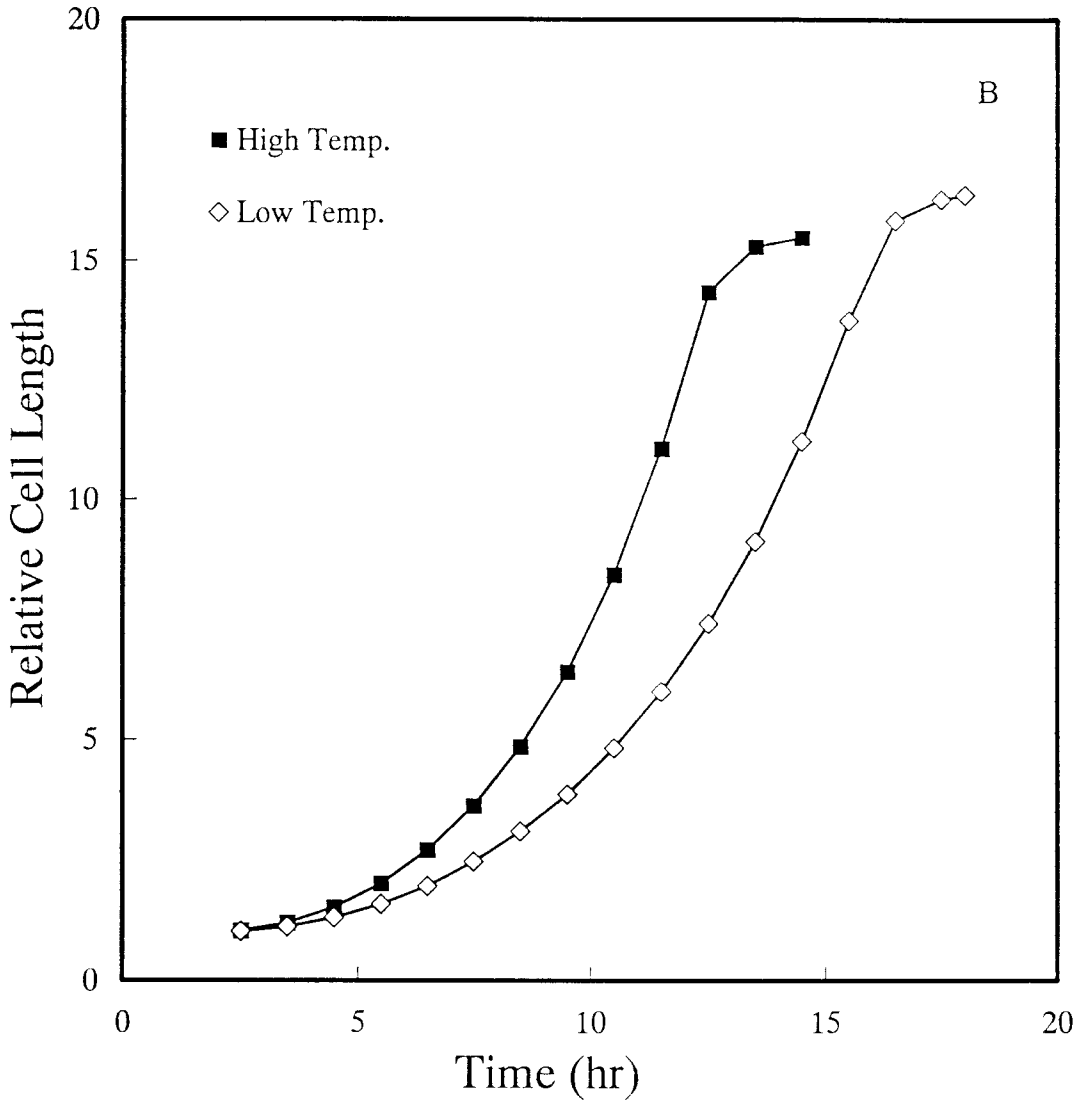

Figure 6.18. Effect of temperature on the elongation process of cells produced at t=2.5 hr. Relative cell length is the current length of the cell divided by its initial length.

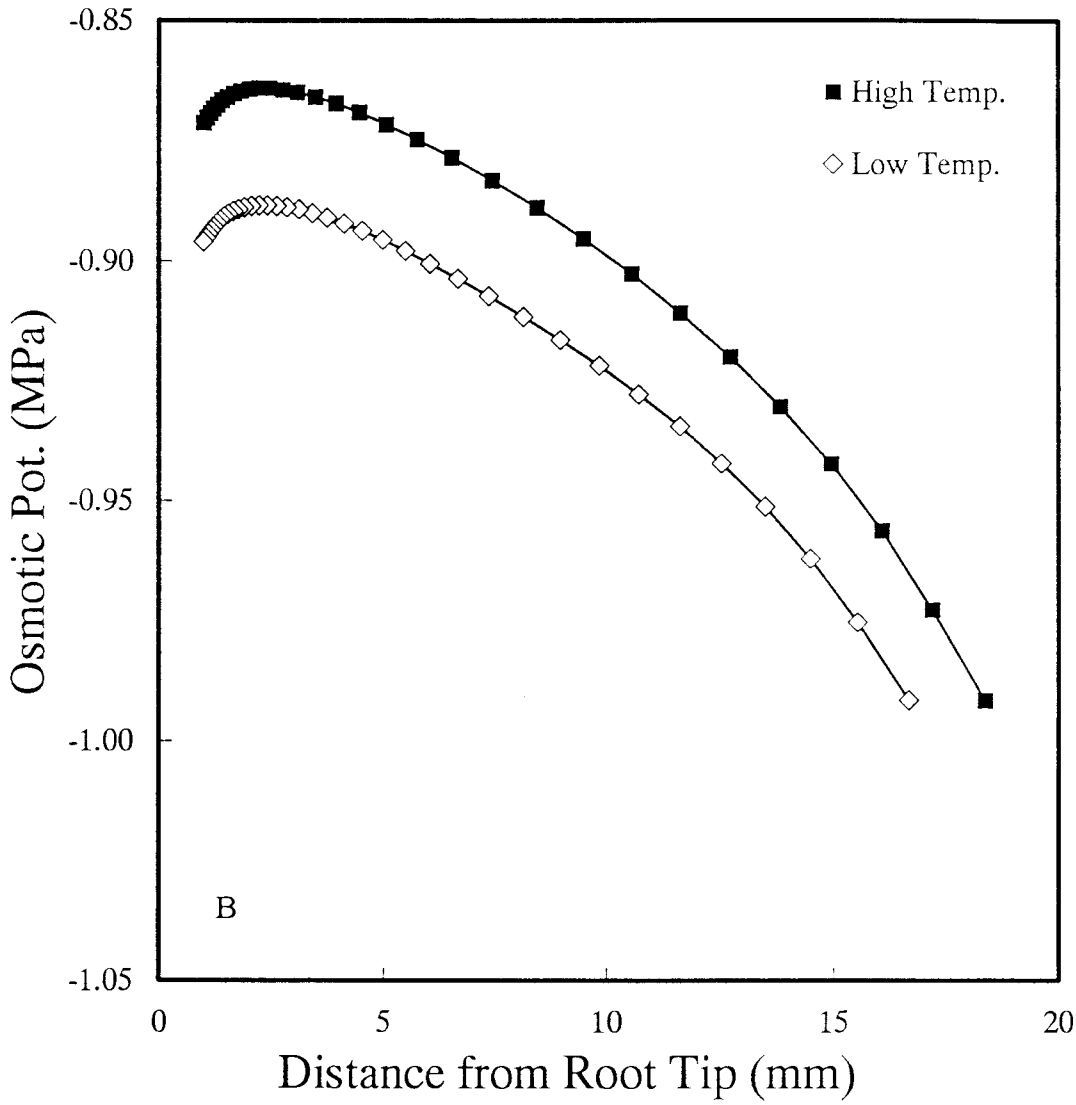

Figure 6.19. Effect of temperature on the distribution of osmotic potential along root axis after 15 hr of growth.

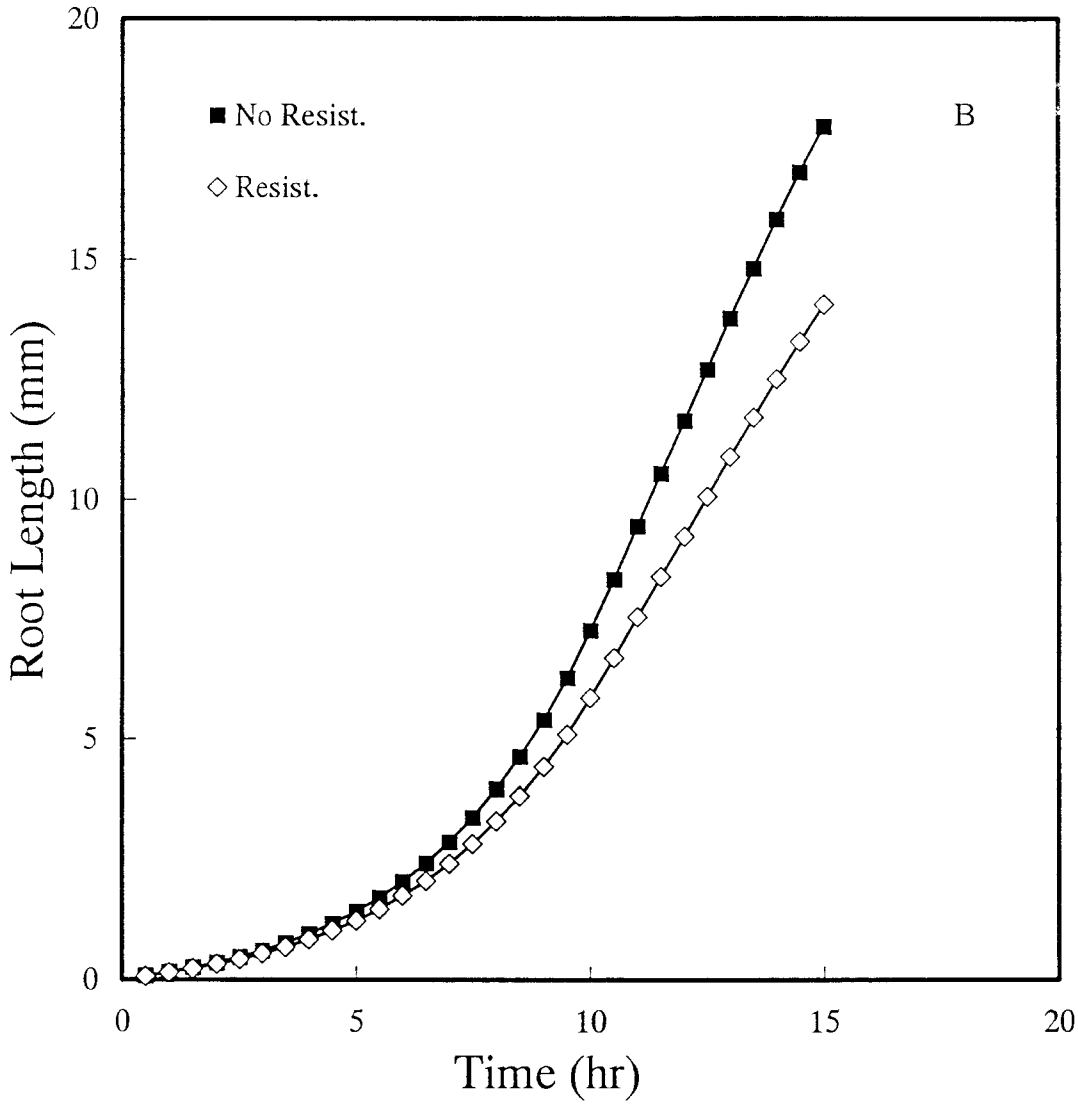

Figure 6.20. Effect of soil resistance on root length as functions of time.

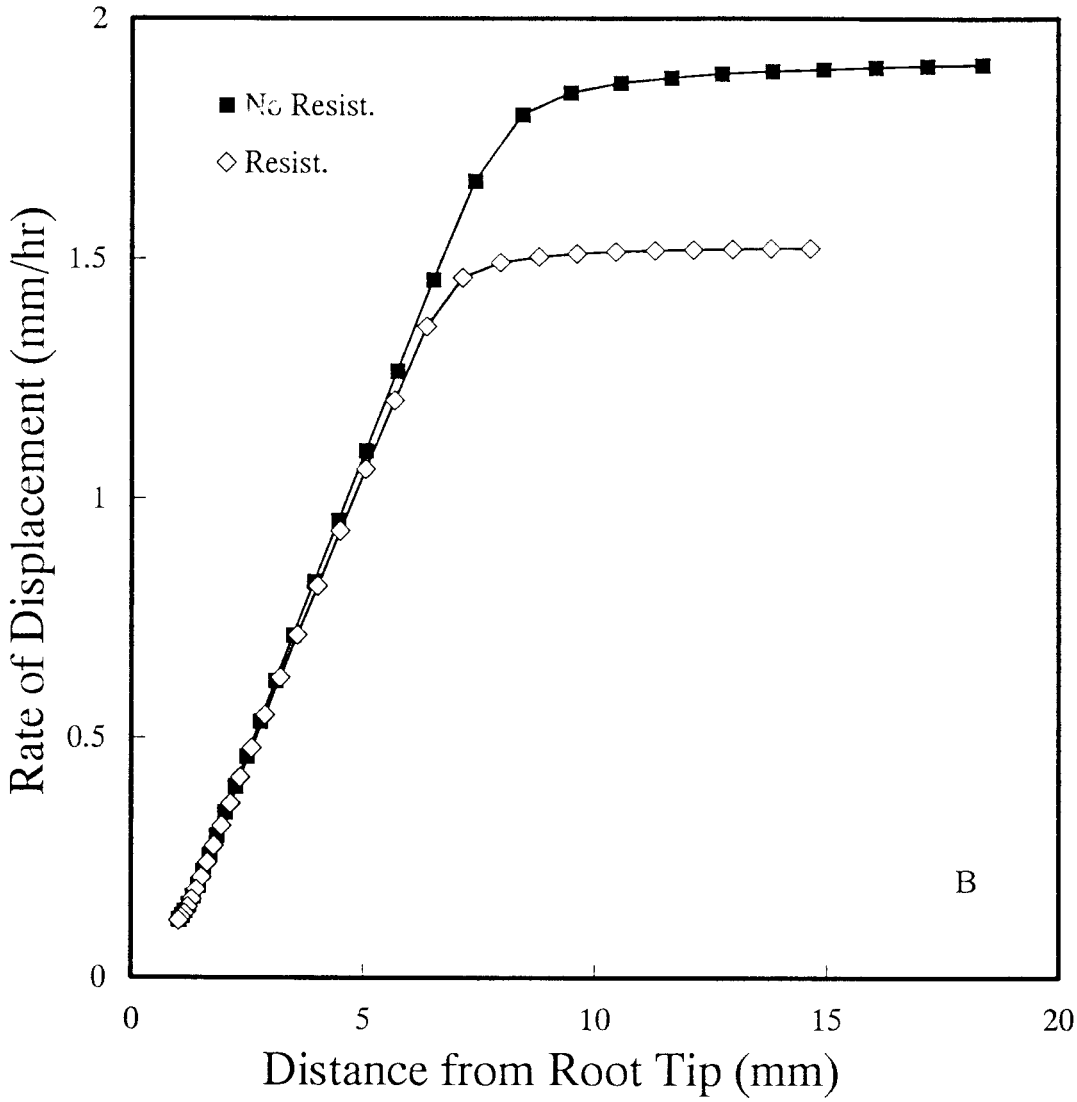

Figure 6.21. Effect of soil resistance on the rate of displacement of material points along the root axis from root tip as functions of spatial distance along the root axis.

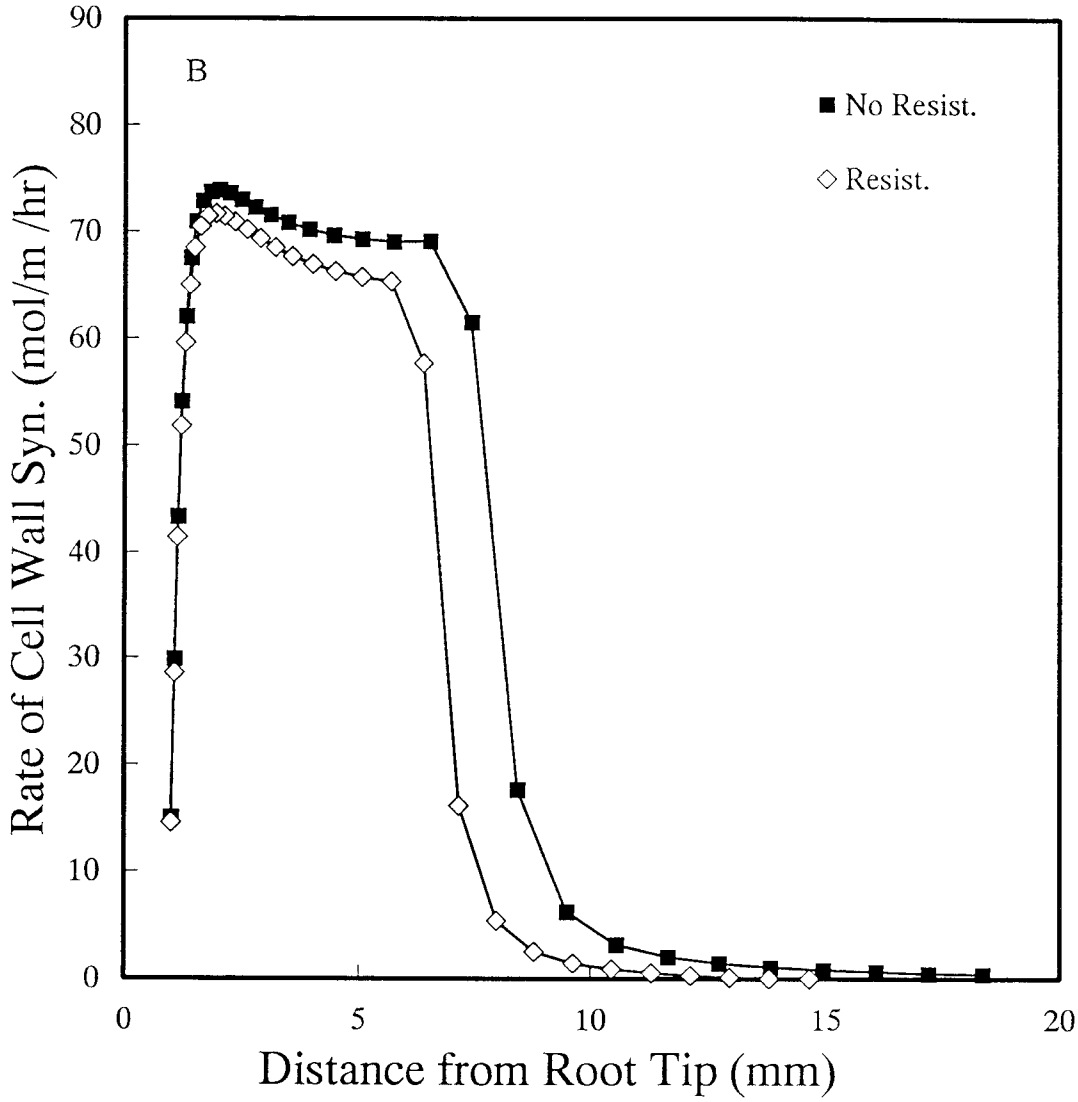

Figure 6.22. Effect of soil resistance on the rate of cell wall synthesis as functions of spatial distance along the root axis. It is assumed in the model to be proportional to the rate of cell elongation by a constant factor.

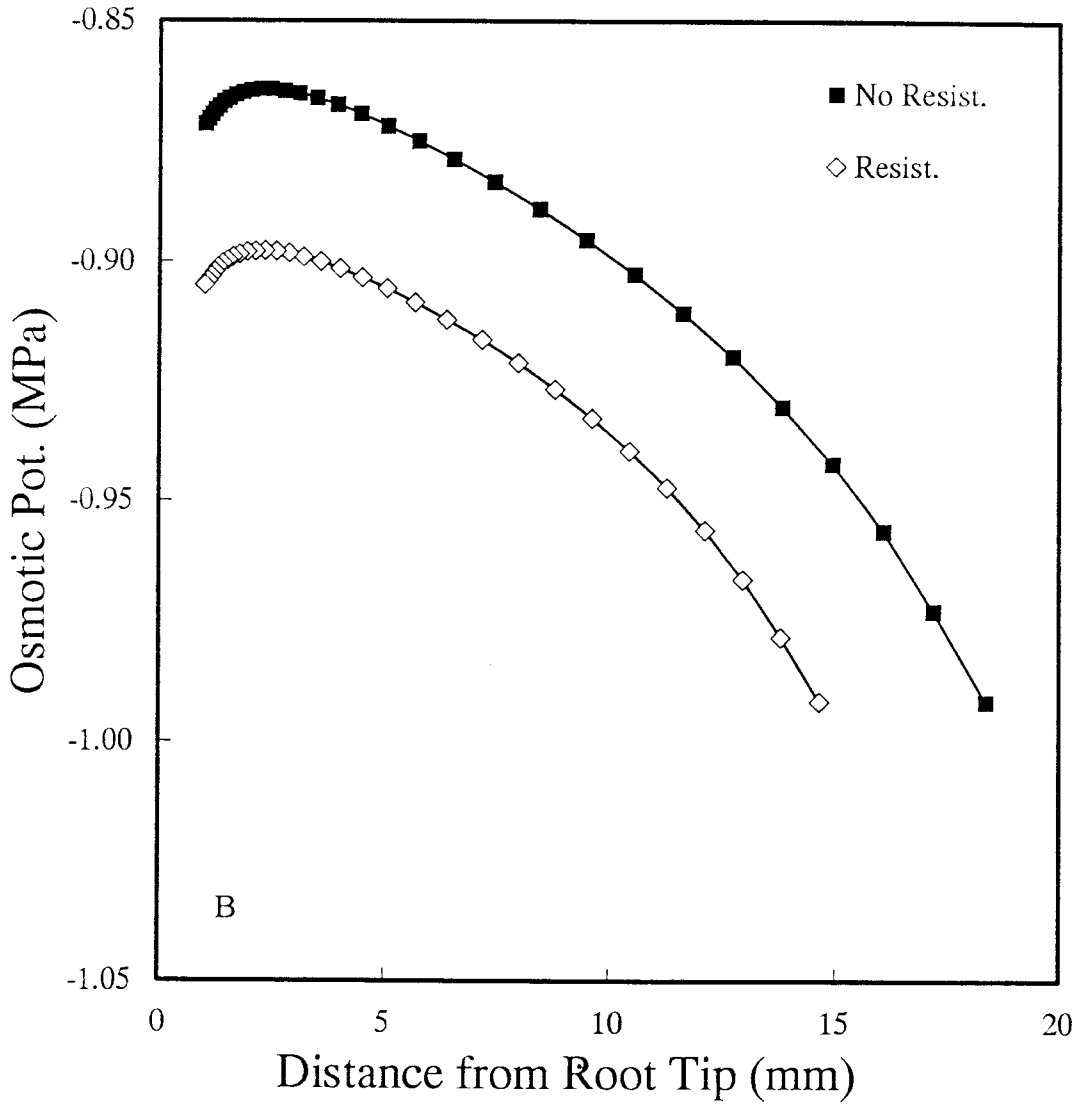

Figure 6.23. Effect of soil resistance on the distribution of osmotic potential along the root axis.

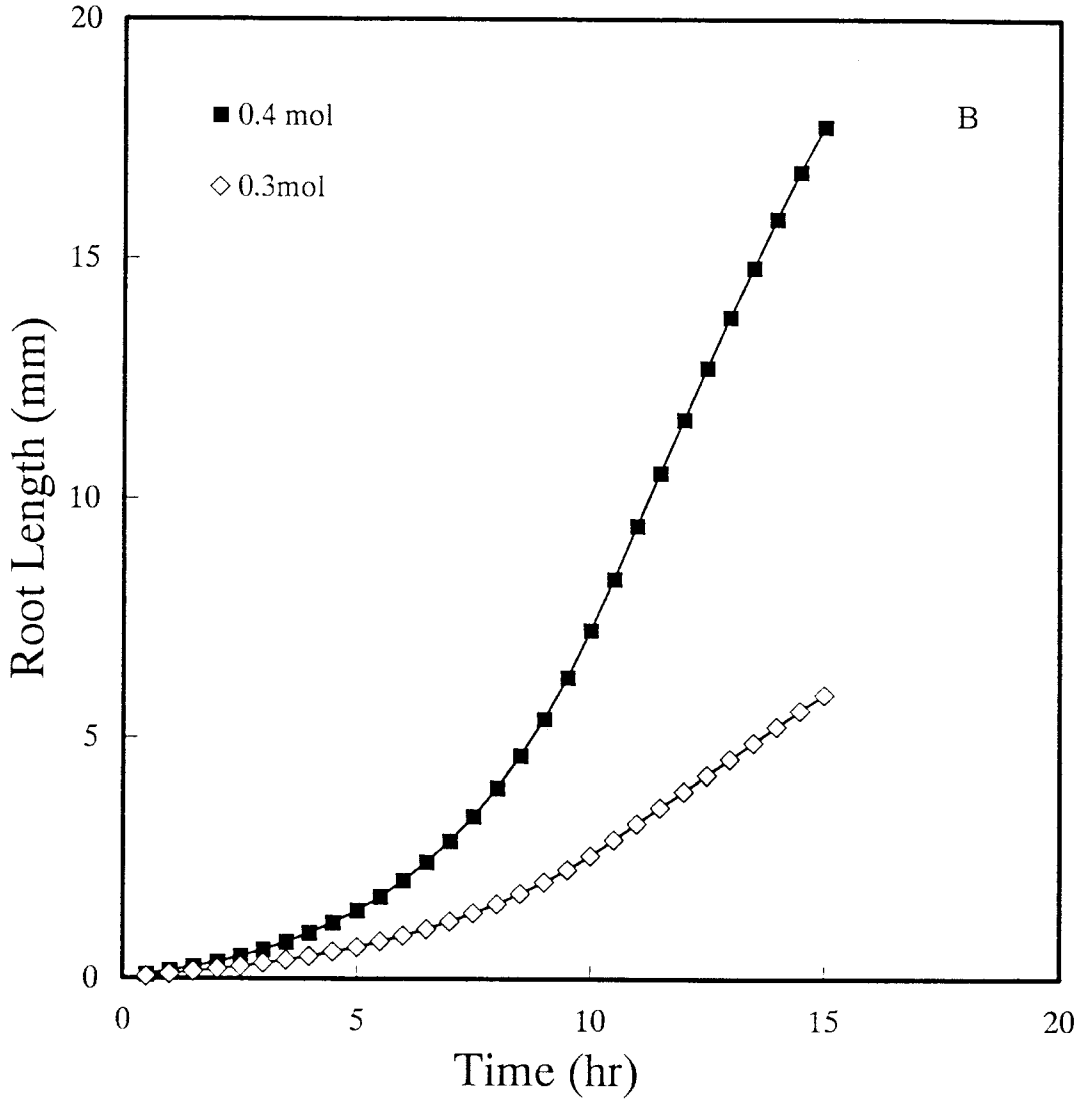

Figure 6.24. Effect of carbohydrate availability on root length as functions of time.

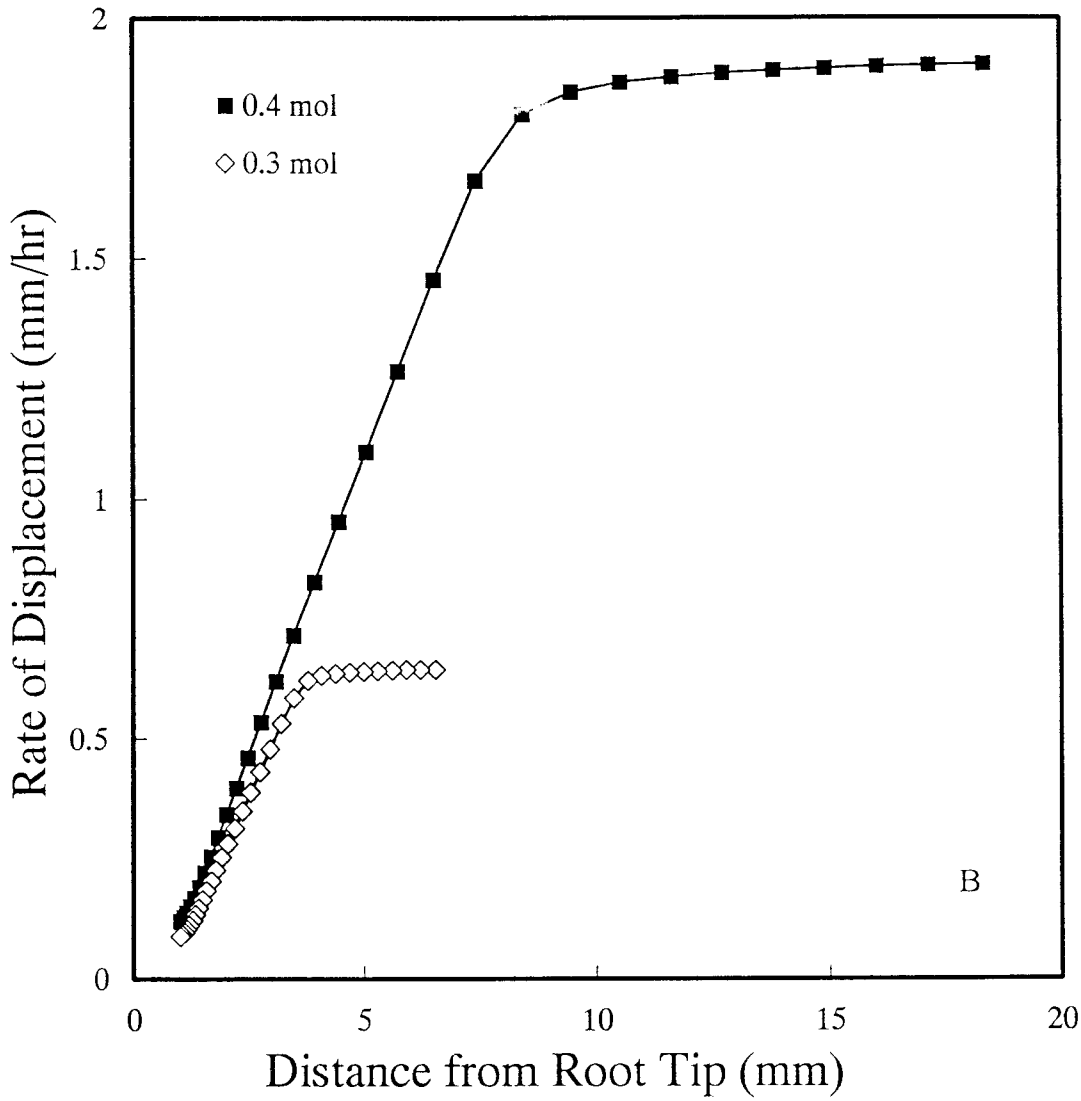

Figure 6.25. Effects of carbohydrate availability on the rate of displacement of material points along the root axis from the root tip as functions of spatial distance along the root axis.

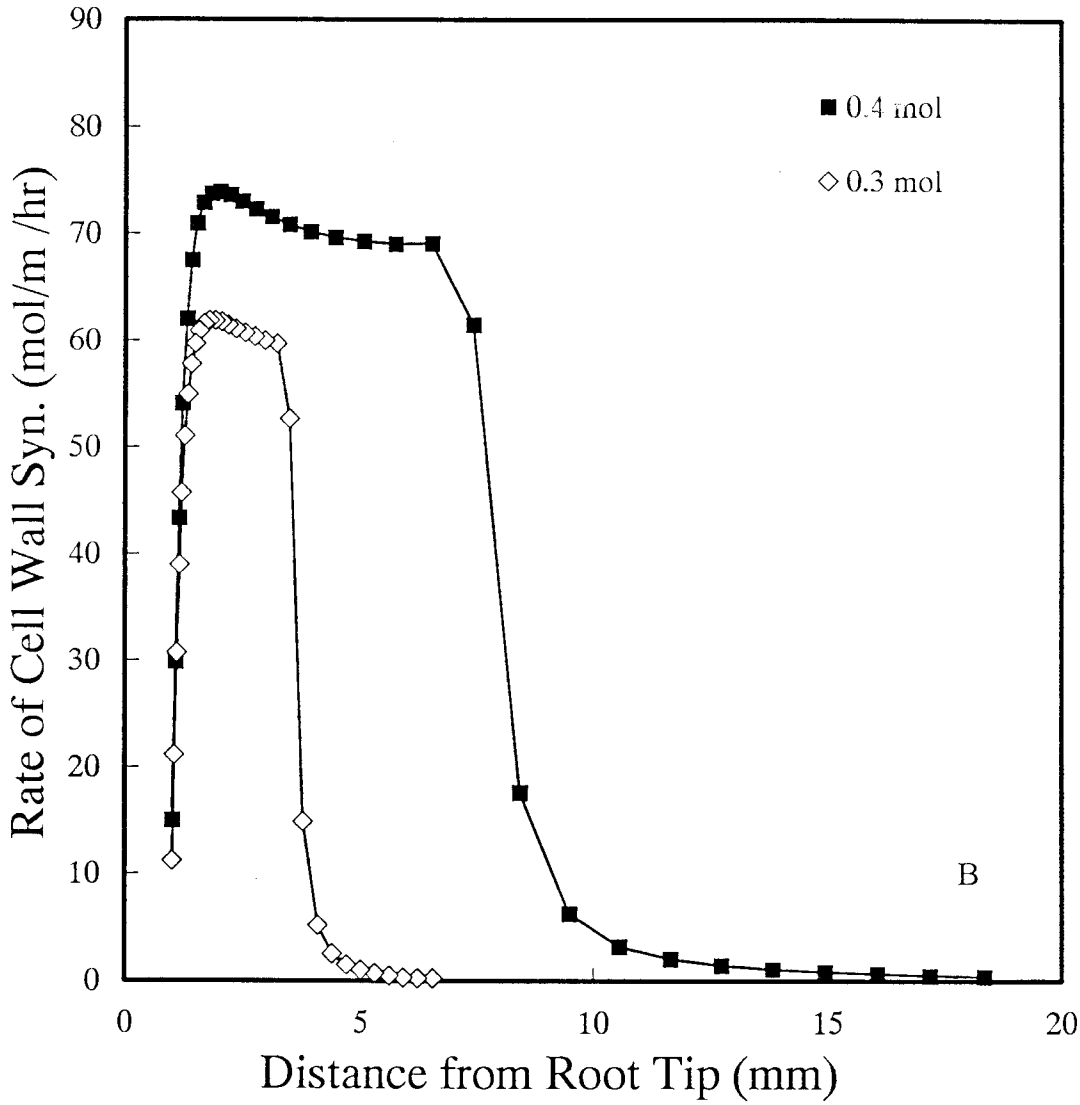

Figure 6.26. Effect of carbohydrate availability on the rate of cell wall synthesis along the root axis. It is assumed in the model to be proportional to the rate of cell elongation by a constant factor.

LIST OF SYMBOLS AND UNITS

$A(C)$	rate of active transport	mol m^{-2} s^{-1}
B	discrete divergence operator	m^{-2}
C	solute concentration in symplast	mol m^{-3}
D_a	active solute transport coefficient	dimensionless
D_d	solute dispersion coefficient	m^2 s^{-1}
D_m	membrane dispersion coefficient	m s
D_q	convection coefficient	dimensionless
D_o	cytoplasm dispersion coefficient	m^2 s^{-1}
H	discrete gradient operator	m^{-1}
K_a	axial apoplast water permeability	kg m^{-1}
K_{as}	water permeability between sympast and apoplast	kg m^{-2}
K_d	rate of metabolic cell wall loosening system degradation	s^{-1}
K_s	axial symplast water permeability	kg m^{-1}
K_{sr}	water permeability between soil and root	kg m^{-2}
K_κ	rate of metabolic cell wall loosening system synthesis	s^{-2}
L	root length	m
L_c	lateral membrane permeability	kg m^{-2}
L_{mstm}	length of meristem	m
L_x	axial membrane permeability	kg m^{-2}
M	discrete flux gradient operator	kg m^{-3}
P	turgor potential	MPa

R	universal gas constant	J $mol^{-1}K^{-1}$
R_r	rate of respiration	mol m^{-3} s^{-1}
R_{rm}	rate of respiration in meristem	mol m^{-3} s^{-1}
S_s	rate of cytoplasm synthesis	mol m^{-3} s^{-1}
S_{sm}	rate of cytoplasm synthesis in meristem	mol m^{-3} s^{-1}
S_w	rate of cell wall synthesis	mol m^{-3} s^{-1}
S_w	rate of cell wall synthesis in meristem	mol m^{-3} s^{-1}
T	absolute temperature	K
X	material coordinate	m
s_x	axial membrane reflection coefficient	dimensionless
s_ℓ	lateral membrane reflection coefficient	dimensionless
t	time	s
x	spatial longitudinal coordinate	m
Π	osmotic potential	MPa
Ψ_a	apoplast water potential	MPa
Ψ_s	symplast water potential	MPa
Ψ_{soil}	soil water potential	MPa
α_f	coefficient of facilitated diffusion	dimensionless
ϵ	strain	dimensionless
$\dot{\epsilon}$	rate of deformation	s^{-1}
$\dot{\epsilon}_m$	rate of deformation in meristem	s^{-1}
κ	time coefficient of biochemical cell wall loosening	s
μ	viscosity of water	kg m^{-1} s^{-1}
θ	porosity of cell wall	dimensionless
ρ_ℓ	density of water	kg m^{-3}

σ	cell wall stress	N m^{-2}
σ_e	elastic component of wall stress	N m^{-2}
σ_v	viscoelastic component of wall stress	N m^{-2}
τ	time constant of physical cell wall stress relaxation	s
ω_s	volume fraction of symplast	dimensionless
ω_a	volume fraction of apoplast	dimensionless
ω_w	volume fraction of cell walls	dimensionless

LITERATURE CITED

Bertaud, D. S., and P. W. Gandar, 1985. Referential descriptions of cell proliferation in roots illustrated using Phleum pralense L. Bot. Gaz., 146:275–287.

Boyer, J. S., 1988. Cell enlargement and growth–induced water potentials. Physiol. Plant., 73:311–316.

Carmona, M. J., and A. Cuadrado, 1986. Analysis of growth components in Allium roots. Planta, 168:183–189.

Chen, G., and J. B. Russel, 1989. Transport of glutamine by *Streptococcus bovis* and conversion of glutamine to pyroglutamic acid and amonia. J. Bacteriol., 171:2981–2985.

Dainty, J., 1976. Water relations of plant cells. in U. Luttge and M. G. Pitman (ed.) Encyclopedia of plant physiology, vol. 2; Transport in plants II, part A: cells. Springer–Verlag, Berlin, 400 pp.

Epstein, E., 1976. Kinetics of ion transport and the carrier concept. in U. Luttge and M. G. Pitman (ed.) Encyclopedia of plant physiology, vol. 2: Transport in plants II, part B: Tissues and organs. Springer–Verlag, Berlin, 456 pp.

Erickson, R. O., and K. B. Sax, 1956a. Rates of cell division and cell elongation in the growth of the primary root of *Zea mays*. Proc. Am. Phil. Soc., 100:499–514.

Erickson, R. O., and K. B. Sax, 1956b. Elememtal growth rates of the primary root of *Zea mays*. Proc. Am. Phil. Soc., 100:499–513.

Gandar, P. W., 1983a. Growth in root apices. I. The kinematic description of growth. Bot. Gaz., 144:1–10.

Gandar, P. W., 1983b. Growth in root apices. II. Deformation and the rate of deformation. bot. Gaz., 144:11–19.

Green, P. B., R. O. Erickson, and J. Buggy, 1971. Metabolic and physical control of cell elongation rate. *In vivo* studies in *Nitella*. Plant Physiol., 47:423–430.

Grenetz, P. S., and A. List Jr., 1973. A model for predicting growth responses in plants to changes in external water potenntial: *Zea mays* primary roots. J. Theor. Biol., 39:29–45.

Lauchli, A., 1976. Apoplasmic transport in tissues. in U. Luttge and M. G. Pitman (ed.) Encyclopedia of plant physiology, vol. 2; Transport in plants II, part B: Tissues and organs. Springer–Verlag, Berlin. 456pp.

List, A. Jr., 1969. Transient growth responses of the primary roots of *Zea mays*. Planta, 87:1–19.

Lockhart, J. A., 1965. An analysis of irreversible plant cell elongation. J. Theor. Biol., 8:264–275.

Lockhart, J. A., 1967. Physical nature of of irreversible deformation of plant cells. Plant Physiol., 42:1545–1552.

McCoy, L. E. and L. Boersma, 1984. The principles of continuum mechanics applied to transport processes and deformation in plant tissues. J. Theor. Biol., 111:687–705.

Molz, F. J., 1976. Water transport through plant tissue: the apoplasm and symplasm pathways. J. Theor. Biol., 59:277–292.

Molz, F. J., and J. S. Boyer, 1978. Growth–induced water potentials in plant cells and tissues. Plant Pjusiol., 62:423–429.

Nobel, P. S., 1983. Biophysical plant physiology and ecology. W. H.

Freeman and Company, San Francisco. 608pp.

Pahlavanian, A. M., and W. K. Silk, 1988. Effect of temperature on spatial and temporal aspects of growth in the primary Maize root. Plant Physiol., 87:529–532.

Plant, R. E., 1982. A continuum model for root growth. J. Theor. Biol., 98:45–59.

Sharp, R. E., W. K. Silk, and T. C. Hsiao, 1988. Growth of the Maize primary root at low water potentials. I. Spatial distribution of expansive growth. Plant Physiol., 87:50–57.

Silk, W. K., and R. O. Erickson, 1979. Kinematics of plant growth. J. Theor. Biol., 76:481–501.

Silk, W. K., and R. O. Erickson, 1980. Local biosynthesis rates of cytoplasmic constituents in growing tissue. J. Theor. Biol., 76:481–501.

Silk, W. K., R. C. Walker, and J. Labavitch, 1984. Uronide deposition rates in the primary roots of *Zea mays*. Plant Physiol., 74:721–726.

Silk, W. K., and K. K. Wagner, 1980. Growth sustaining water potential distributions in the primary corn root. A non–compartmental continuum model. Plant Physiol., 66:859–863.

Tyson, J. J., 1986. Sloppy size control of the cell division cycle. J. Theor. Biol., 118:405–426.

BIBLIOGRAPHY

Abdu–Baki, A. A., and P. M. Ray, 1971. Regulation by auxin of carbohydrate metabolism involved in cell wall synthesis by pea stem tissue. Plant Physiol., 47:537–544.

Bertaud, D. S., and P. W. Gandar, 1985. Referential descriptions of cell proliferation in roots illustrated using *Phleum pratense L.* Bot. Gaz., 146:275–287.

Biggs, K. J., and S. C. Fry, 1987. Phenolic cross linking in the cell wall. *In* D. J. Cosgrove and D. P. Knievel (ed.) Physiology of cell expansion during plant growth. Am. Soc. Plant Physiol., Penn. State Univ..

Boyer, J. S., 1985. Water transport. Ann. Rev. Plant Physiol., 36:473–516.

Boyer, J. S., 1988. Cell enlargement and growth–induced water potentials. Physiol. Plant., 73:311–316.

Boyer, J. S., and G. Wu, 1978. Auxin increases the hydraulic conductivity of auxin–sensitive hypocotyl tissue. Planta, 139:227–237.

Brummel, D. A., and J. L. Hall, 1985. The role of cell wall synthesis in sustained auxin–sensitive hypocotyl tissue. Planta, 63:406–412.

Burstrom, H. G., 1974. Patterns of synthesis during internodal growth of *Pisum* stems. Z. Pflanzenphysiol., 74:1–13.

Carmona, M. J., and A. Cuadrado, 1986. Analysis of growth components in Allium roots. Planta, 168:183–189.,

Canny, M. J., 1971. Translocation: Mechanisms and kinetics. Ann. Rev. Plant Physiol., 22:237–260.

Chen, G., nd J. B. Russel, 1989. Transport of glutamine by *Streptococcus bovis* and conversion of glutamine to pyroglutamic acid and amonia. J. Bacteriol., 171:2981–2985.

Christy, A. L., and J. M. Ferrier, 1973. A mathematical treatment of Munch's pressure flow hypothesis of phloem translocation. Plant Physiol, 52:531–538.

Cleland, W. W., 1970. Steady state kinetics. In P. D. Boyer (ed.) The enzymes, kinetics and mehanism, II. Academic press, New York. 584pp.

Cleland, R., 1971. Cell wall extension. Ann. Rev. Plant Physiol., 22:197–221.

Cleland, R. E., 1987. The mechanisms of wall loosening and wall extension. In D. J. Cosgrove and D. P. Knievel (ed.) Physiology of cell expansion during plant growth. Am. Soc. Plant Physiol., Pennsylvania State Univ..

Cleland, R., and P. M. Haughton, 1971. The effect of Auxin on stress relaxation in isolated *Avena* coleoptiles. Plant Physiology, 47:812–815.

Collins, J. F., and M. H. Richmond, 1962. Rate of growth of Bacillus cereus between divisions. J. Gen. Microbiol., 28:15–33.

Cosgrove, D. J., 1981. Analysis of the dynamic and steady–state responses of growth rate and turgor pressure to changes in cell parameters. Plant Physiol., 68:377–405.

Cosgrove, D. J., 1985. Cell wall yield properties of growing tissue:

Evaluation by *in vivo* stress relaxation. Plant Physiology, 78:347–356.

Cosgrove, D. J., 1986. Biophysical control of plant cell growth. Ann. Rev. Plant Physiol., 37:377–405.

Cosgrove, D. J., 1987. Wall relaxation and the driving forces for cell expansive growth. Plant PHysiol., 84:561–564.

Dale, J. E., 1988. The control of leaf expansion. Ann. Rev. Plant Physiol., 39:267–295.

Dainty, J., 1976. Water relations of plant cells. in U. Luttge and M. G. Pitman (ed.) Encyclopedia of plant physiology, vol. 2; Transport in plants II, part A: cells. Springer–Verlag, Berlin. 400pp.

Dainty, J., 1985. Studies of root function in Zea mays. III. Xylem sap composition at maximum root pressure provides evidence of active transport into the xylem and a measurement of the reflection coefficient of the root. Plant Physiol., 77:162–167.

Dalton, F. N., P. A. C. Raats, and W. R. Gardner, 1975. Simultaneous uptake of water and solutes by plant roots. Agron. J., 67:334–339.

Danielli, J. F., 1952. Theories of cell permeability. In H. Davson and J. Danielli (ed.) Permeability of natural membranes. p. 294–323. Cambridge Univ. Press, Cambridge. 365pp.

De Mechelis, M. I., M. Radice, R. Columbo, and P. Lado, 1978. Evidences for an active transport of methyl–α–D–glucopyranoside in pea stem segments. Plant Sci. Lett., 12:93–99.

Dixon, M., and E. L. Webb, 1964. Enzymes. Longmans, London. 1116pp.

Dorrington, K. L., 1980. The theory of viscoelasticity in biomaterials. *In*

The mechanical properties of biological materials. Symp. Soc. Exp. Biol., 34:315–329. Cambridge Univ. Press, Cambridge.

Epstein, E., 1976. Kinetics of ion transport and the carrier concept. in U. Luttge and M. G. Pitman (ed.) Encyclopedia of plant physiology, vol. 2; Transport in plants II, part B: Tissues and organs. Springer–Verlag, Berlin. 456pp.

Erickson, R. O., 1976. Modeling of plant growth. Annual Review of Plant Physiology, 27:407–434.

Erickson, R. O., and K. B. Sax. 1956a. Elemental growth rates of the primary root of *Zea mays*. Proc. Am. Phil. Soc., 100:487–497.

Erickson, R. O., and K. B. Sax. 1956b. Elemental growth rates of the primary root of *Zea mays*. Proc. Am. Phil. Soc., 100:499–513.

Feher, J. J., 1983. Facilitated calcium diffusion by intestinal calcium–binding proterin. Am. J. Physiol., 244:303–307.

Feng, Y., X. Li, and L. Boersma, 1990. The Arrhenius equation as a model for explaining plant responses to temperature and water stresses. Ann. Bot., 66:237–244.

Ferry, J. D., 1970. Viscoelastic properties of polymers. Second Edition. John Wiley and Sons, New York. 671pp.

Fiscus, E. L., 1975. The interaction between osmotic– and pressure–induced water flow in plant roots. Plant Physiol., 55:917–922.

Fry, S. C., 1986. Cross–linking of matrix polymers in the growing cell walls of angiosperms. Ann. Rev. Plant Physiol., 37:165–186.

Gandar, P. W., 1980. The analysis of growth and cell production in root apices. Bot. Gaz. 141:131–138.

Gandar, P. W., 1983a. Growth in root apices. I. Kinematic description of growth. Bot. Gaz. 144:1–10.

Gandar, P. W., 1983b. Growth in root apices. II. Deformation and rate of deformation. Bot. Gaz. 144:11–19.

Gardner, W. R., 1960. Dynamic aspects of water availability to plants. Soil Sci., 89:63–73.

Gayler, K. R., and K. T. Glasziou, 1972. Carrier mediated active transport of glucose. Plant Physiol., 49:563–568.

Goodwin, R. H., and W. Stepka, 1945. Growth and differentiation in the root tip of Phleum pralense. Am. J. Bot., 32:36–46.

Greecen, E. L., and J. S. Oh, 1972. Physics of root growth. Nature, New Biol. 235:24–25.

Green P. B., 1968. Growth physics in *Nitella*: A method for continuous *in vivo* analysis of extensibility based on a micro–manometer technique for turgor pressure. Plant Physiol., 43:1169–1184.

Green, P. B., R. O. Erickson, and J. Buggy, 1971. Metabolic and physical control of cell elongation rate. *In vivo* studies in *Nitella*. Plant Physiol., 47:423–430.

Green, P. B., 1976. Growth and cell pattern formation on an axis. Critique of concepts, terminology, and modes of study. Bot. Gaz. 137:187–202.

Green, P. B., K. Bauer, and fW. R. Cummins, 1977. Biophysical model for plant growth: auxin effect. in A. M. Jungreis et al. (ed.) Water relations in membrane transport in plants and animals. Academic press, New York.

Greenetz, P. S. and A. List, 1973. A model for predicting growth response in plants to changes in external water otential: *Zea mays* primary root. J. Theor. Biol., 39:29–45.

Ho, L. C. and D. A. Baker, 1982. Regulation of loading and unloading in long distance transport systems. Physiol. Plant., 56:225–230.

Hanson, P. J., Sucoff E. I., and Markhart A. H., 1985. Quantifying apoplast flux through red pine root systems using tri–sodium, 3–hydroxy–5, 8, 10–pyrenetri–sulfonate. Plant Physiol., 77:21–24.

Haughton, P. M., and D. B. Sellen, 1969. Dynamic mechanical properties of the cell walls of some green algae. J. Exp. Bot. 20:516–535.

Haughton, P. M., and D. B. Sellen, 1973. Stress relaxation in regenerated cellulose. J. Physics, D: Applied Physics, 6:1998–2011.

Haughton, P. M., D. B. Sellen, and R. D. Preston, F. R. S., 1968. Dynamic mechanical properties of the cell wall of *Nitella opaca*. J. Exp. Bot., 19:1–12.

Hejnowicz, Z., 1982. Vector and scalar fields in modeling of growth response in plants to changes in external water potential: Zea mays primary root. J. Theor. Biol. 96:161–173.

Hettiaratchi, D. R. P., and J. R. O'Callaghan, 1974. A membrane model of plant cell extension. J. Theor. Biol., 45:459–465.

Hillel, D., 1982. Introduction to soil physics. Academic Press, New York. 364pp.

Kirkham, M. B., W. R. Gardner, and G. C. Gerloff, 1972. Regulation of cell division and cell enlargement by turgor pressure. Plant Physiol. 49:961–962.

Komor, E., M. Thom, and A. Maretzki, 1981. The mechanism of sugar uptake by sugarcane suspension cells. Planta, 153:181–192.

Kramer, P. J., 1983. Water relations of plants. Academic Press, Orlando. 489pp.

Lang A. R. G., and W. R. Gardner, 1970. Limitation to water flux from soil to plants. Agron. J., 62:693–695.

Lauchli, A., 1976. Apoplasmic transport in tissues. in U. Luttge and M. G. Pitman (ed.) Encyclopedia of plant physiology, vol. 2; Transport in plants II, part B: Tissues and organs. Springer–Verlag, Berlin, 456pp.

List, A. Jr., 1969. Transient growth responses of the primary roots of *Zea mays*. Planta 87:1–19.

Lockhart, J. A., 1965. An analysis of irreversible plant cell elongation. J. Theor. Biol., 8:264–275.

Lockhart, J. A., 1967. Physical nature of irreversible deformation of plant cells. Plant Physiol., 42:1545–1552.

Luttge, U., and M. G. Pitman, 1976. Transport and energy. in Luttge, U., and M. G. Pitman (ed.) Encycl. Plant Physiol., vol. 2: Transport in plants II, Part A: Cells. Spring–Verlag, Berlin. 400pp.

Madore, M. A., and W. J. Lucas, 1989. Transport of photoassimilates between leaf cells. In D. A. Baker and J. A. Milburn (ed.) Transport of photoassimilates. Longman Sci. Tech.. 384pp.

Mathews, M. A., E. Van Volkenburgh, and J. S. Boyer, 1984. Acclimation of leaf growth to low water potentials in sunflower plant. Cell Environ., 7:199–206.

McCoy, E. L., and L. Boersma, 1984. The principles of continuum mechanics applied to transport processes and deformation in plant tissue. J. Theor. Biol. 111:687–705.

McCully, M. E., and M. J. Canny, 1988. Pathways and processes of water and nutrient movement in roots. Plant and Soil, 159–170.

Meyer, R. F., and J. S. Boyer, 1972. Sensitivity of cell division and cell elongation to low water potentials in soybean hypocotyls. Planta. 108:77–87.

Milburn, J. A., and K. Kallarackal, 1989. Physiological aspects of pholoem translocation. In D. A. Baker and J. A. Milburn (ed.) Transport of photoassimilates. Longmam Sci. Tech.. 384pp.

Molz, F. J., 1976. Water transport through plant tissue: the apoplasm and symplasm pathways. J. Theor. Biol., 59:277–292.

Molz, F. J., and J. S. Boyer, 1978. Growth induced water potentials in plant cells and tissues. Plant Physiol., 62:423–429.

Moon, G. J., B. F. Clough, C. A. Peterson, and W. G. Allaway, 1986. Apoplastic and symplastic pathways in *Avicenia merina (Forsk) Vierh.* roots reveled by fluorescent tracer dyes. Aust. J. Plant Physiol., 13:637–648.

Morris, D. A., and E. D. Arthur, 1985. Invertase activity, carbohydrate metabolism and cell expansion in the stem of *Phaseolus vulgaris L.* J. Exp. Bot., 36:623–633.

Newman, E. I., 1976. Interaction between osmoti– and pressure– induced water flow in plant roots. Plant Physiol., 57:738–739.

Nobel, P. S., 1983. Biophysical plant physiology and ecology. Freeman and Company, New York. 608pp.

Pahlavanian, A. M., and W. K. Silk, 1988. Effect of temperature on spatial and temporal aspects of growth in the primary Maize root. Plant Physiol. 87:529–532.

Passioura, J. B., 1980. The transport of water from soil to shoot in wheat seedlings. J. Exp. Bot., 31:333–345.

Passioura, J. B., 1984a. Hydraulic resistance of plants. I. Constant or variable? Aust. J. Plant. Physiol., 11:333–339.

Passioura, J. B., 1984b. Hydraulic resistance of plants. II. Effects of rooting medium, and time of day, in barley and lupin. Aust. J. Plant Physiol., 11:341–350.

Passioura, J. B., 1988. Water transport in and to roots. Ann. Rev. Plant Physiol., 39:245–265.

Phillip. J. R., 1957. The physical principles of soil water movement during the irrigation cycle. Proc. Int. Congr. Irrig. Drain., 8:125–154.

Plant, R. E., 1982. A continuum model for root growth. J. Theor. Biol. 98:45–59.

Prat, R., B. Vian, D. Reis, and J. Roland, 1977. Evolution of internal pressure, vacuolation and membrane flow during cell growth in mung bean hypocotyls. Biol. Cellulaire, 28:269–280.

Pritchard, J., R. G. Wyn Jones and A. D. Tomos, 1988. Control of wheat root growth. The effects of excision on growth, wall rheology and root anatomy. Planta, 176:399–405.

Ortega. J. K. E., 1985. Augmented growth equation for cell wall expansion. Plant Physiology, 79:318–320.

Raats, P. A. C., and A. Klute, 1968a. Transport in soils: the balance of mass. Soil Sci. Soc. Am. Proc., 32:161–166.

Raats, P. A. C., and A. Klute, 1968b. Transport in soils: the balance of momentum. Soil Sci. Soc. Am. Proc., 32:452–456.

Ray, P. M., 1987. Principles of plant cell growth. In D. J. Cosgrove and D. P. Knievel (ed.) Physiology of cell expansion during plant growth. Am. Soc. Plant Physiol., Penn. State Univ..

Ray, P. M., 1987. Principles of plant cell growth. in D. J. Cosgrove and D. P. Knievel (ed.) Physiology of cell expansion during plant growth. Am. Soc. Plant Physiol., Rockville, Maryland.

Ray, P. M., and A. W. Reusink, 1962. Kinetic experiments on the nature of the growth mechanism in oat coleoptile cells. Dev. Biol., 4:377–397.

Reicosky, D. C., Ritchie J. T., 1976. Relative importance of soil resistance and plant resistance in root water absorption. Soil Sci. Soc. Am. Proc., 40:293–297.

Reinhold, L., and A. Kaplan, 1984. Membrane transport of sugars and amino acids. Ann. Rev. Plant Physiol., 35:45–83.

Sachio, M. R. M. and J. S. Boyer, 1988. Rapid wall relaxation in elongating tissues. Plant Physiol., 86:1163–1167.

Salamon, P. A., A. List and P. S. Grenetz, 1973. Mathematical analysis of plant growth. *Zea mays* primary roots. Plant Physiol. 51:653–640.

Sellen, D. B., 1980. The mechanical properties of plant cell walls. In The mechanical properties of biological materials. Symp. Soc. Exp. Biol. 34:315–329. Cambridge Univ. Press, Cambridge.

Sharp, R. E., W. K. Silk, and T. C. Hsiao, 1988. Growth of the Maize primary root at low water potentials. I. Spatial distribution of expansive growth. Plant Physiol. 87:50–57.

Silk, W. K., 1984. Quantitative descriptions of development. Ann. Rev. Plant Physiol., 35:479–518.

Silk, W. K., and R. O. Erickson. 1978. Kinematics of hypocotyl curvature. Am. J. Bot. 65:310–319.

Silk, W. K., and R. O. Erickson. 1979. Kinematics of plant growth. J. Theor. Biol. 76:481–501.

Silk, W. K., and R. O. Erickson, 1980. Local biosynthesis rates of cytoplasmic constituents in growing tissue. J. Theor. Biol. 83:701–703.

Silk, W. K., and K. K. Wagner, 1980. Growth sustaining water potential distributions in the primary corn root. A noncompartmental continuum model. Plant physiol., 66:859–863.

Silk, W. K., R. C. Walker, and J. Labavitch, 1984. Uronide deposition rates in the primary root of *Zea mays*. Plant Physiol., 74:721–726.

Silk, W. K., T. C. Hsiao, U. Diedenhofen, and C. Matson, 1986. Spatial distributions of ptasium, solutes, and their deposition rates in the growth zone of the primary corn root. Plant Physiol., 82:853–858.

Sposito. G., 1978a. The statistical mechanical theory of water transport through unsaturated soil. 1. The conservation laws. Water Res. Res., 14:474–478.

Sposito. G., 1978b. The statistical theory of water transport through unsaturated soil. 2. Derivation of the Buckingham–Darcy flux law. Water Res. Res., 14:479–484.

St. Aubin, G., Canny M. J., and McCully M. E., 1986. Living vessel elements in the late metaxylem of sheathed maize roots. Ann. Bot. 58:577–588.

Stein, W. D., 1977. Testing and characterizing a simple carrier model for co–transport. in M. Kramer and F. Lauterbach (ed.) Intestinal permeation. p. 262–274. Excerpta Medica, Amsterdam. 449pp.

Steudle, E., R. Oren, and E. D. Schulze, 1987. Water transport in maize roots: Measurement of hydrolic conductivity, solute permeability, and of reflection coefficients of excised roots using the root pressure probe. Plant Physiol., 84:1220–1232.

Taiz, L., 1984. Plant cell expansion: Regulation of cell wall mechanical properties. Annual Review of Plant Physiology, 35:585–657.

Theologis, A., 1987. Possible link between auxin regulated gene expression, H^+ secretion, and cell elongation: a hypothesis. in D. J. Cosgrove and D. P. Knievel (ed.) Physiology of cell expansion during plant growth. Am. Soc. Plant Physiol., Penn. State Univ..

Thorne, J. H., 1982. Characterization of the active sucrose transport system of immature soybean embryos. Plant Physiol., 70:953–958.

Tobolsky, A., and H. Eyring, 1943. Mechanical properties of polymeric materials. J. Chem. Physics, 11:125–134.

Turner, N. C., 1986. Adaptation to water deficits: a changing perspective. Aust. J. Plant Physiol., 13:175–190.

Turner, N. C., 1987. Crop water deficits: a decade of progress. Adv. Agron., 39:1–51.

Tyree, M. T., and J. Dainty, 1975. Theoretical considerations. in M. H. Zimmermann and J. A. Milnurn (ed.) Encycl. Plant Physiol., vol.

1. Transport in plants I: Phloem transport. Spring–Verlag, Berlin. 535pp.

Tyson, J. J., 1986. Sloppy size control of the cell division cycle. J. Theor. Biol., 118:405–426.

Van Volkenburgh, E., and R. E. Cleland, 1981. Control of light–induced bean leaf expansion: Role of osmotic potential, wall yield stress, and hydraulic conductivity. Planta, 153:527–577.

Wyse, R., 1979. Sucrose uptake by sugar beet tap root tissue. Plant Physiol., 64:837–841.

APPENDIX

APPENDIX. SUMMARY OF EQUATIONS

Kinematic equaitons

$$x[\mathbf{X}(t'),t] = \int_0^{t'} \aleph(g)\Lambda(g,t)dg \quad [A1]$$

$$L(t) = x[\mathbf{X}(t),t] = \int_0^{t} \aleph(g)\Lambda(g,t)dg \quad [A2]$$

$$v(t) = \int_0^{t} \aleph(g)\frac{\partial\Lambda(g,t)}{\partial t}\,dg + \aleph(t) \quad [A3]$$

$$J = \frac{dx}{d\mathbf{X}} = \Lambda(t',t) \quad [A4]$$

$$\dot{\epsilon} = \frac{1}{\Lambda(t',t)}\frac{\partial\Lambda(t,t)}{\partial t} = \frac{1}{J}\frac{\partial J}{\partial t} \quad [A5]$$

Meristem growth:

$$\frac{d\sigma_{em}}{dt} = G_e\dot{\epsilon}_m - \frac{1}{\kappa}\sigma_e \quad [A6]$$

$$\frac{d\sigma_{vm}}{dt} = G_v\dot{\epsilon}_m - (\frac{1}{\kappa} + \frac{1}{\tau})\sigma_v \quad [A7]$$

$$\frac{d\sigma_m}{dt} = (G_e + G_v)\dot{\epsilon}_m - \frac{1}{\kappa}\sigma_m - \frac{1}{\tau}\sigma_v \quad [A8]$$

$$\frac{d}{dt}\frac{1}{\kappa} = K_{\kappa m} - (K_{dm} + \dot{\epsilon}_m)\frac{1}{\kappa} \quad [A9]$$

$$\frac{d\omega_{am}}{dt} = \frac{1-\omega_{am}}{\theta\rho_{wm}}S_{wm} - \omega_{wm}\dot{\epsilon}_m \quad [A10]$$

$$\frac{d\rho_{sm}}{dt} = S_{sm} + \frac{\rho_{sm}}{\omega_{sm}}\frac{d\omega_{am}}{dt} - \omega_{sm}\dot{\epsilon}_m \quad [A11]$$

$$\frac{dr_m}{dt} = (\dot{\epsilon}_m - b)r_m \quad [A12]$$

where

$$K_{\kappa m} = \rho_{sm}\frac{K_{\kappa m}C_m}{k_{\kappa m} + C_m} \quad [A13]$$

$$S_{sm} = K_{sm}\dot{\epsilon}_m \quad [A14]$$

$$S_{wm} = K_{wm}\dot{\epsilon}_m \quad [A15]$$

$$\begin{cases} b = \dfrac{A(x-a)^2}{1-x}\ \dot{\epsilon}_m, & a<x=\dfrac{r_m}{r_{m,max}}<1 \\ b = 0, & x\geq 1,\ 0<x\leq a \end{cases} \qquad [A16]$$

and

$$\sigma_m = \frac{1}{\theta\omega_{am}}(\omega_{sm}P_m - f_p) \qquad [A17]$$

Growth in the elongation region

$$\frac{d\sigma_e}{dt} = G_e\dot{\epsilon} - \frac{1}{\kappa}\ \sigma_e \qquad [A18]$$

$$\frac{d\sigma_v}{dt} = G_v\dot{\epsilon} - (\frac{1}{\kappa} + \frac{1}{\tau})\sigma_v \qquad [A19]$$

$$\frac{d\sigma}{dt} = (G_e + G_v)\dot{\epsilon} - \frac{1}{\kappa}\sigma - \frac{1}{\tau}\sigma_v \qquad [A20]$$

$$\frac{d}{dt}\ \frac{1}{\kappa} = K_\kappa - (K_d + \dot{\epsilon})\frac{1}{\kappa} \qquad [A21]$$

$$\frac{d\omega_a}{dt} = \frac{1-\omega_a}{\theta\rho_w}\ S_w - \omega_w\dot{\epsilon} \qquad [A22]$$

$$\frac{d\rho_s}{dt} = S_s + \frac{\rho_s}{\omega_s}\ \frac{d\omega_a}{dt} - \omega_s\dot{\epsilon} \qquad [A23]$$

where

$$\begin{cases} K_\kappa = \rho_s \dfrac{K_\kappa\ C}{k_\kappa + C}, & 0\leq t-t'\leq t_g \\ K_\kappa = 0, & t-t'>t_g \end{cases} \qquad [A24]$$

$$S_{s.} = K_s\ \dot{\epsilon} \qquad [A25]$$

$$S_{w.} = K_w\ \dot{\epsilon} \qquad [A26]$$

$$\sigma = \frac{1}{\theta\omega_a}\left[\omega_s P + \omega_a(\Psi_a - \Psi_{a,tip}) - \int_{X(t')}^{tip} f_r J\ dX - f_p\right] \qquad [A27]$$

Apoplast water transport

$$\frac{\partial}{\partial X}(K_a\frac{\partial\Psi_a}{\partial X}) - \frac{K_{sr}}{\omega_a}(\Psi_a - \Psi_{soil}) - \frac{K_{as}}{\omega_a}[\Psi_a - (P + s_\ell\Pi) - \mu\rho_\ell\theta\dot{\epsilon}J = 0 \qquad [A28]$$

where

$$K_a = \frac{K_{a,o}}{J} \quad [A29]$$

$$K_{as} = \frac{L_{m\ell}\omega_s}{r_{ci}\omega_a}(2J + 1) \quad [A30]$$

$$K_{sr} = J\left[\frac{2K_{soil}}{r_r \ln(r_d/r_r)}\right] \quad [A31]$$

Symplast water transport:

$$\frac{\partial}{\partial X}\left\{K_s\frac{\partial}{\partial X}(P + s_x\Pi)\right\} + \frac{K_{as}}{\omega_s}[\Psi_a - (P + s_\ell\Pi)] = \mu\rho_\ell\dot{\epsilon}J \quad [A32]$$

where

$$\Pi = -CRT \quad [A33]$$

$$K_s = \frac{2r_{ci}}{\frac{1}{L_{mx}} + \frac{2r_{ci}}{K_{s,o}}(J-\omega_{ai})} \quad [A34]$$

Solute transport:

$$J\frac{\partial C}{\partial t} = \frac{\partial}{\partial X}\left[\alpha_f D_d\frac{\partial C}{\partial X} - (1-s_x)CQ_{sx} - \alpha_a D_a\right] - J(\dot{\epsilon}C+S_w+S_s+R_r) \quad [A35]$$

where

$$Q_{sx} = -K_s\frac{\partial}{\partial X}(P + s_x\Pi) \quad [A36]$$

$$\alpha_f = \rho_s\frac{K_f C}{k_f + C} \quad [A37]$$

$$\alpha_a = \rho_s\frac{K_a C}{k_a + C} \quad [A38]$$

$$R_r = \rho_s\frac{K_r C}{k_r + C} \quad [A39]$$

$$D_d = \frac{2r_{ci}}{\frac{1}{D_m} + \frac{2r_{ci}}{D_o}(J - \omega_{ai})} \quad [A40]$$

$$D_a = \frac{1}{1 + 2r_{ci}(J - \omega_{ai})\frac{D_m}{D_o}} \quad [A41]$$

Boundary conditions at the root tip

$$\omega_a K_a \frac{\partial \Psi_a}{\partial X} + \omega_s K_s \frac{\partial}{\partial X}(P + s_x \Pi) + L_{mstm} K_{sr}(\Psi_a - \Psi_{soil}) = - \mu \rho_\ell (\omega_{sm} + \theta \omega_{am}) \dot{\epsilon}_m L_{mstm} \quad [A42]$$

$$L_{mstm} K_{as}[(P + s_\ell \Pi) - \Psi_a] + \omega_s K_s \frac{\partial}{\partial X}(P + s_x \Pi) = -\mu \rho_\ell \omega_{sm} \dot{\epsilon}_m L_{mstm} \quad [A43]$$

$$- \alpha_f D_d \frac{\partial C}{\partial X} + (1 - s_x) Q_{sx} + \alpha_a D_a = (S_{sm} + S_{wm} + R_{rm}) L_{mstm} \quad [A44]$$

where

$$R_{rm} = \rho_{sm} \frac{K_{rm} C_m}{K_{rm} + C_m} \quad [A45]$$